Author/s:
Yatipanthalawa, Bhagya Subashini

Title:
Processing microalgae for the recovery of high value products

Date:
2022

Persistent Link:
https://hdl.handle.net/11343/310313

Processing microalgae for the recovery of high value products

Bhagya Yatipanthalawa
ORCID: 0000-0001-7332-8371

Doctor of Philosophy

March 2022

Department of Chemical Engineering

Submitted in total fulfilment of the requirements for the Degree of Doctor of Philosophy

The University of Melbourne

Abstract

Microalgae are a diverse range of photosynthetic organisms that inhabit aquatic environments. They are characterised by their microscopic size and their ability to photosynthesize, converting solar energy into high-value metabolites. Their high productivity and ability to be grown on non-arable land make them an attractive potential source of sustainable food and fuel. Microalgal metabolites include lipids that can be converted to produce biodiesel, polysaccharides that can be functional for food application or used to produce bioethanol, proteins that can be used to produce food and feed, and higher-value products such as vitamins, carotenoids and polyunsaturated fatty acids with potential nutraceutical applications. Despite this, microalgal products are scarcely commercialised due to the lack of processes to efficiently extract the high-value components.

When the extraction of lipids for biodiesel production from microalgae is considered, wet lipid extraction is favoured over lipid extraction from dried microalgae due to the high energy costs associated with drying. Further, biphasic lipid extraction from wet paste is deemed to be the most economically feasible way of extracting the lipids from microalgae, which avoids energy intensive distillation to separate the solvents from water as in monophasic systems. Microalgal lipid droplets are stored intercellularly and are often inaccessible to a biphasic lipid extraction system. Hence cell rupture or physically breaking the cells apart is a critical step. However, there is still little understanding of how different microalgae species behave under different lipid extraction processes, particularly in relation to the differences in cell wall structure amongst the diversity of microalgae species.

Among the different microalgae, the marine *Nannochloropsis* sp. has been widely researched owing to its rapid and robust growth and its ability to accumulate high lipid contents. However, their cell walls are robust, necessitating energy-intensive methods to rupture the cells, to enable the subsequent extraction of high-value components. Dark anoxic incubation, where highly concentrated microalgae slurries are incubated in the dark at an elevated temperature, depriving them of sunlight and oxygen, has been identified as a low-cost method to weaken the cell walls of *Nannochloropsis* via induction of autolysis, making the subsequent cell rupture easier. When other microalgae species such as *Chlamydomonas* are subjected to dark anoxic conditions, they undergo glycolytic and fermentative pathways to produce energy. Similar fermentative end products have previously been observed in *Nannochloropsis* during dark anoxia incubation, but the cellular response and the biochemical pathways *Nannochloropsis* undertake are still unclear. The presence of enzymes such as lipases, proteases and cellulases in microalgae cells could also lead to the uncontrolled degradation of biomacromolecules when the cells undergo external stresses. In addition to dark anoxia incubation, *Nannochloropsis* could undergo such dark anoxic conditions in natural marine environment, or during prolonged storage of harvested biomass. Therefore, understanding the cellular response to dark anoxia will enable understanding of the behaviour and decomposition of *Nannochloropsis* as well as to identify the appropriate strategies to preserve and stabilise the biomass and its composition.

Therefore, the first part of this thesis investigated the cellular responses of *Nannochloropsis* to dark anoxia incubation through an in-depth proteomic analysis and investigated the potential effects on the integrity of the proteins and lipids. The cells were found to alter their metabolism to undertake glycolytic and fermentative pathways to produce energy and to maintain the redox balance. During prolonged incubation, the cells were eventually overcome, leading to loss of membrane integrity. As a result, uncontrolled action of proteases and lipases led to the hydrolysis of proteins and lipids into peptides and free fatty acids (FFAs), respectively. The study concluded that while incubation can facilitate cell disruption by weakening the cell walls, the breakdown of proteins and lipids may have detrimental effects for food and fuel applications. This emphasizes the importance of optimizing the incubation time to achieve cell weakening while minimising the unnecessary degradation of biomacromolecules.

The need for cell rupture prior to biphasic lipid extraction from *Nannochloropsis*, and the observed degradation of lipids during prolonged incubation, negates much of the advantages of extracting lipids from this alga. In the second part of this work, the diatom *Navicula* sp. is introduced as a potential alternative to *Nannochloropsis* sp. While *Navicula* sp. can also produce high amounts of lipids, it does not have the robust cellulosic cell walls of *Nannochloropsis* sp. Instead, *Navicula* sp. has a very different cell structure that includes siliceous plates and mucilaginous extracellular polymeric substances (EPS) bound to the exterior of the cell. This unique structure and surface chemistry of diatom cells might alter their behaviour during lipid extraction using biphasic systems. Unexpectedly, and in contrast to other microalgae, it was discovered that biphasic lipid extraction was possible from *Navicula* sp. without prior cell rupture. Investigations into the extraction kinetics, interfacial behaviour and cell structure revealed that nonpolar hexane could infiltrate through the pores present in the cell coverings of these diatoms. High yields (>80%) of intracellular lipids were extracted from intact cells over the course of hours upon low-shear contacting with hexane. Applying high shear forces greatly accelerated lipid extraction due to increased mass transfer from mixing and emulsification, as well as the rupture of some of the cells. Dynamic interfacial tension measurements and electron microscopic analysis revealed that the EPS bound to the cell walls of the diatoms acted as a barrier to solvent penetration into the cells, and power ultrasound could remove these from the cell surfaces, further accelerating lipid extraction. The combination of high-shear in the presence of hexane resulted in the in-situ rupture of the cells, which greatly accelerated lipid extraction and allowed high yields of neutral lipid (>95%) to be recovered from freshly harvested cells within less than 5 min. This was the first study revealing a different mechanism for biphasic lipid extraction from the diatom *Navicula* compared to other previously studied microalgae species such as *Chlorella* and *Nannochloropsis* which possess cellulosic cell walls.

Apart from lipids, diatoms produce high amounts of EPS that are typically carbohydrate-rich polymers that have potential application as functional polysaccharides. Having demonstrated the ability of power ultrasound to remove EPS from *Navicula* sp. without causing significant cell rupture, the third phase of the thesis investigated the use of ultrasonication to remove EPS as a

potential by-product stream, while in parallel investigating the effect of EPS removal on downstream biomass processing, including slurry rheology, dewatering and biphasic lipid extraction. Ultrasonication was effective at removing the EPS, while only causing limited cell rupture specifically at higher EPS yields. The energy requirement for ultrasound assisted EPS removal could be minimised by applying higher intensity ultrasound. The removal of EPS was shown to facilitate downstream processing by improving the slurry rheology and the dewaterability of the cell suspensions. For a 5 wt. % cell slurry, EPS removal by sonication for 30 s reduced the shear-dependent viscosity by about 10-fold and increased the solid concentrations following centrifugation by >sevenfold. It was also found that the removal of EPS could accelerate subsequent biphasic lipid extraction as a result of removing the barrier between the cells and the solvent.

This thesis is the first to systematically investigate the physicochemical mechanisms of mechanical cell rupture and biphasic lipid extraction from two structurally diverse species of microalgae. Through this body of work, important insights into the connections between cell biology and the processability and biochemistry of microalgal suspensions are revealed. These understandings are crucial for the development and optimisation of future processes for microalgae based biorefineries.

Declaration

This is to certify that:

i) The thesis comprises of my original work towards the PhD;

ii) Due acknowledgement has been given in the text to all related parties and other materials used;

iii) The thesis is fewer than 100,000 words in length, excluding tables, maps, bibliographies and appendices.

Bhagya Subashini Yatipanthalawa

March 2022

Acknowledgement

This PhD journey has not been easy, it has been a long and a challenging learning experience for me. Leading to this final thesis were so many people involved, that helped me in numerous ways, and I make this an opportunity to pay my utmost gratitude for them, who made the journey enjoyable and fulfilling.

First and foremost, I would like to extend my heartfelt gratitude to my three supervisors, A/Prof. Greg Martin, Prof. Peter Scales and Prof Muthupandian Ashokkumar for their guidance and supervision throughout my PhD study. Greg has been a wonderful supervisor, always making himself available for the numerous problems I had and ran into. His breadth of knowledge, research expertise and patience played a major role in making this research a success. His involvement has helped me to improve my ability to approach scientific questions, performing sound scientific research trying to look at the bigger picture had allowed me to grow as a research scientist. Peter's expertise in rheology and Ashok's expertise in Sonochemistry made a great addition to this research work. Apart from research they were always open for friendly chats and always made sure I was on track. I'm grateful to A/Prof. Kathryn Mumford, my committee chair for her encouragements and suggestions in our progress review meetings throughout the past 3.5 years.

I would also like to thank the University of Melbourne for the Melbourne research scholarship and the conference travel scholarship that funded my stay and research here in Melbourne. Coming this far would have not been possible if not for the free education I received back in Sri Lanka, from Grade 1 till finishing my bachelors. I am extremely grateful for all the tax paying citizens both in Sri Lanka and Australia and the free education system in Sri Lanka for supporting my education and research.

I am grateful for all the past and present members of the algal processing group, sonochemistry group and the sludge group, particularly, Dr. Sam Law, Dr. Charitha Gamlath, Dr. Nature Poddar, Dr. Erico Baroni, Dr. Ronald Halim, Raul Cavalida, Dr. Shane Usher, Dr. Rachana Pathak, Haiyan Zhu, Stephen Yao, Dr. Srinivas Mettu, Dr. Shirley Xu, and David Liu all who helped me in getting started in the labs and giving me good company while working in the lab. A special thank goes to Dr. David Hill for the help with microalgae cultures and sharing his knowledge and passion on microalgae. The assistance of Zlatan Trifunovic in taking TEM images is gratefully acknowledged.

I would also like to thank Esther Mienis and Prof. Imogen Foubert from KU Leuven, Belgium for the helpful analysis and discussions on microalgal lipids. I would like to pay my special gratitude to the Proteomic and mass spectrometry facility and the advanced microscopy facility at the University of Melbourne.

The trust and confidence my parents; amma, appachchi and my two sisters had on me and their love and care were a key driving force for me to pass this hurdle. I am also grateful for my parents-in-law and sister-in-law, who showered me with unconditional love. My stay here in Melbourne away from my family, was made less stressful thanks to a bunch of friends who deserve a special mention. My Sri Lankan friend circle, Charitha, Sachi, Nilanka, Sachini, Sulochana, Chaminga, Manula and Mevan made me feel home, and were always there cheering for the smallest achievement. I would also like to thank Hongjiao and Shareen, my first two friends I made at the University of Melbourne for being there for my moral support throughout the PhD journey.

Last but not least, this whole PhD rollercoaster would not have been easier if not for my loving husband Tharindu, for all the constant love, support, understanding and encouragement throughout the past few years and also the trust on me that I am built for bigger and better things. If not for you, I could have easily given up my PhD long ago!.

Publications arising from this thesis

Published:

Yatipanthalawa, B., Li, W., Hill, D. R., Trifunovic, Z., Ashokkumar, M., Scales, P. J., & Martin, G. J. (2021). "Interplay between interfacial behaviour, cell structure and shear enables biphasic lipid extraction from whole diatom cells (*Navicula* sp.)". Journal of Colloid and Interface Science, 589, 65-76.

Yatipanthalawa, B., & Martin, G. (2021). "Conventional and novel approaches to extract food ingredients and nutraceuticals from microalgae". In Cultured Microalgae for the Food Industry (pp. 73-96). Academic Press.

Yatipanthalawa, B. S., Ashokkumar, M., Scales, P. J., & Martin, G. J. (2022). "Ultrasound-Assisted Extracellular Polymeric Substance Removal from the Diatom *Navicula* sp.: A Route to Functional Polysaccharides and More Efficient Algal Biorefineries". ACS Sustainable Chemistry & Engineering.

Manuscripts in preparation:

Yatipanthalawa, B. S., Mienis, E., Halim, R., Foubert, I., Ashokkumar, M., Scales, P. J., & Martin, G. J. "Induced biochemical and metabolic changes during dark anoxic incubation of *Nannochloropsis*".

Conference presentations

Yatipanthalawa, B., Li, W., Hill, D. R., Trifunovic, Z., Ashokkumar, M., Scales, P. J., & Martin, G. J. (2021). "Biphasic lipid extraction from unruptured diatom cells – a new mechanism for algae lipid extraction driven by wall structure and interfacial behaviour" Presented at the 10th Algal Biomass, Biofuels and Bioproducts Conference, Online.

Table of contents

List of figures

ACDC Acetyl CoA deacylase, ADH Aldehyde dehydrogenase, AcDH Alcohol Dehydrogenase, ALAT Alanine aminotransferase, CS Citrate synthase, ME malic enzyme, OGDH oxoglutarate dehydrogenase, SCL Succinyl CoA lyase, SDH Succinate dehydrogenase, FHy fumarate hydratase, MDH Malate dehydrogenase, AAT Aspartate aminotransferase, LDH Lactate dehydrogenase. Green: significantly increased. Grey: increased but not significantly. Orange: decreased but not significantly Black: not found.

Figure 4.1: (a) Kinetics of biphasic lipid extraction from wet slurries (2.1% solids) of freshly harvested, intact *Navicula* sp. cells using hexane under low-shear mixing. The kinetics are expressed as a percentage of the total neutral lipids extracted using a Bligh and Dyer method. Error bars represent the standard deviation of duplicate measurements of triplicate experiments. Representative SEM images of (b, d) fresh *Navicula* sp. cells harvested by centrifugation and (c, e) *Navicula* sp. cells after 23 h of low-shear mixing with hexane.

Figure 4.2. Change in the interfacial tension between hexane and *Navicula* sp. slurry (0.1% solids concentration) phases as a function of time plotted on a linear (a) and log (b) timescale. The different regimes are separated by vertical dashed lines and the possible mechanisms underlying each are briefly described.

Figure 4.3. TEM images of (a) a freshly harvested *Navicula* sp. cell, and (b) a cell contacted with hexane only via diffusional interfacial adsorption for 2 h. Red circles show the position of the filled (a) and emptied (b) lipid bodies (Cl = chloroplast; M = mitochondrion). Red arrows are used to point the difference in the extracellular material present on the cell walls in the insert images. The scale bars represent 1 µm.

Figure 4.4: (a) Kinetics of biphasic lipid extraction from wet slurries (2.1% solids) of freshly harvested, unruptured *Navicula* sp. cells using hexane mixed by ultrasonication and rotor stator mixing. The kinetics are expressed as a percentage of the total neutral lipids extracted using Bligh and Dyer method. Error bars represent the standard deviation of duplicate measurements of triplicate experiments. Representative SEM images of (b) cells subjected to ultrasonication for 60 s in the presence of hexane (1:1 hexane: paste) (c) cells mixed with hexane (1:1 hexane: paste) using rotor stator mixing for 20 mins. The inserts show representative cells at a higher magnification. The scale bars represent 10 µm.

Figure 4.5. Representative SEM images of (a) freshly harvested *Navicula sp.* cells and (b) cells subjected to 1-min ultrasonication. The scale bars represent 5 µm. (c) TEM image of a *Navicula sp.* cell ultrasonicated for 1 min, revealing a cell wall lacking attached extracellular polymeric substances (M = mitochondria; N = nucleus; C = chloroplast). The scale bars represent 500 nm.

Figure 4.6: Dynamic interfacial tension (DIFT) profiles between hexane and suspensions of *Navicula* sp. cells (1.5% solids) in relation to prior treatment with ultrasound (for 5 s, 30 s, or 1 min) to remove bound EPS. Trendlines in red indicate the DIFT in regime III. Dashed lines indicate the times and IFT associated with the onset of regime IV.

Figure 4.7: Schematic of the proposed mechanism of biphasic lipid extraction from the diatom *Navicula* with and without high shear forces. A detailed description of the mechanism is included in the main text.

Figure 5.1: Extracted EPS (as estimated by the polysaccharide content of the supernatant) and cell rupture as a function ultrasonication time at (A) two different power densities and intensities and (B) at two different power intensities at the same power density of 1.5 W/ml. The data points and error bars represent the average and standard deviation of process triplicates, respectively. The same 1.5 W/ml, 0.27 MW/m^2 data is presented in both panels to facilitate comparisons.

Figure 5.2: EPS recovery yield (as estimated by the supernatant polysaccharide content) in relation to cell rupture (A) and energy use (B) as a function ultrasound power intensity (low = blue circles = 0.12 MW/m^2; medium = orange triangles = 0.27 MW/m^2; high = grey squares = 4.24 MW/m^2) and power density (low = 0.688 W/mL; high = 1.5 W/mL). The data points and the error bars represent the average and standard deviation of process triplicates.

Figure 5.3: (A) Shear dependent viscosity of *Navicula* sp. slurries at increasing shear rates from 1 to 300 s^{-1} and different solid concentrations. (B) Shear dependent viscosity of *Navicula* sp. slurries following removal of EPS by ultrasonication for different time periods (power intensity = 4.24 MW/m^2; power density = 1.5 W/mL) and removal of the EPS-rich supernatant to obtain a solids concentration of approximately 5%. (C) The viscosity at a shear rate of 145 s^{-1} as a function of the biomass concentration of untreated *Navicula* slurries (■) and following ultrasonic and centrifugal EPS removal (●). The slight decrease in biomass concentration following ultrasonication is due to mass loss associated the EPS are removal. In (A) and (B), duplicated measurements are shown for each data set, in coloured and empty symbols. In (C), the data points and error bars represent the average and standard deviation of duplicate measurements, respectively.

Figure 5.4: (A) The effect of ultrasonic removal of EPS on the rate of separation efficiency (defined as the percentage of water removed from the biomass). (B) The final biomass concentration obtained after centrifugation for 20 min at 2330 g as a function of the amount of EPS removed/dislodged using ultrasonication for 5 s, 15 s, or 30 s (power intensity = 4.3 MW/m^2; power density = 1.5 W/ml). (C) Shear dependent viscosity of the EPS fractions separated by centrifugation after ultrasonication.

Figure 5.5: Biphasic lipid extraction kinetics from suspensions of the diatom *Navicula* sp. with EPS removed by ultrasound pretreatment and concentrated to 5% solids. Lipid yields represent the % of total neutral lipids in the algae that were recovered. (A) Extraction kinetics under high shear mixing using ultrasonication. (B) Extraction kinetics under low shear mixing. Both sets of data were obtained at room temperature. The data points and error bars represent the average and standard deviation of triplicated experiments.

Figure 5.6: Summary of the improvements to a biorefinery enabled by ultrasonic pre-treatment to remove EPS. This process results in a concentrated EPS stream and improves the processability of the microalgae suspension by decreasing the overall suspension viscosity, by enabling higher solids concentration slurries to intensify processing, and by accelerating lipid extraction.

List of tables

Nomenclature

AAT	Aminotransferase
ABF	Actinobacterium Bioflocculant
AcDH	Alcohol Dehydrogenase
ACK	Acetate Kinase
ACN	Acetonitrile
ACST	Acetate Succinate CoA Transferase
ADH	Aldehyde Dehydrogenase
ALAT	Alanine Aminotransferase
AOM	Algogenic Organic Matter
ASCT	Acyl CoA Thioesterase
ATP	Adenosine triphosphate
BCA	Bicinchoninic acid
CER	Cation Exchange Resin
DAG	Diacylglycerols
DGI	Dangerous Goods International
DHA	Docosahexaenoic Acid
DIFT	Dynamic Interfacial Tension
DME	Dimethyl Ether
DNA	Deoxyribonucleic Acid
EPA	Eicosapentaenoic Acid
EPS	Extracellular Polymeric Substances
ER	Endoplasmic reticulum
F1P	Fructose-1-phosphate
FAMEs	Fatty Acid Methyl Esters
FBA	Fructose Bisphosphate Aldolase
FDA	Food and Drug Administration

FFAs	Free Fatty Acids
FK	Fructokinase
G3P	Glycerol-3-phosphate
G3PDH	Glyceraldehyde 3 Phosphate Dehydrogenase
GK	Glucokinase
HPH	High-pressure Homogenisation
iBAQ	Intensity Based Absolute Quantification
IFT	Interfacial Tension
LDH	Lactate Dehydrogenase
LC/MS/MS	Liquid chromatography tandem mass spectrometry
MAG	Monoacylglycerols
MDH	Malate Dehydrogenase
mRNA	Messenger ribonucleic acid
NAC	N-acetyl Cysteine
NAD	Nicotinamide adenine dinucleotide
OAA	Oxaloacetate
OGDH	Oxoglutarate Dehydrogenase
OPA	O-phthalaldehyde
PAC	Poly Aluminium Chloride
PBS	Phosphate Buffered Saline
PDH	Pyruvate Dehydrogenase Complex
PEF	Pulsed Electric Fields
PEI	Polyethyleneimine
PFK	Phosphofructokinase
PFL	Pyruvate Formate Lyase
PFO	Pyruvate Ferredoxin Oxidoreductase
PGK	Phosphoglycerate Kinase
PHy	Pyruvate Hydratase

PK	Pyruvate Kinase
PTA	Phosphotransacetylase
PUFAs	Polyunsaturated Fatty Acids
ROS	Reactive Oxygen Species
RSLC	Rapid Separation Liquid Chromatography
SCL	Succinyl CoA Lyase
SDS	Sodium Dodecyl Sulphate
SEM	Scanning Electron Microscopy
SPE	Solid Phase Extraction
SQDG	Sulfoquinovosl Diacylglycerol
TAGs	Triacylglycerols
TCEP	Tris(2-carboxyethyl) phosphine
TEAB	Triethylammonium Bicarbonate
TFA	Trifluoro Acetic Acid
tRNA	Transfer ribonucleic acid
UDP	Uridine Diphosphate
UHPH	Ultra-high-pressure Homogenisation
PV	Peroxide Value

Chapter 1

1. Introduction

Microalgae are an important and diverse group of photosynthetic microorganisms that inhabit freshwater marine environments. Their ability to efficiently utilise sunlight to convert carbon into lipids, proteins, carbohydrates, and high-value pigments (Minhas et al., 2016, Dong et al., 2013, Sirajunnisa and Surendhiran, 2016) have led to increasing research into their use as a source of sustainable food, fuel, and biochemicals. In particular, the high lipid content that can be accumulated in some microalgae make them a potential feedstock for biodiesel production. The ability to produce high-value metabolites such as polyunsaturated fatty acids (PUFAs), proteins and polysaccharides makes them great sources for food and nutraceutical applications (Aguirre et al., 2013, Minhas et al., 2016). However, isolating and recovering such components from microalgae involves a series of operations including culturing, harvesting and biomass processing, which may involve cell rupture, component extraction and purification.

Microalgae grow as dilute suspensions and hence efficient harvesting of the biomass is necessary for efficient biorefineries. This can include concentration steps to reduce the process volumes followed by a thermal drying step to remove the moisture. However, the thermal drying step consumes very high amounts of energy, considerably reducing the energy efficiency of the process (Cooney et al., 2011b, Chisti, 2013). Therefore, processing wet concentrated microalgal biomass during the extraction of the valuable components has gained increasing interest in research (Dong et al., 2016a, Martin, 2016a). When considering wet processing of microalgae, extraction of the lipids is considered a major bottleneck (Dong et al., 2016a). Biphasic lipid extraction systems in which nonpolar solvents are used, are preferred over monophasic systems (polar solvents, or polar and non-polar solvent mixtures that are water miscible) due to the ease of physical separation of the lipid-rich solvent fraction, which avoid energy-intensive distillation from water (Dong et al., 2016a, Martin, 2016a).

Microalgae being a diverse group of organisms, selecting the most suitable strain for the industrial production is a challenging and important consideration. The effect of different culture conditions on different strains has long been studied, focussing on optimising the accumulation of targeted end-products. However, there is currently less knowledge about how differences in the cell properties of different strains affects downstream biomass processing. Different microalgal species have differences in cell wall structure, size, shape and extracellular and intracellular compositions. These differences can affect the accessibility of intracellular components (Balduyck et al., 2015), the need for and difficulty of cell rupture (Spiden et al., 2013b), the rheology of concentrated slurries (Bernaerts et al., 2017), dewaterability (Uduman et al., 2010), and surface interactions (Hao et al., 2017), thus affecting downstream processing. Therefore, understanding the cellular and cell wall structure is necessary when developing efficient biorefinery processes for microalgae.

Nannochloropsis sp. is a widely studied genus of microalgae, identified as a suitable precursor for biodiesel production. *Nannochloropsis* cells include strong cellulosic cell walls that are physically robust, making cell rupture difficult (Yap et al., 2015). In a previous study, a low-cost process for extracting lipids from wet concentrated *Nannochloropsis* sp. was proposed (Olmstead et al., 2013b). Here the cells were weakened before mechanical cell rupture using dark anoxic incubation. Subjecting the cells to dark anoxic conditions was later found to lead to cell wall thinning from cell autolysis (Halim et al., 2019a, Olmstead et al., 2013b). Of practical importance, it was found that the total lipid and protein contents of the biomass were not reduced, while cellulose in the cell walls was degraded (Halim et al., 2019a). However, potential biochemical alterations in the lipid and protein fractions that could result during this process are not yet known (Halim et al., 2019a, Halim et al., 2016a). Hence the chapter 3 focusses on the effect of dark anoxia incubation on the biomacromolecules, while trying to elucidate the underlying cellular responses to dark anoxia incubation. Such an understanding will benefit development of efficient lipid extraction processes and will provide a foundation for future studies on *Nannochloropsis* and dark anoxic fermentation of microalgae species more broadly.

Diatoms are another class of microalgae that possess fundamentally different cell wall structures to those of *Nannochloropsis* sp. Diatom cell walls consist of two separate silica frustules that are attached to each other, which makes the diatom cells comparatively more susceptible to mechanical rupture than microalgae with cellulosic cell walls such as *Chlorella* and *Nannochloropsis* (Spiden et al., 2013b). Diatoms can also produce large amounts of extracellular polymeric substances (EPS) that are excreted out of the cells (Klein et al., 2014). The effects of these differences in the cell wall structure and extracellular composition on biphasic lipid extraction and downstream processing are investigated in the Chapters 4 and 5 using a marine diatom, *Navicula* sp.

This thesis begins with an in-depth literature review on the current knowledge pertaining to microalgae cell biology and processing, and methods for the extraction of high-value components including lipids, proteins and polysaccharides (Chapter 2). From this review knowledge gaps in the literature are identified that are to be addressed in this thesis. Chapters 3 to 5 cover the experimental work done in the thesis, focussing on the issues highlighted above. Each chapter includes a separate introduction followed by the experimental work, its findings and conclusions, and contains its own references section. The first experimental chapter (Chapter 3) aims at providing a fundamental understanding of a previously studied cell weakening process on the microalgae *Nannochloropsis* sp. Chapters 4 and 5 focus on a structurally different type of microalgae called diatoms. The mechanisms of biphasic lipid extraction are studied in Chapter 4, while Chapter 5 focuses on a biorefinery concept involving the pre-removal of EPS (extracellular polysaccharides) as a means to improve the processability of the microalgal slurries for subsequent lipid extraction, while recovering a potentially useful co-product. The findings and conclusions are brought together in the final chapter (Chapter 6) to form an overall understanding of the

processing microalgae for the recovery of high-value products, along with recommendations for future work.

References

AGUIRRE, A.-M., BASSI, A. & SAXENA, P. 2013. Engineering challenges in biodiesel production from microalgae. *Critical reviews in biotechnology,* 33**,** 293-308.

BALDUYCK, L., GOIRIS, K., BRUNEEL, C., MUYLAERT, K. & FOUBERT, I. 2015. Stability of Valuable Components during Wet and Dry Storage. *Handbook of Marine Microalgae.* Elsevier.

BERNAERTS, T. M., PANOZZO, A., DOUMEN, V., FOUBERT, I., GHEYSEN, L., GOIRIS, K., MOLDENAERS, P., HENDRICKX, M. E. & VAN LOEY, A. M. 2017. Microalgal biomass as a (multi) functional ingredient in food products: Rheological properties of microalgal suspensions as affected by mechanical and thermal processing. *Algal research,* 25**,** 452-463.

CHISTI, Y. 2013. Constraints to commercialization of algal fuels. *Journal of biotechnology,* 167**,** 201-214.

COONEY, M. J., YOUNG, G. & PATE, R. 2011. Bio-oil from photosynthetic microalgae: Case study. *Bioresource Technology,* 102**,** 166-177.

DONG, H.-P., WILLIAMS, E., WANG, D.-Z., XIE, Z.-X., HSIA, R.-C., JENCK, A., HALDEN, R., CHEN, F. & PLACE, A. 2013. Responses of *Nannochloropsis* oceanica IMET1 to long-term nitrogen starvation and recovery. *Plant physiology***,** pp. 113.214320.

DONG, T., KNOSHAUG, E. P., PIENKOS, P. T. & LAURENS, L. M. 2016. Lipid recovery from wet oleaginous microbial biomass for biofuel production: a critical review. *Applied energy,* 177**,** 879-895.

HALIM, R., HILL, D. R. A., HANSSEN, E., WEBLEY, P. A., BLACKBURN, S., GROSSMAN, A. R., POSTEN, C. & MARTIN, G. J. O. 2019. Towards sustainable microalgal biomass processing: anaerobic induction of autolytic cell-wall self-ingestion in lipid-rich *Nannochloropsis* slurries. *Green Chemistry,* 21**,** 2967-2982.

HALIM, R., WEBLEY, P. A. & MARTIN, G. J. 2016. The CIDES process: fractionation of concentrated microalgal paste for co-production of biofuel, nutraceuticals, and high-grade protein feed. *Algal Research,* 19**,** 299-306.

HAO, W., YANPENG, L., ZHOU, S., XIANGYING, R., WENJUN, Z. & JUN, L. 2017. Surface characteristics of microalgae and their effects on harvesting performance by air flotation. *International journal of agricultural and biological engineering,* 10**,** 125-133.

KLEIN, G. L., PIERRE, G., BELLON-FONTAINE, M.-N., ZHAO, J.-M., BRERET, M., MAUGARD, T. & GRABER, M. 2014. Marine diatom *Navicula* jeffreyi from biochemical composition and physico-chemical surface properties to understanding the first step of benthic biofilm formation. *Journal of Adhesion Science and Technology,* 28**,** 1739-1753.

MARTIN, G. J. 2016. Energy requirements for wet solvent extraction of lipids from microalgal biomass. *Bioresource technology,* 205**,** 40-47.

MINHAS, A. K., HODGSON, P., BARROW, C. J. & ADHOLEYA, A. 2016. A review on the assessment of stress conditions for simultaneous production of microalgal lipids and carotenoids. *Frontiers in microbiology,* 7**,** 546.

OLMSTEAD, I. L., KENTISH, S. E., SCALES, P. J. & MARTIN, G. J. 2013. Low solvent, low temperature method for extracting biodiesel lipids from concentrated microalgal biomass. *Bioresource technology,* 148**,** 615-619.

SIRAJUNNISA, A. R. & SURENDHIRAN, D. 2016. Algae–a quintessential and positive resource of bioethanol production: a comprehensive review. *Renewable and sustainable energy reviews,* 66**,** 248-267.

SPIDEN, E. M., YAP, B. H. J., HILL, D. R. A., KENTISH, S. E., SCALES, P. J. & MARTIN, G. J. O. 2013. Quantitative evaluation of the ease of rupture of industrially promising microalgae by high pressure homogenization. *Bioresource Technology,* 140**,** 165-171.

UDUMAN, N., QI, Y., DANQUAH, M. K., FORDE, G. M. & HOADLEY, A. 2010. Dewatering of microalgal cultures: a major bottleneck to algae-based fuels. *Journal of renewable and sustainable energy,* 2**,** 012701.

YAP, B. H., DUMSDAY, G. J., SCALES, P. J. & MARTIN, G. J. O. 2015. Energy evaluation of algal cell disruption by high pressure homogenization. *Bioresource Technology,* 184**,** 280-285.

Chapter 2

2. Literature Review

2.1. An overview of microalgae production and biomass processing

2.1.1. Microalgae cell structure and functions

As described in the Introduction, this thesis will investigate the processing of microalgal biomass in relation to cell structure and function. This section provides an overview of microalgae cell structure as a basis for the research. Microalgae are a very diverse group of photosynthetic microorganisms which have been traditionally classified based on their structural and morphological differences. This thesis will focus on two main classes of algae within the Chromista Kingdom, Eustigmatophyceae and Bacillariophyceae (i.e. diatoms). Despite the dramatic differences in their external characteristics, internally, the cellular organelles and functions are mostly similar amongst eukaryotic algae. The various organelles have different functions that are ultimately catalysed and carried out by specific proteins or enzymes. The protoplast, which is the protoplasmic content of a cell, is surrounded by a lipoproteinaceous external boundary called the cell membrane. The cell membrane is comprised of lipids and proteins, is thin and elastic, and is selectively permeable, thus controlling the passage of materials in and out of the cells. This transport of molecules in and out of the cells can be aided by transport proteins. In eukaryotic algal cells, there are membrane-bound organelles including the nucleus, chloroplasts, Golgi apparatus, endoplasmic reticulum, and mitochondria. The nucleus is bound by the nuclear membrane, which has two layers, of which the outer layer is continuous with the endoplasmic reticulum. External to the membrane, the outer cell wall protects and holds the macroscopic structure of the cell together and is a feature of diversity amongst different algae. The cell wall is physically much stronger than the cell membrane and also more permeable. Beyond the cell wall, many microalgae excrete biopolymers, referred to general as extracellular polymeric substances (EPS). Both the cell wall and the EPS will be important aspects of this thesis. Table 2.1 provide a basic understanding of the microalgal cell structure and functions associated with each organelle.

Table 2.1: Functions and location of the organelles in a microalgal cell.

Organelle	Cellular location and function
Endoplasmic reticulum (ER)	Located inside the cytoplasm traversing throughout. It folds to create an internal space named “lumen” which connects to the nuclear envelope. Consists of two parts, the rough ER and the smooth ER (Alberts et al., 2002b).
Rough ER	Surface studded with ribosomes which are responsible for the production of proteins (Alberts et al., 2002b).
Ribosomes	Synthesising proteins using messenger ribonucleic acid (mRNA) and transfer-ribonucleic acid (tRNA).

Smooth ER	Lack bound ribosomes. Makes lipids and steroids. Contains ER exit sites that transport newly synthesized proteins and lipids (Alberts et al., 2002b).
Golgi complex	Sorting and correctly transporting the proteins produced in the endoplasmic reticulum. Formation of new plasma membrane to support growth (Palade, 1956).
Mitochondrion	Performs cellular respiration and breaks down sugars to produce energy. A double layer membrane envelope surrounds the mitochondrion, of which the inner membrane encloses an aqueous matrix of solutes, mitochondrial glucose and soluble enzymes. The matrix is finely granular and highly proteinaceous. This has a circular deoxyribonucleic acid (DNA) and ribosomes of its own which can synthesize some of its own proteins.
Chloroplast	A membrane bound organelle in the cytosol carrying out photosynthesis (Alberts et al., 2002a).
Pyrenoid	Found in the chloroplast. Occupied by a proteinaceous matrix which is involved in carbon fixation, starch formation and storage (Dodge, 2012).
Thylakoid	A membrane bound compartment in the chloroplast. Contains light harvesting complexes and pigments including chlorophyll, carotenoids and phycobiliproteins (Büchel, 2020).
Nucleus	Cell's genetic material are stored here. DNA trapped around proteins is stored in a gel like substance called nucleoplasm (Alberts et al., 2017).
Nucleolus	Located inside the nucleus and is responsible for the assembling of new ribosomes (Alberts et al., 2017).
Lipid droplets	Globular organelle located in the cytosol enclosing the neutral lipids (mainly triacylglycerols (TAGs)), covered by a layer of membrane lipids and proteins (Alberts et al., 2017).
Cell membrane	Lipoproteinaceous membrane which controls the passage of different compounds in and out of the cell (Alberts et al., 2017).
Cell walls	Composed of biopolymers, often primarily cellulose other polysaccharides, or of silica in the case of diatoms. In addition, other polysaccharides like pectin and hemicellulose and proteins can be found in cell walls. Gives the cell its shape and supports the plasma (Dodge, 2012).

The cell walls of microalgae controls/limits the accessibility to the internal components from the external environment. As briefly described in Table 2.1, the composition and the strength of microalgal cell walls is species dependent, and they vary in composition, where some can contain

polysaccharides like cellulose, xylan, mannose, and different other components such as uronic acids, proteins, glycoproteins, algaenan and sometimes even silica (Lee et al., 2012, Scholz et al., 2014). Also, not all the algal cells are covered with cell walls. Some genera like *Dunaliella* and *Ochromona*s are bounded only by the plasma membrane (Dodge, 2012).

Cellulosic cell walls are composed of cellulose microfibrils of varying thickness, remaining variously oriented in a granular matrix. It has been found that the cell walls of *K. antarctica,* which is a green filamentous microalga having the ability to grow at different salinity conditions, consist of a matrix of polysaccharides containing mainly glucan chains and some minor sugars including rhamnose and mannose (Piro et al., 2000). This thesis investigates *Nannochloropsis* sp. and a diatom, *Navicula* sp.. The cell walls of *Nannochloropsis* sp., which is deemed to be one of the most promising algae for the production of biodiesel (Beacham et al., 2014), consists of a cellulosic inner cell wall. This is protected by an outer layer of algaenan that is comprised of long, straight chain saturated aliphatics with ether cross links that are mainly hydrophobic (Scholz et al., 2014). Diatoms on the other hand have silica frustules as cell coverings, which would be discussed in detail in section 2.6.

2.1.2. Microalgae production and concentration

2.1.2.1. Overview of microalgae cultivation and harvesting

Microalgae are aquatic phototrophic microorganisms that grow in water in the presence of the basic necessary nutrients. Extensive research has been carried out to identify the optimal growth conditions under various growth modes, looking at different microalgal species and different target molecules. The growth conditions would generally include the nutrient content, CO_2 concentration, light intensity (Simionato et al., 2011), pH and temperature, and different stress conditions such as nitrogen and phosphorous starvation. Different growth modes include photoautotrophic, heterotrophic and mixotrophic conditions, classified based on the energy and carbon source used for cellular anabolism. The cultivation of microalgae is not a topic of investigation in this thesis, but rather a prerequisite activity of downstream processing.

Nevertheless, an important aspect of cultivation is that due to self-shading of the available light, the concentration of biomass that can be reached in photoautotrophic cultivation is very low – in the order of 1 g/L (0.1% w/w solids) (Yatipanthalawa and Martin, 2021). This means that the cells must be harvested from large volumes of culture medium. Volume reductions in microalgal processing is a key principle of achieving equipment and energy efficiency in the downstream processes. To achieve a concentrated slurry for biomass processing, the culture needs to be concentrated first (e.g. to *ca* 5% w/w solids via flocculation (Şirin et al., 2013)) and then dewatered (e.g. to *ca* 25% w/w solids via centrifugation (Vandamme et al., 2013)). Water removal beyond this requires thermal drying which is highly energy demanding and can damage sensitive biological components (Cooney et al., 2011b, Lardon et al., 2009).

2.1.2.2. Microalgae harvesting/pre-concentration

Microalgae cells do not settle well without being aggregated, due to their small size and relatively similar density to water. Therefore, various pre-concentration techniques such as chemical flocculation, self-flocculation, gravity sedimentation, electro coagulation and flotation are used to pre-concentrate microalgae cells, which can then be further concentrated by filtration or centrifugation (Yatipanthalawa and Martin, 2021). Flocculants have the ability to coalesce small particles/cells in the suspension into larger aggregates that would make their subsequent settling easier (Barros et al., 2015).

Chemical flocculants include metal salts such as alum and ferric chloride, synthetic cationic polymers such as poly aluminium chloride (PAC) and polyferric chloride, and biopolymers such as chitosan and guar gum (Pugazhendhi et al., 2019, Verma et al., 2012). Metal salts are commonly used as flocculants in industries such as wastewater treatment, but not recommended for the use in microalgae flocculation due to the possible issues associated with contaminating the biomass with these chemicals (Vandamme et al., 2013). Nonetheless, the lipolytic stability during storage of the microalgae species *T. isochrysis* was improved when $FeCl_3$ was used as a chemical flocculant (Balduyck et al., 2019a), indicating that the addition of chemical flocculants to microalgae systems could have some advantages. Synthetic polymer flocculants are costly compared with metal salts hence are not generally preferred for microalgae harvesting (Pugazhendhi et al., 2019).

When considering microalgae specifically for food products, biopolymer flocculants such as chitosan are preferred because of their non-toxicity and biodegradability (Verma et al., 2012). However, molecules such as chitosan are relatively expensive and their use for harvesting microalgae is still emerging. Bacteria-derived bioflocculants such as Actinobacterium bioflocculant (ABF) from *Streptomyces* sp., have been used to effectively recover *Nannochloropsis* sp. cells (Sivasankar et al., 2020). These are harmless to microalgae, allowing them to be reused and recycled, and can be produced at a low cost (Sivasankar et al., 2020).

Self-flocculation is another potentially low-cost method for harvesting microalgae, which does not require any external flocculants allowing the simple reuse of the growth medium. However, only a few species of microalgae have shown the capability of self-flocculation, which has led to more efforts being directed towards co-culturing microalgae with other microorganisms that induce flocculation (Zhao et al., 2019, Salim et al., 2012). Several microalgae species such as *Chlorella vulgaris* (Alam et al., 2014), *Scenedesmus obliquus* (Guo et al., 2013), *Ettlia texensis* (Salim et al., 2014) have shown spontaneous self-flocculating abilities, predominantly due to the composition of the cell wall, and cell wall bound EPS produced by them.

Importantly, the presence of flocculants can affect downstream extraction processes due to the alteration of rheological properties in flocculated and concentrated biomass (Yap et al., 2016a).

2.1.2.3. Dewatering

Following harvesting/pre-concentration, centrifugation and filtration are often used to further concentrate microalgae into pastes. Filtration is typically best used as a thickening step, with centrifugation then applied to produce a concentrated, dewatered slurry (Yatipanthalawa and Martin, 2021).

Filtration require a pressure drop to be maintained to force the microalgae suspension to flow through a membrane (Barros et al., 2015). However, there are limits to the extent of dewatering, as the deposition of microalgae on the filter bed leads to fouling and a reduced flux. Chemical cleaning can recover flux, but this leads to high operational costs (Barros et al., 2015) and potential chemical contamination of the product. Therefore, filtration is only preferred for smaller scale harvests and in cases where the size of the cells is very small. Very small algal cells are difficult to recover in centrifugation as they require higher speeds and retention times.

Although centrifugation incurs high capital costs, it is highly effective at concentrating microalgae and can be used in a continuous operation without requiring the addition of any chemicals (Yatipanthalawa and Martin, 2021). Operational costs incurred during centrifugal dewatering are dependent on the rotational speed and residence time required which are a function of the size and the volume of the algae suspension. Centrifuging pre-concentrated streams is most energy efficient due to the reduced volumes. Therefore, centrifugation is often used as the final step in algae harvesting to obtain a concentrated paste, that can approach the close-packing limit of the cells. The 'effective' close packed limit is dependent on the species of microalgae and is typically about 15 – 40% (w/w) (Yatipanthalawa and Martin, 2021).

2.1.2.4. Drying

Dried microalgal powders are often produced for commercial microalgae for food applications (e.g. *Chlorella* and *Spirulina* to be consumed as whole cell proteins). Dry powders of whole microalgae are relatively stable and easy to transport (Balduyck et al., 2016, de Farias Neves et al., 2019). Drying of algae can also be applied prior to extraction of food ingredients and nutraceuticals, for instance to facilitate solvent extraction of microalgal lipids (Balasubramanian et al., 2013). However, the choice of drying needs to be made wisely as this can deteriorate the quality of microalgae by degrading heat sensitive components in the cells (Stramarkou et al., 2017). In addition, producing a dry powder requires thermal drying to remove intracellular water remaining at concentrations beyond the close-packing limit of the cells. A lot of energy is required to overcome the latent heat of vaporisation, which can make drying impractical, particular for biofuel application for which the drying energy can exceed that of the energy contained in the resultant fuel (Cooney et al., 2011b). Solar drying, spray drying, drum drying and lyophilisation can all be used for drying microalgae. Solar drying and drum drying are lower cost and more energy efficient than the other methods but are also harsher on sensitive food and nutraceutical components. The slow drying rates during solar drying causes biomass degradation and increased bacterial counts (Chen et al., 2015). Lyophilisation, or freeze-drying, is the gentlest method, but by far the costliest (Balasubramanian et al., 2013). As a reasonably gentle yet efficient method,

spray drying is the most widely used method for food applications (Cooney et al., 2011b, de Farias Neves et al., 2019). Cell structure degradation during drying as a result of the fast water evaporation damaging the cell membrane irrespective of the method used, can also result in losing valuable components if stored under unfavourable conditions (de Farias Neves et al., 2019). For example, storing spray-dried *Dunaliella salina* in the presence of light and air led to the degradation of β-carotene (Orset et al., 1999), while storing freeze dried *Haematococcus pluvialis* under unfavourable conditions led to the degradation of astaxanthin (Ahmed et al., 2015). Storing microalgae under vacuum or lower temperatures was seen to improve the stability of such sensitive components (Ahmed et al., 2015).

As removal of water by thermal drying is highly energy intensive compared to physical dewatering, thickened and dewatered pastes are often subjected to drying to reduce the costs. However, even with this approach, the energy costs of drying are prohibitive for biofuel and low-cost feed applications. As such, processes to extract intracellular components from wet microalgae slurries are being developed (refs and/or see Section 2.5). To reduce potential degradation of high value components during wet storage, a short heat treatment can be used inactivate lipolytic enzymes (Balduyck et al., 2019b).

In conclusion, the selection of an appropriate dewatering technology for microalgal depends on the physical properties of the cells, which define their aggregation, settling behaviour and close packing limits. It also needs to be selected based on the requirements of the final product. The associated costs increases as the required concentration of the algae slurry increases. A sequential process is preferred when obtaining the required algae concentrations, that is preconcentrating the cells, dewatering the thickened suspensions followed by drying to minimise the energy requirement and operational costs owing to the scaled down volumes.

2.2. Valuable components in microalgae

2.2.1. Lipids

Lipids can be categorized as polar and non-polar lipids, based on polarity. Polar lipids include phospholipids and glycolipids whereas non-polar lipids include triacylglycerols (TAGs), monoacylglycerols (MAG), diacylglycerols (DAG), free fatty acids (FFAs), hydrocarbons, sterols and pigments (Callejón et al., 2014). Lipids can also be categorized as saponifiable and unsaponifiable lipids, depending on whether they contain fatty acid moieties or not, respectively. Saponifiable lipids contain one or more fatty acyl chain linked to an alcohol functional group (typically glycerol or derivative) via an ester bond. They can be transesterified to form fatty acid methyl esters (FAMEs) that are the chemical basis of biodiesel. Neutral saponifiable lipids are better for the production of biodiesel than FFAs and polar saponifiable lipids such as phospholipids and glycolipids which are problematic for conventional base-catalysed transesterification (Dong et al., 2016a, Knothe, 2009). In addition, fatty acids with a lower degree of unsaturation result in a greater oxidation stability and cetane number (Callejón et al., 2014, Halim et al., 2012). Although unsaturated fatty acids can also be converted into fatty acid methyl esters (FAMEs), it has been observed that they reduce the thermal efficiency of the engines and emit more oxides of nitrogen

compared that of saturated fatty acids (Gopinath et al., 2010). It has further been found that the microalgal polar lipids tend to have a higher abundance of polyunsaturated fatty acids that can be nutritionally valuable but a poor feedstock for biodiesel. Therefore, when the production of biodiesel is considered, non-polar lipids, the TAGs are most preferred.

Triacylglycerides (TAGs) are located as droplets within microalgae cells, where they function as energy and carbon storage reservoirs (Olmstead et al., 2013a). Polar lipids on the other hand are mostly found as membrane lipids, which contribute to the structure and integrity of the cells. The TAGs in microalgae are in some respects similar to vegetable oils that are widely used in food applications, however, have their own specific fatty acid profile dependent on the species and growth conditions. In microalgae such as *Nannochloropsis*, the omega-3 long chain polyunsaturated fatty acids (ω-3 LC-PUFAs) which include docosahexaenoic acid (DHA) and eicosapentaenoic acid (EPA) are predominantly associated with the polar membrane lipids, rather than the TAG oils (Martin et al., 2014b, Simionato et al., 2013).

Pigments which have antioxidative properties that can protect the chemical integrity and nutritive value of the ω-3 LC-PUFAs during storage and processing in food applications are also observed in microalgae and can be coextracted with the lipids (Ryckebosch et al., 2013). As food ingredients, these pigments such as carotenoids (e.g. β-carotene, lutein and astaxanthin), chlorophylls, and phycobiliproteins (e.g. phycocyanin, phycoerythrin and allophycocyanin) can be used as food colourings and nutraceuticals, due to their colour and antioxidant, anti-carcinogenic and neuroprotective properties (Cuellar-Bermudez et al., 2015).

2.2.2. Proteins

Microalgae produce proteins to fulfil the full functional and structural requirements of the cells. As such, the available proteins are a highly diverse collection of thousands of different proteins. This contrasts greatly with many protein sources used in food applications, such as wheat, soy or milk, which contain a limited number of storage proteins. In the limited nutritional studies performed to date, microalgae proteins have shown equal or sometimes even superior quality compared to other plant proteins and have not shown any short or long term negative effects on toxicological tests done so far including human studies (Becker, 2007). Therefore, studies on using microalgae as a protein supplement are of increasing interest. Microalgae proteins are also used as fish feed in the aquaculture industry for which the costs of feed contributes 40-70% of the costs associated with the aquaculture production (Garcia Gonzalez et al., 2018). Thus, microalgal proteins can be used as an alternative for fish meal for different fish species, particularly is EPA and DHA are included in the algal lipids (Garcia Gonzalez et al., 2018).

Apart from using microalgae as whole-cell proteins, protein concentrates, isolates or hydrolysates can be produced from microalgae (Soto-Sierra et al., 2018). These microalgal proteins are mostly intracellular, residing freely in the cytosol and organelle interiors, or associated with cell walls and cell membranes, and therefore require cell rupture in order to be accessible (Safi et al., 2014, Yatipanthalawa and Martin, 2021). Following cell rupture cytosolic proteins will be released into

the medium, whereas the cell and membrane bound proteins would need specific protein extraction techniques such as extraction under alkaline conditions to improve their solubility (Parimi et al., 2015).

Furthermore, microalgal proteins have been observed to have good emulsifying properties. Ursu et al. (2014) observed that the emulsions made using proteins extracted from *Chlorella vulgaris*, were at least 10% more stable than those made using commercial emulsifiers. In addition, protein hydrolysates of different microalgae species have been observed to have antioxidant and anti-aging activities (Medina et al., 2015, Norzagaray-Valenzuela et al., 2017). Protein hydrolysis involves the enzymatic breakdown of proteins into peptides, which will be a topic of the research presented in Chapter 3. The formation of free radicals in the body can lead to cancer, cardiovascular diseases and others, which can be minimised by consuming compounds with antioxidant properties (Norzagaray-Valenzuela et al., 2017). Proteins and protein hydrolysates have been observed to inherit antioxidant properties depending on their amino acid composition, structure and hydrophobicity (Medina et al., 2015). In the study of Medina et al. (2015), a protein hydrolysate obtained from *Nannochloropsis sp.* was shown to have good antioxidant properties. The protein hydrolysate showed an EC_{50} equal to 26 mg Trolox Equivalents/ml (where EC_{50} corresponds to the effective concentration required to quench 50% of the initial radicals). This is 28 times greater than that for the protein extract before hydrolysis and 89 times greater than that of microalgal biomass. The protein hydrolysate was not shown to have any emulsification capacity, possibly due to the presence of smaller peptides that have a lower ability to form interfacial films covering the lipid droplets due to the presence of high amounts of polar groups (Medina et al., 2015). Thus, the nutritional and functional properties of the proteins not only depends on the species and the growth conditions of the microalgae, but also the treatment conditions used to extract and isolate these proteins from the cells.

Microalgae have also been identified as capable of recombinant protein production due to them being genetically accessible (Chiong et al., 2017). They can be expressed from the nuclear, chloroplast and mitochondrial genomes as they can be genetically transformed to produce various transgenic proteins (Chiong et al., 2017).

2.2.3. Polysaccharides

Polysaccharides in microalgae are mostly either storage polysaccharides or structural carbohydrates that make up the cell walls and the overall structure of the cells (Bernaerts et al., 2019a). Storage carbohydrates are located in the intercellular compartments, as explained in section 2.1, typically as starch or laminarin granules that serve as sugar reserves (Scholz et al., 2014). Along with the proteins, starch granules can be released from the interior of the microalgae cells once the cells are ruptured.

In comparison, structural carbohydrates are compositional components of the cell wall, forming a large part of the cell debris upon rupture. Extracellular polysaccharides, cell wall bound polysaccharides and cell wall polysaccharides are observed across many microalgae species. The

cell walls of most microalgae are composed of polysaccharides and are covered by a layer of external polymers, known as extracellular polymeric substances or exopolysaccharides (EPS) (Bernaerts et al., 2019a). The EPS content varies among the species and the growth conditions, and typically includes a considerable carbohydrate component (Henderson et al., 2008c, Baroni et al., 2020). Section 2.7 examines microalgal extracellular polymeric substances in more detail.

Cell wall polysaccharides often include heteropolysaccharides with a substantial amount of uronic acids and sulphate groups (Bernaerts et al., 2018b). These polysaccharides have the ability to act as functional food material, as gelling agents, thickeners and even as antioxidants (Bernaerts et al., 2019a, Zhang et al., 2010). Furthermore, these polysaccharides or carbohydrates are studied as an alternative source for fermentative processes, to produce bioethanol (Lupatini et al., 2017).

Bernaerts et al. (2018b) found the cell wall polysaccharides represented around 10% of the cellular composition in the microalgae species *P. cruentum, C. vulgaris, O. aurita, D. lutheri, A. platensis* and *T. chuii* and around 5% in microalgae species *P. tricornutum, Nannochloropsis sp., Schizochytrium sp.* and *T. lutea*, and these were sulphated to different extents. Some microalgal polysaccharides have considerable amounts of uronic acids and sulphate groups which provide them with anionic characteristics. Therefore, they can display various bioactive properties such as antiviral, anti-inflammatory and antioxidant properties (de Jesus Raposo et al., 2014, Bernaerts et al., 2018b).

Chrysolaminarin or β (1,3) glucan is the storage polysaccharide in various diatom species, where the length of the backbone chain and the degree of ramnification varies between species. These polysaccharides are currently marketed for their bioactivity, including immuno-stimulatory, anti-tumour and wound-healing activities (Gügi et al., 2015).

2.3. Cell rupture

The outer cell wall protects and holds the macroscopic structure of the cell together and limits the accessibility to the internal components. Within this, the cell membrane is physically weak compared to the cell wall but relatively impermeable, helping to contain intracellular molecules. If the cell wall and membrane have been ruptured, the cytoplasm and its contents will be accessible. The latter holds all the organelles and thus the proteins, lipids and other high value components inside. Upon cell rupture, periplasmic enzymes, proteins and lipids will be readily released into the medium, whereas the release of components inside cell organelles will be dependent on the breakage of those organelles and the relative binding of the compounds to the organelles (Harrison, 1991). Although the solubility of the components depends on the hydrophobicity and whether they are bound to the membranes, cell rupture will increase the accessibility of these compounds for subsequent extraction steps.

Cell rupture can also improve the bioavailability of microalgal cell components, even if they are not extracted (Bernaerts et al., 2020). For instance, it has been shown that the proteins and lipids inside intact *Nannochloropsis* sp. cells are not accessed by the mammalian digestive enzymes, whereas cell rupture increased the accessibility (Cavonius et al., 2016).

The presence of lipids, proteins, polysaccharides and cell debris from ruptured microalgae can also affect the overall functional properties of the slurry (Law et al., 2018). Many cellular components are surface active and can enhance emulsion stability (Law et al., 2018), suggesting that rupturing the cell can improve the functional properties of microalgae for some food applications apart from their nutritional value.

Moreover, the overall rheological properties of the microalgal slurry can be altered due to cell rupture. Bernaerts et al. (2017) have found that the rheological or the flow properties of microalgal slurries are significantly altered during mechanical and thermal processing. The release of intercellular components into the slurry medium increases the slurry viscosity and therefore would have an effect on downstream processing (Yao et al., 2018b).

However, wet storage of ruptured biomass can increase the FFA content compared with that of intact cells due to the release of lipolytic enzymes, which is disadvantageous for food applications (Balduyck et al., 2017). Thus, it may be preferable to deactivate the lipolytic enzymes for instance using a mild heat treatment (Balduyck et al., 2019b). Further, lipid stability has been found to be higher in foods formulated with the inclusion of intact or disrupted *Nannochloropsis* biomass than with extracted oils (Gheysen et al., 2019).

The following section is aimed at giving a broader understanding on the different cell disruption techniques that are widely studied in the literature. Section 2.3.1 focus on physical cell disruption methods, whereas sections 2.3.2 and 2.3.3 will focus on review literature on chemical and biological treatments used for microalgal cell disruption or permeabilization. The selection of the cell disruption method needs to be made considering the feasibility for process scale-up, energy requirements and the efficiency of the particular method for a given species.

2.3.1. Physical disruption

Cell rupture or breaking the cell walls through an external physical force is referred to as physical cell disruption. These include mechanical methods that promote cell rupture through shear forces such as high-pressure homogenization and bead milling, methods that transfer energy through waves such as ultrasonication and microwave irradiation, electromagnetic fields such as pulsed electric field and heat such as different thermal treatment methods. A few of the more commonly used physical disruption methods will be discussed in detail in the next section.

2.3.1.1. Ultrasonication

The action of sound waves, leads to the formation of gas or vapor bubbles which then grow and collapse releasing a large shock wave of high pressure, converting the sonic energy to mechanical energy (Leong et al., 2011). This shock wave will result in an intense shear action that can cause the cells to rupture.

There are two dominant types of sonication device, namely horn and bath. Horn type sonicators are more efficient than baths for cell rupture, as they can produce much more intensely focussed cavitational areas (Liu et al., 2013). An optimum volumetric energy density is observed, above

which cell rupture is reduced due to the excessive cavitation interactions between cavitating bubbles, reducing the energy translated into shear forces that can rupture the cells (Keris-Sen et al., 2014). Beyond cavitation effects, ultrasonication can produce radiation forces and acoustic streaming, however their contribution towards algae cell disruption at large scale is quite small (Kurokawa et al., 2016).

While ultrasonication is not energy-efficient if applied to dilute slurries, it can be used for the disruption of microalgae cells even at high solid concentrations (Yao et al., 2018b). However, the effect of ultrasound attenuates as the viscosity of the slurry increases significantly at increasing solids concentrations, meaning it may not be sufficiently energy efficient for the rupture of microalgae with tough cell walls (Yao et al., 2018b). Ultrasonic rupture of microalgal cells will depend on the acoustic power, ultrasonic frequency, time and the cell concentration.

Apart from using ultrasound to rupture the cells, ultrasonic assisted extraction has been used to accelerate the mass transfer of the components of interest such as lipids and pigments to the solvent phase (Li et al., 2019). Partial denaturation of proteins has been observed during ultrasonication whereas it has been suggested that ultrasonication itself does not hydrolyse the lipids (Li et al., 2019, Yao et al., 2018b). Ultrasonic processing units can be used at industrial scale and can be operated in a continuous mode however not as efficiently as high-pressure homogenisation.

2.3.1.2. High Pressure Homogenisation

High-pressure homogenisation (HPH) has been widely used for the disruption of microalgae cells where it has been found to be efficient for a wide range of species (Spiden et al., 2013b, Yap et al., 2014). This is considered to be an industrially scalable and energy-efficient method of rupture specifically for microalgae with strong cell walls (Yap et al., 2015). The rupture efficiency of a microalgae slurry during HPH depends solely on the homogeniser pressure and the species used, thus, high solid concentrations can be used to minimise energy consumption (Yap et al., 2015).

The robustness of microalgae in relation to mechanical rupture by HPH varies considerably across different species (Spiden et al., 2013b). In particular, some industrially relevant microalgae species such as *Nannochloropsis* and *Chlorella* have strong cell walls which require the use of several passes at 100 MPa pressure, whereas algae with larger, weaker cells like *Tetraselmis* are susceptible to cell rupture at much lower pressures (Spiden et al., 2013b). It has been shown that the strong cell walls of *Nannochloropsis* sp. can be weakened by incubating the cells, thereby reducing the required HPH pressure and energy demands (Olmstead et al., 2013c). Ultra-high-pressure homogenisation (UHPH) at 250 MPa can effectively rupture *Nannochloropsis* cells, which reduces the number of passes required to achieve a specific cell disruption (Bernaerts et al., 2019b). However, formation of aggregates of the released intracellular material due to extensive heating has been observed at ultra-high pressures, representing possible degradation of the heat sensitive components (Bernaerts et al., 2019b).

Apart from the advantages observed for homogenization, several disadvantages of using HPH for cell disruption have also been identified. The release of compartmentalised lipases as a result of

the loss of cell integrity during cell disruption has resulted in the formation of FFAs (Balduyck et al., 2018). Furthermore, HPH results in non-selective intracellular compound release and can generate fine cell debris which may not be suitable for the isolation of fragile functional compounds (Günerken et al., 2015). The potential impact of this on downstream extraction processes and the quality of microalgae lipid products needs to be considered for food applications.

It has also been noted that acid and thermal pre-treatment for *Chlorella sp*. and *Navicula sp.* significantly hindered the subsequent cell rupture using high pressure homogenisation (Spiden et al., 2015). Therefore, the choice of cell rupture techniques needs to be selected appropriately.

2.3.1.3. Pulsed electric field

The use of pulsed electric fields (PEF) is a novel method for permeabilising microalgae cells, rather than completely rupturing them. As such, PEF allows targeted release of the free proteins, whereas more efficient cell disruption techniques such as HPH result in the release of organelle related and structural proteins (Buchmann et al., 2019). The technique involves using short, high voltage pulses that induce the formation of pores in the cell membranes, also termed as electroporation. When placed in a pulsed electric field, an additional transmembrane voltage (membrane potential across the cell membrane) is induced which if high enough makes the cell permeable to relatively larger molecules (Frey et al., 2017).

This technology has been used to permeabilise the cells of freshwater microalgae such as *Chlorella vulgaris* (Buchmann et al., 2019) and cyanobacteria (*Arthrospira*) (Buchmann et al., 2018), enabling the release of soluble proteins. Continuous extraction of proteins from viable microalgae cell cultures of freshwater *Chlorella vulgaris* using PEF has also been achieved (Buchmann et al., 2019). This allows the reuse of the microalgal cells, due to them not being extensively damaged. Selective release of proteins from a cell wall mutant of *Chlamydomonas reinhardtii* was obtained using PEF treatment which permeabilised the microalgae cells instead of completely fragmenting them (‘t Lam et al., 2017). However, the presence of a rigid cell wall can adversely affect the release of intracellular proteins using PEF, with comparatively high amounts of carbohydrates and small ionic solutes released instead (Postma et al., 2016). Incubation of microalgae cells after PEF treatment has been shown to improve subsequent protein and lipid extraction efficiencies (Silve et al., 2018). One limitation of PEF is that the energy consumption is impractically high if the conductivity is too high. This limits its application to microalgae in low-salinity media.

2.3.1.4. Bead Milling

Bead milling can be used to disrupt microalgae species via shear forces creating by colliding beads. It uses glass or silicon beads that are loaded into a drum and rotated resulting in the milling of microalgae fed into the chamber and can be operated in both batch and continuous modes. Over 97% disintegration of *Chlorella vulgaris* has been achieved by bead milling at biomass concentrations varying from 2.5% - 14.5% (w/w) (Postma et al., 2015), with the rupture efficiency observed to be independent of the cell concentration (Postma et al., 2015). The process was mild being able to retain the native structure of the protein, Rubisco (Postma et al., 2017). The efficiency

of this process will depend on the bead type, microalgae species, bead filling ratio and the flow rate of the suspension (Postma et al., 2017). Unfortunately, although potentially effective at disrupting microalgae, the method is highly energy intensive and therefore likely not viable for biofuel applications (Doucha and Lívanský, 2008).

2.3.2. Chemical cell rupture

Dilute acid hydrolysis is a thermochemical process used to release fermentable sugars from lignocellulosic biomass via acid-catalysed hydrolysis. This method has also been applied to microalgae biomass at temperatures between 120-170 °C to break apart the cells and depolymerise the polysaccharides (Dong et al., 2016c). However, as these temperatures will denature proteins and likely cause some chemical degradation, for instance via the Maillard reaction (van Boekel, 2001), this method may not be suitable for the extraction of food additives and nutraceuticals.

Treating heterotrophic *Chlorella* cells with sulphuric acid at a concentration of 0.5 M at 120 °C for 1h been shown to effectively overcome cell wall recalcitrance and enable a lipid yield of 44% following biphasic lipid extraction using the solvent dichloromethane (Zhang et al., 2018). However, use of such concentrated acid and high temperatures is not likely to be economically viable and will degrade any valuable algae components. Alkaline treatment has also been able to weaken the interaction of biopolymers in the cell wall cleaving some recalcitrant linkages (Wu et al., 2017). Further increasing protein yields requires accessing the membrane- and wall-bound protein fraction. Alkaline conditions have shown to be improve the solubility of microalgal proteins, although the functional properties of the proteins can also be altered (Gerde et al., 2013, Parimi et al., 2015).

2.3.3. Biological cell rupture

Biological processes for the degradation of cell walls of microalgae are attractive due to the high energy costs associated with mechanical cell disruption methods. Autolysis and enzymatic hydrolysis are two established methods for breaking down microbial biomass (Middelberg, 1995, Demuez et al., 2015a) and producing food extracts, for example from yeast and microalgae (Mitsuda and Shikanai, 1959). Microalgae cell walls mainly consist of polysaccharides and glycoproteins (Scholz et al., 2014), which can be broken down by selective enzymes under mild reaction conditions. For example, enzymes have been found effective in degrading the cell walls of *Nannochloropsis sp*. (Wu et al., 2017) and *Chlamydomonas reinhardtii* (Sierra et al., 2017) resulting in higher lipid yields.

As enzymes can be expensive and their recovery and reuse difficult (Sierra et al., 2017), autolysis is an alternative approach that utilises the native hydrolytic enzymes of a cell to degrade itself (Demuez et al., 2015a, Kightlinger et al., 2014, Middelberg, 1995). Autolysis can be induced at low cost, simply by incubating the cells at elevated temperatures (e.g., 30-50 ºC) (Halim et al., 2019a, Halim et al., 2016a, Kightlinger et al., 2014, Middelberg, 1995). This method has minimal energy and equipment requirements and could therefore be beneficially incorporated into industrial scale microalgal biorefineries. The use of in-situ enzymes generated under stress conditions that

degrade cell wall material can be used both to weaken the cells prior to mechanical cell rupture (Halim et al., 2016a), or for cell permeabilization (Sierra et al., 2017). However, the effect of autolysis on proteins, lipids and polysaccharides of interest needs to be further explored, since it is likely that the autolytic enzymes will also break down these biomolecules (e.g., via proteolysis or lipolysis). This is a key research questions that will be addressed in Chapter 3 of the thesis and is reviewed in depth in Section 2.4. Further, the response to stress conditions will vary between different microalgae species, suggesting the requirement of species-specific techniques for autolysis.

2.4. Dark anoxic incubation as a means to weaken microalgal cell walls

As discussed in Section 2.3, biological processes such as enzyme hydrolysis and autolysis can be used to weaken the strong cell walls of microalgae. Of particular relevance to this thesis, dark anoxic incubation has been found to weaken the cell walls of *Nannochloropsis* sp. by inducing cell autolysis (Halim et al., 2019a, Halim et al., 2019b).

2.4.1. Current understanding of the effect of dark anoxic incubation on microalgae

In nature, microalgae photosynthesise during the day and meet cellular energy demands via respiration at night, using O_2 as an electron acceptor. However, in the absence of oxygen, which can sometimes occur in the environment, microalgae must have the necessary enzymes to produce Adenosine triphosphate (ATP) via fermentative pathways to generate cellular energy needed for survival. Some microalgae are known to have the necessary pathways to survive dark anoxic conditions for limited periods (Yu et al., 2011), with dark anoxia having been seen to activate fermentative pathways in *Chlamydomonas reinhardtii* (Mus et al., 2007).

In the marine microalga *Nannochloropsis* sp., it was found that subjecting concentrated slurries of cells to incubation at moderate temperatures (35-40 °C) increased their susceptibility to mechanical cell rupture by HPH (Olmstead et al., 2013b). In the subsequent work of Halim et al. (2016b), the conditions of incubation were defined as dark anoxia, which were proposed to weaken the otherwise strong cell walls of *Nannochloropsis* sp. Although the exact mechanism was not confirmed, it was found that the cellulosic layer of the cell walls was thinned during the prolonged incubation, which could explain the increased susceptibility of the cells to mechanical rupture (Halim et al., 2019a). Figure 2.1 presents a simple schematic overview of the dark anoxic incubation process on the microalgae *Nannochloropsis* sp. and its identified mechanism as detailed in Halim et al. (2019a).

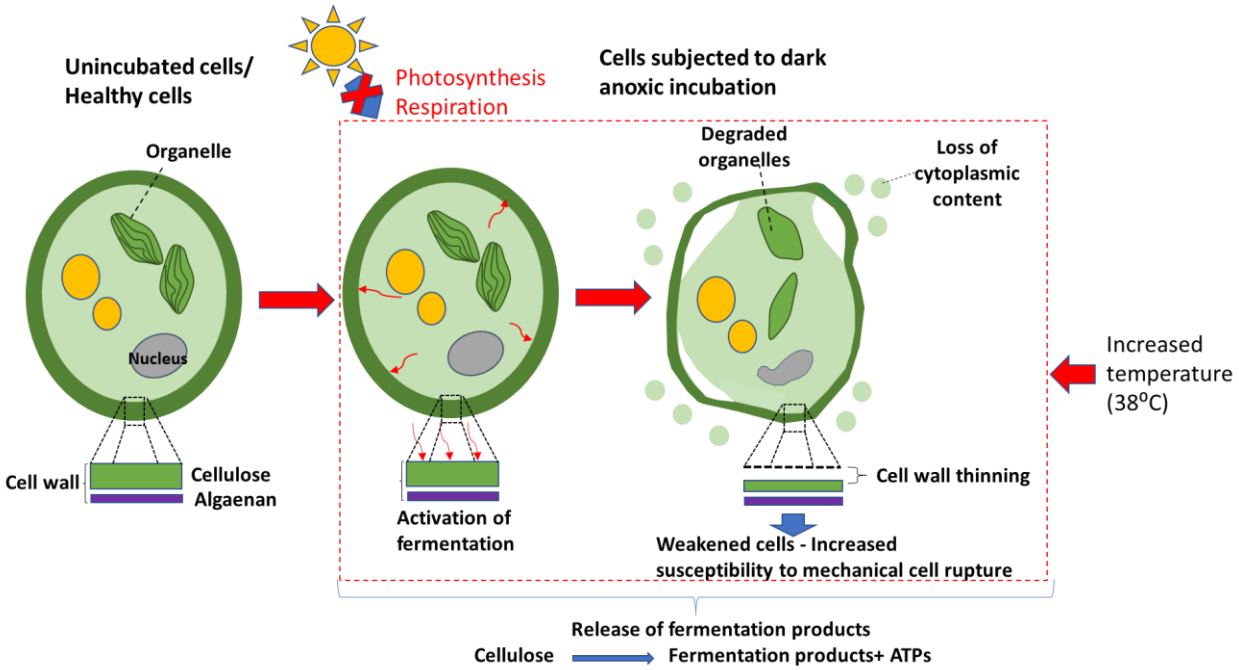

Figure 2.1: Schematic representation of the process of dark anoxia incubation on *Nannochloropsis* sp. and its observed effects. Image adapted from Halim et al. (2019a).

During dark anoxia incubation, *Nannochloropsis* sp., cells were found to produce organic acids including succinic acid, malic acid, lactic acid, fumaric acid, oxalic acid, acetic acid and propionic acid. These were identified as fermentation end products, which were presumed to be produced as an active response to the dark anoxic stress conditions, and could be linked to the consumption of intercellular carbohydrate reserves including the cellulosic layer of the cell walls (Halim et al., 2019a). Similarly, organic acids have been seen to be produced during dark anaerobic conditions by other eukaryotic algae such as *Euglena gracilis* (Tomita et al., 2016), *Selenastrum minutum* (Vanlerberghe et al., 1990), *Chlamydomonas reinhardtii* (Mus et al., 2007). However, in these other microalgae species the organic acids were derived from consumption of plastidic starch rather than the cell wall polysaccharides apparently utilised by *Nannochloropsis* (Mus et al., 2007).

2.4.2. Effect of heat and dark anoxic conditions on algal proteins and lipids

2.4.2.1. Proteins

Proteins are critical to cellular metabolism (i.e. enzymes) and structure. The entirety of proteins in a microalgae cell (i.e. it's proteome) is dynamic, changing according to the cellular growth phase and the environmental conditions. As microalgal proteins are a potential product for applications such as food, the profile of proteins is important. Individually, proteins are complex biochemicals, with dynamic and hierarchical 3-dimenstional structures. In cells, proteins adopt native conformations which confer the required functions, however these structures can be disrupted by physical (e.g. temperature) or chemical forces.

The environmental stresses caused by dark anoxic incubation can be expected to change the protein profile (proteome) of the cells as they respond metabolically. This could include changes in the profile of enzymes associated with basic metabolism as well as stress-specific responses. In particular, the elevated temperatures represent a heat stress that could increase the rate of cellular metabolism and lead to the consumption of proteins for maintaining cellular respiration. In eukaryotic cells protein degradation can happen via the ubiquitin-proteasome pathway or through the autophagy lysosomal system (Sha et al., 2018). The proteasome is a protease complex that carries out selective hydrolysis/degradation of proteins, collaborating with the ubiquitin enzymes that act as markers for regulated proteolysis in eukaryotic cells (Tanaka, 2009). This degradation of proteins through the proteasome requires metabolic energy. During degradation, proteins are broken down into smaller peptides and amino acids. The induction of several proteases under abiotic stress conditions have previously been observed in microalgae (Segovia et al., 2003, Segovia and Berges, 2009). For example, under prolonged darkness, the eukaryote *Dunaliella tertiolecta* showed an increased induction of cell death associated proteases or caspases, and activated apoptotic like cell death (Segovia et al., 2003). Heat stress on eukaryotic microalgae *Chlorella saccharophila* has also led to an increase of apoptotic like cell death, which was significantly reduced following the inhibition of caspase like enzymes (Zuppini et al., 2007).

Importantly, such proteases can cleave the peptide bonds in extracellular matrix proteins (Demuez et al., 2015a) leading to cellular degradation and autolysis. It is possible that such protease activity could contribute to the observed cellular degradation and weakening in *Nannochloropsis* sp. during dark anoxia incubation (Halim et al., 2019a). While protease activity could be beneficial in terms of improving cell rupture, it could have a negative impact on the quality of the proteins and other nutritional components in microalgae (Balduyck et al., 2017). Protein hydrolysis destroys native functionality and results in the formation of peptides that can affect the sensory and nutritional qualities in food applications (Liu et al., 2019). Peptides typically confer bitterness and have altered biophysical functionality (Medina et al., 2015), with some peptides possessing specific and favourable bioactivities (Medina et al., 2015).

It was previously found that the total protein content (based on total elemental nitrogen measurement) in *Nannochloropsis* sp. did not change over the period of dark anoxic incubation (Halim et al., 2019a). However, the effect of dark anoxic incubation on both the profile and integrity of the proteins requires further investigation.

2.4.2.2. Lipids

As discussed in Section 2.2.1, microalgae possess a range of lipids that have potential for various applications. Similar to proteins, the biochemical integrity of lipids in critical to their value, in particular hydrolysis of saponifiable lipids can be detrimental, resulting in problematic free fatty acids and promoting lipid oxidation. Lipid hydrolysis is catalysed by lipases, which are natively present in microalgae cells and used for different cellular purposes. These include releasing the carbon and energy stored in TAG for growth, remodelling membrane lipid composition to enhance cell functioning, and generating signalling molecules (Kong et al., 2018). The use of lipids to

producing carbon and energy for growth involves fatty acid beta oxidation which requires the presence of oxygen in the system. Therefore, during anoxic conditions, it is not possible for microalgae to utilise this pathway. Accordingly, the total lipid content *Nannochloropsis* sp. was found to remain unchanged during dark anoxic incubation confirming that lipids were not oxidising for energy (Halim et al., 2019a).

Beyond the total amount of lipids, potential changes in the quality of the lipids during dark anoxic incubation must be considered. Wet storage of microalgae slurries can be considered as a prolonged, cold form of dark anoxic incubation. Under such conditions, microalgae *T. Isochrysis* and *Nannochloropsis* sp. have showed an increase in the FFA content suggesting lipolytic activity (Balduyck et al., 2016, Balduyck et al., 2017). Lipolytic stability was seen to be dependent on the cells' integrity, where *Nannochloropsis* sp. with stronger cell walls were able to maintain lipid stability for a longer period of time (Balduyck et al., 2017) than *T. Isochrysis*. Similar observations were made in *Tetraselmis sueica* where cell viability was lost along with an increase of FFAs during long-term wet storage at low temperature, while the overall fatty acid profile remained unchanged (Montaini et al., 1995). It has yet to be investigated whether formation of FFA occurs during dark anoxic incubation of *Nannochloropsis* sp. when used to weaken cell walls.

Such lipid hydrolysis and the resultant increase in FFA is not preferred for biodiesel production (as discussed in Section 2.2.1) and in food applications due to the rancidity or off-flavour generation (Balduyck et al., 2015). Moreover, such FFAs are known to be readily oxidised by lipoxygenase enzymes (Balduyck et al., 2017). Lipid peroxidation also has detrimental effects on the lipid quality, negatively impacting the flavour and nutritional profile, and causing bleaching when considering food applications (Gordon, 2001), and forming deposits that interfere with biodiesel production systems (Singer and Rühe, 2014).

2.4.3. Proteomics to predict biological processes

Post-genomic, systems biology approaches are being increasingly used to understand how microorganisms respond and adapt to changes in their physical environment (Guarnieri et al., 2011). Among these, proteomics, or the study of the proteome in an organism, has gained special attention as a method of analysing different metabolic responses. Proteins in cells carry out almost all the work, in particular the enzymes that catalyse biochemical reactions, as well as other proteins that maintain the structure, function and regulation of the cells (Sinitcyn et al., 2018). Therefore, analysing the changes in the proteome under different stress or treatment conditions can reveal the physiological responses of these organisms (Tran et al., 2016). With the advancement in technology, these complex proteomes can be analysed and studied comprehensively using mass spectrometry based technologies (Sinitcyn et al., 2018). For proteomic analyses, the quantitation of the individual proteins is done through labelling or label-free approaches. However, considering the vast diversity of microalgal proteomes and the requirements for time consuming optimisations and specific mass spectrometry acquisition methods for labelling approaches, label-free techniques are preferred (Fabre et al., 2014). Several label-free MS-based relative quantification techniques have therefore been introduced and are widely used in proteomics and the iBAQ or the intensity

based absolute quantification technique is found to give reliable and reproducible results (Arike et al., 2012).

As the use of proteomic analysis requires knowledge of the whole proteome of the organism of interest, it is typically limited to species that are widely studied and whose proteomes and genomes have been characterised/sequenced. For example, microalgae genera such as *Chlamydomonas* and *Nannochloropsis* are very commonly studied which contain sequenced genomes and proteomes. Although limited, proteomic analyses are currently being increasingly used in microalgae, to predict the cellular responses and mechanisms during nitrogen deprivation (Tran et al., 2016), effect of dark stresses on lipid biosynthesis (Bai et al., 2016), responses to low CO_2 conditions (Wei et al., 2019) and have been successful in revealing the underlying mechanisms. Bai et al. (2016) used proteomic analysis to investigate the effect of dark stress on lipid biosynthesis in the diatom *Phaeodactylum tricornutum*, revealing the induction of glycolysis and synthesis of fatty acids in the dark. Analysing the differently expressed proteins in the proteome following the treatment revealed the responses and the affected pathways. Similarly, Tran et al. (2016) carried out a detailed proteomic analysis on *Nannochloropsis occulata* to describe the mechanism that regulates carbon partitioning during nitrogen deprivation. Thus, these proteomics studies could reveal the underlying cellular responses of microalgae cells to different external physiological conditions such as dark anoxic incubation.

2.4.4. Research gaps in the knowledge on dark anoxia incubation

As discussed, dark anoxic incubation of *Nannochloropsis* sp. presents a low-cost scalable technology to weaken the strong cell walls and to improve cell rupture by cell wall thinning (Halim et al., 2019a, Halim et al., 2016a, Olmstead et al., 2013c). The total protein and lipid content were not affected significantly during the process (Halim et al., 2019a). However, as reviewed above, in other microalgae species, such stress conditions have induced metabolic changes, lipid and protein degradation, and cell death. There is currently little understanding of how the stress conditions of dark anoxia affect the overall protein profile and biochemical integrity of proteins and lipids in *Nannochloropsis*, which is important in the context of recovering high-value products.

In addition, marine microalgae such as *Nannochloropsis* can experience periods of dark anoxic conditions in its natural habitats. Previous studies on the well-characterised microalga *Chlamydomonas*, have revealed the adoption of glycolytic, fermentative pathways to generate the energy needed to survive in these conditions (Mus et al., 2007, Grossman et al., 2011). However, while fermentation end-products have been in *Nannochloropsis* (Halim et al., 2019a) an in-depth analysis on the biochemical pathways that the *Nannochloropsis* sp. cells undertake to cope with these dark anoxic conditions are yet to be elucidated. This knowledge is needed to enable optimisation of the dark anoxic incubation process and to allow a better understanding of how they acclimate to such environments in natural systems.

2.5. Lipid extraction from microalgae

2.5.1. Dry versus wet lipid extraction

A lipid extraction method should be highly selective towards the group of targeted lipids, as discussed in detail in section 2.2.1. There are two broad strategies for the extraction of lipids from microalgae: extraction from dried biomass or from wet biomass. Lipids can be extracted from dried biomass using organic solvents (Mahmood et al., 2017, Jiménez Callejón et al., 2020) or supercritical CO_2 (Halim et al., 2011). Non-polar solvents such as hexane can also be used to directly extract TAGs from dried algal biomass (Dos Santos et al., 2015), which when blended with polar solvents like ethanol, can also recover the polar membrane lipids. Alternative to adding a blend of polar and non-polar solvents, such pairs of solvents can be added sequentially. For instance, a recent study initially used hexane to extract the neutral lipids from dried algae biomass, and then extracted the polar lipids in a second extraction using ethanol (Jiménez Callejón et al., 2020). This method requires two extraction and solvent separation steps but has the benefit of producing two distinct lipid streams.

Extracting lipids from wet algal biomass is more technically challenging than from dried biomass, however wet lipid extraction may be preferred due to the high energy cost associated with obtaining a dried biomass (Cooney et al., 2011b, Dong et al., 2016b). Therefore, the discussion will mainly focus on lipid extraction from wet microalgae systems. The presence of water during the solvent extraction process makes it more complicated than extraction from dry biomass (Kim et al., 2013). In addition to the cell wall, the water itself presents a barrier between the extractant and the lipids.

Lipid extraction from wet algae biomass can be performed using organic solvents (Jiménez Callejón et al., 2014, Olmstead et al., 2013c) or so-called switchable solvents whose polarity can be changed to facilitate recovery (Du et al., 2013, Samorì et al., 2013). Both monophasic and biphasic systems can be used (Yap et al., 2014). Monophasic systems involve organic solvents that are miscible with water and often comprise of polar and non-polar solvent mixtures. As water-miscible solvents, they are able to penetrate whole algae cells and can recover both polar and non-polar lipids (Yap et al., 2014). As a result, monophasic solvent systems are often used as total lipid extraction methods for analytical purposes and for the recovery of high-value polar lipids containing long-chain omega-3 fatty acids (Ryckebosch et al., 2013). Biphasic systems on the other hand involve organic solvents that are immiscible with water, which results in two distinct phases. Here the organic solvent forms an emulsion with the wet algal slurry and requires the cells to be ruptured in order to extract the lipids (Yap et al., 2014), as the nonpolar solvent droplets cannot penetrate the cell walls (Yap et al., 2014). Mixing or emulsification is one parameter to consider during biphasic lipid extraction. The non-polar solvent needs to be properly emulsified or mixed to create sufficient interfacial area for the direct contact between the solvent and the lipid droplets. Figure 2.2 gives a graphical overview of lipid extraction in monophasic and biphasic systems. In addition to extracting the lipids into the solvent, efficient separation of the lipid-rich

solvent from the delipidated biomass is important. Following this, the solvent must be recovered from the lipid to be recycled. During lipid extraction from dried biomass, the lipid-rich solvent can be easily recovered using physical separation methods such as centrifugation. Wet lipid extraction also relies on physically recovering the lipid-rich solvent from the biomass, which can be a significant challenge due to the stability of the emulsion formed during extraction. The solvent phase forms stable emulsions in the ruptured algae slurry, which can make centrifugal separation of the lipid rich solvent phase problematic (Law et al., 2017b). It has been shown that strong emulsifying properties of the ruptured algae cells can limit the separation process, by acting as a barrier to coalescence of the droplets (Law et al., 2017b).

The lipid rich solvent layer, once separated, can be evaporated and recycled. Importantly, complete recovery of water-miscible solvents used in monophasic extraction systems cannot be achieved solely by physical methods, and requires energy-intensive distillation. This is needed to separate the water-miscible solvents used in monophasic systems out of the aqueous phase, meaning energy is required to vaporise the water, obviating the energetic benefit of avoiding drying the biomass.

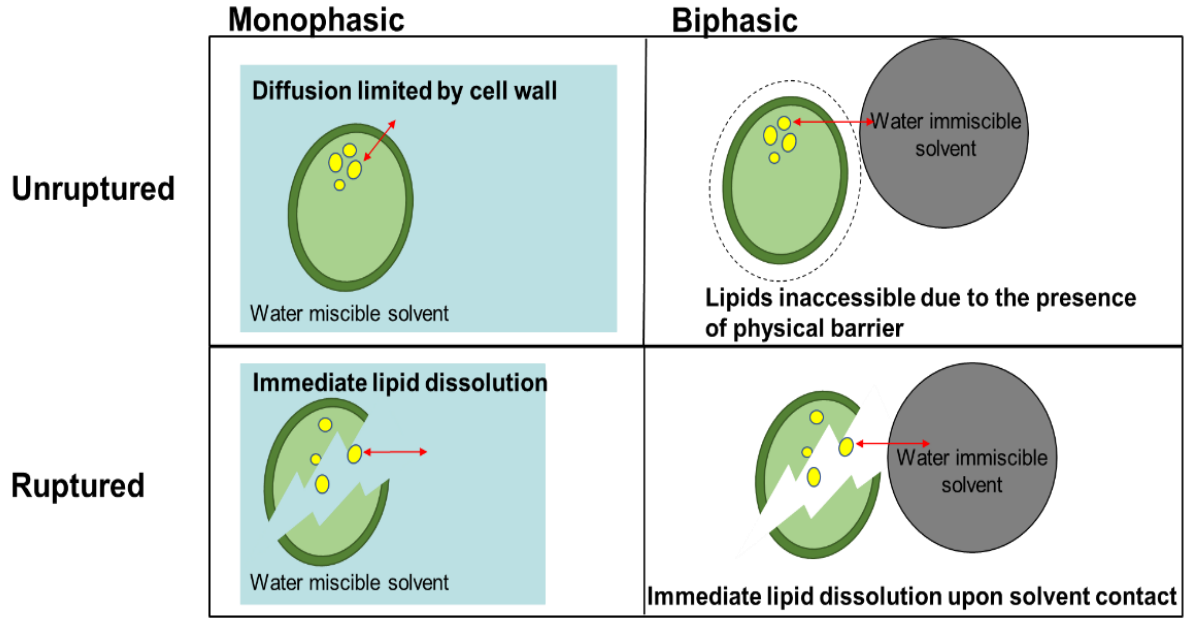

Figure 2.2: Schematic summary of monophasic and biphasic lipid extraction (figure adapted and recreated from (Yap et al., 2014)).

Therefore, the use of biphasic systems is preferred over monophasic systems from an energy perspective due to the avoidance of distillation of the solvent. However, it is important to note that since biphasic systems preferentially extract the neutral lipids, they may not effectively extract the polar lipid-associated PUFAs (Olmstead et al., 2013a), which may or may not be desirable.

2.5.2. Need for biphasic lipid extraction

As discussed, wet algal biomass is preferred in the processing of microalgae since drying of algae consumes around 90% of the total energy cost. The presence of polar lipids can strongly influence the quality and the processing of the product in biodiesel production, thus they are not preferred in producing biodiesel (Kröger and Müller-Langer, 2012). It is also known that the polar lipids and FFAs interfere with the transesterification process (Dong et al., 2016a).

Microalgal TAGs are nonpolar lipids that can be used as food oils or as precursors for biodiesel production. Based on the 'like dissolve like' principle, non-polar lipids will favourably dissolve in a non-polar solvent, whereas polar lipids will not be extracted that easily (Dong et al., 2016a). Hence, non-polar water immiscible solvents are preferred for TAG extraction from wet algal biomass (Dong et al., 2016a). For an industrial scale operation, the selected solvent should also be inexpensive, volatile, free from toxic or reactive impurities and be able to form a two phase system with water for the easy separation and selective recovery of the neutral saponifiable lipids (Kröger and Müller-Langer, 2012).

A preliminary cell disruption step for intracellular compound release has found to be important in controlling biphasic lipid extraction efficiency (Angles et al., 2017, Yap et al., 2014). A key requirement for energy efficiency during wet lipid extraction is to maximise the concentration of the slurry and to reduce the content of solvent used in relation to the amount of TAG recovered (Martin, 2016b).

2.5.3. Mechanisms of lipid extraction

In general, wet lipid extraction from algal biomass can happen via two main mechanisms. For monophasic systems, solvent can diffuse through unruptured cell walls and dissolve the lipids, thereby producing a concentration gradient that can drive the diffusion of lipids out of the cells. In comparison, biphasic systems require direct contact between the immiscible solvent droplets and the lipid droplets, which can then coalesce. In this case, prior cell lysis is essential to effective biphasic lipid extraction, as previously demonstrated for microalgae species including *Chlamydomonas reinhardtii* (Bensalem et al., 2018), *Chlorella vulgaris* (Yap et al., 2014).

One exception is *Botryococcus braunii* Frenz et al. (1989), which produces hydrocarbons that can be extracted after a short contact with hexane, without impacting the cells. The mechanism by which the hydrocarbons are extracted without cell rupture from these cells has been studied but is not completely clear. *Botrycoccus braunii* have previously been identified to have the ability to transport lipid globules from the cytoplasm to the space in between the cell membrane and the cell wall through exocytosis (Zhang et al., 2011). Adding tetradecane to the algae growth medium increased the permeability of the cell membrane, further increasing this extraction of the lipid bodies to the space in between the cell wall and membrane. The lipid droplets could then be extracted to the solvent phase as a result of the looser cell walls structure in the presence of tetradecane (Zhang et al., 2011). Similar observations have been made for the unicellular microalga *Dunaliella salina* in the presence of dodecane (Hejazi et al., 2004). *Dunaliella salina*

lacks a rigid cell wall, and direct contact between the cells and the organic solvent was seen to be not necessary, rather the presence of the organic solvent accelerated the exocytosis process (Hejazi et al.). Dodecane was taken up by the cells, which induced morphological changes in the cells and led to more active diffusion and transport at the cell membrane. resulting in β-carotene rich lipid globules being excreted out through exocytosis. This scenario was identified as the cells "milking" out the β-carotene in the presence of biocompatible organic solvents, without affecting viability (Hejazi et al., 2004).

Lipid extraction using liquefied dimethyl ether (DME) without any prior cell rupture from wet microalgal biomass of the diatom *Chaetoceros gracilis* and coccolithophore *Pleurochrysis carterae* has been able to achieve similar extraction efficiencies as that of monophasic extractions (Kanda et al., 2020). Liquified DME is a supercritical fluid (that is above its critical temperature and pressure) that has a medium polarity and is partially miscible in water. Lipid extraction using liquified DME from wet microalgae is therefore similar to a monophasic system, but avoids the tedious separation requirements (Eckert et al., 2004). The cell wall of microalgae was not affected by the liquefied DME extraction, however the very costly requirement of pressurised systems to liquefy the gas undermines the other advantages seen in this system (Kanda et al., 2020).

The nature of the cell wall of the microalgae species is seen to play a major role when it comes to lipid extraction, and their susceptibility to organic solvents (Miazek et al., 2017). The current understanding of biphasic extraction is that cells that contain rigid cell walls need to be ruptured in order to access the lipid droplets located inside the cell walls. However, as pointed out, nonpolar solvents have been found to be capable of extracting intracellular lipids from some microalgae that lack encapsulating cell walls have been found without prior cell rupture. Diatoms, which are another type of microalgae having a high lipid content, have not been properly investigated to date in terms of the underlying mechanism of biphasic lipid extraction. Given their differences in the cell wall structure, this is the topic of investigation in Chapters 4 and 5 of this thesis. The following section aims at giving a broad understanding of the cell structure of diatoms in the context of lipid extraction.

2.6. Diatoms as feedstock for microalgal biorefineries

2.6.1. An overview of diatom cell structure

Bacillariophyceae or more commonly, diatoms, are a broad group of microalgae distinguished by the presence of a siliceous cell wall comprised of so-called frustules. This characteristic differentiates this class from all other microalgae species. As highly abundant marine phytoplankton, they are the main contributors to global oxygen production. Traditionally, diatoms have been divided into two main groups, namely pennate diatoms, being bilaterally symmetrical, and centric diatoms that are radially symmetrical (Shnyukova and Zolotariova, 2015). The siliceous frustules make two overlapping valves, that are linked together by girdle bands that encircle the cell. Almqvist et al. (2001) have found that the hardness of the diatom's shell was similar to that of known silicas. However, it has been observed that this varies with the region of interest. Certain localized regions of the shell have shown high elasticities and hardness.

Some diatoms release adhesive biopolymers through the raphe, which is a slit in the surface of the silica frustule, in order to interact with the substratum (Arce et al., 2004). The EPS of these diatoms are said to serve numerous functions including motility, sessile adhesion, colony formation, habitat stabilization and anti-desiccation (Hoagland et al., 1993). The EPS excreted through the raphe hydrates and swells upon release into the medium and therefore pushes the cell forward with respect to the substrate (Stal and Défarge, 2005). This mucilaginous EPS layer also protects the cells from sudden environmental changes by forming an envelope around them (Shnyukova and Zolotariova, 2015). A comprehensive review of the functions, chemistry, fine structure and physiology of diatom EPS can be found in Hoagland et al. (1993).

The EPS associated with benthic diatoms are comprised of polysaccharides, proteins and glycoproteins (Underwood and Paterson, 2003). However, the specific composition of these is highly dependent on the species, physiological state of the cells and the environmental conditions (Underwood and Paterson, 2003). Diatomaceous EPS have been seen in many forms such as apical pads, tubes, cell coatings, fibrils, stalks and adhering films. Therefore, the morphology of these EPS material can vary dramatically, ranging from rigid fibril like structures to highly hydrated mucilaginous capsules, that are loosely or tightly bound or even integrated into the cell wall (Gügi et al., 2015, Hoagland et al., 1993, Underwood and Paterson, 2003).

The diatom frustule consists of three successive layers (Gügi et al., 2015). These include i) the diatotepum (the inner most organic layer that is in direct contact with the plasma membrane), ii) silicified shell or frustule, and iii) the cell wall bound EPS (an external organic coating that is trapped in secreted mucilage) (Tesson and Hildebrand, 2013). In addition to the EPS layer, the frustules may be further bound by an external organic membrane of which the composition varies based on the species. This external organic membrane is highly water insoluble and reported to mainly consist of polysaccharides that are tightly bound to the frustule (Tesson and Hildebrand, 2013).

2.6.2. Applications of diatoms

As highly abundant marine organisms, diatoms are said to be responsible for 40% of total global primary production in marine systems (Underwood and Paterson, 2003). When comparing with other microalgae species, apart from the cell ultrastructure, their high growth rates and the dependence of the growth on the presence of silicates in the medium are the key differences (Wang and Seibert, 2017, Coombs et al., 1967). Importantly for biotechnological applications and the topic of this thesis, some oleaginous diatoms can hyperaccumulate TAG, to reach total lipid contents up to 40 – 60% of the biomass. In addition, some species can synthesize high-value omega 3 LC-PUFAs, including EPA and DHA (Sayanova et al., 2017). Diatoms that have been recognised for potential lipid production include *Phaeodactylum tricornutum* (Branco-Vieira et al., 2017), *Amphora exigua* (Chen, 2012), *Cylindrotheca sp*. (Chen, 2012, Suman et al., 2012), *Thalassiosira pseudonana* (Meksiarun et al., 2015) and *Navicula sp*. (Bielsa et al., 2016, Nurachman et al., 2012). An extensive report of twelve marine diatoms, investigating their growth and total lipid content, found the diatom *Amphora exigua* to have the highest lipid content of the studied diatoms, reaching

up to around 45% of the dry biomass (Chen, 2012). The pennate benthic diatom *Cylindrotheca*, sp. could also accumulate considerable amounts of lipids (18-27%), containing comparatively high amounts of PUFAs (around 40% total lipids) following adjustments in the culture medium (Suman et al., 2012). The fatty acid composition of the marine diatom *Phaeodactylum tricornutum* was found to be suitable with respect to the international biodiesel standards, showing potential as a raw material for biodiesel production (Branco-Vieira et al., 2017).

Amongst many studied diatoms, *Navicula cincta* has been identified as a suitable feedstock for biodiesel production due to its high growth rates, ability to grow under low light irradiation, and its propensity to store a high content of TAGs with fatty acids favoured for biodiesel production (Bielsa et al., 2016, Sayanova et al., 2017). In addition, it has a characteristically high EPS content, which can be used as a potential valuable by-product (Bielsa et al., 2016).

Diatoms can be favoured over other algae or cyanobacteria in various water and wastewater applications. Nualgi is a patented product which contains a silicon rich micronutrient tablet formula that can induce diatom domination in wastewater, which in turn photosynthesize and produce oxygen, providing a suitable environment for aerobic bacteria (Thothathri, 2009). This product has been used commercially due to several factors, including the ability of diatoms to photosynthesise at a higher rate compared with other microalgae species and cyanobacteria, therefore producing oxygen, while consuming extra nitrogen and phosphorous in wastewater systems at a higher rate, and providing a healthy food for zooplankton and fish in water systems.

Diatom frustules are studied and used for different applications including enzyme immobilization, separation of heavy metals, selective protein adsorption and drug delivery as a result of their highly organised porous structures, chemical inertness, biocompatibility and due to them being approved as a food grade material by the US Food and Drug Administration (FDA) (Lim et al., 2015).

2.6.3. Lipid extraction from diatoms

The current understanding of biphasic extraction is that cells that contain rigid cell walls need to be ruptured in order to access the lipid droplets located inside the cell walls. However, as pointed out in Section 2.5.3, nonpolar solvents have been found to be capable of extracting intracellular lipids from some microalgae that lack encapsulating cell walls without prior cell rupture, including the diatom *Diadesmis confervaceae* which has the ability to excrete lipids out from the cells (Vinayak et al., 2014). As described in Section 2.6.1, diatoms possess unique cell walls that would generally be expected to be a barrier for biphasic lipid extraction. Various studies have investigated the extraction of lipids from diatoms before and after cell disruption. Lorente et al. (2015) explored biphasic lipid extraction using hexane before and after cell rupture from the diatom *P. tricornutum*, with cell rupture increasing lipid extraction efficiency by about 10 fold. Svenning et al. (2020) studied lipid extraction from the diatom *Porosira glacialis* using different solvent systems (both monophasic and biphasic) and cell rupturing techniques to explore the lipid extractability. Interestingly, cell disruption did not have a significant impact on the lipid extractability in a monophasic system while ultrasound assisted mixing showed a slight improvement in the biphasic

lipid extraction system. This was observed for the diatom *O. aurita* as well (Svenning et al., 2020). While these studies provide some useful knowledge, they do not provide a complete understanding of the underlying mechanism of biphasic lipid extraction from diatoms. Given the unique cell wall structure of diatoms, it is not clear whether there could be mechanistic differences in biphasic lipid extraction compared with other microalgae species with cellulosic cell walls. This is the topic of investigation in Chapters 4 and 5 of this thesis.

2.6.4. Research gaps in biphasic lipid extraction from diatoms

As discussed, the completely different cell wall structure observed in diatoms could result in mechanistic differences in lipid extraction. The surface characteristics of the diatom cell walls and the associated EPS are novel considerations in producing a better understanding of their interactions with the nonpolar solvents used for biphasic lipid extraction.

It has previously been observed that *Navicula* cells are released more easily from hydrophilic surfaces as compared to hydrophobic surfaces, suggesting the importance of looking at cell surface interactions (Krishnan et al., 2006). Further to this, Klein et al. (2014) observed that the diatom *Navicula jeffreyi* show a moderately hydrophobic character and their attachment densities were higher on hydrophobic surfaces compared with hydrophilic surfaces. Similar observations were made by Finlay et al. (2002) for the diatom *Amphora*. Therefore, there is need to explore the underlying mechanism of biphasic lipid extraction from diatoms, considering the surface chemistry of the system, which will affect the interactions between the cells and biphasic solvent droplets. *Navicula* sp. has been widely used as a model pennate diatom to study for example the underwater locomotion strategy of pennate diatoms (Wang et al., 2013, Chen et al., 2019), the protein adsorption ability of diatom frustules (Lim et al., 2015), and the dependence of the growth of marine diatoms on different forms of particulate silica (Penna et al., 2003).

2.7. Microalgal EPS

Already briefly covered in section 2.6.1, EPS are also referred in the literature as extracellular organic matter (EOM) (Baroni et al., 2020) or algogenic organic matter (AOM) (Pivokonsky et al., 2016). The following section will cover the existing knowledge of microalgal EPS, its extraction and applications.

2.7.1. Nature and composition of EPS

Microalgal cells produce and release various EPSs into their living environment, to produce a hydrated biofilm matrix (Xiao and Zheng, 2016). These EPS are known to comprise of proteins, neutral and charged polysaccharides (which can comprise up to 80-90% of the EPS material), nucleic acids, lipids and small molecules (Henderson et al., 2008b). However, the nature and composition of microalgal EPS can vary dramatically based on the algal species, culture conditions age of the culture, growth phase and external factors such as nutrient status (Baroni et al., 2020, Stal and Défarge, 2005).

Diatoms are considered to be the most abundant group of EPS producing microalgae that excrete large quantities of organic carbon into their growth environment (Xiao and Zheng, 2016). Thus,

they contribute greatly as a source of organic matter for the planktonic and benthic inhabitants (Shnyukova and Zolotariova, 2015). Diatom EPS is comprised of sulphated heteropolysaccharides consisting of 6-9 different monosaccharides [131]. They also have considerable amounts of uronic acids, resulting in higher anionic components, which are hypothesised to play important roles in sediment binding and stabilisation [140].

These microalgal polymeric substances or EPS maintain a stable matrix structure and form 3D polymer networks. The cells mediate their adhesion to surfaces and interact with each other as a result (Xiao and Zheng, 2016). Their various functions include transport and transformation of organic matter, biogeochemical cycling of elements, and complexation of dissolved metals (Xiao and Zheng, 2016). Studies on the nature of EPS from four different algae species (*Chlorella vulgaris*, *Microcystis aeruginosa*, *Asterionella formsa* and *Melosira* sp.) have found them predominantly hydrophilic (Henderson et al., 2008b), comprising of hydrophilic polysaccharides and hydrophobic proteins. It has also been observed when the EPS comprise of large molecular weight proteins (>500kDa), they tend to associate to form larger "gel-like" substances as a result of their hydrophobicity. The hydrophilic fraction of EPS decreases when going from exponential phase growth to stationary phase growth in the diatoms studied (*Asterionella formsa* and *Melosira* sp.), although the predominant fraction was still hydrophilic (Henderson et al., 2008b). This further supports the idea that EPS is dependent on the growth state of the algae.

2.7.2. Uses of EPS as functional polysaccharides

EPS from microorganisms such as bacteria and yeast have been widely studied and sometimes used commercially as food hydrocolloids (Ikeda et al., 2019). Further to this, EPS extracted and isolated from microalgae species have also shown high intrinsic viscosities compared to commercially used hydrocolloids, showing promise as thickening and gelling agents in the food industry (Bernaerts et al., 2018a).

Microalgal EPS have also been found to have several bioactivities including anti-inflammatory, antiadhesive, antivirus and antioxidant properties(Parra-Riofrío et al., 2020). A very comprehensive review on diatom EPS can be found in Xiao and Zheng (2016). The presence of a high uronic acid content in some microalgal EPS, is hypothesised to play an important role in sediment binding and stabilisation (Staats et al., 1999). These are reported to have high adhesive properties which are found to be mainly determined by the groups with negative charges such as uronic acids and sulphated sugars (Staats et al., 1999).

EPS has been used in wastewater treatment, following its ability to successfully adsorb heavy metal ions (Ajao et al., 2020). The presence of functional groups such as (–COO-, –NH2, OH) and mainly the carboxyl and hydroxyl groups of uronic acids, neutral polysaccharides and proteins are assumed to be responsible for the ability to bind these metal ions. In addition, having many charges distributed on the long polymeric chains along with the resulting electrostatic repulsions, are likely to keep the polymer in an uncoiled state, providing binding sites for adsorption that are accessible. These properties of EPS, (high molecular weight and high charge density) have made them

effective heavy metal adsorbents (Ajao et al., 2019). Naveed et al. (2019) presents a comprehensive review on the interactions of microalgal EPS with metals.

Most interestingly Guil-Guerrero et al. (2004) have observed defatted diatoms, *Porphyridium cruentum* and *Phaeodactylum tricornutum*, to have exceptional functional properties for food application, such as water absorption capacity, emulsification capacity and oil absorption capacity compared with soybean flour, as a result of the high percentage of exopolysaccharides.

The exceptional functional properties expressed by these EPS, in particular their ability to form gels, could be used as active thickeners or texturizing agents (Pierre et al., 2019). Moreover, there is increasing attention on the microalgal EPS as bio-lubricants.

2.7.3. Techniques for EPS removal/disintegration

Despite the promising applications for algal EPS, extracting these EPS efficiently remains a challenge. EPS removal and disintegration from activated sludge and bacterial cultures has been studied widely. Similar techniques are being explored for microalgal systems as well. EPS which is dissolved in the culture medium can be easily extracted using centrifugation or ultrafiltration (Delattre et al., 2016). However, the concentrations of EPS readily dissolved in the medium are relatively low, therefore the loosely or tightly bound EPS need to be extracted using other treatment methods. Different physical and chemical treatment methods have been investigated for EPS disintegration and extraction from microalgal cells. However, an effective EPS extraction method should have a high extraction efficiency, while minimising cell rupture, in order to avoid the release of intracellular impurities (Lv et al., 2019, Takahashi et al., 2009).

Physical treatments include ultrasonication, the use of a cation exchange resin (CER), high speed centrifugation and heating, whereas chemical treatments include using different buffer solutions, which dissolve the EPS from the cells. There have been efforts to extract EPS using different combinations of these methods. However physical treatments have generally produced higher EPS yields. For instance, CER and heat treatment extracted more EPS from the microalgae *Neocystis mucosa* compared with EDTA, acidic treatment or alkaline treatment (Lv et al., 2019). Takahashi et al. (2010) explored six methods for EPS extraction from the diatom *Navicula jeffreyi*, and optimized EPS extraction with respect to minimizing cell rupture. CER (Dowex) has been found to outperform chemical methods such as “artificial seawater of half salinity” and extractions after pre-treatment with glutaraldehyde using water, Dowex water and Dowex buffer in extracting the EPS while minimising cell rupture (Takahashi et al., 2009). The extracted carbohydrate/polysaccharide content was highest when warm water was used as the buffer. However, the extracted amounts of EPS were still too low to be used commercially. Warm water extraction at 30 °C for 1 h has been used to extract EPS from diatom cells (Staats et al., 1999), however the efficacy is contested (Chiovitti et al., 2004). Chiovitti et al. (2004) raised an argument that the extraction compromises the cell wall integrity and hence extracts intracellular chrysolaminarin. Among these different methods CER has been found to give the best extraction

yields, without leading to cellular lysis (Delattre et al., 2016). Nevertheless, in a commercial scale the applicability of this method remains questionable.

Ultrasonication on the other hand has been widely used for EPS extraction from sludge and other microorganisms (Han et al., 2013), with the ultrasound power applied found to affect the EPS extraction yield. However, ultrasound can also be used to rupture microalgae (Yao et al., 2018a), so its application for EPS removal while minimising cell rupture needs to be carefully considered.

2.7.4. Effects of EPS removal on the processability of algal slurries

The presence of AOM or EPS can have several effects on the overall properties of the algal slurries. Considering upstream processing, EPS can affect the coagulation and flotation properties of the algae cells. EPS can affect coagulation of the cells by sterically interference, to prevent agglomeration. The presence of these components may also result in the fouling of membranes during upstream or downstream processing of microalgae. The hydrophobicity of these components is said to determine the ability of them to foul membranes as well as their ability to be removed by coagulation and adsorption onto activated carbon. Hydrophilic, high molecular weight components have found to be the main membrane foulants, whereas high MW ones have seen to be more amenable to coagulation (Henderson et al., 2008b).

The presence of EPS has found to significantly affect various physicochemical properties of algae aggregates including the viscosity, surface charge, flocculation, and settling properties (Xiao and Zheng, 2016). Proteins present in EPS that are capable of capturing and making complexes with coagulants have been identified, which increases the coagulant requirement; further showing the implications associated with the presence of EPS on upstream processing (Takaara et al., 2004, Henderson et al., 2010). On the other hand, the physiochemical characteristics of the EPS present will also have an effect on their behaviour during downstream processing (Gonzalez-Torres et al., 2019). Rao et al. (2020) observed that the presence of three serine-based and two threonine-based proteins detected in *M. aeruginosa* interacted with the carbohydrates and cells in the presence of coagulants by forming numerous localised networks, therefore maintaining a low coagulant requirement. In addition, the presence of EPS has been seen to have a positive effect on the floc size during coagulation (Filipenska et al., 2019, Rao et al., 2020), enhancing the cell separation due to the carbohydrates and proteins bridging with cells and forming supra-structures in the presence of flocculants (Rao et al., 2021).

Ultrasonication has previously been observed to destroy sludge flocs and cell walls, thus improving the sedimentation and dewatering performance by reducing the viscosity and boundary layer effect of the sludge particles (Xu et al., 2019).

The rheological characteristics of microalgal suspensions also depend on the microalgal species and culture conditions (Bernaerts et al., 2017). The presence of EPS affects should affect the rheological properties of the microalgal suspensions, by effecting cell interactions and hydrodynamics. Thermal or mechanical processing of the slurries can alter their rheological properties (Bernaerts et al., 2017, Yap et al., 2016a).

2.7.5. Current research gaps in microalgal EPS recovery and downstream processing

As discussed above, although the presence of microalgal EPS seems likely to affect the overall processability of microalgae slurries, to date there have been no direct investigations into the effect of microalgal EPS removal on downstream processing parameters. Such an approach seems promising, as similar studies on wastewater sludge systems have yielded favourable and improved processability with respect to the viscosity and dewaterability (Ruiz-Hernando et al., 2013). Therefore, it is worthwhile looking at the link between EPS removal and downstream processing parameters such as the slurry rheology and the dewaterability of microalgal suspensions, which will in turn improve the processability of microalgae for the production of food and fuel-based products.

2.8. Knowledge gaps to be addressed in this thesis

As reviewed above, microalgae based food and fuel production depends on the selection of a suitable strain choice of microalgae, in conjunction with the most appropriate upstream and downstream processing. This thesis comprises three experimental chapters, aimed at developing a better mechanistic understanding of key aspect so downstream processing of microalgae. The basis for the three experimental chapters is briefly summarised here.

Chapter 3: Effect of dark anoxia incubation in *Nannochloropsis* sp.

The first experimental chapter of the thesis (Chapter 3) was based on a previously identified scalable, low cost, low solvent method for aiding the extraction of lipids from the microalgae *Nannochloropsis sp*. – dark anoxic incubation (Halim et al., 2016a, Halim et al., 2019a, Olmstead et al., 2013c). Dark anoxic incubation has been found to weaken *Nannochloropsis* sp. cells through cell wall thinning (Halim et al., 2019a). This facilitates subsequent mechanical rupture by improving the energy efficiency and the cost effectiveness (Olmstead et al., 2013c). Beyond its effectiveness, there is currently limited understanding of the underlying mechanism leading to the cell wall weakening and the effect of dark anoxic incubation on the biomacromolecules.

Other microalgae species such as *Chlamydomonas* are understood to switch from photosynthesis to glycolytic and fermentative pathways under dark anoxic conditions for energy production and to maintain the redox state of the cells (Mus et al., 2007, Catalanotti et al., 2013a). The lowered energy production rates and the stress conditions under dark anoxic conditions have different effects on the protein and lipid fractions in plant cells leading to changes in the protein profile and also degradation of lipids through hydrolysis and lipid peroxidation. However, these processes and effects have yet to be identified in *Nannochloropsis*. Gaining this knowledge could help explain the underlying mechanism for the cell wall thinning, membrane degradation and eventual cell autolysis, and facilitate process optimisation and translation to other species.

Chapter 3 addresses this research gap by studying the effects of incubation on the biomacromolecules including protein and lipids as a function of incubation time. The underlying biochemical pathways are investigated through studying the protein profiles of the cells using

proteomics, and identifying the changes caused in the protein profile as a result of dark anoxia incubation.

Chapter 4: Biphasic lipid extraction from the diatom *Navicula* sp.

As pointed out in the above sections, biphasic lipid extraction is preferred over wet extraction due to the increased energy efficiency and the cost effectiveness of the process. As discussed, the suitability of diatoms as a source of algal oil for biodiesel production or food applications, in combination with their distinctive cell structure, give rise to the importance of studying biphasic lipid extraction from this group of microalgae. Further to this, mixing or the application of shear is necessary in a biphasic lipid extraction system. However, the role of shear is not fully understood in relation to the kinetics of biphasic lipid extraction from algae with different cell wall structures, such as diatoms. The pennate diatom *Navicula* sp. is recognised as a viable feedstock for biodiesel production and has been quite widely researched (Spiden et al., 2015, Bielsa et al., 2016). As such, it was selected as a model diatom for study in this thesis, to better understand how to design effective processes for recovering products for food and fuel applications from this class of microalgae.

Chapter 4 probes the feasibility of biphasic lipid extraction from slurries of the model diatom, *Navicula* sp. by investigating the underlying mechanics of biphasic lipid extraction in relation to diatom cell structure and the application of shear. This chapter aims at gaining a fundamental understanding of biphasic lipid extraction from diatoms that can be applied to the design of effective lipid recovery processes.

Chapter 5: Ultrasound-assisted EPS removal from the diatom *Navicula* sp. and its effect on downstream processing parameters

EPS, rich in polysaccharides are another important product produced by microalgae. As reviewed in Section 2.7, the potential application of microalgal EPS as functional polysaccharides makes them of interest for extraction and use as a by/co- product of lipid and protein production. Diatoms such as *Navicula* sp. have been found to produce high amounts of EPS, however their extraction and separation are scantily studied as reviewed in Section 2.7.3. Moreover, the presence of EPS in slurries can affect the processability of the algal suspensions as reviewed in Section 2.7.4, and there is still little understanding of these effects in general.

Following the findings in Chapter 4, Chapter 5 investigates the application of power ultrasound for the removal of EPS as a potential co-product, with the aim of maximising EPS extraction while minimising the cell rupture. Following EPS removal, the processability of the slurries are studied specifically looking at the dewaterability, rheology and biphasic lipid extraction. This chapter therefore aims to develop a fundamental understanding of EPS removal from the diatoms such as *Navicula* and its effect on the downstream processing parameters leading to the extraction of lipids.

2.9. References

'T LAM, G. P., VAN DER KOLK, J. A., CHORDIA, A., VERMUË, M. H., OLIVIERI, G., EPPINK, M. H. & WIJFFELS, R. H. 2017. Mild and selective protein release of cell wall deficient microalgae with pulsed electric field. *ACS sustainable chemistry & engineering,* 5**,** 6046-6053.

AHMED, F., LI, Y., FANNING, K., NETZEL, M. & SCHENK, P. M. 2015. Effect of drying, storage temperature and air exposure on astaxanthin stability from Haematococcus pluvialis. *Food Research International,* 74**,** 231-236.

AJAO, V., MILLAH, S., GAGLIANO, M. C., BRUNING, H., RIJNAARTS, H. & TEMMINK, H. 2019. Valorization of glycerol/ethanol-rich wastewater to bioflocculants: recovery, properties, and performance. *Journal of hazardous materials,* 375**,** 273-280.

AJAO, V., NAM, K., CHATZOPOULOS, P., SPRUIJT, E., BRUNING, H., RIJNAARTS, H. & TEMMINK, H. 2020. Regeneration and reuse of microbial extracellular polymers immobilised on a bed column for heavy metal recovery. *Water research,* 171**,** 115472.

ALAM, M. A., WAN, C., GUO, S.-L., ZHAO, X.-Q., HUANG, Z.-Y., YANG, Y.-L., CHANG, J.-S. & BAI, F.-W. 2014. Characterization of the flocculating agent from the spontaneously flocculating microalga Chlorella vulgaris JSC-7. *Journal of bioscience and bioengineering,* 118**,** 29-33.

ALBERTS, B., JOHNSON, A., LEWIS, J., MORGAN, D., RAFF, M., ROBERTS, K., WALTER, P., WILSON, J. & HUNT, T. 2017. *Molecular biology of the cell*, WW Norton & Company.

ALBERTS, B., JOHNSON, A., LEWIS, J., RAFF, M., ROBERTS, K. & WALTER, P. 2002a. Chloroplasts and photosynthesis. *Molecular Biology of the Cell. 4th edition.* Garland Science.

ALBERTS, B., JOHNSON, A., LEWIS, J., RAFF, M., ROBERTS, K. & WALTER, P. 2002b. The endoplasmic reticulum. *Molecular Biology of the Cell. 4th edition.* Garland Science.

ALMQVIST, N., DELAMO, Y., SMITH, B., THOMSON, N., BARTHOLDSON, Å., LAL, R., BRZEZINSKI, M. & HANSMA, P. 2001. Micromechanical and structural properties of a pennate diatom investigated by atomic force microscopy. *Journal of microscopy,* 202**,** 518-532.

ANGLES, E., JAOUEN, P., PRUVOST, J. & MARCHAL, L. 2017. Wet lipid extraction from the microalga *Nannochloropsis* sp.: Disruption, physiological effects and solvent screening. *Algal Research,* 21**,** 27-34.

ARCE, F. T., AVCI, R., BEECH, I. B., COOKSEY, K. E. & WIGGLESWORTH-COOKSEY, B. 2004. A live bioprobe for studying diatom-surface interactions. *Biophysical journal,* 87**,** 4284-4297.

ARIKE, L., VALGEPEA, K., PEIL, L., NAHKU, R., ADAMBERG, K. & VILU, R. 2012. Comparison and applications of label-free absolute proteome quantification methods on Escherichia coli. *Journal of proteomics,* 75**,** 5437-5448.

BAI, X., SONG, H., LAVOIE, M., ZHU, K., SU, Y., YE, H., CHEN, S., FU, Z. & QIAN, H. 2016. Proteomic analyses bring new insights into the effect of a dark stress on lipid biosynthesis in Phaeodactylum tricornutum. *Scientific reports,* 6**,** 1-10.

BALASUBRAMANIAN, R. K., DOAN, T. T. Y. & OBBARD, J. P. 2013. Factors affecting cellular lipid extraction from marine microalgae. *Chemical Engineering Journal,* 215**,** 929-936.

BALDUYCK, L., BIJTTEBIER, S., BRUNEEL, C., JACOBS, G., VOORSPOELS, S., VAN DURME, J., MUYLAERT, K. & FOUBERT, I. 2016. Lipolysis in T-Isochrysis lutea during wet storage at different temperatures. *Algal research,* 18**,** 281-287.

BALDUYCK, L., BRUNEEL, C., GOIRIS, K., DEJONGHE, C. & FOUBERT, I. 2018. Influence of High Pressure Homogenization on Free Fatty Acid Formation in *Nannochloropsis* sp. *European Journal of Lipid Science and Technology,* 120.

BALDUYCK, L., DEJONGHE, C., FOUBERT, I. & VANDAMME, D. 2019a. Simultaneous harvesting and inhibition of lipolytic reactions in T-Isochrysis by FeCl3 flocculation.

BALDUYCK, L., DEJONGHE, C., GOOS, P., JOOKEN, E., MUYLAERT, K. & FOUBERT, I. 2019b. Inhibition of lipolytic reactions during wet storage of T-Isochrysis lutea biomass by heat treatment. *Algal research,* 38**,** 101388.

BALDUYCK, L., GOIRIS, K., BRUNEEL, C., MUYLAERT, K. & FOUBERT, I. 2015. Stability of Valuable Components during Wet and Dry Storage. *Handbook of Marine Microalgae.* Elsevier.

BALDUYCK, L., STOCK, T., BIJTTEBIER, S., BRUNEEL, C., JACOBS, G., VOORSPOELS, S., MUYLAERT, K. & FOUBERT, I. 2017. Integrity of the microalgal cell plays a major role in the lipolytic stability during wet storage. *Algal research,* 25**,** 516-524.

BARONI, E., CAO, B., WEBLEY, P. A., SCALES, P. J. & MARTIN, G. J. O. 2020. Nitrogen availability and the nature of extracellular organic matter of microalgae. *Industrial & Engineering Chemistry Research*.

BARROS, A. I., GONÇALVES, A. L., SIMÕES, M. & PIRES, J. C. 2015. Harvesting techniques applied to microalgae: a review. *Renewable and Sustainable Energy Reviews,* 41**,** 1489-1500.

BEACHAM, T. A., BRADLEY, C., WHITE, D. A., BOND, P. & ALI, S. T. 2014. Lipid productivity and cell wall ultrastructure of six strains of *Nannochloropsis*: implications for biofuel production and downstream processing. *Algal research,* 6**,** 64-69.

BECKER, E. 2007. Micro-algae as a source of protein. *Biotechnology advances,* 25**,** 207-210.

BENSALEM, S., LOPES, F., BODÉNÈS, P., PAREAU, D., FRANÇAIS, O. & LE PIOUFLE, B. 2018. Understanding the mechanisms of lipid extraction from microalga Chlamydomonas reinhardtii after electrical field solicitations and mechanical stress within a microfluidic device. *Bioresource technology,* 257**,** 129-136.

BERNAERTS, T. M., GHEYSEN, L., FOUBERT, I., HENDRICKX, M. E. & VAN LOEY, A. M. 2019a. The potential of microalgae and their biopolymers as structuring ingredients in food: A review. *Biotechnology advances***,** 107419.

BERNAERTS, T. M., KYOMUGASHO, C., VAN LOOVEREN, N., GHEYSEN, L., FOUBERT, I., HENDRICKX, M. E. & VAN LOEY, A. M. 2018a. Molecular and rheological characterization of different cell wall fractions of Porphyridium cruentum. *Carbohydrate polymers,* 195**,** 542-550.

BERNAERTS, T. M., PANOZZO, A., DOUMEN, V., FOUBERT, I., GHEYSEN, L., GOIRIS, K., MOLDENAERS, P., HENDRICKX, M. E. & VAN LOEY, A. M. 2017. Microalgal biomass as a (multi) functional ingredient in food products: Rheological properties of microalgal suspensions as affected by mechanical and thermal processing. *Algal research,* 25**,** 452-463.

BERNAERTS, T. M. M., GHEYSEN, L., FOUBERT, I., HENDRICKX, M. E. & VAN LOEY, A. M. 2019b. Evaluating microalgal cell disruption upon ultra high pressure homogenization. *Algal Research,* 42.

BERNAERTS, T. M. M., GHEYSEN, L., KYOMUGASHO, C., JAMSAZZADEH KERMANI, Z., VANDIONANT, S., FOUBERT, I., HENDRICKX, M. E. & VAN LOEY, A. M. 2018b. Comparison of microalgal biomasses as functional food ingredients: Focus on the composition of cell wall related polysaccharides. *Algal Research,* 32**,** 150-161.

BERNAERTS, T. M. M., VERSTREKEN, H., DEJONGHE, C., GHEYSEN, L., FOUBERT, I., GRAUWET, T. & VAN LOEY, A. M. 2020. Cell disruption of *Nannochloropsis* sp. improves in vitro bioaccessibility of carotenoids and ω3-LC-PUFA. *Journal of Functional Foods*.

BIELSA, G. B., POPOVICH, C. A., RODRÍGUEZ, M. C., MARTÍNEZ, A. M., MARTÍN, L. A., MATULEWICZ, M. C. & LEONARDI, P. I. 2016. Simultaneous production assessment of triacylglycerols for biodiesel and exopolysaccharides as valuable co-products in *Navicula* cincta. *Algal research,* 15**,** 120-128.

BRANCO-VIEIRA, M., SAN MARTIN, S., AGURTO, C., SANTOS, M. A., FREITAS, M. A. & CAETANO, N. S. 2017. Analyzing Phaeodactylum tricornutum lipid profile for biodiesel production. *Energy Procedia,* 136**,** 369-373.

BÜCHEL, C. 2020. Light harvesting complexes in chlorophyll c-containing algae. *Biochimica et Biophysica Acta (BBA)-Bioenergetics,* 1861**,** 148027.

BUCHMANN, L., BLOCH, R. & MATHYS, A. 2018. Comprehensive pulsed electric field (PEF) system analysis for microalgae processing. *Bioresource Technology,* 265**,** 268-274.

BUCHMANN, L., BRÄNDLE, I., HABERKORN, I., HIESTAND, M. & MATHYS, A. 2019. Pulsed electric field based cyclic protein extraction of microalgae towards closed-loop biorefinery concepts. *Bioresource Technology,* 291.

CALLEJÓN, M. J. J., MEDINA, A. R., SÁNCHEZ, M. D. M., PEÑA, E. H., CERDÁN, L. E., MORENO, P. A. G. & GRIMA, E. M. 2014. Extraction of saponifiable lipids from wet microalgal biomass for biodiesel production. *Bioresource technology,* 169**,** 198-205.

CATALANOTTI, C., YANG, W., POSEWITZ, M. C. & GROSSMAN, A. R. 2013. Fermentation metabolism and its evolution in algae. *Frontiers in plant science,* 4**,** 150.

CAVONIUS, L. R., ALBERS, E. & UNDELAND, I. 2016. In vitro bioaccessibility of proteins and lipids of pH-shift processed *Nannochloropsis* oculata microalga. *Food & function,* 7.

CHEN, C.-L., CHANG, J.-S. & LEE, D.-J. 2015. Dewatering and drying methods for microalgae. *Drying technology,* 33**,** 443-454.

CHEN, L., WENG, D., DU, C., WANG, J. & CAO, S. 2019. Contribution of frustules and mucilage trails to the mobility of diatom *Navicula* sp. *Scientific reports,* 9**,** 1-12.

CHEN, Y.-C. 2012. The biomass and total lipid content and composition of twelve species of marine diatoms cultured under various environments. *Food Chemistry,* 131**,** 211-219.

CHIONG, T., ACQUAH, C., LAU, S., KHOR, E. & DANQUAH, M. 2017. Microalgal-Based Protein By-Products: Extraction, Purification, and Applications. *Protein Byproducts.* Elsevier.

CHIOVITTI, A., MOLINO, P., CRAWFORD, S. A., TENG, R., SPURCK, T. & WETHERBEE, R. 2004. The glucans extracted with warm water from diatoms are mainly derived from intracellular chrysolaminaran and not extracellular polysaccharides. *European Journal of Phycology,* 39**,** 117-128.

COOMBS, J., DARLEY, W., HOLM-HANSEN, O. & VOLCANI, B. 1967. Studies on the biochemistry and fine structure of silica shell formation in diatoms. Chemical composition of *Navicula* pelliculosa during silicon-starvation synchrony. *Plant Physiology,* 42**,** 1601-1606.

COONEY, M. J., YOUNG, G. & PATE, R. 2011. Bio-oil from photosynthetic microalgae: Case study. *Bioresource Technology,* 102**,** 166-177.

CUELLAR-BERMUDEZ, S. P., AGUILAR-HERNANDEZ, I., CARDENAS-CHAVEZ, D. L., ORNELAS-SOTO, N., ROMERO-OGAWA, M. A. & PARRA-SALDIVAR, R. 2015. Extraction and purification of high-value metabolites from microalgae: essential lipids, astaxanthin and phycobiliproteins. *Microbial biotechnology,* 8**,** 190-209.

DE FARIAS NEVES, F., DEMARCO, M. & TRIBUZI, G. 2019. Drying and Quality of Microalgal Powders for Human Alimentation. *Microalgae-From Physiology to Application.* IntechOpen.

DE JESUS RAPOSO, M. F., DE MORAIS, A. & DE MORAIS, R. 2014. Bioactivity and applications of polysaccharides from marine microalgae. Springer: Cham, Switzerland.

DELATTRE, C., PIERRE, G., LAROCHE, C. & MICHAUD, P. 2016. Production, extraction and characterization of microalgal and cyanobacterial exopolysaccharides. *Biotechnology advances,* 34**,** 1159-1179.

DEMUEZ, M., MAHDY, A., TOMAS-PEJO, E., GONZALEZ-FERNANDEZ, C. & BALLESTEROS, M. 2015. Enzymatic cell disruption of microalgae biomass in biorefinery process. *Biotechnology and Bioengineering,* 112**,** 1955-1966.

DODGE, J. D. 2012. *The fine structure of algal cells*, Elsevier.

DONG, T., KNOSHAUG, E. P., PIENKOS, P. T. & LAURENS, L. M. 2016a. Lipid recovery from wet oleaginous microbial biomass for biofuel production: a critical review. *Applied energy,* 177**,** 879-895.

DONG, T., KNOSHAUG, E. P., PIENKOS, P. T. & LAURENS, L. M. L. 2016b. Lipid recovery from wet oleaginous microbial biomass for biofuel production: A critical review. *Applied Energy,* 177**,** 879-895.

DONG, T., VAN WYCHEN, S., NAGLE, N., PIENKOS, P. T. & LAURENS, L. M. L. 2016c. Impact of biochemical composition on susceptibility of algal biomass to acid-catalyzed pretreatment for sugar and lipid recovery. *Algal Research,* 18**,** 69-77.

DOS SANTOS, R. R., MOREIRA, D. M., KUNIGAMI, C. N., ARANDA, D. A. G. & TEIXEIRA, C. M. L. L. 2015. Comparison between several methods of total lipid extraction from Chlorella vulgaris biomass. *Ultrasonics Sonochemistry,* 22**,** 95-99.

DOUCHA, J. & LÍVANSKÝ, K. 2008. Influence of processing parameters on disintegration of Chlorella cells in various types of homogenizers. *Applied microbiology and biotechnology,* 81**,** 431-440.

DU, Y., SCHUUR, B., SAMORÌ, C., TAGLIAVINI, E. & BRILMAN, D. W. F. 2013. Secondary amines as switchable solvents for lipid extraction from non-broken microalgae. *Bioresource technology,* 149**,** 253-260.

ECKERT, C. A., LIOTTA, C. L., BUSH, D., BROWN, J. S. & HALLETT, J. P. 2004. Sustainable reactions in tunable solvents. *The Journal of Physical Chemistry B,* 108**,** 18108-18118.

FABRE, B., LAMBOUR, T., BOUYSSIÉ, D., MENNETEAU, T., MONSARRAT, B., BURLET-SCHILTZ, O. & BOUSQUET-DUBOUCH, M.-P. 2014. Comparison of label-free quantification methods for the determination of protein complexes subunits stoichiometry. *EuPA Open Proteomics,* 4**,** 82-86.

FILIPENSKA, M., VASATOVA, P., PIVOKONSKA, L., CERMAKOVA, L., GONZALEZ-TORRES, A., HENDERSON, R. K., NACERADSKA, J. & PIVOKONSKY, M. 2019. Influence of COM-peptides/proteins on the properties of flocs formed at different shear rates. *Journal of Environmental Sciences,* 80**,** 116-127.

FINLAY, J. A., CALLOW, M. E., ISTA, L. K., LOPEZ, G. P. & CALLOW, J. A. 2002. The influence of surface wettability on the adhesion strength of settled spores of the green alga Enteromorpha and the diatom Amphora. *Integrative and comparative biology,* 42**,** 1116-1122.

FRENZ, J., LARGEAU, C. & CASADEVALL, E. 1989. Hydrocarbon recovery by extraction with a biocompatible solvent from free and immobilized cultures of Botryococcus braunii. *Enzyme and microbial technology,* 11**,** 717-724.

FREY, W., GUSBETH, C., SAKUGAWA, T., SACK, M., MUELLER, G., SIGLER, J., VOROBIEV, E., LEBOVKA, N., ÁLVAREZ, I. & RASO, J. 2017. Environmental applications, food and biomass processing by pulsed electric fields. *Bioelectrics.* Springer.

GARCIA GONZALEZ, M. C., HERNÁNDEZ, D., MOLINUEVO-SALCES, B., RIAÑO, B., LARRÁN-GARCÍA, A. M. & TOMÁS-ALMENAR, C. 2018. RECOVERY OF PROTEIN CONCENTRATES FROM MICROALGAL BIOMASS GROWN IN MANURE FOR FISH FEED AND VALORIZATION OF THE BY-PRODUCTS THROUGH ANAEROBIC DIGESTION. *Frontiers in Sustainable Food Systems,* 2**,** 28.

GERDE, J. A., WANG, T., YAO, L., JUNG, S., JOHNSON, L. A. & LAMSAL, B. 2013. Optimizing protein isolation from defatted and non-defatted *Nannochloropsis* microalgae biomass. *Algal Research,* 2**,** 145-153.

GHEYSEN, L., LAGAE, N., DEVAERE, J., GOIRIS, K., GOOS, P., BERNAERTS, T., VAN LOEY, A., DE COOMAN, L. & FOUBERT, I. 2019. Impact of *Nannochloropsis* sp. dosage form on the oxidative stability of n-3 LC-PUFA enriched tomato purees. *Food Chemistry,* 279**,** 389-400.

GONZALEZ-TORRES, A., PIVOKONSKY, M. & HENDERSON, R. 2019. The impact of cell morphology and algal organic matter on algal floc properties. *Water research,* 163**,** 114887.

GOPINATH, A., PUHAN, S. & NAGARAJAN, G. 2010. Effect of unsaturated fatty acid esters of biodiesel fuels on combustion, performance and emission characteristics of a DI diesel engine. *International Journal of Energy & Environment*.

GORDON, M. H. 2001. The development of oxidative rancidity in foods. *Antioxidants in food.* Elsevier.

GROSSMAN, A. R., CATALANOTTI, C., YANG, W., DUBINI, A., MAGNESCHI, L., SUBRAMANIAN, V., POSEWITZ, M. C. & SEIBERT, M. 2011. Multiple facets of anoxic metabolism and hydrogen production in the unicellular green alga Chlamydomonas reinhardtii. *New Phytologist,* 190**,** 279-288.

GUARNIERI, M. T., NAG, A., SMOLINSKI, S. L., DARZINS, A., SEIBERT, M. & PIENKOS, P. T. 2011. Examination of triacylglycerol biosynthetic pathways via de novo transcriptomic and proteomic analyses in an unsequenced microalga. *PLoS One,* 6**,** e25851.

GÜGI, B., LE COSTAOUEC, T., BUREL, C., LEROUGE, P., HELBERT, W. & BARDOR, M. 2015. Diatom-specific oligosaccharide and polysaccharide structures help to unravel biosynthetic capabilities in diatoms. *Marine Drugs,* 13**,** 5993-6018.

GUIL-GUERRERO, J., NAVARRO-JUÁREZ, R., LÓPEZ-MARTıNEZ, J., CAMPRA-MADRID, P. & REBOLLOSO-FUENTES, M. 2004. Functional properties of the biomass of three microalgal species. *Journal of food engineering,* 65**,** 511-517.

GÜNERKEN, E., D'HONDT, E., EPPINK, M., GARCIA-GONZALEZ, L., ELST, K. & WIJFFELS, R. H. 2015. Cell disruption for microalgae biorefineries. *Biotechnology advances,* 33**,** 243-260.

GUO, S.-L., ZHAO, X.-Q., WAN, C., HUANG, Z.-Y., YANG, Y.-L., ALAM, M. A., HO, S.-H., BAI, F.-W. & CHANG, J.-S. 2013. Characterization of flocculating agent from the self-flocculating microalga Scenedesmus obliquus AS-6-1 for efficient biomass harvest. *Bioresource technology,* 145**,** 285-289.

HALIM, R., DANQUAH, M. K. & WEBLEY, P. A. 2012. Extraction of oil from microalgae for biodiesel production: a review. *Biotechnology advances,* 30**,** 709-732.

HALIM, R., GLADMAN, B., DANQUAH, M. K. & WEBLEY, P. A. 2011. Oil extraction from microalgae for biodiesel production. *Bioresource technology,* 102**,** 178-185.

HALIM, R., HILL, D. R. A., HANSSEN, E., WEBLEY, P. A., BLACKBURN, S., GROSSMAN, A. R., POSTEN, C. & MARTIN, G. J. O. 2019a. Towards sustainable microalgal biomass processing: anaerobic induction of autolytic cell-wall self-ingestion in lipid-rich *Nannochloropsis* slurries. *Green Chemistry,* 21**,** 2967-2982.

HALIM, R., HILL, D. R. A., HANSSEN, E., WEBLEY, P. A. & MARTIN, G. J. O. 2019b. Thermally coupled dark-anoxia incubation: A platform technology to induce auto-fermentation and thus cell-wall thinning in both nitrogen-replete and nitrogen-deplete *Nannochloropsis* slurries. *Bioresource Technology,* 290**,** 121769.

HALIM, R., WEBLEY, P. A. & MARTIN, G. J. 2016a. The CIDES process: fractionation of concentrated microalgal paste for co-production of biofuel, nutraceuticals, and high-grade protein feed. *Algal Research,* 19**,** 299-306.

HALIM, R., WEBLEY, P. A. & MARTIN, G. J. O. 2016b. The CIDES Process: fractionation of concentrated microalgal paste for co-production of biofuel, nutraceuticals, and high-grade protein feed. *Algal Research,* 19**,** 299-306.

HAN, X., WANG, Z., ZHU, C. & WU, Z. 2013. Effect of ultrasonic power density on extracting loosely bound and tightly bound extracellular polymeric substances. *Desalination,* 329**,** 35-40.

HARRISON, S. T. 1991. Bacterial cell disruption: a key unit operation in the recovery of intracellular products. *Biotechnology advances,* 9**,** 217-240.

HEJAZI, M., KLEINEGRIS, D. & WIJFFELS, R. 2004. Mechanism of extraction of β-carotene from microalga Dunaliellea salina in two-phase bioreactors. *Biotechnology and bioengineering,* 88**,** 593-600.

HENDERSON, R. K., BAKER, A., PARSONS, S. A. & JEFFERSON, B. 2008a. Characterisation of algogenic organic matter extracted from cyanobacteria, green algae and diatoms. *Water research,* 42**,** 3435-3445.

HENDERSON, R. K., BAKER, A., PARSONS, S. A. & JEFFERSON, B. 2008b. Characterisation of algogenic organic matter extracted from cyanobacteria, green algae and diatoms. *Water Research,* 42**,** 3435-3445.

HENDERSON, R. K., PARSONS, S. A. & JEFFERSON, B. 2010. The impact of differing cell and algogenic organic matter (AOM) characteristics on the coagulation and flotation of algae. *Water research,* 44**,** 3617-3624.

HOAGLAND, K. D., ROSOWSKI, J. R., GRETZ, M. R. & ROEMER, S. C. 1993. Diatom extracellular polymeric substances: function, fine structure, chemistry, and physiology. *Journal of phycology,* 29**,** 537-566.

IKEDA, S., MURAYAMA, D., TSURUMAKI, A., SATO, S., URASHIMA, T. & FUKUDA, K. 2019. Rheological characteristics and supramolecular structure of the exopolysaccharide produced by Lactobacillus fermentum MTCC 25067. *Carbohydrate polymers,* 218**,** 226-233.

JIMÉNEZ CALLEJÓN, M. J., ROBLES MEDINA, A., GONZÁLEZ MORENO, P. A., ESTEBAN CERDÁN, L., ORTA GUILLÉN, S. & MOLINA GRIMA, E. 2020. Simultaneous extraction and fractionation of lipids from the microalga *Nannochloropsis* sp. for the production of EPA-rich polar lipid concentrates. *Journal of Applied Phycology*.

JIMÉNEZ CALLEJÓN, M. J., ROBLES MEDINA, A., MACÍAS SÁNCHEZ, M. D., HITA PEÑA, E., ESTEBAN CERDÁN, L., GONZÁLEZ MORENO, P. A. & MOLINA GRIMA, E. 2014. Extraction of saponifiable lipids from wet microalgal biomass for biodiesel production. *Bioresource Technology,* 169**,** 198-205.

KANDA, H., HOSHINO, R., MURAKAMI, K., ZHENG, Q. & GOTO, M. 2020. Lipid extraction from microalgae covered with biomineralized cell walls using liquefied dimethyl ether. *Fuel,* 262**,** 116590.

KERIS-SEN, U. D., SEN, U., SOYDEMIR, G. & GUROL, M. D. 2014. An investigation of ultrasound effect on microalgal cell integrity and lipid extraction efficiency. *Bioresource technology,* 152**,** 407-413.

KIGHTLINGER, W., CHEN, K., POURMIR, A., CRUNKLETON, D. W., PRICE, G. L. & JOHANNES, T. W. 2014. Production and characterization of algae extract from *Chlamydomonas reinhardtii*. *Electric Journal of Biotechnology,* 17**,** 14-18.

KIM, J., YOO, G., LEE, H., LIM, J., KIM, K., KIM, C. W., PARK, M. S. & YANG, J.-W. 2013. Methods of downstream processing for the production of biodiesel from microalgae. *Biotechnology advances,* 31**,** 862-876.

KLEIN, G. L., PIERRE, G., BELLON-FONTAINE, M.-N., ZHAO, J.-M., BRERET, M., MAUGARD, T. & GRABER, M. 2014. Marine diatom *Navicula* jeffreyi from biochemical composition and physico-chemical surface properties to understanding the first step of benthic biofilm formation. *Journal of Adhesion Science and Technology,* 28**,** 1739-1753.

KNOTHE, G. 2009. Improving biodiesel fuel properties by modifying fatty ester composition. *Energy & Environmental Science,* 2**,** 759-766.

KONG, F., ROMERO, I. T., WARAKANONT, J. & LI-BEISSON, Y. 2018. Lipid catabolism in microalgae. *New Phytologist,* 218**,** 1340-1348.

KRISHNAN, S., WANG, N., OBER, C. K., FINLAY, J. A., CALLOW, M. E., CALLOW, J. A., HEXEMER, A., SOHN, K. E., KRAMER, E. J. & FISCHER, D. A. 2006. Comparison of the fouling release properties of hydrophobic fluorinated and hydrophilic PEGylated block copolymer surfaces: attachment strength of the diatom *Navicula* and the green alga Ulva. *Biomacromolecules,* 7**,** 1449-1462.

KRÖGER, M. & MÜLLER-LANGER, F. 2012. Review on possible algal-biofuel production processes. *Biofuels,* 3**,** 333-349.

KUROKAWA, M., KING, P. M., WU, X., JOYCE, E. M., MASON, T. J. & YAMAMOTO, K. 2016. Effect of sonication frequency on the disruption of algae. *Ultrasonics sonochemistry,* 31**,** 157-162.

LARDON, L., HÉLIAS, A., SIALVE, B., STEYER, J.-P. & BERNARD, O. 2009. Life-Cycle Assessment of Biodiesel Production from Microalgae. *Environmental Science & Technology,* 43**,** 6475-6481.

LAW, S. Q., METTU, S., ASHOKKUMAR, M., SCALES, P. J. & MARTIN, G. J. 2018. Emulsifying properties of ruptured microalgae cells: Barriers to lipid extraction or promising biosurfactants? *Colloids and Surfaces B: Biointerfaces*.

LAW, S. Q. K., CHEN, B., SCALES, P. J. & MARTIN, G. J. O. 2017. Centrifugal recovery of solvent after biphasic wet extraction of lipids from a concentrated slurry of *Nannochloropsis* sp. biomass. *Algal Research,* 24**,** 299-308.

LEE, A. K., LEWIS, D. M. & ASHMAN, P. J. 2012. Disruption of microalgal cells for the extraction of lipids for biofuels: processes and specific energy requirements. *Biomass and bioenergy,* 46**,** 89-101.

LEONG, T., ASHOKKUMAR, M. & KENTISH, S. 2011. The fundamentals of power ultrasound-a review.
LI, W., GAMLATH, C. J., PATHAK, R., MARTIN, G. J. & ASHOKKUMAR, M. 2019. Ultrasound–The Physical and Chemical Effects Integral to Food Processing. *In:* KNOERZER, K. & MUTHUKUMARAPPAN, K. (eds.) *Innovative Food Processing Technologies.* Elsevier.
LIM, G., LIM, J., AHMAD, A. & CHAN, D. 2015. Influences of diatom frustule morphologies on protein adsorption behavior. *Journal of Applied Phycology,* 27**,** 763-775.
LIU, D., ZENG, X.-A., SUN, D.-W. & HAN, Z. 2013. Disruption and protein release by ultrasonication of yeast cells. *Innovative Food Science & Emerging Technologies,* 18**,** 132-137.
LIU, S., ZHANG, Y., ZHOU, G., BAO, Y., REN, X., ZHU, Y. & PENG, Z. 2019. Protein degradation, color and textural properties of low sodium dry cured beef. *International Journal of Food Properties,* 22**,** 487-498.
LORENTE, E., FARRIOL, X. & SALVADÓ, J. 2015. Steam explosion as a fractionation step in biofuel production from microalgae. *Fuel Processing Technology,* 131**,** 93-98.
LUPATINI, A. L., DE OLIVEIRA BISPO, L., COLLA, L. M., COSTA, J. A. V., CANAN, C. & COLLA, E. 2017. Protein and carbohydrate extraction from S. platensis biomass by ultrasound and mechanical agitation. *Food Research International,* 99**,** 1028-1035.
LV, J., ZHAO, F., FENG, J., LIU, Q., NAN, F. & XIE, S. 2019. Extraction of extracellular polymeric substances (EPS) from a newly isolated self-flocculating microalga Neocystis mucosa SX with different methods. *Algal Research,* 40**,** 101479.
MAHMOOD, W. M. A. W., THEODOROPOULOS, C. & GONZALEZ-MIQUEL, M. 2017. Enhanced microalgal lipid extraction using bio-based solvents for sustainable biofuel production. *Green Chemistry,* 19**,** 5723-5733.
MARTIN, G. J. O. 2016. Energy requirements for wet solvent extraction of lipids from microalgal biomass. *Bioresource Technology,* 205**,** 40-47.
MARTIN, G. J. O., HILL, D. R. A., OLMSTEAD, I. L. D., BERGAMIN, A., SHEARS, M. J., DIAS, D. A., KENTISH, S. E., SCALES, P. J., BOTTÉ, C. Y. & CALLAHAN, D. L. 2014. Lipid profile remodeling in response to nitrogen deprivation in the microalgae *Chlorella* sp. (Trebouxiophyceae) and *Nannochloropsis* sp. (Eustigmatophyceae). *PlosOne,* 9**,** e103389.
MEDINA, C., RUBILAR, M., SHENE, C., TORRES, S. & VERDUGO, M. 2015. Protein fractions with techno-functional and antioxidant properties from *Nannochloropsis* gaditana microalgal biomass. *Journal of Biobased Materials and Bioenergy,* 9**,** 417-425.
MEKSIARUN, P., SPEGAZZINI, N., MATSUI, H., NAKAJIMA, K., MATSUDA, Y. & SATO, H. 2015. In vivo study of lipid accumulation in the microalgae marine diatom Thalassiosira pseudonana using Raman spectroscopy. *Applied spectroscopy,* 69**,** 45-51.
MIAZEK, K., KRATKY, L., SULC, R., JIROUT, T., AGUEDO, M., RICHEL, A. & GOFFIN, D. 2017. Effect of organic solvents on microalgae growth, metabolism and industrial bioproduct extraction: a review. *International journal of molecular sciences,* 18**,** 1429.
MIDDELBERG, A. P. J. 1995. Process-scale disruption of microorganisms. *Biotechnology Advances,* 13**,** 491-551.
MITSUDA, H. & SHIKANAI, T. 1959. Studies on the utilization of Chlorella for food. *Journal of Japanese Society of Food Nutrition,* 12**,** 40-58.
MONTAINI, E., ZITTELLI, G. C., TREDICI, M., GRIMA, E. M., SEVILLA, J. F. & PÉREZ, J. S. 1995. Long-term preservation of Tetraselmis suecica: influence of storage on viability and fatty acid profile. *Aquaculture,* 134**,** 81-90.
MUS, F., DUBINI, A., SEIBERT, M., POSEWITZ, M. C. & GROSSMAN, A. R. 2007. Anaerobic acclimation in Chlamydomonas reinhardtii: anoxic gene expression, hydrogenase induction, and metabolic pathways. *Journal of Biological Chemistry,* 282**,** 25475-25486.

NAVEED, S., LI, C., LU, X., CHEN, S., YIN, B., ZHANG, C. & GE, Y. 2019. Microalgal extracellular polymeric substances and their interactions with metal (loid) s: A review. *Critical Reviews in Environmental Science and Technology,* 49**,** 1769-1802.

NORZAGARAY-VALENZUELA, C. D., VALDEZ-ORTIZ, A., SHELTON, L. M., JIMÉNEZ-EDEZA, M., RIVERA-LÓPEZ, J., VALDEZ-FLORES, M. A. & GERMÁN-BÁEZ, L. J. 2017. Residual biomasses and protein hydrolysates of three green microalgae species exhibit antioxidant and anti-aging activity. *Journal of applied phycology,* 29**,** 189-198.

NURACHMAN, Z., BRATANINGTYAS, D. S. & PANGGABEAN, L. M. G. 2012. Oil from the tropical marine benthic-diatom *Navicula* sp. *Applied biochemistry and biotechnology,* 168**,** 1065-1075.

OLMSTEAD, I. L., HILL, D. R., DIAS, D. A., JAYASINGHE, N. S., CALLAHAN, D. L., KENTISH, S. E., SCALES, P. J. & MARTIN, G. J. 2013a. A quantitative analysis of microalgal lipids for optimization of biodiesel and omega-3 production. *Biotechnology and bioengineering,* 110**,** 2096-2104.

OLMSTEAD, I. L., KENTISH, S. E., SCALES, P. J. & MARTIN, G. J. 2013b. Low solvent, low temperature method for extracting biodiesel lipids from concentrated microalgal biomass. *Bioresource technology,* 148**,** 615-619.

OLMSTEAD, I. L. D., KENTISH, S. E., SCALES, P. J. & MARTIN, G. J. O. 2013c. Low solvent, low temperature method for extracting biodiesel lipids from concentrated microalgal biomass. *Bioresource Technology,* 148**,** 615-619.

ORSET, S., LEACH, G. C., MORAIS, R. & YOUNG, A. J. 1999. Spray-drying of the microalga Dunaliella salina: effects on β-carotene content and isomer composition. *Journal of agricultural and food chemistry,* 47**,** 4782-4790.

PALADE, G. E. 1956. The endoplasmic reticulum. *The Journal of Cell Biology,* 2**,** 85-98.

PARIMI, N. S., SINGH, M., KASTNER, J. R., DAS, K. C., FORSBERG, L. S. & AZADI, P. 2015. Optimization of protein extraction from Spirulina platensis to generate a potential co-product and a biofuel feedstock with reduced nitrogen content. *Frontiers in Energy Research,* 3**,** 30.

PARRA-RIOFRÍO, G., GARCÍA-MÁRQUEZ, J., CASAS-ARROJO, V., URIBE-TAPIA, E. & ABDALA-DÍAZ, R. T. 2020. Antioxidant and Cytotoxic Effects on Tumor Cells of Exopolysaccharides from Tetraselmis suecica (Kylin) Butcher Grown Under Autotrophic and Heterotrophic Conditions. *Marine drugs,* 18**,** 534.

PENNA, A., MAGNANI, M., FENOGLIO, I., FUBINI, B., CERRANO, C., GIOVINE, M. & BAVESTRELLO, G. 2003. Marine diatom growth on different forms of particulate silica: evidence of cell/particle interaction. *Aquatic microbial ecology,* 32**,** 299-306.

PIERRE, G., DELATTRE, C., DUBESSAY, P., JUBEAU, S., VIALLEIX, C., CADORET, J.-P., PROBERT, I. & MICHAUD, P. 2019. What is in store for EPS microalgae in the next decade? *Molecules,* 24**,** 4296.

PIRO, G., LENUCCI, M., DALESSANDRO, G., LA ROCCA, N., RASCIO, N., MORO, I. & ANDREOLI, C. 2000. Ultrastructure, chemical composition and biosynthesis of the cell wall in Koliella antarctica (Klebsormidiales, Chlorophyta). *European Journal of Phycology,* 35**,** 331-337.

PIVOKONSKY, M., NACERADSKA, J., KOPECKA, I., BARESOVA, M., JEFFERSON, B., LI, X. & HENDERSON, R. 2016. The impact of algogenic organic matter on water treatment plant operation and water quality: a review. *Critical Reviews in Environmental Science and Technology,* 46**,** 291-335.

POSTMA, P., MIRON, T., OLIVIERI, G., BARBOSA, M., WIJFFELS, R. & EPPINK, M. 2015. Mild disintegration of the green microalgae Chlorella vulgaris using bead milling. *Bioresource technology,* 184**,** 297-304.

POSTMA, P., PATARO, G., CAPITOLI, M., BARBOSA, M., WIJFFELS, R. H., EPPINK, M., OLIVIERI, G. & FERRARI, G. 2016. Selective extraction of intracellular components from the microalga Chlorella vulgaris by combined pulsed electric field–temperature treatment. *Bioresource technology,* 203**,** 80-88.

POSTMA, P., SUAREZ-GARCIA, E., SAFI, C., YONATHAN, K., OLIVIERI, G., BARBOSA, M., WIJFFELS, R. H. & EPPINK, M. 2017. Energy efficient bead milling of microalgae: effect of bead size on disintegration and release of proteins and carbohydrates. *Bioresource technology,* 224**,** 670-679.

PUGAZHENDHI, A., SHOBANA, S., BAKONYI, P., NEMESTÓTHY, N., XIA, A. & KUMAR, G. 2019. A review on chemical mechanism of microalgae flocculation via polymers. *Biotechnology Reports,* 21**,** e00302.

RAO, N., GRANVILLE, A. & HENDERSON, R. 2021. Understanding variability in algal solid-liquid separation process outcomes by manipulating extracellular protein-carbohydrate interactions. *Water Research,* 190**,** 116747.

RAO, N., GRANVILLE, A., WICH, P. & HENDERSON, R. 2020. Detailed algal extracellular carbohydrate-protein characterisation lends insight into algal solid-liquid separation process outcomes. *Water research,* 178**,** 115833.

RUIZ-HERNANDO, M., MARTINEZ-ELORZA, G., LABANDA, J. & LLORENS, J. 2013. Dewaterability of sewage sludge by ultrasonic, thermal and chemical treatments. *Chemical Engineering Journal,* 230**,** 102-110.

RYCKEBOSCH, E., BRUNEEL, C., TERMOTE-VERHALLE, R., LEMAHIEU, C., MUYLAERT, K., VAN DURME, J., GOIRIS, K. & FOUBERT, I. 2013. Stability of omega-3 LC-PUFA-rich photoautotrophic microalgal oils compared to commercially available omega-3 LC-PUFA oils. *Journal of Agricultural and Food Chemistry,* 61**,** 10145-10155.

SAFI, C., URSU, A. V., LAROCHE, C., ZEBIB, B., MERAH, O., PONTALIER, P.-Y. & VACA-GARCIA, C. 2014. Aqueous extraction of proteins from microalgae: effect of different cell disruption methods. *Algal Research,* 3**,** 61-65.

SALIM, S., KOSTERINK, N., WACKA, N. T., VERMUË, M. & WIJFFELS, R. 2014. Mechanism behind autoflocculation of unicellular green microalgae Ettlia texensis. *Journal of biotechnology,* 174**,** 34-38.

SALIM, S., VERMUË, M. & WIJFFELS, R. 2012. Ratio between autoflocculating and target microalgae affects the energy-efficient harvesting by bio-flocculation. *Bioresource technology,* 118**,** 49-55.

SAMORÌ, C., LÓPEZ BARREIRO, D., VET, R., PEZZOLESI, L., BRILMAN, D. W. F., GALLETTI, P. & TAGLIAVINI, E. 2013. Effective lipid extraction from algae cultures using switchable solvents. *Green Chemistry,* 15**,** 353-356.

SAYANOVA, O., MIMOUNI, V., ULMANN, L., MORANT-MANCEAU, A., PASQUET, V., SCHOEFS, B. & NAPIER, J. A. 2017. Modulation of lipid biosynthesis by stress in diatoms. *Philosophical Transactions of the Royal Society B: Biological Sciences,* 372**,** 20160407.

SCHOLZ, M. J., WEISS, T. L., JINKERSON, R. E., JING, J., ROTH, R., GOODENOUGH, U., POSEWITZ, M. C. & GERKEN, H. G. 2014. Ultrastructure and composition of the *Nannochloropsis* gaditana cell wall. *Eukaryotic cell,* 13**,** 1450-1464.

SEGOVIA, M. & BERGES, J. A. 2009. INHIBITION OF CASPASE-LIKE ACTIVITIES PREVENTS THE APPEARANCE OF REACTIVE OXYGEN SPECIES AND DARK-INDUCED APOPTOSIS IN THE UNICELLULAR CHLOROPHYTE DUNALIELLA TERTIOLECTA 1. *Journal of Phycology,* 45**,** 1116-1126.

SEGOVIA, M., HARAMATY, L., BERGES, J. A. & FALKOWSKI, P. G. 2003. Cell death in the unicellular chlorophyte Dunaliella tertiolecta. A hypothesis on the evolution of apoptosis in higher plants and metazoans. *Plant physiology,* 132**,** 99-105.

SHA, Z., ZHAO, J. & GOLDBERG, A. L. 2018. Measuring the overall rate of protein breakdown in cells and the contributions of the ubiquitin-proteasome and autophagy-lysosomal pathways. *The Ubiquitin Proteasome System.* Springer.

SHNYUKOVA, E. & ZOLOTARIOVA, Y. K. 2015. Diatom exopolysaccharides: a review. *International Journal on Algae,* 17.

SIERRA, L. S., DIXON, C. K. & WILKEN, L. R. 2017. Enzymatic cell disruption of the microalgae Chlamydomonas reinhardtii for lipid and protein extraction. *Algal research,* 25**,** 149-159.

SILVE, A., KIAN, C. B., PAPACHRISTOU, I., KUBISCH, C., NAZAROVA, N., WÜSTNER, R., LEBER, K., STRAESSNER, R. & FREY, W. 2018. Incubation time after pulsed electric field treatment of microalgae enhances the efficiency of extraction processes and enables the reduction of specific treatment energy. *Bioresource technology,* 269**,** 179-187.

SIMIONATO, D., BLOCK, M. A., LA ROCCA, N., JOUHET, J., MARECHAL, E., FINAZZI, G. & MOROSINOTTO, T. 2013. The Response of *Nannochloropsis* gaditana to Nitrogen Starvation Includes De Novo Biosynthesis of Triacylglycerols, a Decrease of Chloroplast Galactolipids, and Reorganization of the Photosynthetic Apparatus. *Eukaryotic Cell,* 12**,** 665-676.

SIMIONATO, D., SFORZA, E., CARPINELLI, E. C., BERTUCCO, A., GIACOMETTI, G. M. & MOROSINOTTO, T. 2011. Acclimation of *Nannochloropsis* gaditana to different illumination regimes: effects on lipids accumulation. *Bioresource technology,* 102**,** 6026-6032.

SINGER, P. & RÜHE, J. 2014. On the mechanism of deposit formation during thermal oxidation of mineral diesel and diesel/biodiesel blends under accelerated conditions. *Fuel,* 133**,** 245-252.

SINITCYN, P., RUDOLPH, J. D. & COX, J. 2018. Computational methods for understanding mass spectrometry–based shotgun proteomics data. *Annual Review of Biomedical Data Science,* 1**,** 207-234.

ŞIRIN, S., CLAVERO, E. & SALVADÓ, J. 2013. Potential pre-concentration methods for *Nannochloropsis* gaditana and a comparative study of pre-concentrated sample properties. *Bioresource Technology,* 132**,** 293-304.

SIVASANKAR, P., POONGODI, S., LOBO, A. O. & PUGAZHENDHI, A. 2020. Characterization of a novel polymeric bioflocculant from marine actinobacterium Streptomyces sp. and its application in recovery of microalgae. *International Biodeterioration & Biodegradation,* 148**,** 104883.

SOTO-SIERRA, L., STOYKOVA, P. & NIKOLOV, Z. L. 2018. Extraction and fractionation of microalgae-based protein products. *Algal research,* 36**,** 175-192.

SPIDEN, E. M., SCALES, P. J., YAP, B. H., KENTISH, S. E., HILL, D. R. & MARTIN, G. J. 2015. The effects of acidic and thermal pretreatment on the mechanical rupture of two industrially relevant microalgae: Chlorella sp. and *Navicula* sp. *Algal research,* 7**,** 5-10.

SPIDEN, E. M., YAP, B. H. J., HILL, D. R. A., KENTISH, S. E., SCALES, P. J. & MARTIN, G. J. O. 2013. Quantitative evaluation of the ease of rupture of industrially promising microalgae by high pressure homogenization. *Bioresource Technology,* 140**,** 165-171.

STAATS, N., DE WINDER, B., STAL, L. J. & MUR, L. R. 1999. Isolation and characterization of extracellular polysaccharides from the epipelic diatoms Cylindrotheca closterium and *Navicula* salinarum. *European Journal of Phycology,* 34**,** 161-169.

STAL, L. J. & DÉFARGE, C. 2005. Structure and dynamics of exopolymers in an intertidal diatom biofilm. *Geomicrobiology Journal,* 22**,** 341-352.

STRAMARKOU, M., PAPADAKI, S., KYRIAKOPOULOU, K. & KROKIDA, M. 2017. Effect of drying and extraction conditions on the recovery of bioactive compounds from Chlorella vulgaris. *Journal of Applied Phycology,* 29**,** 2947-2960.

SUMAN, K., KIRAN, T., DEVI, U. K. & SARMA, N. S. 2012. Culture medium optimization and lipid profiling of Cylindrotheca, a lipid-and polyunsaturated fatty acid-rich pennate diatom and potential source of eicosapentaenoic acid. *Botanica marina,* 55**,** 289-299.

SVENNING, J. B., DALHEIM, L., VASSKOG, T., MATRICON, L., VANG, B. & OLSEN, R. L. 2020. Lipid yield from the diatom Porosira glacialis is determined by solvent choice and number of extractions, independent of cell disruption. *Scientific reports,* 10**,** 1-10.

TAKAARA, T., SANO, D., KONNO, H. & OMURA, T. 2004. Affinity isolation of algal organic matters able to form complex with aluminium coagulant. *Water Science and Technology: Water Supply,* 4**,** 95-102.

TAKAHASHI, E., LEDAUPHIN, J., GOUX, D. & ORVAIN, F. 2009. Optimising extraction of extracellular polymeric substances (EPS) from benthic diatoms: comparison of the efficiency of six EPS extraction methods. *Marine and Freshwater Research,* 60**,** 1201-1210.

TANAKA, K. 2009. The proteasome: overview of structure and functions. *Proceedings of the Japan Academy, Series B,* 85**,** 12-36.

TESSON, B. & HILDEBRAND, M. 2013. Characterization and localization of insoluble organic matrices associated with diatom cell walls: insight into their roles during cell wall formation. *PloS one,* 8**,** e61675.

THOTHATHRI, S. K. 2009. Composition for growth of diatom algae. Google Patents.

TOMITA, Y., YOSHIOKA, K., IIJIMA, H., NAKASHIMA, A., IWATA, O., SUZUKI, K., HASUNUMA, T., KONDO, A., HIRAI, M. Y. & OSANAI, T. 2016. Succinate and lactate production from Euglena gracilis during dark, anaerobic conditions. *Frontiers in microbiology,* 7**,** 2050.

TRAN, N.-A. T., PADULA, M. P., EVENHUIS, C. R., COMMAULT, A. S., RALPH, P. J. & TAMBURIC, B. 2016. Proteomic and biophysical analyses reveal a metabolic shift in nitrogen deprived *Nannochloropsis* oculata. *Algal research,* 19**,** 1-11.

UNDERWOOD, G. J. & PATERSON, D. M. 2003. The importance of extracellular carbohydrate productionby marine epipelic diatoms. *Advances in botanical research,* 40**,** 183-240.

URSU, A.-V., MARCATI, A., SAYD, T., SANTE-LHOUTELLIER, V., DJELVEH, G. & MICHAUD, P. 2014. Extraction, fractionation and functional properties of proteins from the microalgae Chlorella vulgaris. *Bioresource technology,* 157**,** 134-139.

VAN BOEKEL, M. A. J. S. 2001. Kinetic aspects of the Maillard reaction: a critical review. *Food / Nahrung,* 45**,** 150-159.

VANDAMME, D., FOUBERT, I. & MUYLAERT, K. 2013. Flocculation as a low-cost method for harvesting microalgae for bulk biomass production. *Trends in Biotechnology,* 31**,** 233-239.

VANLERBERGHE, G. C., FEIL, R. & TURPIN, D. H. 1990. Anaerobic metabolism in the N-limited green alga Selenastrum minutum: I. Regulation of carbon metabolism and succinate as a fermentation product. *Plant physiology,* 94**,** 1116-1123.

VERMA, A. K., DASH, R. R. & BHUNIA, P. 2012. A review on chemical coagulation/flocculation technologies for removal of colour from textile wastewaters. *Journal of environmental management,* 93**,** 154-168.

VINAYAK, V., GORDON, R., GAUTAM, S. & RAI, A. 2014. Discovery of a diatom that oozes oil. *Advanced Science Letters,* 20**,** 1256-1267.

WANG, J.-K. & SEIBERT, M. 2017. Prospects for commercial production of diatoms. *Biotechnology for biofuels,* 10**,** 16.

WANG, J., CAO, S., DU, C. & CHEN, D. 2013. Underwater locomotion strategy by a benthic pennate diatom *Navicula* sp. *Protoplasma,* 250**,** 1203-1212.

WEI, L., EL HAJJAMI, M., SHEN, C., YOU, W., LU, Y., LI, J., JING, X., HU, Q., ZHOU, W. & POETSCH, A. 2019. Transcriptomic and proteomic responses to very low CO 2 suggest multiple carbon concentrating mechanisms in *Nannochloropsis* oceanica. *Biotechnology for biofuels,* 12**,** 1-21.

WU, C., XIAO, Y., LIN, W., LI, J., ZHANG, S., ZHU, J. & RONG, J. 2017. Aqueous enzymatic process for cell wall degradation and lipid extraction from *Nannochloropsis* sp. *Bioresource technology,* 223**,** 312-316.

XIAO, R. & ZHENG, Y. 2016. Overview of microalgal extracellular polymeric substances (EPS) and their applications. *Biotechnology Advances,* 34**,** 1225-1244.

XU, X., CAO, D., WANG, Z., LIU, J., GAO, J., SANCHUAN, M. & WANG, Z. 2019. Study on ultrasonic treatment for municipal sludge. *Ultrasonics sonochemistry,* 57**,** 29-37.

YAO, S., METTU, S., LAW, S. Q., ASHOKKUMAR, M. & MARTIN, G. J. 2018a. The effect of high-intensity ultrasound on cell disruption and lipid extraction from high-solids viscous slurries of *Nannochloropsis* sp. biomass. *Algal research,* 35**,** 341-348.

YAO, S., METTU, S., LAW, S. Q. K., ASHOKKUMAR, M. & MARTIN, G. J. O. 2018b. The effect of high-intensity ultrasound on cell disruption and lipid extraction from high-solids viscous slurries of *Nannochloropsis* sp. biomass. *Algal Research,* 35**,** 341-348.

YAP, B. H., CRAWFORD, S. A., DUMSDAY, G. J., SCALES, P. J. & MARTIN, G. J. 2014. A mechanistic study of algal cell disruption and its effect on lipid recovery by solvent extraction. *Algal Research,* 5**,** 112-120.

YAP, B. H., DUMSDAY, G. J., SCALES, P. J. & MARTIN, G. J. O. 2015. Energy evaluation of algal cell disruption by high pressure homogenization. *Bioresource Technology,* 184**,** 280-285.

YAP, B. H., MARTIN, G. J. & SCALES, P. J. 2016. Rheological manipulation of flocculated algal slurries to achieve high solids processing. *Algal Research,* 14**,** 1-8.

YATIPANTHALAWA, B. & MARTIN, G. 2021. Conventional and novel approaches to extract food ingredients and nutraceuticals from microalgae. *In:* LAFARGA, T. & ACIÉN, G. (eds.) *Cultured Microalgae for the Food Industry.* Elsevier.

YU, W.-L., ANSARI, W., SCHOEPP, N. G., HANNON, M. J., MAYFIELD, S. P. & BURKART, M. D. 2011. Modifications of the metabolic pathways of lipid and triacylglycerol production in microalgae. *Microbial cell factories,* 10**,** 1-11.

ZHANG, C., TANG, X. & YANG, X. 2018. Overcoming the cell wall recalcitrance of heterotrophic Chlorella to promote the efficiency of lipid extraction. *Journal of Cleaner Production,* 198**,** 1224-1231.

ZHANG, F., CHENG, L.-H., GAO, W.-L., XU, X.-H., ZHANG, L. & CHEN, H.-L. 2011. Mechanism of lipid extraction from Botryococcus braunii FACHB 357 in a biphasic bioreactor. *Journal of biotechnology,* 154**,** 281-284.

ZHANG, Z., WANG, F., WANG, X., LIU, X., HOU, Y. & ZHANG, Q. 2010. Extraction of the polysaccharides from five algae and their potential antioxidant activity in vitro. *Carbohydrate Polymers,* 82**,** 118-121.

ZHAO, F., XIAO, J., DING, W., CUI, N., YU, X., XU, J.-W., LI, T. & ZHAO, P. 2019. An effective method for harvesting of microalga: Coculture-induced self-flocculation. *Journal of the Taiwan Institute of Chemical Engineers,* 100**,** 117-126.

ZUPPINI, A., ANDREOLI, C. & BALDAN, B. 2007. Heat stress: an inducer of programmed cell death in Chlorella saccharophila. *Plant and Cell Physiology,* 48**,** 1000-1009.

Chapter 3

3. Induced biochemical and metabolic changes during dark anoxic incubation of *Nannochloropsis*

This chapter aims at developing an in depth understanding on the cellular response of *Nannochloropsis* sp. to dark anoxia incubation. The effect on the proteins and lipids in the cells are investigated to obtain a unified understanding on the effect of dark anoxia on biomacromolecules. Such an understanding will benefit future studies on *Nannochloropsis* and dark anoxic fermentation on microalgae more broadly.

3.1 Introduction

With increasing demand for sustainable resources, microalgae are increasingly being researched as a renewable feedstock for food and fuel (Aguirre et al., 2013, Minhas et al., 2016). Microalgae contain lipids, carbohydrates, proteins and can produce high-value metabolites such as long chain polyunsaturated fatty acids, carotenoids and vitamins (Minhas et al., 2016). Due to the presence of robust cell walls, the extraction of value components often requires cell rupture. Amongst the diverse range of microalgae, cell walls are often composed of polysaccharides including cellulose, xylan, mannose and other components such as uronic acids, proteins, glycoproteins, algaenan and sometimes even silica (Lee et al., 2012, Scholz et al., 2014).

Nannochloropsis sp., a promising precursor for algae-based lipid production due to its high TAG accumulating ability, have particularly strong cell walls that are resistant to cell rupture (Spiden et al., 2013b). A low-cost method was introduced previously to weaken these strong cell walls, making the subsequent physical rupture easier (Olmstead et al., 2013b, Halim et al., 2016a). In that work, concentrated slurries of cells were subjected to dark anoxic incubation (deprivation of light and oxygen) at an elevated temperature, which led to self-digestion of the cell walls (Halim et al., 2019a).

When photosynthetic microalgae are deprived of light, they cease photosynthetic oxygen production, and instead consume oxygen for respiration, drawing on internal carbon reserves (Napan et al., 2015). This can eventually lead to anoxic conditions. Oxygen is essential for energy production through oxidative phosphorylation, and certain biosynthetic pathways requiring oxygen as an oxidant or a reagent (Hemschemeier et al., 2013). The lack of oxygen therefore requires adjustment of cellular pathways through differential expression of genes. Previous studies have found microalgae such as *Chlamydomonas* have the necessary enzymes and pathways to survive dark anoxic conditions. To generate the energy needed for survival, they ferment plastidic starch into a variety of end products such as ethanol, acetate, glycerol, formate, lactate, CO_2 and H_2. Some microalgae excrete the fermentation products while others accumulate them inside the cells (Atteia et al., 2013, Mus et al., 2007). For an example, *Chlamydomonas* was found to excrete different fermentation products such as ethanol, malic acid, acetic acid and formic acid into the surrounding medium (Mus et al., 2007), whereas *Euglena gracilis* undertakes wax ester fermentation, during which the wax ester products are retained within the cells (Inui et al., 1982).

Previously it was found that subjecting *Nannochloropsis* sp., to dark anoxic incubation led to the formation of fermentative end products, and concomitant depletion of carbohydrate reserves, suggesting they employ fermentative pathways similar to other studied microalgae species (Halim et al., 2019a). However, the exact biochemical pathways used by *Nannochloropsis* sp. to respond to dark anoxic stress conditions are unresolved.

Enzymes are the catalysts of cellular metabolic pathways. Studying the differential expression of these proteins enables identification of the metabolic responses of the cells used to survive dark anoxic stresses. The advancement in mass spectrometric techniques has enabled in depth

understanding on the different biological processes in cells using various 'omics' approaches. Transcriptomics relates to the study of gene expression and regulation, while proteomics involves studying protein expression and post translational modification. Of these, proteomics is often preferred as proteins are more directly related to the physiological responses of the cells. Previous proteomics studies of microalgae have revealed the cellular responses to nitrogen deprivation in *Nannochloropsis occulata* (Tran et al., 2016), the effect of dark stress on the lipid biosynthesis in *Phaeodactylum tricornutum* (Bai et al., 2016), and low CO_2 responses in *Nannochloropsis oceanica* (Wei et al., 2019). However the response of dark anoxic incubation on microalgae has been limited mostly to *Chlamydomonas* and usually involved transcriptomic studies (Mus et al., 2007) rather than proteomics (Terashima et al., 2010). Changes in algal physiology and biochemical pathways in response to stress conditions are reflected in changes to the proteome (Tran et al., 2016). Therefore, a proteomic study of *Nannochloropsis* sp. during dark anoxia has the potential to provide a deeper understanding of the process.

In addition to their role in metabolism, proteins are of practical interest as a product from microalgae. The compositional profile will influence the nutritional and functional value of proteins. Further, the quality of the proteins could be affected by the incubation process. It is possible that proteolysis may occur, which could have several practical implications. Some peptides could be bioactive (Caporgno and Mathys, 2018, Soto-Sierra et al., 2018), while others could be bitter (Maehashi and Huang, 2009) or have altered biophysical functionality (Medina et al., 2015). In addition, the release of peptides from the cells could affect protein yields.

Lipids are another potential commercial product from microalgae. Lipid hydrolysis and lipid peroxidation can reduce lipid quality, and these processes have been observed in plants during anoxic conditions (Blokhina et al., 2003). Previously, Balduyck et al. (2017) also found that the FFA content in *Nannochloropsis* sp. increased during wet storage at 4 °C. The storage conditions were both dark and anoxic, while the temperature was lower and the incubation period longer (around 7 days) than that used for cell weakening (<2 days). It was seen that the polar lipids were mostly affected, and the activity of a phospholipase was proposed. Such degradation of the lipids can have implications in different applications, such as problems associated with downstream processing in biodiesel production and rancid flavours and loss of nutritional value considering food applications (Balduyck et al., 2016).

Microalgae cells contain lipases, proteases and cellulases of which the activity is systematically controlled by and compartmentalised within the cells. It is possible that dark anoxic incubation could result in active over-expression of these enzymes or decompartmentalization/ intracellular release resulting in inadvertent degradation of cellular proteins, lipid and cell wall material.

Much is already known about the metabolic responses of the well-characterised and studied microalgae *Chlamydomonas*. Less is known about other microalgae, but it is clear that the metabolic responses of different microalgae species under stress conditions can differ. For example, in a previous study, the diatom *T. weissoflogii* could survive under darkness, whereas 6

days of darkness resulted in cell death of the chlorophyte *D. tertiolecta* (Berges and Falkowski, 1998). While some effects of dark anoxic incubation on the cell physiology of *Nannochloropsis* have been revealed, it is of interest to understand the cellular responses in more details, which can then be compared with other species. *Nannochloropsis* sp. is a marine alga that dwells in marine environments. These environments frequently become anoxic. An in-depth understanding of the cellular response of *Nannochloropsis* sp. is relevant to understanding the behaviour and decomposition of this microalgae in the marine environment. In addition, this knowledge is needed to evaluate and improve the inclusion of dark anoxic incubation processes to facilitate efficient recovery of high-value components without compromising the quality of the products.

Halim et al. (2019a) previously observed that the total lipid and protein content of *Nannochloropsis* sp. was not significantly impacted by dark anoxic incubation. However, no measurements were performed to investigate potential biochemical alterations to the proteins or lipids. The current study aimed at investigating whether dark anoxic incubation can cause proteolysis or lipolysis, and to identify the cellular response to dark anoxia incubation using proteomic analysis.

3.2 Materials and Methods

3.2.1 Microalgae strain and cultivation

A previously studied microalgae *Nannochloropsis salina* was grown indoors at 20 °C in multiple 12 L carboys in parallel with a light:dark cycle of 14:10 hours (Halim et al., 2016a). A modified f/2 medium (Olmstead et al., 2013a) was used. An aquarium air pump (Stellar 380D, Aqua One, China) was used to aerate each bioreactor at a flow rate of 190 L/h by splitting the airflow into two air stones. Algae were harvested using a disc stack centrifuge (Separator OTC 2-02-137, GEA Westfalia, Italy) at the end of a 14-day growth cycle.

3.2.2 Dark anoxia incubation

Three separate batches of freshly harvested microalgal biomass cultivated under identical conditions were used in independent investigations into the effect of dark anoxic incubation on i) the release of proteins and peptides, ii) lipid hydrolysis and oxidation, and iii) proteomic profile and degree of hydrolysis.

Algae paste was diluted in synthetic seawater medium (30 g/L Red Sea Coral Pro salt dissolved in deionised water) to a salt-free dry weight solids concentration of ~12% w/w. For each experimental replicate, 80 ml of algae slurry was put into 100 ml Schott bottles and covered in aluminium foil to create dark conditions. Two holes in the lid were used to allow entry and exit of nitrogen gas which was sparged for 30 s prior to incubation to ensure anoxic conditions. For incubation, the bottles were kept in a water bath maintained at 38±1 °C. Stirring was not provided during incubation as mixing had previously been shown to have no impact on incubation except for maintaining a uniform temperature in a large vessel (Halim et al., 2019a). In the small vessels used in these experiments, a consistent temperature was monitored and maintained using a hot plate stirrer (Stuart CC162, Crown scientific, NSW). Duplicate 7.5 ml samples of algae slurry were

taken from each vessel after 8 h, 24 h and 48 h of incubation for analysis. Before sampling, the contents in the vessel were hand mixed and pipetted in and out several times to ensure homogeneity of the sample.

3.2.3 Protein and peptide release during incubation

Samples taken from the incubation vessels were centrifuged at 9000 g for 10 min (Allegra X-30R, fixed-angle rotor F0685, Beckman Coulter, Victoria, Australia). The supernatant was carefully recovered without disturbing the algae pellet. The total protein in the supernatant fraction was quantified using a modified Lowry protein assay kit following appropriate dilutions using synthetic seawater medium. Peptides in the supernatant fraction were separated from whole proteins usingm a Microcon-30 kDa membrane filter (Millipore, Merck) and centrifuged at 10,000 g for 10 mins using an Eppendorf 5702 fitted with an A-4-38 rotor (Eppendorf, North Ryde, NSW, Australia) to obtain the peptide-rich fraction in the supernatant. The total peptide content was measured using the modified Lowry assay.

3.2.4 Cell rupture and protein extraction

To assist in the complete recovery of proteins for total protein quantification, degree of hydrolysis measurement and proteomic analysis, cells were first ruptured by high-pressure homogenisation. Samples of algae from the incubation experiments and the unincubated/fresh algae were diluted with deionised water 10 times to obtain a sufficient volume to be processed in the high-pressure homogeniser (Panda 2K NS1001L, GEA Niro Soavi, Parma, Italy) and a protease inhibitor (Sigmafast protease inhibitor, Sigma-Aldrich) was added to halt any proteolysis. The algae slurry was passed through the homogeniser 5 times at a pressure of 1000±100 bar. Following cell disruption, 35 ml of the algae slurry was put into a 50 ml centrifuge tube (Falcon) and centrifuged at 4000 *g* for 10 min (Allegra X-30R, fixed-angle rotor F0685, Beckman Coulter, Victoria, Australia). Supernatants were collected and the pellets redispersed in 10 ml of 2.5% SDS, 50 mM Tris pH 8.1 buffer to maximise the protein extraction for the subsequent proteomic studies. Samples were vortexed for 1 min, following which they were centrifuged again at 4000 *g* for 10 min to remove cell debris. Supernatants from the repeated centrifugations were pooled together and used for subsequent quantification of the total protein content, degree of hydrolysis measurements and proteomics.

3.2.5 Degree of hydrolysis measurement

The degree of hydrolysis of the protein content in the supernatants described above, was measured using the O-phthalaldehyde (OPA) reagent. OPA reagent was prepared as previously described (Spellman et al., 2003). In brief, 10 ml, 10 ml and 5 ml respectively of 50 mM OPA solution in methanol, 50 mM N-acetyl cysteine (NAC) in water and 20% w/v sodium dodecyl sulphate (SDS) solution were dissolved in 75 ml of 0.1M borate buffer (pH 9.5). A volume of 20 µl of the diluted supernatant fraction was mixed with 2.4 ml of the reagent. The absorbance measurement at 340 nm was read after a 2 min incubation period using a UV-Vis spectrophotometer (Cary 3E UV-Vis absorbance spectrophotometer, Agilent Technologies, Mulgrave, VIC, Australia). The background

noise of the supernatant was measured at 340 nm after diluting 20 µl of the diluted supernatant fraction in 2.4 ml of deionised water and subtracted as a baseline. A standard calibration curve of leucine was used to represent free amino acids. The degree of hydrolysis was calculated using the following equation:

$$DH_x = \frac{\Delta Abs\ 340nm\ of\ x\ h\ incubation}{\Delta Abs\ 340nm\ of\ 0\ h\ incubation} \times \frac{Average\ protein\ content\ at\ t{=}0h}{Average\ protein\ content\ at\ t{=}xh}, \text{ where } x = 8h, 24h, 48h.$$

Samples were measured in duplicate for triplicated experiments. The average protein content was measured using a BCA assay kit using the microplate procedure according to the supplier's procedure.

3.2.6 Protein sample preparation for LC/MS/MS

Protein samples obtained following cell rupture were purified for proteomic study using a previously described procedure (Nguyen et al., 2017). Based on the protein content measured using the BCA assay, an appropriate volume was pipetted into a 2 ml microfuge tube to obtain a protein mass of around 0.1 mg. To precipitate the proteins, ice-cold acetone was added (at 4x the volume of the pipetted sample) and the tubes left in the freezer at -20 °C overnight. The tubes were then centrifuged at 16,000 g for 10 min using an Eppendorf 5702 fitted with an A-4-38 rotor (Eppendorf, North Ryde, NSW, Australia). The supernatant was removed, and the pellet was slowly washed with 1 ml of ice-cold acetone, recentrifuged, and the supernatant removed. The remaining pellet was resuspended in 100 µl of 8 M urea in 50 mM triethylammonium bicarbonate (TEAB) (Sigma-Aldrich) and vortexed to solubilise the pellet completely. The protein content was quantified to verify that a protein concentration of 1 ± 0.2 mg/ml was achieved.

Tris(2-carboxyethyl) phosphine (TCEP) was added to obtain a concentration of 10 mM in the sample (2 µl of 0.5 M TCEP) and mixed for 45 min at 37 °C. Iodoacetamide was added to reach a concentration of 55 mM (22 µl of 0.25 M iodoacetamide in 25 mM TEAB) and again mixed for 45 min at 37 °C. Finally, the solution was diluted to reach a final concentration of 1 M urea using 25 mM TEAB and was digested with trypsin (1:40) (Trypsin singles, Proteomics grade, Sigma-Aldrich, USA) shaking overnight at 37 °C using an incubated shaker (New Brunswick, Eppendorf, USA). Following trypsin digestion, solid phase extraction (SPE) was performed to purify the peptide fractions. The solution was acidified by adding pure formic acid to a concentration of 1% (v/v). SPE cartridges (Oasis HLB 1 cc Vac Cartridge, 10 mg Sorbent per Cartridge, Waters, Australia) were washed with 1 ml of 80% acetonitrile (ACN) containing 0.1% trifluoro acetic acid (TFA) (A), followed by two sequential washes with 1.2 ml of 0.1% TFA (B). The sample containing the peptide fractions was loaded into the SPE column and washed with 1.5 ml of B. The peptide fraction was eluted with 800 µl of solution A and collected in a 1 ml Eppendorf tube. Samples were dried in a SpeedVac concentrator (Labcono Centrivap Concentrator, Kansas, MO, USA) for 20 min to remove ACN and then were freeze dried overnight using a freeze dryer (Christ Alpha 1-2 LD Plus).

3.2.7 Proteomic analysis

The freeze-dried peptide fractions were redispersed in 1 ml of the loading buffer (2% ACN and 0.1% formic acid) and centrifuged at 16,000 g for 10 min (Eppendorf 5702 fitted with an A-4-38 rotor, Eppendorf, North Ryde, NSW, Australia) to remove any undispersed particles. The samples were run in a LC/MS/MS using an Orbitrap Elite mass spectrometer (Thermo Fisher Scientific) coupled online to a rapid separation liquid chromatography (RSLC) nano High performance Liquid chromatography (HPLC) (Ultimate 3000 UHPLC, Thermo Fisher Scientific) following the same method described previously (Ruethers et al., 2019). Results were analysed using MaxQuant (v.1.6.2.3) against a UniProt database (Bateman, 2021) for both *Nannochloropsis gaditana* and *Nannochloropsis salina*. The intensity based absolute quantification (iBAQ%) value was used for comparisons (Ruethers et al., 2021). Identified protein groups with a minimum of two peptides were included in the analysis. Data pre-processing was done using Perseus software. Three process replicates were used for the incubation time intervals. Sample groups were filtered to remove the proteins with a zero iBAQ intensity.

Proteins were filtered such that the iBAQ intensity was >0 in at least 80% of the samples in at least one time interval. Values were then converted into log 2 values, which assigned "NAN" (i.e. Not a number as $\log_2 0$=NAN) to the entries with an iBAQ intensity = 0. These values were imputed using the software guidelines to obtain a normal distribution. Following pre-processing, data were further manually analysed using Microsoft Excel. The relative abundance of the proteins was obtained using the iBAQ intensity following the equation below (Shin et al., 2013):

$$riBAQ\ of\ protein\ P = \frac{iBAQ\ of\ protein\ P}{\sum_{i=1}^{n} iBAQ_i}.$$

This gives an estimation of the protein concentration of the protein P in each individual sample. The average relative abundance of the protein P for the replicated samples were then obtained to compare between the incubation time intervals. The fold change was obtained by comparing the average relative abundance of the incubated samples for a given time t (t = 8 h, 24 h, or 48 h) with that of the fresh/unincubated sample (t = 0 h).

$$Fold\ change\ of\ protein\ P = \frac{Average\ riBAQ(t)\ of\ P}{Average\ riBAQ\ (0h) of\ P}, \qquad (t = 8\ h, 24\ h, 48\ h).$$

The proteins were manually categorised into different protein groups based on their key cellular functions in *Nannochloropsis* sp. All these details are included in Supplementary 2.

3.2.8 Lipid analysis

A separate batch of *Nannochloropsis* was prepared for lipid analysis using the same procedures described above, and subjected to dark anoxic incubation in three separate, replicate vessels, again following the same process discussed above. Samples taken during incubation were frozen at -80 °C and then freeze dried. Freeze-dried samples were then stored at -80 °C until being transported to KU Leuven, Kortrijk, Belgium for lipid analysis. The samples were transported in dry ice, via rapid air transport by Dangerous Goods International (DGI global). The integrity of the samples

was confirmed by the presence of dry ice on arrival at KU Leuven and a comparison of the cell permeability using hexane isopropanol extractions done at both The University of Melbourne and KU Leuven.

3.2.9 Total lipid extraction and quantification

Total lipid content of the freeze-dried *Nannochloropsis* biomass was gravimetrically determined using chloroform/methanol (1:1 v/v) as described by Ryckebosch et al. (2012). Briefly, 4 ml, 2 ml and 0.4 ml of methanol, chloroform and demineralised water respectively were added to 100 mg freeze-dried biomass and the sample was vortexed. 2 ml of both chloroform and demineralised water was added to the resulting sample, followed by vortexing and centrifugation. The upper phase was discarded, and the lower organic solvent phase was collected. The remaining biomass was re-extracted using 4 ml chloroform/methanol (1:1 v/v) followed by vortexing and centrifugation. The organic solvent phase was pooled with the previously collected organic solvent phase. The remaining biomass was subjected to a second extraction according to the same protocol and the organic solvent phases of both extractions were pooled. The collected organic solvent was filtered through a sodium sulphate layer. The total lipid content was gravimetrically determined after evaporation of the organic solvent.

3.2.10 FFA quantification

The total FFA quantification was performed by derivatisation of the FFA to ethylamine derivatives based on the method developed by Kangani et al. (2008) with slight modifications as described by Gheysen et al. (2018). In brief, 10 mg of lipids obtained as described in Section 3.2.9 were dissolved in 1 ml dichloromethane, following which a volume of 10 µl of diisopropylethylamine and a volume of 30 µl of diethylamine were added and the mixture was cooled to 0 ºC. A 40 µl volume of bis(2-methoxyethyl) aminosulfur trifluoride was added dropwise into the mixture obtained, and the solution was vortexed for 5 seconds and kept at 0 ºC for 5 minutes. Then the solutions were brought back to room temperature (25 minutes), 2 ml of demineralised water and 4 ml of hexane was added, and the solutions were mixed for 1 minute. The solutions were centrifuged (750g, 10min) and the upper hexane layer containing the FFA derivatives were analysed using gas chromatography (GC) with cold on-column injection and flame ionization detection (FID) (Trace GC Ultra, Thermo Scientific, Interscience, Louvain-la-neuve, Belgium) using a temperature profile as follows: 100-160 ºC (20 ºC/min), 160-240 ºC (4 ºC/min), 240 ºC (27 min). The total FFA content was quantified by obtaining the sum of the peak areas and comparing it to the area of the internal standard used (C13:0).

3.2.11 Lipid peroxidation quantification

The quantification of primary lipid peroxidation was performed by determining the peroxide value (PV) using the spectrophotometric FOX method as described by [84]. 10 mg of lipids obtained as described in 'Total lipid extraction and quantification', was dissolved in chloroform/methanol (7:3 v/v), diluted 1/10 and the absorbance (A_{DS}) was measured at 560 nm. 50 µl of xylenol orange and 50 µl acidified Fe (II) chloride solution were added. The absorbance of the blank of the Fe(II)

chloride solution (A_B) and the absorbance of the sample solution (A_s) at 560 nm was measured after exactly 5 minutes. Fe (III) chloride solution (10 µg/ml) was used to prepare a calibration curve of Fe (III) against its absorbance at 560 nm. The PV value was calculated according to:

$$PV = \frac{(A_S - A_{DS} - A_B) * m_i}{W * 55.84 * 2}.$$

With m_i the inverse of the slope of the calibration curve, and W the mass of the lipid (g). The PV were normalised against the PV value of unincubated/fresh sample to obtain the change in peroxide value (ΔPV).

3.2.12 Statistics and reproducibility

Incubation experiments were performed as triplicates, with three separate vessels used to incubate microalgae grown and harvested as a single batch. Subsequent protein extraction, degree of hydrolysis measurement, lipid extraction, FFA measurement and lipid peroxidation value were all performed in duplicate for each of the triplicated experiments. The presented data points include the mean and standard deviation of all values (n = 6). For the unincubated/fresh sample, all the above measurements were performed in triplicates instead of duplicates.

For the proteomic analysis, triplicated incubation experiments and duplicated protein extractions were performed. Individual protein samples were analysed, and the protein extraction duplicates were pooled together for each experiment when analysing using the MaxQuant software. Statistical analysis was done on the individual proteins and the categorised protein groups. An ANOVA analysis was done followed by a post-hoc t-tests ($p < 0.05$) to identify the significantly changed proteins and protein groups.

3.3 Results

As the first step, the effect of dark anoxia incubation on the total protein and lipid content was measured and the previous observations by Halim et al. (2019a) were confirmed (Figure 3.1). The biochemical integrity of the protein and lipid content of the algal biomass has important practical implications. The effect of dark anoxic incubation on protein and lipid integrity was investigated by measuring the degree of hydrolysis of the proteins (Figure 3.2a), the release of proteins and peptides from the cells into the supernatant (Figure 3.2b), and the free fatty acid content (Figure 3.2c) and peroxide value (Figure 3.2d) of the lipids as a function of incubation time.

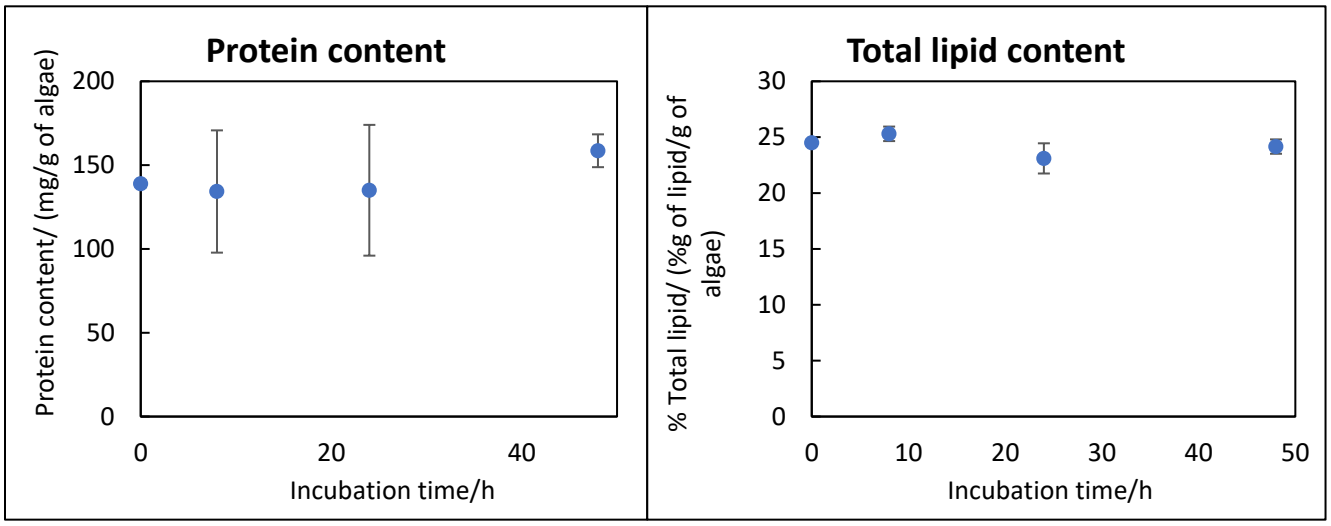

Figure 3.1: Total protein and total lipid content of *Nannochloropsis* sp. measured at different incubation time intervals. The error bars represent the standard deviation of triplicated experiments.

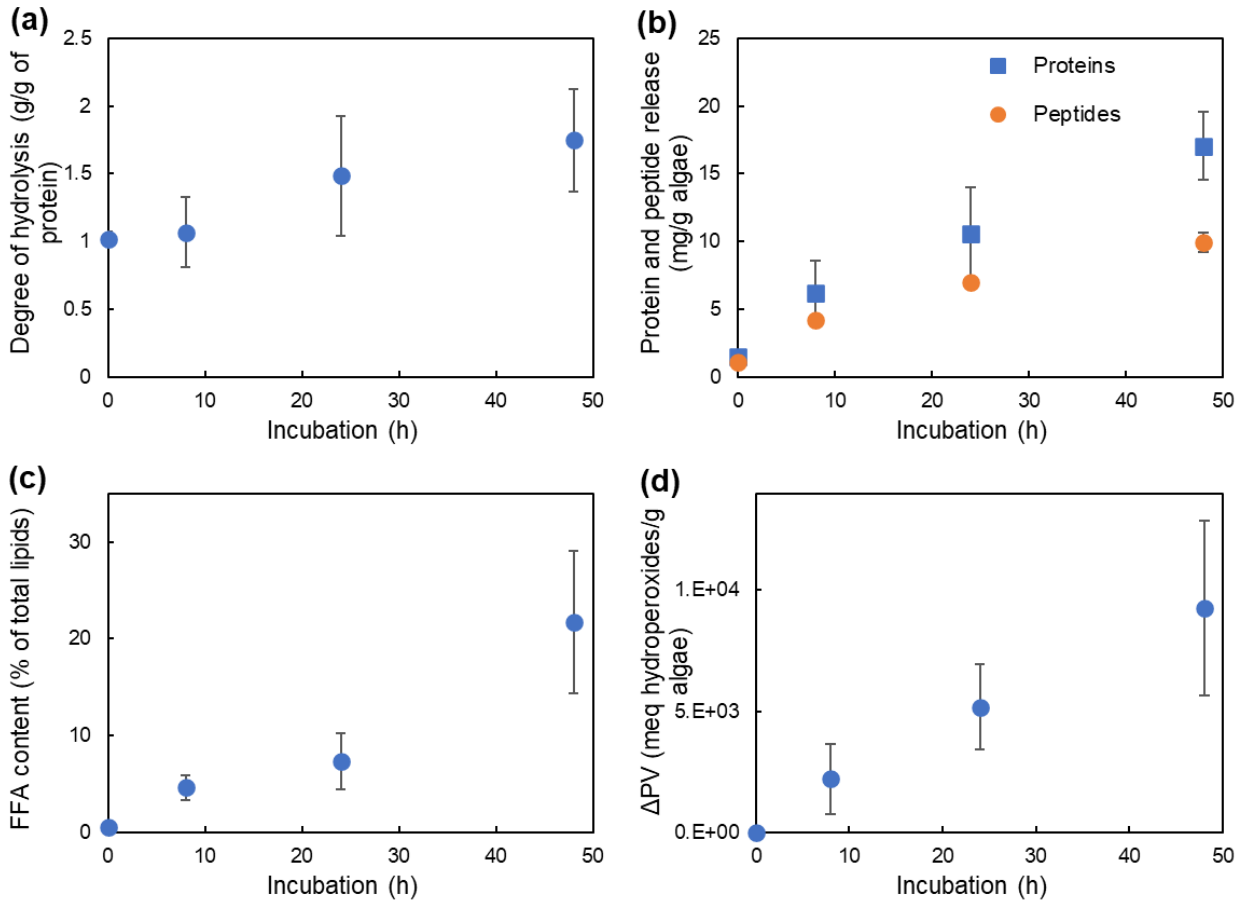

Figure 3.2: The effect of dark anoxia incubation on (a) the degree of hydrolysis of proteins, (b) protein and peptide release from cells into the supernatant, and the (c) FFA content and (d) peroxide value (ΔPV) of the lipids. The data points and the error bars represent the average and standard deviation of duplicate measurements of triplicated experiments.

For the proteins, the degree of hydrolysis increased with increasing incubation time (Figure 3.2a) and proteins and peptides progressively leaked from the cells into the supernatant (Figure 3.2b). Initially, peptides were the majority of released proteinaceous material, reflecting their smaller size. As the incubation time increased, the peptide-to-protein ratio decreased suggesting the cells progressively became sufficiently permeable to release whole proteins/larger peptides.

Figure 3.2c shows that the FFA content increased with increasing incubation time. As the total lipid content did not change during incubation (Figure 3.1), the increase in FFA suggests lipolysis is taking place during dark anoxic incubation. Notably, the FFA content is seen to increase dramatically between 24 h and 48 h of dark anoxia incubation. The peroxide value is an indicator of lipid peroxidation, which is detrimental to lipid quality. The peroxide value increased approximately linearly with respect to incubation time (Figure 3.2d). The increase in FFA content and peroxide value demonstrates that dark anoxic incubation results in degradation of lipid quality, particularly beyond 24 h.

Table 3.1: Proteins identified to be differentially expressed during incubation ($p < 0.05$). Grey shading represents overexpressed proteins while the unshaded proteins were significantly downregulated. Protein fold increase shows the difference of the abundance of the proteins at a specific incubation time relative to that in the control, unincubated sample.

Majority protein IDs	Protein name	Protein fold increase compared with the non-incubated cells		
		8h	24h	48h
Lipid metabolism				
A0A4D9CUP3	PLA2c domain-containing protein	41.10	43.18	47.41
A0A4D9CUK9	[Acyl-carrier-protein] S-malonyltransferase (EC 2.3.1.39)	2.21	1.83	3.18
A0A4D9CYN6	Udp-sulfoquinovose synthase	1.56	1.70	1.78
Energy/carbohydrate metabolism				
W7TQI2	Endo-1,3(4)-beta-glucanase (EC 3.2.1.6)	2.46	1.38	2.36
A0A4D9D2P9	Alpha-glucosidase ii	1.88	2.77	3.36
A0A4D9D252	Fructokinase	1.28	2.96	2.68
W7U0D4	Succinyl-CoA synthetase subunit alpha	1.22	1.82	1.51
A0A4D9CXW9	Acetyl-coenzyme A synthetase (EC 6.2.1.1)	2.09	2.54	2.95
A0A4D9D596	Dihydrolipoyllysine-residue succinyltransferase (EC 2.3.1.61)	2.32	2.96	3.58
A0A4D9CQ74	Ferredoxin--NADP(+) reductase (EC 1.18.1.2)	1.08	1.13	1.40
A0A4D9CX97	Dihydrolipoyl dehydrogenase (EC 1.8.1.4)	0.75	0.64	0.49
A0A4D9D2R7	Exo-beta--glucanase	0.45	0.25	0.34
W7U1X5	Transaldolase (EC 2.2.1.2)	0.33	0.78	0.78

A0A4D9DBL2	Isovaleryl-dehydrogenase	0.38	0.73	0.56
A0A4D9D7Z1	UDPglucose pyrophosphorylase	0.70	0.52	0.90
A0A4D9DC52	Rhamnose biosynthetic enzyme expressed	0.33	0.44	0.47
Proteases and protein metabolism				
A0A4D9CPY1	26s protease regulatory subunit 8	13.11	11.14	13.31
A0A4D9D6A4	ATP-dependent Clp protease proteolytic subunit	0.79	0.98	3.60
T1RI58	ATP-dependent zinc metalloprotease FtsH (EC 3.4.24.-)	1.17	1.15	1.56
A0A4D9D8Q8	Ubiquitin-activating enzyme e1	0.94	1.39	2.14
A0A4D9D849	Ubiquitin-conjugating enzyme catalytic domain protein	2.55	2.99	6.10
W7TFQ1	Mitochondrial-processing peptidase subunit beta	1.51	1.79	1.49
A0A4D9CWF8	Carboxyl-terminal processing protease	0.54	0.35	0.16
A0A4D9D808	26S proteasome regulatory subunit RPN11	0.80	0.47	0.58
Gene expression				
K9ZV80	30S ribosomal protein S10, chloroplastic	88.63	112.40	137.40
K9ZV97	30S ribosomal protein S18, chloroplastic	2.82	3.93	1.98
A0A4D9CZW2	50S ribosomal protein L5, chloroplastic	2.46	1.87	3.08
A0A4D9D8D6	Uncharacterized protein	4.10	2.39	4.13
A0A4D9D6Q8	30s ribosomal protein s1	0.87	0.80	1.26
W7THS5	Peptidyl-prolyl cis-trans isomerase (PPIase) (EC 5.2.1.8)	2.18	2.26	3.88
W7TD66	Peptidyl-prolyl cis-trans isomerase (PPIase) (EC 5.2.1.8)	1.41	1.36	1.86
A0A4D9D029	Rna binding protein	2.30	2.81	0.67
A0A4D9D910	Rna binding s1 domain protein	1.73	1.68	1.68
W7UA52	Histone h3	2.32	4.41	4.77
W7TJJ6	Proliferating cell nuclear antigen	1.43	3.73	2.76
A0A4D9CVG6	Elongation factor ef-3	1.23	1.29	10.31
W7TRP0	Eukaryotic initiation factor 4a	1.12	0.92	1.76
W7TD18	DNA ligase (EC 6.5.1.1), Ribulose-phosphate 3-epimerase (EC 5.1.3.1)	1.12	1.70	0.99
A0A4D9CXK5	U1 small nuclear ribonucleoprotein a	4.13	9.89	7.11
A0A4D9CYW1	Adenylosuccinate lyase (ASL) (EC 4.3.2.2) (Adenylosuccinase)	5.28	7.84	4.74
A0A4D9D2A5	GrpE nucleotide exchange factor	1.48	1.23	2.17
A0A4D9CVP5	Chaperonin cpn60 tcp-1	0.89	1.20	1.85
W7TPW8	Rubisco expression protein	1.65	1.56	1.58
A0A4D9D9K7	Prolyl-tRNA synthetase (EC 6.1.1.15)	0.76	1.35	2.04
A0A4D9DB93	Asparagine--tRNA ligase (EC 6.1.1.22)	1.74	2.15	4.94
A0A4D9D1E6	Uncharacterized protein	0.36	0.52	0.45
A0A4D9DC93	Peptidyl-prolyl cis-trans isomerase	0.45	0.38	0.42
A0A4D9DAP6	Peptidylprolyl isomerase (EC 5.2.1.8)	0.63	0.47	0.32
W7TWV9	Peptidylprolyl isomerase (EC 5.2.1.8)	0.89	0.50	0.14
A0A4D9D874	Peptidylprolyl isomerase (EC 5.2.1.8)	0.19	0.17	0.34
Amino acid biosynthesis				
A0A4D9CQT5	Acetohydroxy-acid reductoisomerase	0.94	1.01	1.39

W7TX01	Pyrroline-5-carboxylate reductase (EC 1.5.1.2)	1.01	1.28	1.35
A0A4D9CME1	Aspartate aminotransferase	1.65	2.34	1.80
A0A4D9CVJ1	Branched-chain amino acid aminotransferase	0.37	0.27	0.42
A0A4D9CYV5	Cysteine synthase	0.46	0.37	0.39
Oxidoreductases and stress induced proteins				
A0A4D9D3X6	Betaine aldehyde dehydrogenase	1.30	3.52	4.64
A0A4D9D429	Short-chain dehydrogenase reductase sdr	5.22	5.93	6.23
W7UAI2	PKS_ER domain-containing protein, Cinnamyl alcohol dehydrogenase	2.28	4.32	4.74
A0A4D9D7K1	Heat shock protein	1.96	1.77	2.28
A0A4D9CWW7	Stress-inducible protein sti1	1.62	2.45	2.45
A0A4D9D323	Obtusifoliol 14-alpha demethylase	1.37	1.32	2.32
A0A4D9CXV0	Hypersensitive-induced response protein,PHB domain-containing protein	2.20	2.81	1.96
A0A4D9D7Y8	Glutathione s-transferase	1.82	2.83	3.03
A0A4D9CUC9	Nucleoredoxin	0.96	1.25	1.65
A0A4D9D7N4	Arogenate dehydrogenase	1.30	2.44	2.03
A0A4D9CYT4	Short-chain dehydrogenase	0.47	0.23	0.14
A0A4D9D107	VKc domain-containing protein	0.52	0.20	0.19
A0A4D9D5I9	Cytochrome c peroxidase	0.37	0.38	0.39
W7TH17	Glutathione peroxidase	0.48	0.30	0.12
A0A4D9DC12	Glutathione reductase (EC 1.8.1.7)	0.36	0.27	0.22
Signalling proteins and transport				
A0A4D9DC09	PDZ domain protein	5.19	6.91	10.80
A0A4D9CQ73	MFS domain-containing protein	1.55	4.21	6.82
A0A4D9CY02	metal ion transmembrane transporter activity [GO:0046873]	1.90	2.89	1.07
A0A4D9D9I1	Mitochondrial carrier	1.59	2.85	3.44
A0A4D9CTY7	Amino acid transporter, transmembrane	3.94	3.16	4.40
A0A4D9D428	Protein translocase subunit SecA	1.06	1.11	1.70
A0A4D9CNB5	Myosin light chain kinase, Protein kinase domain-containing protein	0.92	1.68	1.97
Photosynthesis and chlorophyll biosynthesis				
A0A4D9DCN1	Geranylgeranyl reductase (EC 1.3.1.83)	1.02	1.06	1.42
T1RGM9	Magnesium chelatase (EC 6.6.1.1)	1.77	1.92	2.30
T1RH13	Photosystem I reaction center subunit VIII (PSI-I)	3.15	1.54	4.22
A0A4D9DHT9	Glutamyl-tRNA synthetase (EC 6.1.1.17)	1.23	1.60	2.87
W7TX20	Light-harvesting protein	0.75	0.93	0.67
W7T8I0	Light-harvesting protein	0.56	0.38	0.56
W7TCZ6	Mg chelatase subunit	0.13	0.29	0.78
K9ZXJ9	Cytochrome c-550 (Cytochrome c550)	0.92	0.56	0.21
Violaxanthin cycle				
A0A4D9DAF3	Violaxanthin de-epoxidase-related protein	4.86	4.47	5.16
A0A4D9CSI8	Zeaxanthin epoxidase	0.99	1.36	1.67
Metabolism				

A0A4D9CXT2	Rnase l inhibitor-like protein	2.16	1.77	4.67
A0A4D9D739	Putative cation-transporting atpase 13a1	20.70	39.09	22.44
W7TSQ4	S-adenosylmethionine synthase (EC 2.5.1.6)	0.84	0.57	0.48
K9ZWY0	AAA family ATPase (Putative AAA domain-containing protein Ycf46	0.36	0.43	0.56
A0A4D9CUN8	Pab-dependent poly-specific ribonuclease subunit 3	0.24	0.05	0.14
A0A4D9DDQ5	Phosphatidylinositide phosphatase sac1	0.47	0.49	0.72
Others				
A0A4D9CQD3	AMP-binding domain-containing protein	2.39	2.65	2.89
A0A4D9DBW7	Proton-translocating NAD(P)(+) transhydrogenase (EC 7.1.1.1)	3.86	3.40	4.13
W7TGL9	Receptor expression-enhancing protein 6	1.01	1.90	1.92
W7TSH6	Tautomerase	2.73	3.35	2.57
W7TFK4	Tubulin alpha chain	2.39	4.11	3.34
A0A4D9DGD2	Asp_Arg_Hydrox domain-containing protein	4.98	13.71	15.46
A0A4D9D9S4	Methyltransf_11 domain-containing protein	0.15	0.09	0.10
W7T5W5	Methyltransf_11 domain-containing protein	0.46	0.79	1.03
W7TIQ3	Protein-l-isoaspartate(D-aspartate) o-methyltransferase	0.55	0.39	0.30
A0A4D9DAM0	ATP-dependent (S)-NAD(P)H-hydrate dehydratase (EC 4.2.1.93) (ATP-dependent NAD(P)HX dehydratase)	0.52	0.58	0.28
A0A4D9D2R3	Nad-dependent epimerase dehydratase	0.55	0.28	0.27
A0A4D9DAA6	Tpr repeat protein	0.19	0.05	0.06
A0A4D9D997	Transmembrane protein, DUF1279 domain-containing protein	0.62	0.55	0.63
A0A4D9CY79	VOC domain-containing protein	0.88	1.07	0.59
A0A4D9D9E7	Ycii-like protein	0.28	0.34	0.40
A0A4D9DCC5	ZnF_CDGSH domain-containing protein	0.77	0.67	0.15

Through the proteomic analysis, around 1700 proteins in the *Nannochloropsis* proteome could be identified. However, among the 1700 proteins, only around 170 were found to be differentially expressed ($p < 0.05$). Proteins involved in protein, lipid and carbohydrate metabolism were seen among these, in addition to the proteins associated with stress responses. Table 3.1 includes the proteins that were seen to be differentially expressed during the process of incubation, categorised based on their major cellular functions. Figure 3.3 presents the number of up- and downregulated proteins grouped by function.

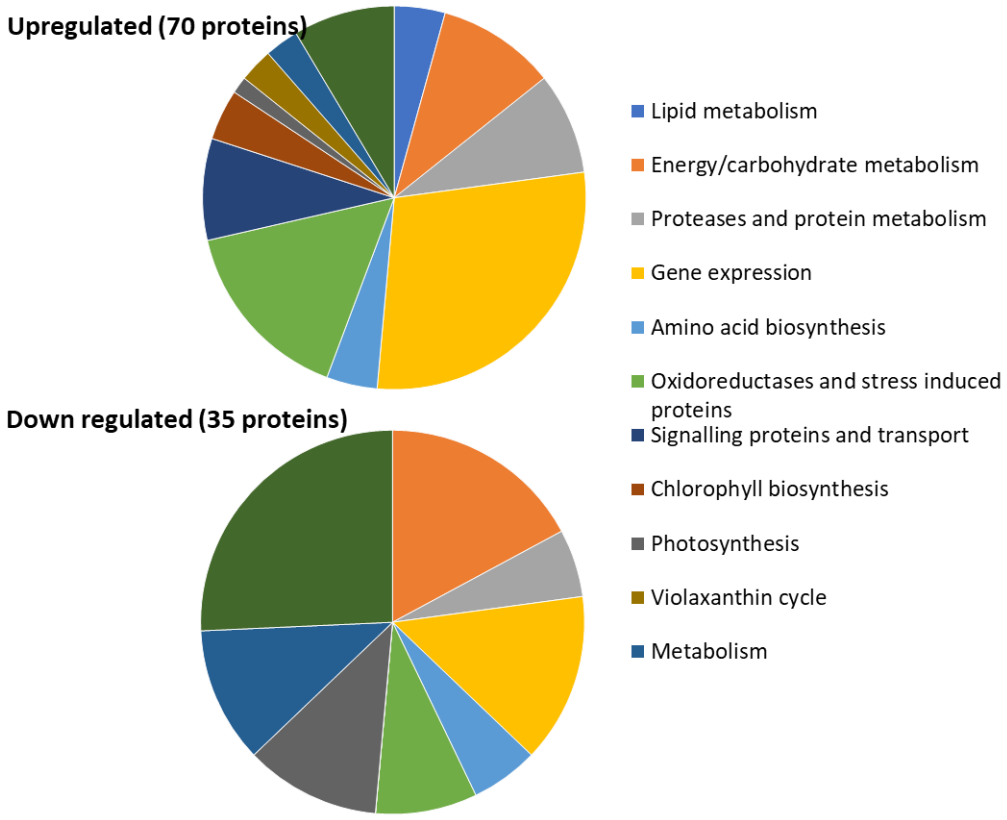

Figure 3.3: Groupings of the significantly changed proteins based on their cellular function.

Figure 3.3 indicates that there were significantly changed proteins involved in a broad range of cellular functions including lipid metabolism, energy/carbohydrate metabolism, protein catabolism, amino acid biosynthesis, photosynthesis, chlorophyll biosynthesis, stress responses, protein translation and transcription, and signalling and transport. More of the proteases and proteins related to protein metabolism (transcription, translation and protein folding) increased than decreased in abundance along with the enzymes related with oxidoreductase activity. The activity of the violaxanthin cycle seemed to be improved as two related enzymes were significantly upregulated. Oxidoreductase and stress response was another group affected during dark anoxia incubation. Considering Table 3.1, it is clear that there were many individual proteins within the functional groups that were variously up and down regulated. The implications of specific proteins of apparent importance will be discussed in the next section.

Apart from identifying the statistically significant proteins and protein groups that were differently abundant/expressed, the effect of incubation on the overall abundance of different protein groups of specific functions, irrespective of whether the individual proteins have changed or not, was considered important. From previous studies of Chlamydomonas, specific functional groups were seen to be affected by dark anoxia incubation (Mus et al., 2007, Hemschemeier et al., 2013). Hence the proteins showing relevance to different catabolic processes, energy production, photosynthesis and stress response, were manually selected and characterised. The sum of the relative abundance

of individual proteins in each functional group was obtained and compared as a function of incubation time and is depicted in Figure 3.4.

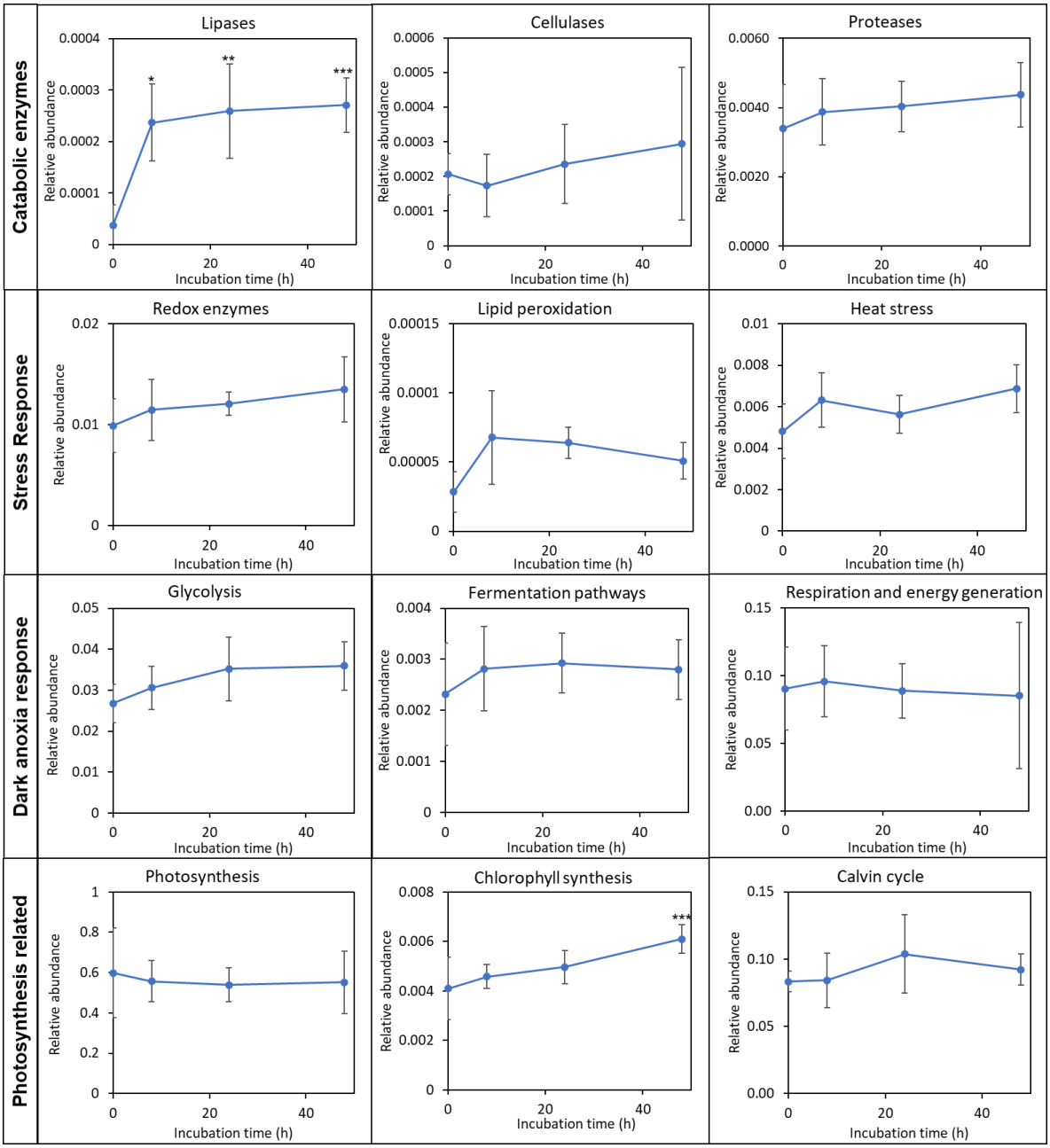

Figure 3.4: The average sum of the relative abundance of protein groups involved in the selected processes of interest. (a) Lipases, (b) cellulases, (c) proteases (sum of all proteases, peptidases and proteasome complex units), (d) redox enzymes (sum of all the enzymes/proteins having oxidoreductase activity), (e) lipid peroxidation (sum of all lipoxygenases), (f) heat stress proteins (induced as a response to heat stress, with the function of these proteins mostly associated with protein folding and refolding), (g) glycolysis (proteins associated with the glycolytic pathway), (h) fermentation pathways (proteins identified to be involved in different fermentative pathways to

maintain the redox balance of the cell), (i) respiration and energy generation (proteins involved in respiratory energy metabolism), (j) photosynthesis (proteins involved in photosynthesis including light harvesting complexes, photosystem I and II complexes and cytochrome proteins), (k) chlorophyll synthesis, (l) Calvin cycle (proteins involved in photosynthetic C fixation through the Calvin cycle). Asterisk symbols represent statistically significant differences compared to the t = 0 time point. Error bars represent the standard deviation of duplicated samples of triplicated experiments.

Statistically significant changes were observed only in the lipase and chlorophyl biosynthesis groups. However, looking at the overall trends, protein groups involved in catabolic and stress response activities such as lipase, proteases, cellulases, heat stress induced, and redox enzymes showed an overall increasing trend during incubation. There was a sudden 2-3 fold increase in lipid peroxidation related enzymes after 8 h of incubation, which subsequently subsided. Of the protein groups involved in dark anoxia responses, glycolysis and fermentation pathways showed an overall increase, while the enzymes involved in respiratory energy generation decreased over the period of incubation. Photosynthesis related proteins progressively decreased, although interestingly the enzymes involved in chlorophyll synthesis showed an increasing trend. Generally, it can be observed that the cellular response within the first 8 h of incubation induction was more pronounced than later in the incubation period. The significance of these protein groups and the variation of the relative abundance are now considered.

3.4 Discussion

3.4.1 Effect of dark anoxic incubation on protein and lipid integrity

The observed increases in the cellular FFA and peptide content (Figure 3.2a and 3.2c) could be a result of either or both of two processes. First, the degradation of lipids and proteins could be a result of an active cellular response to the stress conditions they are undergoing. In this case, the cells would actively express proteolytic and lipolytic enzymes, possibly to as part of cellular reassembly or to maintain energy flux under the stress conditions. Alternatively, it could be an inadvertent effect of the release of compartmentalised or membrane-bound proteases and lipases in the cells as a result of global intracellular degradation. The latter is consistent with the transmission electron microscopy images obtained in a previous study, which revealed that the organelles of the cell slowly lost their integrity over the incubation time period (Halim et al., 2019a).

Proteasomes and proteases function in cells by degrading misfolded or unwanted proteins. The stress conditions provided (high temperature and anoxic conditions) could promote protein misfolding and aggregation, or result in the redundancy of certain enzymes (e.g. those involved in photosynthesis), therefore requiring the degradation of such proteins and overexpressing of proteolytic enzymes (Berges and Falkowski, 1998, Schroda et al., 2015). The observed increase in two proteases, one peptidase and two ubiquitin enzymes (Table 3.1) suggest that the cells are actively increasing the metabolism and degradation of unwanted proteins. In particular, the 26s

protease regulatory subunit 8 increased 13-fold in the first 8 hours, after which it remained constant. Two ubiquitin enzymes also increased in abundance, suggesting the proteasome-ubiquitin pathway is activated. This 26s proteasome pathway is located in the cytoplasm and nucleus and is involved in degrading misfolded and unwanted proteins (Tanaka, 2009). However, degrading the proteins through the ubiquitin-proteasome pathway requires energy, which is highly limited during dark anoxic incubation. Also, while the overall content of proteases available in the cells was seen to increase during prolonged incubation (Figure 3.4), it was quite minor (*ca* +10%).

Apart from this, the ATP-dependent zinc metalloprotease related to cell division and protein catabolic process also increased in abundance (Table 3.1). Most importantly, this was the most abundant protease observed in all the protein samples irrespective of the incubation time. Such zinc metalloproteases have previously been identified to have the ability to degrade the extracellular matrix proteins of the microalgae cell wall, eventually leading to cell autolysis in *Chlamydomonas reinhardtii* (Demuez et al., 2015b, Matsuda et al., 1985, Kinoshita et al., 1992). This protease is likely playing a key role in the above suggested cellular degradation. Abiotic stresses such as light limitation in microalgae have induced proteases that led to autocatalyzed cell death (Berges and Falkowski, 1998, Segovia et al., 2003). In a previous study, the unicellular chlorophyte *Dunaliella tertiolecta* activated apoptotic cell death when placed in prolonged darkness, which was seen to be related to an increase in protease activity and the induction of certain proteases (Segovia and Berges, 2009, Segovia et al., 2003, Berges and Falkowski, 1998). These mainly consisted of cell death-associated proteases or caspases, whereas the inhibition of such proteases had prevented the appearance of reactive oxygen species and apoptosis under dark conditions (Segovia and Berges, 2009). Similarly, heat stress on eukaryotic microalgae *Chlorella saccharophila* has also led to an increase in apoptotic-like cell death, which was significantly reduced following the inhibition of caspase like enzymes (Zuppini et al., 2007).

Importantly, the progressive increase in the degree of hydrolysis of the proteins during prolonged dark anoxic incubation indicates an imbalance between protein degradation and assembly. In healthy cells, protein degradation is balanced by reassembly of correctly folded proteins needed by the cells. The high degree of unbalanced proteolysis suggests an uncontrolled process. It is possible that the initial spike in 26s protease regulatory subunit 8 and the zinc metalloprotease have accelerated this process to some extent. Overall, the evidence supports the idea that protein degradation was initially promoted by proteases expressed as part of apoptotic cellular degradation resulting from the dark, anoxic and heat shock provided to the cells, and then accelerated by unregulated proteolytic activity.

Figure 3.2b shows that the protein content present in the supernatant prior to incubation was mostly peptides. As the incubation time increased, more proteins were released into the supernatant, which were initially also peptides. This reflects the higher permeation rate of peptides relative to whole proteins. Despite the continued progression of proteolysis (Figure 3.2a), whole proteins eventually leaked out from the cells at a higher rate than peptides, presumably due to the continued loss of

cell membrane integrity. Compromised membrane permeability is another reported effect of caspase like proteases leading to apoptotic cell death (Bidle, 2016).

Similar to the protein hydrolysis, the observed lipolysis (as evidenced by the constant total lipid content and increasing FFA) could be an inadvertent consequence of cell degradation or a result of deliberate cellular action. In contrast to the small increase in protease concentration, the total amount of lipases in the cells increased considerably (*ca* +600%) during dark anoxic incubation (Figure 3.4). In particular, the PLA2c domain-containing protein that has phospholipase activity was found to increase in abundance by over 40-fold during dark anoxic incubation (Table 3.1). Previously, similar dark storage of *Nannochloropsis* sp. slurries resulted in an increase in the FFA and monoacylglyceride (MAG) content, with a concurrent decrease in the polar lipids suggesting the lipolysis of membrane lipids (Balduyck et al., 2017). As phospholipases act on the membrane phospholipids, the increase in the free fatty acid content (Figure 3.2b) is consistent with lipolysis of membrane lipids and a loss of membrane integrity. The activity of a phospholipase has been observed to initiate chemical defence in the diatom *Thalassiosira rotula* after cell damage (Pohnert, 2002). This observed increased activity of the phospholipase could be part of a similar defence strategy by the *Nannochloropsis* sp. cells.

Similar observations were made in potato cells by Rawyler et al. (1999), where increased anoxic incubation led to an increase in the FFA concentration. The anoxia-induced FFA accumulation in potato cells was correlated with an increase in electrolyte leakage, suggesting the cell membranes were affected (Rawyler et al., 1999). The loss of membrane integrity resulting from phospholipase activity is consistent with the increased release of whole protein during incubation. Lipolysis, or the formation of FFA, was previously seen to be a sign of microalgae (*Nannochloropsis* and *Isochrysis*) cell damage or cell death-induced mechanisms caused by different stress conditions (Balduyck et al., 2017, Balduyck et al., 2016). Such stress conditions induce lipase activity or make cells fragile and accessible to endogenous lipases, whereas short term heat treatments to inactivate these endogenous lipases have resulted in increased lipid stability (Berge et al., 1995, Balduyck et al., 2019b).

In a previous study on *Chlamydomonas reinhardtii*, a decrease in the total fatty acid content was seen during dark anoxia. This was related to an unexpected accumulation of acyl CoA oxidases (Hemschemeier et al., 2013). It was also observed that the cells accumulated TAGs, despite the decrease in the total fatty acids. It was proposed that the polyunsaturated FAs from the plastid or membrane lipids were likely being redistributed to TAGs (Hemschemeier et al., 2013). Bai et al. (2016) observed increased lipid production in the diatom *Phaeodactylum tricornutum* under dark stress. Similar observations were made by Chua et al. (2020) for *Nannochloropsis oceanica* under dark conditions coupled with cold stress. However, dark anoxic incubation of *Nannochloropsis* did not seem to significantly affect the lipid class distribution or overall FAME composition (Halim et al., 2019a). This is consistent with other studies on microalgae such as *Nannochloropsis salina* (Napan et al., 2015), *Tetraselmis suecica* (Montaini et al., 1995) *D. tertiolecta* where the fatty acid content has not been significantly affected during dark anoxic conditions.

Although dark wet storage of *Nannochloropsis* resulted in membrane lipid hydrolysis, the TAG content did not change significantly (Balduyck et al., 2017). Polar lipids in microalgae have been found to be more sensitive to lipolysis than TAGs (Balduyck et al., 2015, Berge et al., 1995). This could be partly due to the relative inaccessibility of the TAG molecules (largely protected within lipid bodies). In *Nannochloropsis* sp. TAGs have been found to consist mostly of saturated fatty acids whereas polar lipids are richer in unsaturated fatty acids including PUFAs (Martin et al., 2014a, Simionato et al., 2013). Membrane lipids, especially the unsaturated fatty acids, undergo changes under biotic and abiotic stresses, during the induction of defence reactions. Abiotic stress conditions were also seen to affect the degree of fatty acid unsaturation (Samala et al., 1998).

The main cellular functions of lipolysis or lipid degradation include production of carbon and energy for growth, remodelling membrane lipid composition, and generation of signalling molecules (Kong et al., 2018). Lipids can be used to generate energy in dark conditions via lipolysis followed by fatty acid beta oxidation in the presence of oxygen (Kong et al., 2018). However, the lack of oxygen in the environment prevents fatty acid beta oxidation. The stasis of the total FA content in *Nannochloropsis* during dark anoxic incubation (Halim et al., 2019a) suggests the lipids (both TAGs and membrane lipids) are not hydrolysed for energy generation (in which case the overall content would be decreased (Halim et al., 2019b)), but rather an inadvertent effect of cellular degradation, and possibly as a defence mechanism.

In a similar study, long term anaerobic dark storage of the microalgae *Scenedesmus acutus* underwent lactic acid fermentation, resulting in a decrease in the carbohydrate content. The protein and lipid content remained unaffected, however the degradation effects/products were not studied (Wendt et al., 2019). Membrane lipids have been shown to be sensitive to cellular heat stress. Under heat stress, the fluidity of the membrane increases, which can be actively countered by the cells via increasing the degree of fatty acid saturation to maximise hydrophobic interactions (Srirangan et al., 2015). Therefore, the observed increase in the FFAs can be associated with the spike in the phospholipase enzymes that act on the membrane lipids as a stress response trying to remodel the membrane lipids.

Lipid peroxidation is important for lipid quality and is linked with the amount of reactive oxygen species (ROS; hydroxyl radicals ($^{\cdot}OH$), superoxide radicals (O_2^{-}), and hydrogen peroxide (H_2O_2)) present and the presence of FFAs and lipoxygenase enzymes. The activity of lipoxygenases was seen to increase during anoxic incubation of potato cells (Pavelic et al., 2000). In Figure 3.4, although the increase was not statistically significant, there was an apparent increase in the lipoxygenases observed during dark anoxia that could promote lipid peroxidation (Figure 3.2d). In potato cells, lipid peroxidation occurred only when irreversible damage occurred by anoxia triggered lipid hydrolysis (Pavelic et al., 2000). Therefore, the activity of the phospholipase is likely to play a major role in both FFA formation and lipid peroxidation.

As described earlier, the induction of several stress conditions resulted in degradative effects on the proteins and lipids. Therefore, the following section involves a detailed discussion on the

observed differences in the cell proteome and the potential responses of the cells including the response to dark anoxia and heat stress, that provide insights into the mechanism used to survive these stress conditions and trigger the observed biochemical degradation.

3.4.2 Cellular stresses during dark anoxic incubation

Dark anoxic incubation subjects the algae cells to three main stresses: i) dark conditions that prevent photosynthetic carbon assimilation and energy generation, ii) anoxic conditions that prevent oxidative respiration, and iii) heat stress.

Even a small increase in temperature beyond the upper limit for a given microalgae can cause heat stress that can result in protein unfolding, entanglement, and unspecific aggregation (Kobayashi et al., 2014). When microalgal cells are subjected to high temperature stresses, an accelerated expression of heat responsive genes and heat shock proteins has been observed (Fan et al., 2018, Kobayashi et al., 2014). As an example, the expression of heat shock proteins was seen in the red alga *Cyanidioschyzon merolae* and the green alga *Chlamydomonas reinhardtii* when subjected to high temperatures (36 °C for *Chlamydomonas reinhardtii* and 55 °C for *Cyanidioschyzon merolae*) relative to their optimal growth temperatures (22 °C and 42 °C, respectively) (Kobayashi et al., 2014, Tanaka et al., 2000). Although the threshold temperature for heat stress in the studied strain of *Nannochloropsis* has not been determined, *Nannochloropsis* naturally grows in similar climate conditions as does *Chlamydomonas*, which could suggest that activation of heat response could occur at an incubation temperature of 37 °C. The exact role of elevated temperature during the current dark anoxic incubation is not clear, however there are some signs of heat stress in the proteome. In particular, a heat shock protein involved in protein folding (Table 3.1) was overexpressed indicating an active metabolic adjustment to counter these effects.

Beyond the direct effects of heat stress, cells need energy if they are to actively metabolise and express new proteins and recycle the misfolded or damaged proteins. Therefore, the following section discusses the energy production mechanism during dark anoxic incubation, and their link to the other two stresses – darkness and anoxia.

3.4.3 Energy production in *Nannochloropsis* sp. during dark anoxia

To maintain cell integrity and functioning, a means of cellular energy generation is required. Under normal circumstances, microalgal cells produce energy in the form of ATP via photosynthesis when light is available, and by respiration of carbon reserves (e.g. TAG or starch) using O_2 as the main electron acceptor during periods of darkness. However, under dark anoxic conditions, the algae cells are not able to undertake either of these energy generating processes due to the simultaneous lack of both light and oxygen. In the absence of oxygen or other terminal electron acceptors, many microorganisms can resort to substrate level phosphorylation using fermentation pathways, which catabolise organic compounds with no net oxidation.

Fermentation metabolism has been confirmed and studied in detail in the model microalga, *Chlamydomonas reinhardtii* (Catalanotti et al., 2013b). Under dark anoxic conditions *Chlamydomonas* can maintain cellular energy generation and redox balance by fermenting stored

starch via glycolysis into end-products including formate, acetate, ethanol, CO_2 and H_2 (Catalanotti et al., 2013b). Fermentation metabolism has yet to be confirmed in *Nannochloropsis*, but was proposed in our previous studies of dark anoxia incubation of this alga (Halim et al., 2019a). One complication, however, is that for glycolysis to take place, a carbohydrate substrate should be available to ferment. Unlike *Chlamydomonas* that uses starch as its cellular energy and carbon reserve, *Nannochloropsis* is primarily a lipid (TAG) accumulator. As TAG has a much higher degree of reductance than starch, it cannot be readily fermented. However, in addition to TAG, *Nannochloropsis* can retain glucans (chrysolaminarin) as storage carbohydrates and their cell walls contain cellulose (Scholz et al., 2014, Vogler et al., 2018). It was previously observed that the cellulose layer in *Nannochloropsis* sp. was consumed during dark anoxic incubation, and it was proposed that the cellulose may have been metabolised as part of fermentation metabolism (Halim et al., 2019a). For this to occur, there needs to be cellulases present in the cells that can hydrolyse the cellulose and glucans present in the *Nannochloropsis* cells. In the present study we in fact observed a few glycosidic hydrolases including betaglucosidase, endoglucanase, and lactase in the *Nannochloropsis* proteome (Supplementary 2). The overall abundance of proteins with cellulase activity was seen to increase during incubation (albeit, not statistically significantly, Figure 3.4), with alpha glucosidase and endo glucanase found to be significantly upregulated (Table 3.1). These observations coupled with the thinning of the cellulose layer of the cell walls by Halim et al. (2019a), provides further evidence that *Nannochloropsis* cells degrade the cellulose component of their walls as a resource for subsequent glycolysis.

Following cellulose hydrolysis, the glycolytic pathway includes several steps catalysed by different enzymes that lead to the generation of the central metabolite pyruvate. Figure 3.5 summarises the different steps involved in glycolysis along with the associated enzymes found through the proteomic analysis in this study. This comprises of two main stages: upper glycolysis which is energy consuming, and lower glycolysis which is energy yielding. The upper glycolytic pathway produces two glycerol-3-phosphate (G3P) molecules, consuming one glucose molecule and 2ATP molecules that will be eventually converted to two pyruvate molecules along with 4 ATP and 2 NADH via the lower glycolytic pathway. Therefore, the glycolytic pathway is able to produce 2 ATP that can be used as energy reserves for cellular processes (Atteia et al., 2013). The key steps in the glycolytic pathway that generate ATP are catalysed by the enzymes phosphoglycerate kinase (PGK) and pyruvate kinase (PK) resulting in the production of two pyruvate molecules.

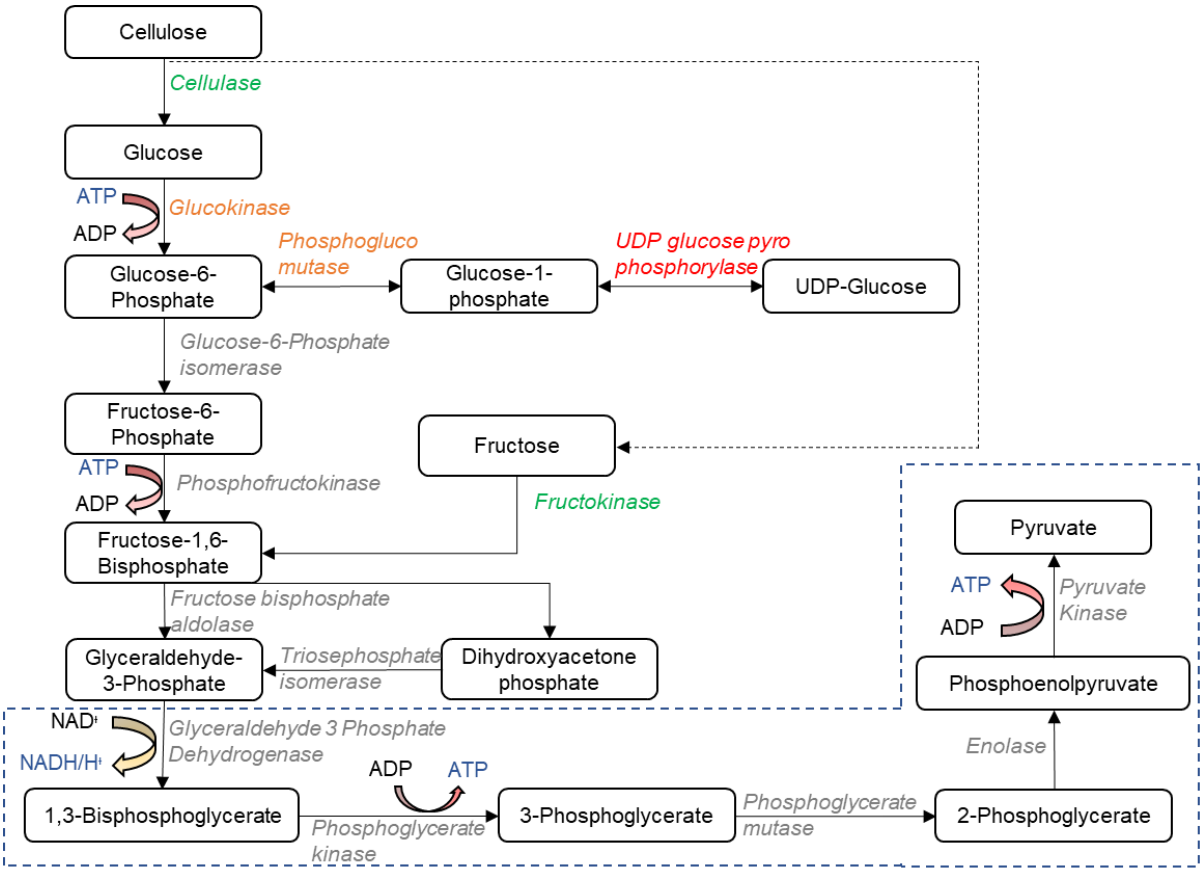

Figure 3.5: Localisation of the main enzymes and intermediates identified in this study involved in ATP production through the glycolytic pathway. Green represents significantly upregulated enzymes, grey upregulated but not significantly, orange down-regulated but not significantly, and red significantly down regulated enzymes. Blue dashed line indicates the reactions in the lower glycolytic pathway.

Importantly, all enzymes involved in glycolysis were observed in the *Nannochloropsis* proteome. Apart from the cellulases mentioned earlier, only fructokinase (FK) catalysing the conversion of fructose to fructose-1-phosphate (F1P) was significantly upregulated during dark anoxic incubation (Table 3.1). However, as fructose was not previously found to be abundant in *Nannochloropsis sp.* (Halim et al., 2019a, Scholz et al., 2014), the reason for this is unclear.

Generally, the limiting steps in the glycolytic pathway have found to be those catalysed by glucokinase (GK) and phosphofructokinase (PFK), as they consume energy for the forward reaction (Abbriano et al., 2018). In the present study, GK was downregulated while PFK was upregulated, although both changes were not statistically significant. Overexpression of PFK has previously led to an increased glycolytic activity in the diatom *Thalassiosira pseudonana* (Abbriano et al., 2018), and it could be that GK is not the rate-limiting step in *Nannochloropsis* sp. glycolytic pathway. Further in-depth studies are required to determine the rate-limiting steps in the *Nannochloropsis* glycolytic pathway.

When considering the other enzymes involved in the glycolytic pathway, although the difference was not statistically significant, most of the enzymes showed an increase in their fold change when compared with the unincubated, fresh cells. This suggests *Nannochloropsis* sp. cells attempt to upregulate glycolytic metabolism to produce the energy required for cellular processes in response to the stress conditions. Reciprocally, Uridine diphosphate (UDP) glucose pyrophosophorylase, which is needed for glucose activation in the synthesis of cellulose and other glucose polymers (Scholz et al., 2014), was downregulated. The absence of photosynthetically fixed carbon during dark anoxia reduces the need for this enzyme for cellulose or chrysolaminarin synthesis.

Among the statistically unchanged enzymes, fructose bisphosphate aldolase (FBA), glyceraldehyde 3 phosphate dehydrogenase (G3PDH), pyruvate hydratase (PHy) and PK nonetheless showed an increasing trend during incubation (Figure 7.4). FBA has been found to be rate-limiting in upper glycolysis in *E.coli* (Kitamura et al., 2021).

The conversion of NAD+ to NADH in the lower glycolytic pathway catalysed by the enzyme G3P leads to an imbalance in the redox state of the cell. Therefore, the pyruvate produced must be metabolised to regenerate the oxidised NADH or FADH2 and to produce more ATP in subsequent processes (Atteia et al., 2013). The following section discusses on the different fermentative and other pathways that were identified in the *Nannochloropsis* proteome that can be used to maintain cellular redox balance.

3.4.4 Fermentation and other related pathways for maintaining cellular redox balance

As discussed, under dark anoxic conditions *Nannochloropsis* cells are proposed to undertake glycolysis to produce energy required for cellular metabolism. In the absence of oxygen needed to re-oxidise the NADH to produce NAD+ via the citric acid /Krebs cycle fermentative pathways are required which lead to the formation of various organic acids, alcohols and gases such as H_2 and CO_2 depending on the pathways undertaken by the cells (Mus et al., 2007, Halim et al., 2019a). In eukaryotes like *Nannochloropsis*, fermentation involves the conversion of the pyruvate produced during glycolysis into a range of end-products including ethanol, lactate, acetate, succinate and propionate, via intermediates such as acetyl CoA (Atteia et al., 2013). Figure 3.6 summarises all the fermentation and associated pathways *Nannochloropsis* cells are proposed to undertake during dark anoxic incubation based on proteomic data obtained. Each of these pathways is discussed in detail in this section.

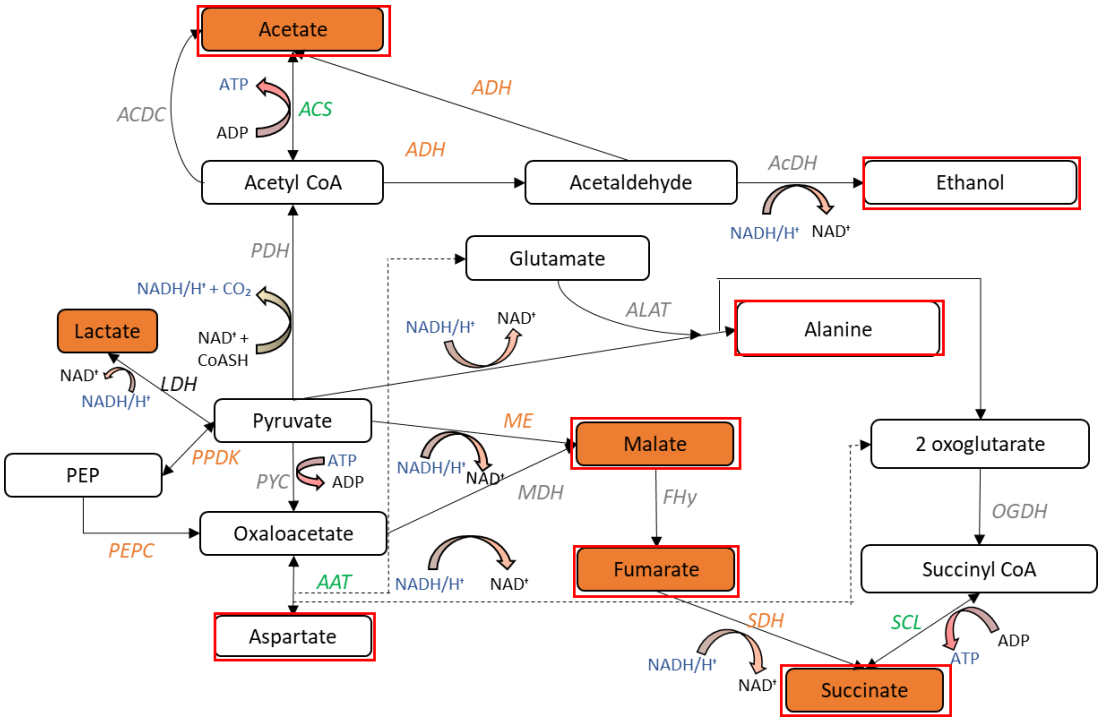

Figure 3.6: Identified enzymes and associated fermentative pathways in *Nannochloropsis* sp. under dark anoxia. Fermentative end products associated with the identified pathways are indicated by red boxes, with filled orange boxes representing end products that were previously detected during dark anoxic incubation of *Nannochloropsis* sp. (Halim et al., 2019a). PPDK Pyruvate phosphate dikinase, PDH Pyruvate dehydrogenase, PYC Pyruvate carboxylase, ACS Acetate synthase, ACDC Acetyl CoA deacylase, ADH Aldehyde dehydrogenase, AcDH Alcohol Dehydrogenase, ALAT Alanine aminotransferase, CS Citrate synthase, ME malic enzyme, OGDH oxoglutarate dehydrogenase, SCL Succinyl CoA lyase, SDH Succinate dehydrogenase, FHy fumarate hydratase, MDH Malate dehydrogenase, AAT Aspartate aminotransferase, LDH Lactate dehydrogenase. Green: significantly increased. Grey: increased but not significantly. Orange: decreased but not significantly Black: not found.

Pyruvate to acetyl CoA conversion is a crucial step in carbon energy metabolism, and this can be catalysed by the pyruvate dehydrogenase complex (PDH), pyruvate:ferredoxin oxidoreductase (PFO) (Atteia et al., 2013), or pyruvate formate lyase (PFL) (Mus et al., 2007), of which only the pathway through PDH was observed in *Nannochloropsis* based on our observations through proteomic analysis. Neither PFO nor PFL were found in the proteome of *Nannochloropsis*. The PDH enzyme complex did not show a significant increase during incubation, but the average relative abundance of the proteins did increase slightly by around 26±5% (Figure 7.4).

Acetyl CoA can be further metabolised into ethanol through alcohol dehydrogenase (AcDH) and aldehyde dehydrogenase (ADH) (also called ethanolic fermentation), as has been confirmed in *Chlamydomonas* (Mus et al., 2007). During dark anoxic incubation of *Nannochloropsis*, AcDH (Figure 7.5) was seen to be upregulated, although the difference was not statistically significant.

Aldehyde dehydrogenase was present, but not changed significantly. The presence of these enzymes indicates the ability of *Nannochloropsis* sp. cells to use these pathways. The lack of upregulation of these enzymes suggests that this pathway was not favoured. This is consistent with our previous study on dark anoxic incubation of *Nannochloropsis* in which ethanol was not detected as a fermentation end product (Halim et al., 2019a). There are reports showing the accumulation of esters following long storage of *Nannochloropsis* and *Isochrysis* under dark conditions (Balduyck et al., 2017), which could indicate that any ethanol that was produced during dark anoxic metabolism was consumed in reactions with lipids to produce esters. Apart from the ethanol fermentation pathway, acetyl CoA can be converted to acetate through 5 different pathways in eukaryotes to convert ADP to ATP. These include acyl CoA thioesterase (ASCT) pathway, acetate succinate CoA transferase (ACST) pathway (Atteia et al., 2013) Acyl CoA deacylase pathway, acyl CoA synthetase pathway and the phosphotransacetylase (PTA) and acetate kinase (ACK) pathway (Mus et al., 2007). Among these the PTA, ACK and ASCT enzymes were not found in the *Nannochloropsis* proteome. The PTA ACK pathway was the dominant pathway under dark anoxic conditions in *Chlamydomonas reinhardtii* (Catalanotti et al., 2013a). However, during incubation of *Nannochloropsis*, only the ACS pathway and the ACDC pathway were observed, with ACS significantly overexpressed (Figure 3.5, Table 3.1), similar to previous observations in *Chlamydomonas* cells (Mus et al., 2007).

The next common pathway of fermentation is the lactate fermentation, catalysed by lactate dehydrogenase (LDH) (Kato-Noguchi, 2006). Lactic acid was previously detected in *Nannochloropsis* subjected to dark anoxic incubation (Halim et al., 2019a) indicating that lactate as well as ethanolic fermentation were used to re-oxidise NADH. LDH is indeed present in the *Nannochloropsis* proteome found through a protein search in the UniProt database (Bateman, 2021), however it was not detected in the proteomic samples in the present study. It is possible that the protein was expressed at low levels and was present below the limits of detection.

A rapid increase in alanine aminotransferase (ALAT) (Rocha et al., 2010) and a resultant accumulation of alanine (Kato-Noguchi, 2006) has been observed in plant cells under anoxia. ALAT catalyses the transamination of pyruvate to alanine and conversion of pyruvate and glutamine to alanine and 2-oxoglutaric acid, playing a key role in carbon and nitrogen metabolism in plants (Kato-Noguchi, 2006). It has been proposed that functions of ALAT during anoxic conditions are to reduce cellular acidity (Catalanotti et al., 2013a), prevent the loss of carbon through the fermentation pathways, and to yield ATP through substrate level phosphorylation (Yang et al., 2015). In addition, the produced 2-oxoglutarate is converted to succinyl CoA catalysed by oxoglutarate dehydrogenase (OGDH) and succinyl CoA to succinate via succinyl CoA lyase (SCL) releasing another ATP molecule (Rocha et al., 2010). In this study, all of these enzymes were found to be present, with ALAT and SCL found to increase in abundance during dark anoxic incubation (the increase in SCL but not ALAT was statistically significant). Although the presence of alanine was not previously verified (Halim et al., 2019a), the presence of all necessary enzymes suggests this pathway could be active in *Nannochloropsis*.

The two pathways discussed above, a part of the reverse tricarboxylic acid (TCA) cycle and part of the TCA cycle starting from 2 oxoglutarate, both lead to the production of succinate, which was previously observed in dark anoxic incubation of *Nannochloropsis* (Halim et al., 2019a). It was proposed previously that succinate biosynthesis occurs through the reductive TCA cycle in *Euglena gracilis* under dark anoxic conditions (Tomita et al., 2016). For this, aspartate is converted to oxaloacetate (OAA), which is then reduced to succinate by aspartate aminotransferase (AAT). A rapid drop in aspartate coupled with an increase in alanine and succinate has previously been observed during dark anaerobic treatment of the microalga *Selenastrum minutum* (Vanlerberghe et al., 1990). The presence of all required enzymes including a significant increase in AAT (Table 3.1), suggests that this is another possible pathway used by *Nannochloropsis* during dark anoxia.

Under anaerobic conditions, a partial reductive TCA cycle where OAA is reduced to malate, fumarate and succinate was shown previously for *Euglena gracilis* under dark anaerobic conditions (Vanlerberghe et al., 1989). OAA is reduced to malate by cytosolic malate dehydrogenase (MDH) to reoxidise nicotinamide adenine dinucleotide (NAD) + hydrogen (H) (NADH) (Atteia et al., 2013). The malate can subsequently be metabolised to succinate through fumarate via part of the reverse TCA cycle (Tomita et al., 2016). Fumarate reduction to succinate results in the oxidation of NADH and ATP production, hence, it is a productive anaerobic metabolism. This pathway seems to be active during dark anoxia incubation in *Nannochloropsis*, with a slight increase in MDH found during incubation, along with the presence of fumarate hydratase and succinate dehydrogenase (Figure 7.5), as well as previously detected malate, fumarate and succinate (Halim et al., 2019a).

In summary, it can be concluded that during dark anoxia *Nannochloropsis* cells produce ATP through glycolysis and a range of fermentative pathways. However, it should be noted that the amount of energy produced during dark anoxia is significantly lower than that which can be produced by photosynthesis or by aerobic respiration of cellular carbon reserves in the presence of oxygen. This represents a secondary stress on the cells, which need to limit energy usage to support only the most critical functions.

3.4.5 Effect of dark anoxic incubation on photosynthetic and light harvesting proteins

Previously, when *Nannochloropsis* sp. cells grown in high light were transferred to low light conditions, the volume of the chloroplasts of the cells, the photosynthetic unit (PSU) density, thylakoid surface area and the pigmentation all increased representing a 1.7-fold increase in the overall light harvesting potential (Fisher et al., 1998). This demonstrates that, when cells still have a photosynthetic energy supply, they can compensate for limited light availability by diverting resources towards increasing their light harvesting ability.

In contrast, due to the complete lack of light during incubation, the cells cannot perform photosynthesis, and as discussed above, have a limited energy supply. While cells could potentially reduce resources devoted to unused photosynthetic apparatus, photosynthetic microalgae are naturally subjected to cyclical light availability and should not be programmed to completely

deconstruct its photosynthetic apparatus during periods of darkness. In line with this, *Chlamydomonas* has been found to retain but downregulate its photosynthetic apparatus and enzymes related to chlorophyll synthesis during dark anoxia (Hemschemeier et al., 2013). In comparison, in this study, while there was a reduction in two light harvesting proteins (W7TX20, W7T8I0), there was an increase in magnesium chelatase and geranylgeranyl reductase, two major enzymes involved in the chlorophyll biosynthetic pathways (Table 3.1).

Photosynthetic pigments are a critical component of photosynthetic apparatus. Halim et al. (2019a) observed the chlorophyll a content in *Nannochloropsis* sp. to be degraded to pheophytin a (which is chlorophyll a lacking a Mg^{2+} ion) during dark anoxic incubation. As discussed above, the elevated temperature and dark anoxic environment stress the cells and limit energy availability. Chlorophyll degradation could be due to uncontrolled reactions with organic acids produced intercellularly due to fermentation or as an action of chlorophyllide oxygenase present in the cells (Halim et al., 2019a, Doi et al., 2001). It has been observed that acidic conditions and high temperatures result in the degradation of chlorophyll a to pheophytin a (Yilmaz and Gökmen, 2016, Sánchez et al., 2014). To compensate for this degradation, cells can try to produce more chlorophyll. Consistent with this hypothesis, the amount of degradation product of chlorophyll a, pheophytin a, was higher in the incubated samples than the chlorophyl content in the cells prior to incubation in Halim et al. (2019a).

Apart from these, other major photosynthetic related enzymes including the light harvesting complexes and Photosystem I and II related proteins showed a slightly decreasing trend although the difference was not found to be significant (Figure 3.4) similar to that previously observed in *Euglena gracilis*.(Yoshida et al., 2016) Light harvesting proteins were previously seen to be down regulated under dark conditions (Kennedy et al., 2019), similarly two light harvesting proteins (W7TX20, W7T8I0) showed a significant decrease in abundance (Table 3.1). There was no significant change in ATP synthases, consistent with what has been previously been observed in other microalgae (*Fragilariopsis cylindrus* and *Chlamydomonas reinhardtii*) (Kennedy et al., 2019, Hemschemeier et al., 2013). The PSI reaction subunit increased in abundance (Table 3.1), although unexpected similar observations have previously been observed (Yang et al., 2015, Gans and Rebeille, 1990). None of the proteins related to the Calvin Benson cycle, used for carbon fixation and light-dependant reactions, were significantly changed over the dark anoxic incubation period. Thus, based on these observations, it appears that as a photosynthetic microorganism, *Nannochloropsis* sp. tries to maintain their photosynthetic machinery even during prolonged dark anoxic stress conditions.

3.4.6 Effect of dark anoxic incubation on other major cellular metabolic processes

Apart from the energy generation and stress responses in the cells, the enzymes related to protein synthesis, including transcription, translation and protein folding were significantly increased (Table 3.1). This is consistent with a previous study on *Chlamydomonas* in which transcripts encoding for transcription/translation regulation factors were seen to be increased during dark

anoxia (Mus et al., 2007). The increased levels of protein synthesis enzymes, despite the limited energy availability, may be a result of retooling in response to dark anoxic stresses. These stresses appear to trigger multifaceted cellular adaptations that require retooling of metabolic pathways, leading to an increased requirement for the synthesis of new/different proteins.

Signalling and transport proteins are required for cellular metabolism and were also affected during dark anoxia incubation (Table 3.1). The up-regulation of signalling proteins in response to different stress conditions has previously been observed in plants as well as microalgae such as Chlamydomonas (Zou et al., 2010, Hemschemeier et al., 2013), where they play a major role when acclimating to stress conditions. The accumulation of amino acid transporters (A0A4D9CTY7) and several transmembrane transporters (A0A4D9CQ73, A0A4D9CY02, A0A4D9D9I1) (Table 3.1) may be related to cell response to the stress conditions. For example, fermentation end-products may need to be transported and excreted from the cells in order to prevent acidosis (Chang et al., 2000).

UDP sulfoquinovose synthase enzyme, which is responsible for the formation of the membrane lipid sulfoquinovosl diacylglycerol (SQDG), was upregulated during dark anoxia (Table 3.1), similar to what was observed in diatoms (Kennedy et al., 2019). SQDG is important for maintaining thylakoid membrane integrity and protecting the functionality of ATP synthase (Kennedy et al., 2019).

3.4.7 Practical implications

Dark anoxia incubation is a low-cost method to weaken the cell walls of *Nannochloropsis* to improve the efficiency of mechanical cell rupture, and facilitate the recovery of lipid or protein products (Halim et al., 2016a). However, it was seen here to affect the integrity of the cell proteins and lipids. This section discusses the practical implications of these findings and possible future research areas that would help widen the understanding of the process.

The weakening of cell walls was found to be due to the degradation of cellulose during anoxic metabolism in *Nannochloropsis* cells (Halim et al., 2019a). However, the results here show that the cell weakening process is intertwined with the degradation of the proteins into peptides and lipids into free fatty acids and lipid peroxides. The presence of high amounts of FFAs can be detrimental for both biodiesel production (López et al., 2015) and food applications (Balduyck et al., 2017) due to the issues associated with downstream processing, and off-flavours and oxidation, respectively. Other aspects of lipid chemistry are also of practical importance, warranting an in-depth analysis to elucidate the effects on the overall lipid profile in *Nannochloropsis*. Production of wax esters has been observed previously in *Euglina gracili*s in response to anoxic fermentation (Tomita et al., 2016), and it is hypothesised that the absence of ethanol as a fermentative end-product in *Nannochloropsis* could be due to reactions with TAG that lead to ester formation. Therefore, in addition to looking at the FFA and lipid peroxidation, an in-depth characterization of the lipid profile will provide a better understanding on how dark anoxia incubation affects the overall quality of the lipids.

When considering the progression of lipid degradation during dark anoxic incubation, it was seen that the FFA content increased most significantly after about 24 h. The late yet dramatic increase in FFA can be related to the loss of cellular integrity as a result of inadequate energy production and the inability of the cells to actively metabolise and control the activity of lipases and other catabolic enzymes (Rawyler et al., 1999). Therefore, the process of incubation will need to be optimised such that it maximises the degree of cell weakening while minimising the degradation of the biomacromolecules to avoid the detrimental effects. As the degradation of cellulose appears to be an active pre-cursor of uncontrolled cellular degradation, it may be possible to find a more favourable incubation temperature (20-37 ℃) and time (< 24 h) combination that achieves cell weakening with minimal lipid hydrolysis. Since the results from previous studies have demonstrated that the majority of cell-wall thinning in *Nannochloropsis* takes place within the first 24 h of dark-anoxia [8, 53], extending the incubation beyond this period can be concluded to confer no further downstream benefit.

As well as valuable lipids, microalgae are rich in pigments containing antioxidative properties. In addition to the effect on the lipids, the heat stress and potential changes in the cytosolic pH could have a negative impact on these pigments and their antioxidative properties. Halim et al. (2019a) found the chlorophyll pigments to degrade to pheophytin during incubation, despite the observed increase in the enzymes in the chlorophyll biosynthetic pathway. Therefore, it is worthwhile looking at the effect on the pigment profile, the antioxidative and other bioactive properties of microalgae cells following dark anoxia incubation.

With respect to the protein content, it would be useful to determine the abundance of free amino acids during dark anoxic incubation to confirm the effects of AAT and ALAT, leading to an increase in alanine and a drop in aspartate proposed in this study. Also, although the proteins can be considered to be ‘degraded’ into peptides, it would be worth characterising these peptides and to look for potential bioactive properties which could be of practical interest for nutritional applications.

3.5 Conclusions

The current study investigated the effects of dark anoxic incubation on the proteins and lipids of *Nannochloropsis* sp., including an in-depth proteomic analysis to gain a mechanistic understanding of the cellular responses.

Dark anoxia incubation induced stress conditions lead to the degradation of lipids and proteins in *Nannochloropsis* sp. over prolonged time periods. The cells altered their metabolism in response to the stress conditions of incubation, in particular the elevated temperature and dark anoxic conditions. In the absence of light and oxygen, glycolytic and fermentative pathways were used to produce energy and to maintain the redox balance of the cells during incubation. The key glycolytic and fermentative pathways used by *Nannochloropsis* cells to survive dark anoxia incubation are identified from the proteomic data and previously reported end-product analysis. Stress conditions led to the over-expression of proteins with oxidoreductase activity, gene expression, some

enzymes in the glycolytic and fermentative pathways, chlorophyll biosynthesis and violaxanthin cycle, suggesting these processes were affected during incubation. Among the proteins showing higher activity, of more interest were a phospholipase, proteases and cellulases that were responsible for the lipid, protein and cellulose degradations, respectively. As the incubation time increased, the energy produced through the glycolytic and fermentative pathways likely becomes inadequate to maintain the cellular integrity and to continue the metabolic processes. This culminated in the break-down of cellular integrity and the uncontrolled degradation of protein and lipids. Considering the aspects of cell weakening and the quality of microalgal products, this study emphasizes the importance of optimising the incubation time, in order to avoid or minimise the unnecessary degradation of cellular components. In addition, the proposed pathways and the identified enzymes will benefit further research on *Nannochloropsis* and dark anoxic fermentation on microalgae species.

3.6 References

ABBRIANO, R., VARDAR, N., YEE, D. & HILDEBRAND, M. 2018. Manipulation of a glycolytic regulator alters growth and carbon partitioning in the marine diatom Thalassiosira pseudonana. *Algal research,* 32**,** 250-258.

AGUIRRE, A.-M., BASSI, A. & SAXENA, P. 2013. Engineering challenges in biodiesel production from microalgae. *Critical reviews in biotechnology,* 33**,** 293-308.

ATTEIA, A., VAN LIS, R., TIELENS, A. G. & MARTIN, W. F. 2013. Anaerobic energy metabolism in unicellular photosynthetic eukaryotes. *Biochimica et Biophysica Acta (BBA)-Bioenergetics,* 1827**,** 210-223.

BAI, X., SONG, H., LAVOIE, M., ZHU, K., SU, Y., YE, H., CHEN, S., FU, Z. & QIAN, H. 2016. Proteomic analyses bring new insights into the effect of a dark stress on lipid biosynthesis in Phaeodactylum tricornutum. *Scientific reports,* 6**,** 1-10.

BALDUYCK, L., BIJTTEBIER, S., BRUNEEL, C., JACOBS, G., VOORSPOELS, S., VAN DURME, J., MUYLAERT, K. & FOUBERT, I. 2016. Lipolysis in T-Isochrysis lutea during wet storage at different temperatures. *Algal research,* 18**,** 281-287.

BALDUYCK, L., DEJONGHE, C., GOOS, P., JOOKEN, E., MUYLAERT, K. & FOUBERT, I. 2019. Inhibition of lipolytic reactions during wet storage of T-Isochrysis lutea biomass by heat treatment. *Algal research,* 38**,** 101388.

BALDUYCK, L., GOIRIS, K., BRUNEEL, C., MUYLAERT, K. & FOUBERT, I. 2015. Stability of Valuable Components during Wet and Dry Storage. *Handbook of Marine Microalgae.* Elsevier.

BALDUYCK, L., STOCK, T., BIJTTEBIER, S., BRUNEEL, C., JACOBS, G., VOORSPOELS, S., MUYLAERT, K. & FOUBERT, I. 2017. Integrity of the microalgal cell plays a major role in the lipolytic stability during wet storage. *Algal research,* 25**,** 516-524.

BATEMAN, A. 2021. (2021) UniProt: the universal protein knowledgebase in. *Nucleic Acids Res,* 49**,** D480-D489.

BERGE, J.-P., GOUYGOU, J.-P., DUBACQ, J.-P. & DURAND, P. 1995. Reassessment of lipid composition of the diatom, Skeletonema costatum. *Phytochemistry,* 39**,** 1017-1021.

BERGES, J. A. & FALKOWSKI, P. G. 1998. Physiological stress and cell death in marine phytoplankton: induction of proteases in response to nitrogen or light limitation. *Limnology and Oceanography,* 43**,** 129-135.

BIDLE, K. D. 2016. Programmed cell death in unicellular phytoplankton. *Current Biology,* 26**,** R594-R607.

BLOKHINA, O., VIROLAINEN, E. & FAGERSTEDT, K. V. 2003. Antioxidants, oxidative damage and oxygen deprivation stress: a review. *Annals of botany,* 91**,** 179-194.

CAPORGNO, M. P. & MATHYS, A. 2018. Trends in microalgae incorporation into innovative food products with potential health benefits. *Frontiers in nutrition,* 5**,** 58.

CATALANOTTI, C., YANG, W., POSEWITZ, M. C. & GROSSMAN, A. R. 2013a. Fermentation metabolism and its evolution in algae. *Frontiers in plant science,* 4**,** 150.

CATALANOTTI, C., YANG, W., POSEWITZ, M. C. & GROSSMAN, A. R. 2013b. Fermentation metabolism and its evolution in algae. *Frontiers in plant science,* 4**,** 150-150.

CHANG, W. W., HUANG, L., SHEN, M., WEBSTER, C., BURLINGAME, A. L. & ROBERTS, J. K. 2000. Patterns of protein synthesis and tolerance of anoxia in root tips of maize seedlings acclimated to a low-oxygen environment, and identification of proteins by mass spectrometry. *Plant physiology,* 122**,** 295-318.

CHUA, E. T., DAL'MOLIN, C., THOMAS-HALL, S., NETZEL, M. E., NETZEL, G. & SCHENK, P. M. 2020. Cold and dark treatments induce omega-3 fatty acid and carotenoid production in *Nannochloropsis* oceanica. *Algal Research,* 51**,** 102059.

DEMUEZ, M., MAHDY, A., TOMÁS-PEJÓ, E., GONZÁLEZ-FERNÁNDEZ, C. & BALLESTEROS, M. 2015. Enzymatic cell disruption of microalgae biomass in biorefinery processes. *Biotechnology and bioengineering,* 112**,** 1955-1966.

DOI, M., INAGE, T. & SHIOI, Y. 2001. Chlorophyll degradation in a Chlamydomonas reinhardtii mutant: an accumulation of pyropheophorbide a by anaerobiosis. *Plant and Cell Physiology,* 42**,** 469-474.

FAN, M., SUN, X., LIAO, Z., WANG, J., LI, Y. & XU, N. 2018. Comparative proteomic analysis of Ulva prolifera response to high temperature stress. *Proteome science,* 16**,** 1-22.

FISHER, T., BERNER, T., ILUZ, D. & DUBINSKY, Z. 1998. The kinetics of the photoacclimation response of *Nannochloropsis* sp.(Eustigmatophyceae): a study of changes in ultrastructure and PSU density. *Journal of Phycology,* 34**,** 818-824.

GANS, P. & REBEILLE, F. 1990. Control in the dark of the plastoquinone redox state by mitochondrial activity in Chlamydomonas reinhardtii. *Biochimica et Biophysica Acta (BBA)-Bioenergetics,* 1015**,** 150-155.

GHEYSEN, L., BERNAERTS, T., BRUNEEL, C., GOIRIS, K., VAN DURME, J., VAN LOEY, A., DE COOMAN, L. & FOUBERT, I. 2018. Impact of processing on n-3 LC-PUFA in model systems enriched with microalgae. *Food chemistry,* 268**,** 441-450.

HALIM, R., HILL, D. R. A., HANSSEN, E., WEBLEY, P. A., BLACKBURN, S., GROSSMAN, A. R., POSTEN, C. & MARTIN, G. J. O. 2019a. Towards sustainable microalgal biomass processing: anaerobic induction of autolytic cell-wall self-ingestion in lipid-rich *Nannochloropsis* slurries. *Green Chemistry,* 21**,** 2967-2982.

HALIM, R., HILL, D. R. A., HANSSEN, E., WEBLEY, P. A. & MARTIN, G. J. O. 2019b. Thermally coupled dark-anoxia incubation: A platform technology to induce auto-fermentation and thus cell-wall thinning in both nitrogen-replete and nitrogen-deplete *Nannochloropsis* slurries. *Bioresource Technology,* 290**,** 121769.

HALIM, R., WEBLEY, P. A. & MARTIN, G. J. 2016. The CIDES process: fractionation of concentrated microalgal paste for co-production of biofuel, nutraceuticals, and high-grade protein feed. *Algal Research,* 19**,** 299-306.

HEMSCHEMEIER, A., CASERO, D., LIU, B., BENNING, C., PELLEGRINI, M., HAPPE, T. & MERCHANT, S. S. 2013. COPPER RESPONSE REGULATOR1–dependent and–independent responses of the Chlamydomonas reinhardtii transcriptome to dark anoxia. *The Plant Cell,* 25**,** 3186-3211.

INUI, H., MIYATAKE, K., NAKANO, Y. & KITAOKA, S. 1982. Wax ester fermentation in Euglena gracilis. *FEBS letters,* 150**,** 89-93.

KANGANI, C. O., KELLEY, D. E. & DELANY, J. P. 2008. New method for GC/FID and GC–C-IRMS analysis of plasma free fatty acid concentration and isotopic enrichment. *Journal of Chromatography B,* 873**,** 95-101.

KATO-NOGUCHI, H. 2006. Pyruvate metabolism in rice coleoptiles under anaerobiosis. *Plant Growth Regulation,* 50**,** 41-46.

KENNEDY, F., MARTIN, A., BOWMAN, J. P., WILSON, R. & MCMINN, A. 2019. Dark metabolism: a molecular insight into how the Antarctic sea-ice diatom Fragilariopsis cylindrus survives long-term darkness. *New Phytologist,* 223**,** 675-691.

KINOSHITA, T., FUKUZAWA, H., SHIMADA, T., SAITO, T. & MATSUDA, Y. 1992. Primary structure and expression of a gamete lytic enzyme in Chlamydomonas reinhardtii: similarity of functional domains to matrix metalloproteases. *Proceedings of the National Academy of Sciences,* 89**,** 4693-4697.

KITAMURA, S., SHIMIZU, H. & TOYA, Y. 2021. Identification of a rate-limiting step in a metabolic pathway using the kinetic model and in vitro experiment. *Journal of bioscience and bioengineering,* 131**,** 271-276.

KOBAYASHI, Y., HARADA, N., NISHIMURA, Y., SAITO, T., NAKAMURA, M., FUJIWARA, T., KUROIWA, T. & MISUMI, O. 2014. Algae sense exact temperatures: small heat shock proteins are expressed at the survival threshold temperature in Cyanidioschyzon merolae and Chlamydomonas reinhardtii. *Genome biology and evolution,* 6**,** 2731-2740.

KONG, F., ROMERO, I. T., WARAKANONT, J. & LI-BEISSON, Y. 2018. Lipid catabolism in microalgae. *New Phytologist,* 218**,** 1340-1348.

LEE, A. K., LEWIS, D. M. & ASHMAN, P. J. 2012. Disruption of microalgal cells for the extraction of lipids for biofuels: processes and specific energy requirements. *Biomass and bioenergy,* 46**,** 89-101.

LÓPEZ, E. N., MEDINA, A. R., MORENO, P. A. G., CALLEJÓN, M. J. J., CERDÁN, L. E., VALVERDE, L. M., LÓPEZ, B. C. & GRIMA, E. M. 2015. Enzymatic production of biodiesel from *Nannochloropsis* gaditana lipids: Influence of operational variables and polar lipid content. *Bioresource technology,* 187**,** 346-353.

MAEHASHI, K. & HUANG, L. 2009. Bitter peptides and bitter taste receptors. *Cellular and molecular life sciences,* 66**,** 1661-1671.

MARTIN, G. J. O., HILL, D. R. A., OLMSTEAD, I. L. D., BERGAMIN, A., SHEARS, M. J., DIAS, D. A., KENTISH, S. E., SCALES, P. J. & BOTTÉ, C. Y. 2014. Lipid profile remodeling in response to nitrogen deprivation in the microalgae *Chlorella* sp. (Trebouxiophyceae) and *Nannochloropsis* sp. (Eustigmatophyceae). *PlosOne,* 9**,** e103389.

MATSUDA, Y., SAITO, T., YAMAGUCHI, T. & KAWASE, H. 1985. Cell wall lytic enzyme released by mating gametes of Chlamydomonas reinhardtii is a metalloprotease and digests the sodium perchlorate-insoluble component of cell wall. *Journal of Biological Chemistry,* 260**,** 6373-6377.

MEDINA, C., RUBILAR, M., SHENE, C., TORRES, S. & VERDUGO, M. 2015. Protein fractions with techno-functional and antioxidant properties from *Nannochloropsis* gaditana microalgal biomass. *Journal of Biobased Materials and Bioenergy,* 9**,** 417-425.

MINHAS, A. K., HODGSON, P., BARROW, C. J. & ADHOLEYA, A. 2016. A review on the assessment of stress conditions for simultaneous production of microalgal lipids and carotenoids. *Frontiers in microbiology,* 7**,** 546.

MONTAINI, E., ZITTELLI, G. C., TREDICI, M., GRIMA, E. M., SEVILLA, J. F. & PÉREZ, J. S. 1995. Long-term preservation of Tetraselmis suecica: influence of storage on viability and fatty acid profile. *Aquaculture,* 134**,** 81-90.

MUS, F., DUBINI, A., SEIBERT, M., POSEWITZ, M. C. & GROSSMAN, A. R. 2007. Anaerobic acclimation in Chlamydomonas reinhardtii: anoxic gene expression, hydrogenase induction, and metabolic pathways. *Journal of Biological Chemistry,* 282**,** 25475-25486.

NAPAN, K., CHRISTIANSON, T., VOIE, K. & QUINN, J. C. 2015. Quantitative assessment of microalgae biomass and lipid stability post-cultivation. *Frontiers in Energy Research,* 3**,** 15.

NGUYEN, H. T., ONG, L., HOQUE, A., KENTISH, S. E., WILLIAMSON, N., ANG, C.-S. & GRAS, S. L. 2017. A proteomic characterization shows differences in the milk fat globule membrane of buffalo and bovine milk. *Food bioscience,* 19**,** 7-16.

OLMSTEAD, I. L., HILL, D. R., DIAS, D. A., JAYASINGHE, N. S., CALLAHAN, D. L., KENTISH, S. E., SCALES, P. J. & MARTIN, G. J. 2013a. A quantitative analysis of microalgal lipids for optimization of biodiesel and omega-3 production. *Biotechnology and bioengineering,* 110**,** 2096-2104.

OLMSTEAD, I. L., KENTISH, S. E., SCALES, P. J. & MARTIN, G. J. 2013b. Low solvent, low temperature method for extracting biodiesel lipids from concentrated microalgal biomass. *Bioresource technology,* 148**,** 615-619.

PAVELIC, D., ARPAGAUS, S., RAWYLER, A. & BRANDLE, R. 2000. Impact of post-anoxia stress on membrane lipids of anoxia-pretreated potato cells. A re-appraisal. *Plant Physiology,* 124**,** 1285-1292.

POHNERT, G. 2002. Phospholipase A2 activity triggers the wound-activated chemical defense in the diatom Thalassiosira rotula. *Plant physiology,* 129**,** 103-111.

RAWYLER, A., PAVELIC, D., GIANINAZZI, C., OBERSON, J. & BRAENDLE, R. 1999. Membrane lipid integrity relies on a threshold of ATP production rate in potato cell cultures submitted to anoxia. *Plant Physiology,* 120**,** 293-300.

ROCHA, M., LICAUSI, F., ARAÚJO, W. L., NUNES-NESI, A., SODEK, L., FERNIE, A. R. & VAN DONGEN, J. T. 2010. Glycolysis and the tricarboxylic acid cycle are linked by alanine aminotransferase during hypoxia induced by waterlogging of Lotus japonicus. *Plant Physiology,* 152**,** 1501-1513.

RUETHERS, T., TAKI, A. C., KARNANEEDI, S., NIE, S., KALIC, T., DAI, D., DADUANG, S., LEEMING, M., WILLIAMSON, N. A. & BREITENEDER, H. 2021. Expanding the allergen repertoire of salmon and catfish. *Allergy,* 76**,** 1443-1453.

RUETHERS, T., TAKI, A. C., NUGRAHA, R., CAO, T. T., KOEBERL, M., KAMATH, S. D., WILLIAMSON, N. A., O'CALLAGHAN, S., NIE, S. & MEHR, S. S. 2019. Variability of allergens in commercial fish extracts for skin prick testing. *Allergy,* 74**,** 1352-1363.

RYCKEBOSCH, E., MUYLAERT, K. & FOUBERT, I. 2012. Optimization of an analytical procedure for extraction of lipids from microalgae. *Journal of the American Oil Chemists' Society,* 89**,** 189-198.

SAMALA, S., YAN, J. & BAIRD, W. V. 1998. Changes in polar lipid fatty acid composition during cold acclimation in 'Midiron'and 'U3'bermudagrass. *Crop Science,* 38**,** 188-195.

SÁNCHEZ, C., BARANDA, A. B. & DE MARAÑÓN, I. M. 2014. The effect of high pressure and high temperature processing on carotenoids and chlorophylls content in some vegetables. *Food chemistry,* 163**,** 37-45.

SCHOLZ, M. J., WEISS, T. L., JINKERSON, R. E., JING, J., ROTH, R., GOODENOUGH, U., POSEWITZ, M. C. & GERKEN, H. G. 2014. Ultrastructure and composition of the *Nannochloropsis* gaditana cell wall. *Eukaryotic cell,* 13**,** 1450-1464.

SCHRODA, M., HEMME, D. & MÜHLHAUS, T. 2015. The Chlamydomonas heat stress response. *The Plant Journal,* 82**,** 466-480.

SEGOVIA, M. & BERGES, J. A. 2009. INHIBITION OF CASPASE-LIKE ACTIVITIES PREVENTS THE APPEARANCE OF REACTIVE OXYGEN SPECIES AND DARK-INDUCED APOPTOSIS IN THE UNICELLULAR CHLOROPHYTE DUNALIELLA TERTIOLECTA 1. *Journal of Phycology,* 45**,** 1116-1126.

SEGOVIA, M., HARAMATY, L., BERGES, J. A. & FALKOWSKI, P. G. 2003. Cell death in the unicellular chlorophyte Dunaliella tertiolecta. A hypothesis on the evolution of apoptosis in higher plants and metazoans. *Plant physiology,* 132**,** 99-105.

SHIN, J.-B., KREY, J. F., HASSAN, A., METLAGEL, Z., TAUSCHER, A. N., PAGANA, J. M., SHERMAN, N. E., JEFFERY, E. D., SPINELLI, K. J. & ZHAO, H. 2013. Molecular architecture of the chick vestibular hair bundle. *Nature neuroscience,* 16**,** 365-374.

SIMIONATO, D., BLOCK, M. A., LA ROCCA, N., JOUHET, J., MARECHAL, E., FINAZZI, G. & MOROSINOTTO, T. 2013. The Response of *Nannochloropsis* gaditana to Nitrogen Starvation Includes De Novo

Biosynthesis of Triacylglycerols, a Decrease of Chloroplast Galactolipids, and Reorganization of the Photosynthetic Apparatus. *Eukaryotic Cell,* 12**,** 665-676.

SOTO-SIERRA, L., STOYKOVA, P. & NIKOLOV, Z. L. 2018. Extraction and fractionation of microalgae-based protein products. *Algal research,* 36**,** 175-192.

SPELLMAN, D., MCEVOY, E., O'CUINN, G. & FITZGERALD, R. 2003. Proteinase and exopeptidase hydrolysis of whey protein: Comparison of the TNBS, OPA and pH stat methods for quantification of degree of hydrolysis. *International dairy journal,* 13**,** 447-453.

SPIDEN, E. M., YAP, B. H. J., HILL, D. R. A., KENTISH, S. E., SCALES, P. J. & MARTIN, G. J. O. 2013. Quantitative evaluation of the ease of rupture of industrially promising microalgae by high pressure homogenization. *Bioresource Technology,* 140**,** 165-171.

SRIRANGAN, S., SAUER, M.-L., HOWARD, B., DVORA, M., DUMS, J., BACKMAN, P. & SEDEROFF, H. 2015. Interaction of temperature and photoperiod increases growth and oil content in the marine microalgae Dunaliella viridis. *PloS one,* 10**,** e0127562.

TANAKA, K. 2009. The proteasome: overview of structure and functions. *Proceedings of the Japan Academy, Series B,* 85**,** 12-36.

TANAKA, Y., NISHIYAMA, Y. & MURATA, N. 2000. Acclimation of the photosynthetic machinery to high temperature in Chlamydomonas reinhardtii requires synthesis de novo of proteins encoded by the nuclear and chloroplast genomes. *Plant Physiology,* 124**,** 441-450.

TERASHIMA, M., SPECHT, M., NAUMANN, B. & HIPPLER, M. 2010. Characterizing the anaerobic response of Chlamydomonas reinhardtii by quantitative proteomics. *Molecular & Cellular Proteomics,* 9**,** 1514-1532.

TOMITA, Y., YOSHIOKA, K., IIJIMA, H., NAKASHIMA, A., IWATA, O., SUZUKI, K., HASUNUMA, T., KONDO, A., HIRAI, M. Y. & OSANAI, T. 2016. Succinate and lactate production from Euglena gracilis during dark, anaerobic conditions. *Frontiers in microbiology,* 7**,** 2050.

TRAN, N.-A. T., PADULA, M. P., EVENHUIS, C. R., COMMAULT, A. S., RALPH, P. J. & TAMBURIC, B. 2016. Proteomic and biophysical analyses reveal a metabolic shift in nitrogen deprived *Nannochloropsis* oculata. *Algal research,* 19**,** 1-11.

VANLERBERGHE, G. C., FEIL, R. & TURPIN, D. H. 1990. Anaerobic metabolism in the N-limited green alga Selenastrum minutum: I. Regulation of carbon metabolism and succinate as a fermentation product. *Plant physiology,* 94**,** 1116-1123.

VANLERBERGHE, G. C., HORSEY, A. K., WEGER, H. G. & TURPIN, D. H. 1989. Anaerobic carbon metabolism by the tricarboxylic acid cycle: evidence for partial oxidative and reductive pathways during dark ammonium assimilation. *Plant physiology,* 91**,** 1551-1557.

VOGLER, B. W., BRANNUM, J., CHUNG, J. W., SEGER, M. & POSEWITZ, M. C. 2018. Characterization of the *Nannochloropsis* gaditana storage carbohydrate: A 1, 3-beta glucan with limited 1, 6-branching. *Algal research,* 36**,** 152-158.

WEI, L., EL HAJJAMI, M., SHEN, C., YOU, W., LU, Y., LI, J., JING, X., HU, Q., ZHOU, W. & POETSCH, A. 2019. Transcriptomic and proteomic responses to very low CO 2 suggest multiple carbon concentrating mechanisms in *Nannochloropsis* oceanica. *Biotechnology for biofuels,* 12**,** 1-21.

WENDT, L. M., KINCHIN, C., WAHLEN, B. D., DAVIS, R., DEMPSTER, T. A. & GERKEN, H. 2019. Assessing the stability and techno-economic implications for wet storage of harvested microalgae to manage seasonal variability. *Biotechnology for biofuels,* 12**,** 1-14.

YANG, W., CATALANOTTI, C., WITTKOPP, T. M., POSEWITZ, M. C. & GROSSMAN, A. R. 2015. Algae after dark: mechanisms to cope with anoxic/hypoxic conditions. *The Plant Journal,* 82**,** 481-503.

YILMAZ, C. & GÖKMEN, V. 2016. Chlorophyll.

YOSHIDA, Y., TOMIYAMA, T., MARUTA, T., TOMITA, M., ISHIKAWA, T. & ARAKAWA, K. 2016. De novo assembly and comparative transcriptome analysis of Euglena gracilis in response to anaerobic conditions. *BMC genomics,* 17**,** 1-10.

ZOU, X., JIANG, Y., LIU, L., ZHANG, Z. & ZHENG, Y. 2010. Identification of transcriptome induced in roots of maize seedlings at the late stage of waterlogging. *BMC plant biology,* 10**,** 1-16.

ZUPPINI, A., ANDREOLI, C. & BALDAN, B. 2007. Heat stress: an inducer of programmed cell death in Chlorella saccharophila. *Plant and Cell Physiology,* 48**,** 1000-1009.

Chapter 4

4. Biphasic lipid extraction from diatom cells (*Navicula* sp.) Interplay between interfacial behaviour, cell structure and shear enables biphasic lipid extraction from whole diatom cells (*Navicula* sp.)

The aim of this study is to develop a mechanistic understanding of biphasic lipid extraction from diatoms. This investigates the role of the cell structure, shear forces and the interfacial behaviour on the biphasic lipid extraction using hexane from the diatom *Navicula* sp.

This chapter has been published as below.

"Interplay between interfacial behaviour, cell structure and shear enables biphasic lipid extraction from whole diatom cells (*Navicula* sp.)" by Yatipanthalawa B, Li W, Hill DR, Trifunovic Z, Ashokkumar M, Scales PJ, Martin GJ (2021). Journal of Colloid and Interface Science 589:65-76

4.1 Introduction

Microalgae includes photosynthetic microorganisms that can yield valuable products including lipids, proteins, carbohydrates, and high-value metabolites such as long-chain polyunsaturated fatty acids, vitamins and carotenoids (Minhas et al., 2016). The ability of some microalgal species to accumulate high amounts of TAG lipids makes them a promising alternative feedstock for the production of food oils and fuels, including biodiesel (Aguirre et al., 2013). Extraction of microalgal lipids, which are present in cell membranes and as lipid bodies inside the cells, is a crucial and challenging process (Dong et al., 2016a). Although lipids can be readily extracted at high yields from thermally dried microalgal biomass, drying consumes very large amounts of energy (Cooney et al., 2011a). Therefore, energy-efficient recovery of algal lipids relies on extraction from concentrated wet algal slurries (Martin, 2016b).

Both polar and non-polar solvents can be used to extract lipids from wet microalgal biomass, which are selective for polar membrane lipids and TAGs, respectively (Olmstead et al., 2013a). Polar solvents such as methanol, ethanol and propanol are water-miscible and can individually or in certain combinations with non-polar solvents and water form a monophasic extraction system. In a monophasic system, the solvent can permeate through algal cell walls and dissolve the intracellular lipids, which can then diffuse out via a concentration gradient (Yap et al., 2014). However, the use of polar solvents is not preferred at an industrial scale as the recovery of these solvents for reuse requires energy-intensive distillation to separate the water-miscible solvent from the water. This effectively cancels out the benefits of extracting lipids from wet slurries instead of dried biomass (Dong et al., 2016a, Martin, 2016b). Water immiscible solvents such as hexane form liquid-liquid biphasic systems in the presence of water, and are therefore preferable, as the lipid-rich solvent can be physically separated (e.g. by centrifugation) from the water in the slurry, thereby avoiding thermal evaporation of water.

In such a biphasic system, the solvent and aqueous slurry need to be mixed so that the solvent phase can contact the lipids. With the exception of a few algae such as *Botryococcus braunii* that excrete extracellular hydrocarbons (Zhang et al., 2011), the lipids of interest are protected within cell walls that must be broken apart to allow the lipid droplets to coalesce into the extracellular hexane droplets. For algae with strong cell walls, such as *Chlorella* sp. and *Nannochloropsis* sp. (Spiden et al., 2013b, Yap et al., 2016b, Bernaerts et al., 2019b), it has been shown that the cells

must be disrupted prior to undertaking biphasic lipid extraction (Law et al., 2017a, Olmstead et al., 2013b, Yap et al., 2014). As these strong cells need intense mechanical stresses to be ruptured, cell rupture has not been found to occur under the mixing conditions used during extraction, necessitating upstream cell disruption using physical or chemical methods such as high-pressure homogenisation, ultrasonication and chemical hydrolysis (Spiden et al., 2013b, Dong et al., 2016a, Yao et al., 2018b).

It is now generally agreed that algal cells must be ruptured prior to performing biphasic lipid extraction. However, if it were possible to simultaneously rupture cells during biphasic lipid extraction, this could increase the overall energy-efficiency of lipid recovery and reduce the number of process steps. Bensalem et al. (2018) showed that it was possible to rupture pre-permeabilised cells of a cell wall-deficient mutant of *Chlamydomonas reinhardtii* during biphasic extraction with hexane. In addition, Kwak et al. (2018) demonstrated the possibility of high-shear assisted simultaneous cell disruption and lipid extraction from cell wall deficient *Aurantiochytrium* sp. However, cell wall-deficient mutants are not industrially applicable. Rupturing robust, industrially relevant algae such as *Chlorella* and *Nannochloropsis* that possess strong, contiguous cellulosic cell walls, presents a more significant challenge.

Instead, it would be preferable to find an alga that is robust with respect to large-scale cultivation, but can also be ruptured during lipid extraction. It was hypothesised here that diatoms such as *Navicula* could be worth investigating, as they have a fundamentally different cell wall structure that may make them more readily ruptured during biphasic extraction. Bacillariophyceae (i.e. diatoms) are an important class of algae that have potential as feedstocks for biorefineries due to their high growth rates, ability to accumulate TAG, and to produce long-chain ω-3 polyunsaturated fatty acids (Bielsa et al., 2016, Yi et al., 2017, Popovich et al., 2019). Rather than having a true cell wall, diatom cells are protected by so-called frustules that are made of amorphous silica and comprising of two separate valves (Chauton et al., 2015). Although these silicon frustules are themselves very hard, breaking them apart to rupture diatom cells has been observed to be easier than rupturing other microalgae surrounded by cellulosic cell walls, such as *Chlorella* or *Nannochloropsis* (Spiden et al., 2013b, Wang and Seibert, 2017, Spiden et al., 2015).

Studies of lipid extraction from diatoms such as *Phaeodactylum tricornutum* and *Chaetoceros calcitrans* have been mostly limited to those involving dried biomass (Ramírez Fajardo et al., 2007,

Cartens et al., 1996, Kanda et al., 2020, Nogueira et al., 2018) or monophasic wet extraction using water-miscible solvents (Derwenskus et al., 2019, Vandamme et al., 2018, Gilbert-López et al., 2017). However as previously mentioned, the use of dried biomass or water-miscible solvents is not energy efficient. Of more relevance here, is the study by Horst et al. (2012), in which the authors investigated enzymatic (papain) cell disruption of the diatom *P. tricornutum* as an alternative to mechanical cell disruption for enabling biphasic lipid extraction using heptane. The study showed that papain could rupture the cells, by enabling the separation of the two halves of the diatom. Importantly, the study also found that prior cell disruption was necessary to obtain high lipid yields using biphasic extraction (Horst et al., 2012), consistent with studies on other algae (Olmstead et al., 2013b). However, the extraction process was performed without intensive mixing and was limited to 1 hour. The possibility of rupturing diatoms by applying shear during lipid extraction is yet to be investigated.

The role of shear, while clearly important to biphasic extraction kinetics, is not fully understood. In particular, the effect of shear on the kinetics of biphasic lipid extraction from algae with different cell wall structures, such as diatoms, warrants further investigation. Increased shear can enhance emulsification, thereby increasing the interfacial area between a water-immiscible solvent and an aqueous algal slurry to accelerate extraction, while potentially making downstream recovery of the solvent (e.g. by centrifugation) more difficult (Law et al., 2017a). Shear also exerts mechanical stresses, which if strong enough in relation to the mechanical properties of the cells, can result in cell rupture (Spiden et al., 2013b, Yap et al., 2016b), albeit under very intense shear conditions for most algal species.

There are various means of producing shear during extraction, including conventional impeller-type devices such as rotor-stator mixers (Kwak et al., 2019). Alternatively, high-intensity, low-frequency power ultrasound can be used to generate much higher levels of shear comparable to high-pressure homogenisation, via acoustic cavitation resulting from pressure fluctuations in the fluid (Li et al., 2018a). Power ultrasound is well-known to enhance mass transfer and accelerate extraction of lipids, proteins and polysaccharides from various plant materials (Vilkhu et al., 2008). It has also been shown that the extreme shear generated by ultrasound can be sufficient to rupture microalgae with strong cellulosic cell walls, such as *Nannochloropsis* (Yao et al., 2018b). The ability of ultrasound to both rupture algal cells and to enhance mass transfer during extraction,

provides an opportunity of applying ultrasound to perform simultaneous cell rupture and biphasic lipid extraction. As discussed above, this could be particularly promising for algae such as diatoms including *Navicula* sp. that have weaker cell wall structures than *Nannochloropsis* or *Chlorella* (Spiden et al., 2013b). In addition, diatom frustules are hard, non-deformable particles, that may be abrasive and damaging to industrial cell rupture equipment such as high-pressure homogenisers, potentially limiting their ability to be ruptured prior to lipid extraction.

In order to design an effective simultaneous cell rupture and lipid extraction process, it is important to understand the influence of shear on both cell structure and the mechanics of biphasic lipid extraction. It is also important to consider physicochemical interactions between the algae and the solvent droplets in relation to shear and emulsification. For example, it has been shown that ruptured cell wall fragments of *Nannochoropsis* are surface active, thereby affecting the emulsion properties during and after biphasic lipid extraction (Law et al., 2018). However, the interfacial behaviour of diatoms during biphasic extraction has yet to be considered.

In this study, slurries of unruptured *Navicula* sp. cells were subjected to different levels of shear (generated by gentle mixing, high-shear rotor-stator mixing, and power ultrasound) in the presence and absence of hexane. *Navicula* sp. was selected as a representative pennate diatom with important cell structural features (i.e. silica frustules) common amongst other Bacillariophyceae but lacking in the more commonly studied *P. tricornutum*. The performance and kinetics of biphasic lipid extraction were investigated in relation to shear and cell structure. Novel mechanisms are revealed and explained in relation to the distinct physicochemical properties of the *Navicula* sp. cells. The study was aimed at providing new insights into biphasic lipid extraction from diatoms and to investigate the potential of simultaneously rupturing algae cells and extracting lipids.

4.2 Materials and Methods

4.2.1 Microalgae cultivation and harvest

The diatom *Navicula* sp., isolated from Wimmera River at Jeparit, Victoria, Australia by Anne and Bob Hill, was isolated into a modified f medium with added silica as previously described (Olmstead et al., 2013a, Spiden et al., 2015). Cultures were grown as described by Law et al. (2018) in 15 L carboys at room temperature (22 ± 2 ºC) under a light: dark cycle of 14:10 h with air continuously delivered via air stones connected to an air pump. The cultures were harvested by

centrifugation using a disc stack centrifuge (Separator OTC 2-02-137, GEA Westfalia, Italy) at 10,000 rpm after a 10-day growth period. The nitrogen content in the medium was measured during the growth cycle using a commercial API® nitrate test kit (Poddar et al., 2020). The harvested cells were nitrogen deprived for the final 4 days of the 10-day cultivation period. The solids concentration of the harvested biomass was determined by measuring the dry weight of the biomass after oven drying overnight at 60 ºC. The effect of salt content was accounted for in the dry weight calculation by assuming the amount of water evaporated by drying had left behind salts accounting for 3% of its weight. Slurries at different concentrations were obtained by diluting the harvested biomass with 3% artificial sea water (Coral Pro Salt, Red Sea Fish Pharm LTD, Israel).

4.2.2 Total lipid extraction and fractionation

Total lipids were extracted in triplicate using a previously described (Olmstead et al., 2013a) modified Bligh and Dyer method in which chloroform (99.8% AR, RCI Labscan, Chem Supply, SA, Australia) and methanol (99.9% HPLC, Fisher Scientific, Ottawa, Canada) were used as the extracting solvents. The extracted lipids were dried under a nitrogen stream at 40 ºC using a dri-block heater (Techne Sample Concentrator, model DB-3D Dri-Block, Bibby Scientific Limited, Stone, UK). The collected lipids were weighed and then resuspended in chloroform-methanol (1:2) for subsequent fractionation of the neutral lipids from the phospho- and glycolipid fractions using solid-phase extraction (SPE) as previously described in Olmstead et al. (2013a). The neutral lipid fraction was found to be 84±1%, which was used to determine the neutral lipid extraction yield.

4.2.3 Biphasic lipid extraction under different mixing conditions

The effect of shear flow on biphasic lipid extraction kinetics from *Navicula* sp. was examined via three different mixing methods: low-shear mixing, rotor stator mixing, and ultrasonication. For all methods, a 1:1 volume ratio of n-hexane (95% HPLC, RCI Labscan, Chem Supply, SA, Australia) and algae suspension was used by mixing 10 mL samples of 2.1% solids algae suspension with 10 mL of n-hexane in 50 mL conical centrifugal tubes. The extraction was continued until the difference in two consecutive concentrations was minimal.

Extraction under low-shear mixing was conducted by rotating at 8 rpm using a rotator (Labquake, Barnstead International, Iowa, USA). The extraction temperature was maintained at 24 ± 1 ºC by placing the mixer in an incubator (Unimax 1010 & Incubator 1000, Heidolph Instruments,

Germany). The maximum power intensity required by this mixing regime was previously estimated to be 0.002 W/mL (Yap et al., 2016c).

To apply more shear during extraction, a high-shear rotor-stator mixer (Ultraturrax, IKA Labortechnik) was applied to the extraction mixture at a rotational speed of 6500 rpm. The sample containers were immersed in a water bath maintained at 24 ± 2 ºC throughout the process. The power consumption of the rotor-stator unit was found to be 0.95 W/mL using an attached power meter.

Ultrasonication was applied to investigate the effect of intense shear on biphasic lipid extraction. A high-intensity low-frequency ultrasonic transducer (Branson Sonifier operating at 20 kHz) having a micro-tip horn of 3 mm diameter was used. The tip of the horn was positioned at the hexane-biomass interface for efficient mixing. The temperature of samples was maintained by a water bath at 24 ± 2 ºC. The power intensity was determined to be 0.57 W/mL.

4.2.4 Quantification of lipid extraction kinetics

Lipid extraction kinetics were investigated by measuring the yield of extracted lipids in 1.5 mL samples taken at different time intervals depending on the total extraction time of the mixing method. These samples were centrifuged at 2330 g for 10 min (Allegra X-30R, fixed-angle rotor F0685, Beckman Coulter, Victoria, Australia) to recover the extracted lipids from the extraction mixture. The pellets were resuspended in fresh hexane up to 1.5 mL, and the resulting material was added back to the extraction vessels to keep the volume constant over the experiment. The lipid-rich hexane supernatant layer was then diluted with n-hexane. The amount of lipid extracted in each time-course sample was quantified by measuring the absorbance at 450 nm using a UV-Vis spectrophotometer (Cary 3E UV-Vis absorbance spectrophotometer, Agilent Technologies, Mulgrave, VIC, Australia). Absorbance between 400 nm – 800 nm was measured at 5 nm increments and 450nm (chlorophyll a) was selected as the wavelength that best matched the lipid response curve over the relevant concentration range. A calibration curve was plotted based on absorbance at 450 nm using known concentrations of hexane-extracted lipids redissolved in 95% n-hexane as the baseline solvent. This curve was used to convert the absorbance to the concentration of lipids.

4.2.5 Scanning Electron Microscopy

Scanning electron microscopy (SEM) was used to image *Navicula* sp. cells to reveal morphological changes and cell rupture resulting from hexane contact and ultrasonication. First, a 0.1% (v/v) polyethyleneimine (PEI) (branched average molecular weight ~25,000 g/mol as measured by light scattering, Sigma Aldrich, NSW, Australia) solution was used to coat diced silicon wafers (13 mm by 13 mm). A drop of PEI was placed on the silicon wafer and was dried under a flame to obtain this coating. The wafers were allowed to cool back to room temperature, following which 200 μL of the cell suspensions were incubated for 1 h. The excess cell suspension on the coated wafer was carefully removed after the incubation. The wafer was immediately immersed in a 2.5% glutaraldehyde in Phosphate buffered saline (PBS) solution for 1 h to allow crosslinking with the PEI film. Fresh PBS was then used to wash the silicon wafer three times. The wafer was left immersed in the solution for 10 mins for each wash. Then dehydrating them sequentially in increasing concentrations of 10, 30, 50, 70, 90 and 100% of ethanol in water (10 min for each step). The wafers were dried in a critical point dryer (Balzers CPD030 Liechtenstein, Germany). A scanning electron microscope (FEI Teneo volumescope) was used to image the cells on the silicon wafers were imaged at a voltage of 5 kV and a current of 25 pA.

4.2.6 Transmission electron microscopy

Samples of *Navicula* sp. that had been subjected to different treatments were prepared for transmission electron microscopy (TEM) analysis. First, cell suspensions were centrifuged in a bench-top centrifuge at 1750g for 5 min (MiniSpin plus, Rotor F-45-12-11, Eppendorf AG, Germany). The supernatant was removed and the cell pellets resuspended in an equal volume of 0.7% low melting point agarose (made up with sea water) (Nixon et al., 2009). The cells were cryo-immobilised by high-pressure freezing using a Leica EM PACT2.

Frozen sample carriers were transferred under liquid nitrogen to a freeze substitution medium. The freeze substitution medium consisted of 1% OsO_4 (4% Aqueous solution electron microscopy grade, ProSciTech, QLD, Australia), 0.5% uranyl acetate (99.6% grade ProSciTech (Electron Microscopy Sciences), QLD, Australia) and 2.5% H_2O in acetone (99.8% AR Grade, Chem Supply, VIC, Australia) (McDonald and Webb, 2011, Walther and Ziegler, 2002) and processed using a previously described rapid freeze substitution protocol (McDonald and Webb, 2011). Upon reaching 0 ºC, fixative was rinsed out with two exchanges of pure acetone, before continuing on to resin infiltration and embedding in Embed 812 (ProSciTec). Once the resin had polymerised,

ultrathin sections (70 nm) were prepared on formvar with carbon coated copper grids (100 mesh) using an ultramicrotome (Leica EM UC7). Sections were poststained with 7% uranyl acetate in methanol and Reynold's citrate. Following this, thin sections were observed on a TEM (FEI Talos L120C).

4.2.7 Interfacial tension measurement

To probe the interfacial behaviour of algal cells during lipid extraction using hexane, a pendant drop tensiometer (OCA20, Dataphysics, Germany) was utilised to measure the interfacial tension between the aqueous phase (microalgae suspension) and the organic phase (n-hexane). These measurements were performed under quiescent conditions to focus on the surface chemistry of the system. Prior to measurement, the solids concentration of the microalgae slurry was reduced to 0.1% using seawater medium. At such solids concentrations, the kinetics of interfacial behaviour of *Navicula* sp. cells could be probed based on the dynamic interfacial tension (DIFT) (Beverung et al., 1999, Law et al., 2018).

For these measurements, a 10 mm x 10 mm solvent-resistant cuvette was used to contain the n-hexane and a PTFE cuvette stopper with a hole in the centre to accommodate the pendant drop needle passing through was used to minimise solvent evaporation. A drop of the aqueous phase was produced using a gas-tight glass syringe with a stainless steel Luer lock needle (22 gauge, outer diameter 0.72 mm) (Law et al., 2018). An integrated camera unit was used to capture images of the droplets and the interfacial tension was calculated within the instrument software using the Young-Laplace equation. Data acquisition was done manually for the first 30 seconds and then switched to automatic data acquisition at a rate of 10 points/min.

4.2.8 Ultrasound assisted EPS removal

Navicula sp. is known to possess a significant amount of EPS (Underwood and Paterson, 2003), which could influence the lipid extraction process. To investigate the possible role of EPS on lipid extraction, ultrasonication was applied in the absence of hexane as a means of physically removing EPS prior to lipid extraction. For this, 20 mL of cell suspensions having 1.5% solid concentration were prepared and ultrasonicated in 50 mL conical centrifugal tubes for 5 s, 30 s and 60 s time intervals using the same high-intensity ultrasonic set up described earlier. EPS rich supernatant was removed by centrifuging the slurry at 3920 g for 10 min, then pipetting out the EPS-rich

supernatant. The EPS-reduced algae suspension was prepared by re-diluting the centrifuged algae pellet with 3% saltwater to reach the same total liquid volume (i.e., 20 mL).

4.2.9 Experimental reproducibility

All experiments were performed in at least duplicate. Total lipid extraction and fractionation and dry weight measurements were performed in triplicate for duplicated samples. The lipid extraction kinetics (lipid concentration) and solvent recovery were measured in duplicate on triplicated experimental samples. The mean and the standard deviation were calculated based on the replicates. The interfacial tension measurements were carried out in duplicate for duplicated samples and a representative data set was presented. SEM and TEM images representative of the whole sample were selected.

4.3 Results and discussion

4.3.1 Biphasic lipid extraction from unruptured *Navicula* cells under low-shear mixing

To provide an initial baseline understanding of biphasic extraction in the absence of shear, experiments were first attempted on whole *Navicula* cells that had not undergone prior cell rupture using low-shear mixing. This was not expected to result in significant lipid extraction, because as mentioned in the introduction, previous studies of biphasic solvent extraction on microalgae have consistently shown that prior cell rupture was required for effective lipid extraction (Yap et al., 2014, Horst et al., 2012). Surprisingly however, it was found that high lipid yields (> 80% of the total neutral lipids) could be obtained, albeit slowly, despite the cells being unruptured and the extraction being performed under low-shear mixing conditions (Figure 4.1). The most obvious explanation for these results would be that cell rupture occurred during the extraction process, and that this led to the release of lipids from the cells and their recovery into the hexane droplets. To investigate this hypothesis, scanning electron microscopy images of the cells were taken following prolonged (23 h) exposure to low-shear mixing with hexane (Figure 4.1c,e) and were compared to fresh cells (Figure 4.1b,d). Interestingly, although low-shear mixing with hexane resulted in high lipid yields (Figure 4.1a), the cells mixed in hexane for 23 h were not in fact physically ruptured (Figure 4.1c). These observations suggest that intracellular lipids were able to leave unruptured *Navicula* cells and pass into hexane droplets via a novel mechanism.

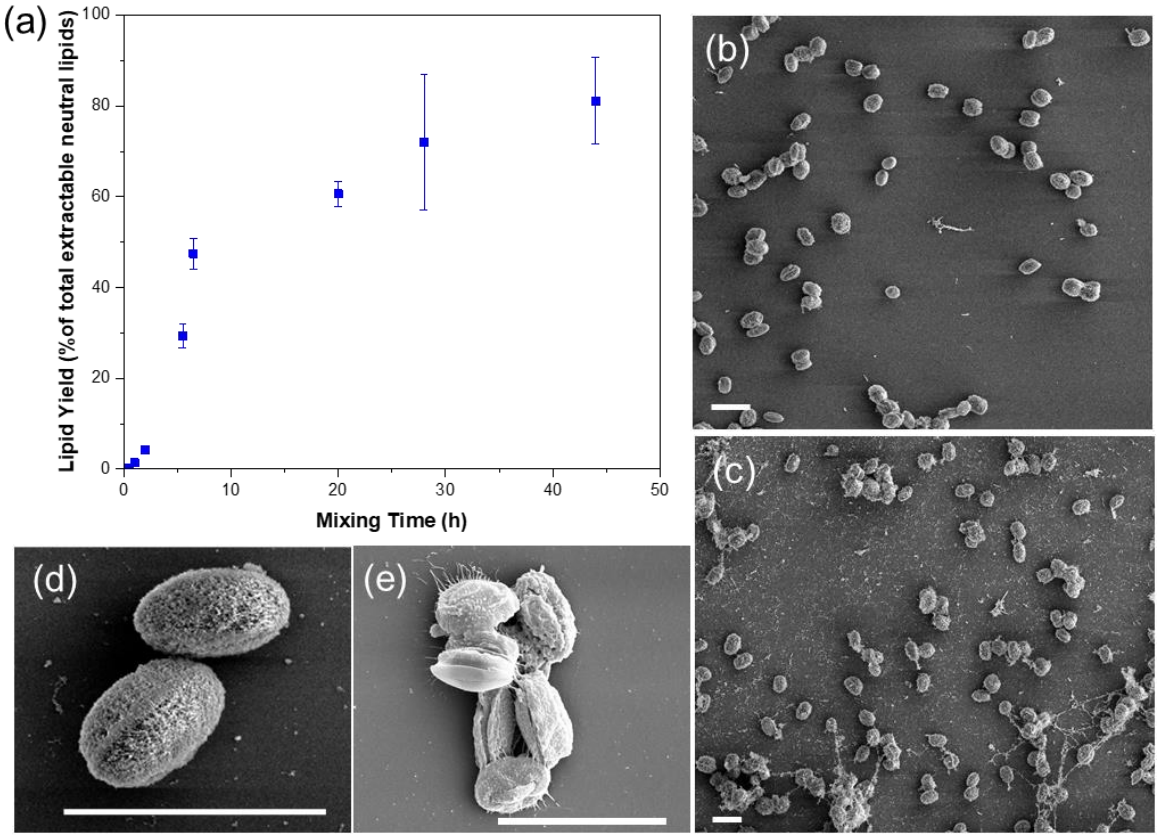

Figure 4.1: (a) Kinetics of biphasic lipid extraction from wet slurries (2.1% solids) of freshly harvested, intact *Navicula* sp. cells using hexane under low-shear mixing. The kinetics are expressed as a percentage of the total neutral lipids extracted using a Bligh and Dyer method. Error bars represent the standard deviation of duplicate measurements of triplicate experiments. Representative SEM images of (b, d) fresh *Navicula* sp. cells harvested by centrifugation and (c, e) *Navicula* sp. cells after 23 h of low-shear mixing with hexane. The scale bars represent 10 µm. Additional SEM images of fresh and hexane-contacted cells are provided in appendices (Figure 7.6 and 7.7, respectively).

As hexane is water immiscible, it remains as emulsion droplets that cannot diffuse into a microalgal cell (Yap et al., 2014). The route by which lipids are extracted out of intact *Navicula* cells into water-immiscible hexane droplets is therefore not immediately obvious. One possibility is that the cells come into direct contact with the hexane droplets and that this somehow enables coalescence of the intracellular lipid bodies into the hexane via passage through the cell wall. Diatoms in fact are covered by hard siliceous shells called frustules rather than true cell walls. These frustules

contain hydrophobic pores of sizes ranging from 40 nm – 1500 nm depending on the species (Rosengarten and Herringer, 2017), that are used for several functions including gas exchange and could serve as the passage for the water-immiscible hexane to contact the lipid bodies within the intact cells (Chauton et al., 2015, Krishnan et al., 2006). This process would require the cells to adhere to hexane droplets to allow intimate contact between the droplets and the cells in order for hexane to penetrate through the frustule pores and coalesce with the lipid bodies. Klein et al. (2014) have found the contact angle of water in air with the marine diatom *Navicula jeffreyi* layers to be 68.6^{O}, indicating that they are moderately hydrophobic which could allow sufficient contact with hexane droplets.

Therefore, the role of the water-hexane interface and the interfacial behaviour of algae cells appear to be central to the unexpected biphasic lipid extraction from unruptured *Navicula* sp. cells. Such factors need to be examined in the absence of shear forces, which could otherwise impact on the extraction kinetics as will be subsequently discussed. Figure 4.1c shows that although *Navicula* sp. cells were not ruptured by prolonged contact with hexane, there is some extraneous material present in the background that provides some initial evidence that the *Navicula* cells interacted directly with the hexane droplets.

4.3.2 Interfacial behaviour during biphasic lipid extraction from unruptured *Navicula* cells in the absence of shear

As the proposed mechanism of extraction necessarily occurs at the hexane-water interface, the presence of cells and extracted lipids at the interface would be expected to affect the interfacial tension (IFT). Therefore, to investigate this further, DIFT measurements were performed on the interface between hexane and aqueous suspensions of *Navicula* sp. cells (Figure 4.2).

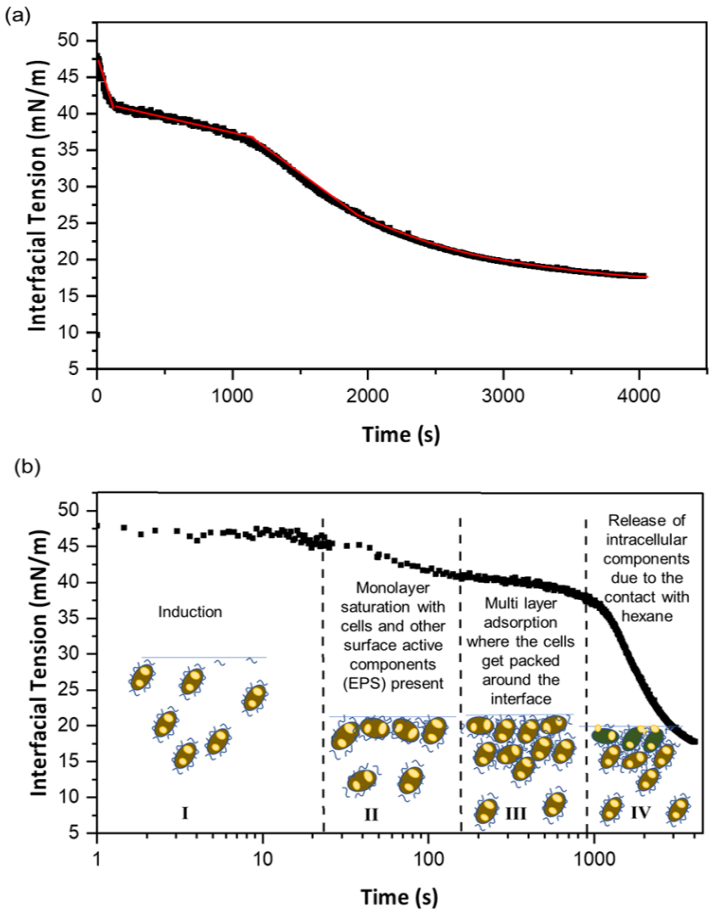

Figure 4.2. Change in the interfacial tension between hexane and *Navicula* sp. slurry (0.1% solids concentration) phases as a function of time plotted on a linear (a) and log (b) timescale. The different regimes are separated by vertical dashed lines and the possible mechanisms underlying each are briefly described.

Four different regimes (I-IV) can be distinguished in the IFT curve (Figure 4.2b), the first three of which align to stages previously identified for particulate-stabilised interfaces (Beverung et al., 1999, Law et al., 2018). The IFT remained essentially unchanged at ~50 nM/m for the first 20 s (I), after which it began to decline (II). After reaching ~40 mN/m, the IFT continued to decline at a slower rate for a few minutes (III), before transitioning at around 1000 s to a period of more rapid, yet progressively decelerating decline (IV), approaching an apparent minimum value of approximately 18 mN/m after about 1 h (3600 s).

Similar dynamic interfacial tension measurements were performed by Beverung et al. (1999) for probing protein adsorption at oil-water interfaces. In that case, a 3-regime model was proposed for interpreting the interfacial tension dynamics in relation to protein adsorption under quiescent conditions. In regime I (induction phase), the IFT remains high for a short period of time until the surface-active proteins diffuse to the interface from the bulk medium. The IFT then begins to reduce in phase II (monolayer formation) as the interface becomes covered by a monolayer of protein molecules, which in the process of adsorption can unfold. In phase III (multilayer adsorption), the IFT continues to decline, but at a slower rate of decline than in phase II. The reduction in IFT in this phase occurs after the interface has been saturated by protein molecules at which point they can undergo further inter-molecular interactions (i.e. close packing or gelation). Algae cells, despite being a few orders of magnitude larger than proteins, are still particles for which similar interfacial adsorption processes can be expected to occur (Beverung et al., 1999, Law et al., 2018). As such, the first three stages in the DIFT curve observed here (Figure 4.2) align to the induction time for cell diffusion to the interface (regime I), the reduction in IFT due to the development of an interfacial monolayer of algae cells (regime II), and further inter-cellular packing and rearrangement at the interface (regime III).

Interestingly, in this biphasic system of hexane and *Navicula* suspensions, a unique fourth regime (regime IV) can be distinguished in the DIFT profile (Figure 4.2b). Instead of reaching a plateau in the IFT following inter-cellular packing (regime III) following these three initial regimes, there was a rapid and dramatic resumption in the reduction of IFT (regime IV). The existence of a fourth stage of IFT reduction has not been reported in macromolecular systems such as proteins (Beverung et al., 1999), nor for slurries of microalgae that have cellulosic cell walls (*Nannochloropsis*) (Law et al., 2018). This indicates the occurrence of a phenomenon beyond that of interfacial particle adsorption and rearrangement. By considering this IFT behaviour in connection with the observed lipid extraction (Figure 4.1a) from unruptured cells (Figure 4.1c), it is posited here that the decrease in IFT in regime IV was due to the uptake of intracellular algae lipids into the interface. These lipids would include surface active polar lipids that could account for the much more dramatic reduction in IFT during regime IV than was possible in the first three stages (the IFT was reduced by around 22 mN/m in regime IV, compared to a total reduction of only about 5 mN/m across regimes I to III).

To further investigate the effect of hexane on the cell structure and associated lipid droplets, TEM images were obtained revealing the internal structure of the diatoms before and after the contact with hexane (Figure 4.3). These images confirm the observations from SEM that the cells remained unruptured by contact with hexane. Figure 4.3(a) shows the lipid bodies in the intact cells were large and located near the cell membrane, making them relatively accessible to hexane droplets onto which the cells may be adsorbed. Importantly, after contact with hexane, the lipid bodies can be seen to have been evacuated, with just a hollow region remaining within the otherwise whole cell (Figure 4.3(b)), indicating that the lipid bodies had indeed coalesced into the extracellular hexane droplets. The fold present in the hollow region could be an artefact of sample preparation or some unextracted material from the lipid body. Such biphasic extraction of lipids from *Navicula* sp. without any apparent cell rupture either prior or during extraction is fundamentally different to the mechanism previously identified for other microalgae that possess cellulosic cell walls (Yap et al., 2014). In addition, it can be observed that the dark layer surrounding the cell wall surface of the untreated cells (Figure 4.3(a)) is much fainter around the cells contacted with hexane (Figure 4.3(b)). This layer is identified here as EPS, which will be discussed in the subsequent sections.

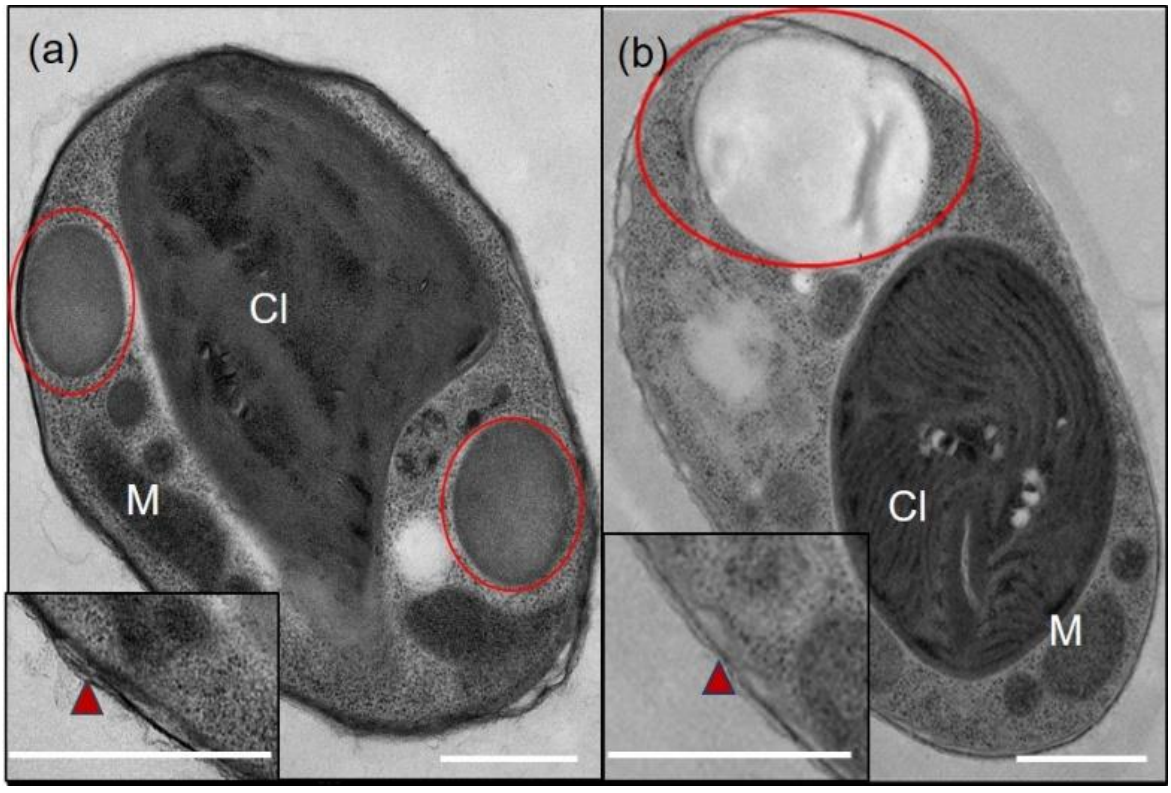

Figure 4.3. TEM images of (a) a freshly harvested *Navicula* sp. cell, and (b) a cell contacted with hexane only via diffusional interfacial adsorption for 2 h. Red circles show the position of the filled (a) and emptied (b) lipid bodies (Cl = chloroplast; M = mitochondrion). Red arrows are used to point the difference in the extracellular material present on the cell walls in the insert images. The scale bars represent 1 μm. Additional TEM images for fresh and hexane contacted cells are provided in appendices (Figure 7.8).

4.3.3 Effect of shear on lipid extraction

Experiments were performed to investigate the effect of shear on the kinetics of biphasic lipid extraction from intact *Navicula* cells using high-shear rotor-stator mixing and ultrasonication (Figure 4.4). Ultrasonication enabled the fastest lipid extraction, followed by rotor stator mixing (Figure 4.4), and low-shear mixing (Figure 4.1), with a 75% yield of the total neutral lipids present as quantified using the Bligh and Dyer method achieved in approximately 1.5 min, 70 min and 2000 minutes, respectively. These results showed that extraction was greatly accelerated by shear, in particular with intense shear provided by power ultrasonication.

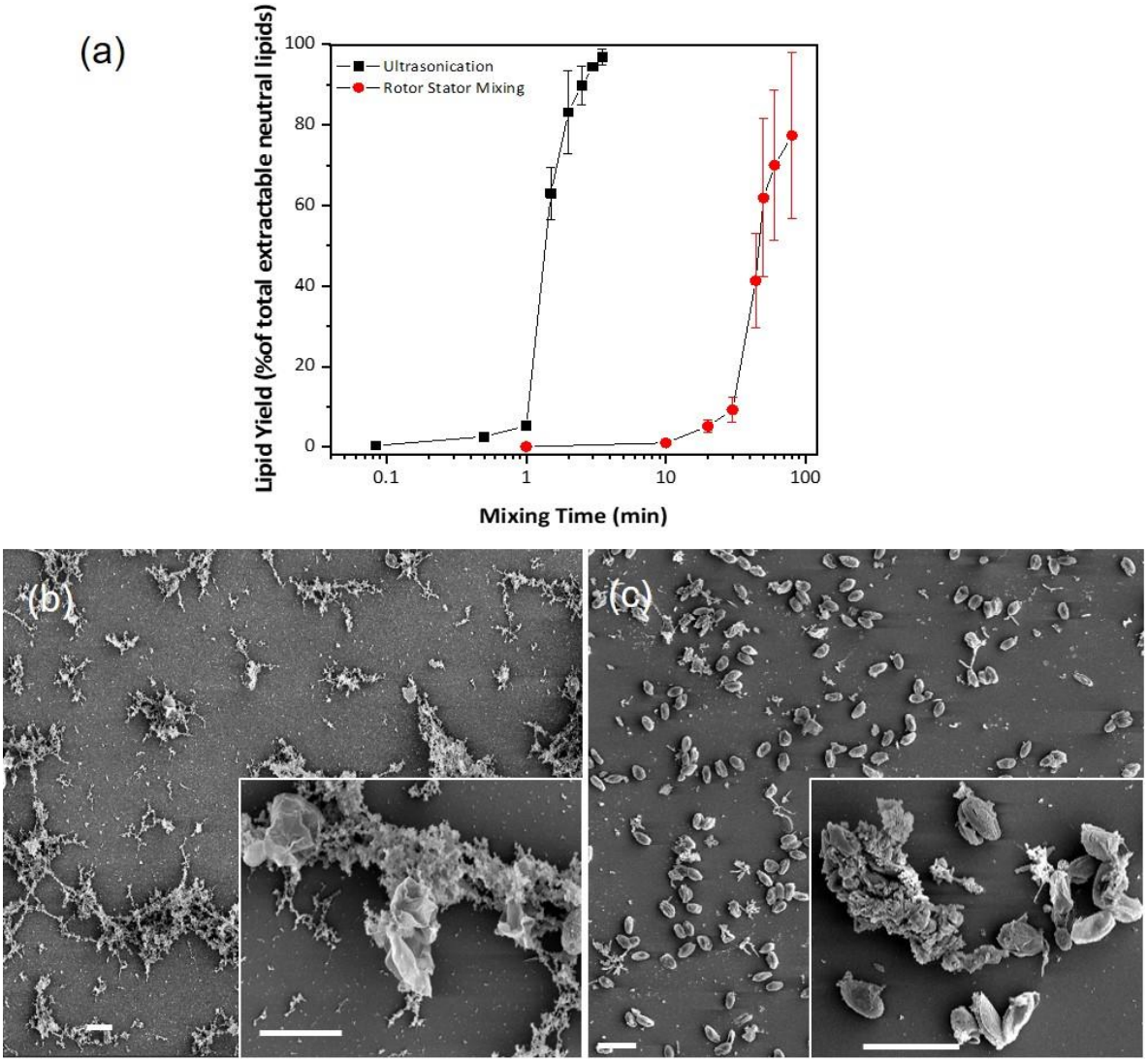

Figure 4.4: (a) Kinetics of biphasic lipid extraction from wet slurries (2.1% solids) of freshly harvested, unruptured *Navicula* sp. cells using hexane mixed by ultrasonication and rotor stator mixing. The kinetics are expressed as a percentage of the total neutral lipids extracted using Bligh and Dyer method. Error bars represent the standard deviation of duplicate measurements of triplicate experiments. Representative SEM images of (b) cells subjected to ultrasonication for 60 s in the presence of hexane (1:1 hexane: paste) (c) cells mixed with hexane (1:1 hexane: paste) using rotor stator mixing for 20 mins. The inserts show representative cells at a higher magnification. The scale bars represent 10 µm.

The difference in the rate of extraction as a function of shear is explained by the degree of emulsification. Higher levels of shear forces can promote emulsion droplet breakup, leading to

smaller droplets. Ultrasonication can produce very small emulsion droplets within a short period of time due to the high shear forces arising from acoustic cavitation (Reddy and Fogler, 1980). High-shear rotor-stator mixing also generates shear forces, but cannot form emulsion droplets as small as is possible with ultrasonication (Li et al., 2018b). The smaller droplets result in a higher specific interfacial area between the dispersed hexane droplets and the continuous algae slurries. This would increase the number of cells that are able to make direct contact with the hexane droplets, with the algal cells acting as the major interfacial stabiliser of this Pickering style emulsion system, thus accelerating direct extraction via the mechanism identified earlier. While the increased interfacial area associated with increased shear (ultrasonication > rotor-stator mixing > low-shear mixing) is consistent with the increased extraction rates, it may not be sufficient to explain the dramatic differences in kinetics. In particular, although the cells were initially unruptured (Figure 4.1a) and were not ruptured by hexane contact in the absence of shear mixing (Figure 4.1b), it is possible that cells were ruptured as a result of shear forces exerted during extraction using ultrasonication and rotor-stator mixing. To investigate whether cell rupture occurred during extraction, SEM images were obtained of cells exposed to ultrasonication (for 60 s) or rotor-stator mixing (for 20 min) in the presence of hexane (Figure 4.4b and 4c). Indeed, the application of shear using ultrasound or rotor-stator mixing in the presence of hexane resulted in cellular disintegration. In the case of ultrasonication, however, the cell rupture appeared to be significantly more extensive than with the rotor-stator mixing, as evidenced by the greater amount of internal cellular debris present in the SEM images. In both cases, cell rupture was shown to have occurred before the onset of the period of very rapid biphasic lipid extraction (Figure 4.4) providing further insights into the enhanced extraction kinetics in the presence of shear.

4.3.4 Role of extracellular polymeric substances (EPS) on biphasic lipid extraction from *Navicula*

Based on the results presented so far, it is evident that the passage of intracellular lipids from unruptured *Navicula* cells occurs at the hexane-water interface. This process will depend on the surface chemistry of the cells. Beyond the cell walls themselves, many microalgae, including diatoms such as *Navicula*, excrete so-called extracellular polymeric substances (EPS) (Doghri et al., 2017, Klein et al., 2014). The EPS of diatoms is functionally, structurally and chemically diverse (Hoagland et al., 1993). In diatoms such as *Navicula*, EPS has been found to completely

encase the cell and to be surface active and adhesive (Mnif and Ghribi, 2015, Klein et al., 2014, Wang et al., 2000). More specifically, *Navicula* is known to have a thick, outer mucilaginous capsule of EPS and a thinner (10 nm) organic 'skin' layer tightly associated with the valve (Hoagland et al., 1993). In this context, the outer mucilaginous EPS layer present on intact *Navicula* cells was speculated to be a barrier against the water-immiscible solvent penetrating the cells and coalescing with intracellular lipid bodies.

To investigate the possible role of EPS in relation biphasic lipid extraction, ultrasonication was applied to remove the mucilaginous EPS layer prior to hexane contact. Indeed, EPS removal from intact *Navicula* cells was achieved by ultrasonication for 60 s in the absence of hexane, importantly without otherwise affecting the cells (Figure 4.5). The SEM and TEM images presented in Figure 4.5 show that ultrasound removed mucilaginous EPS covering the surface of the fresh cells without resulting in any significant cell rupture nor the release of intracellular contents. Following ultrasound, the surface of the silica frustules can be seen to be considerably smoother (Figure 4.5b) than the untreated 'hairy' surface of the fresh cells (Figure 4.5a), while the intracellular organelles and lipid bodies remained intact (Figure 4.5c). Contrasting these images (Figure 4.5) with those of cells following hexane contact under low-shear mixing (Figure 4.3b) in which the lipid bodies were removed from otherwise whole cells, reinforces the novel mechanism of intracellular lipid release from *Navicula* occurring at the water-hexane interface.

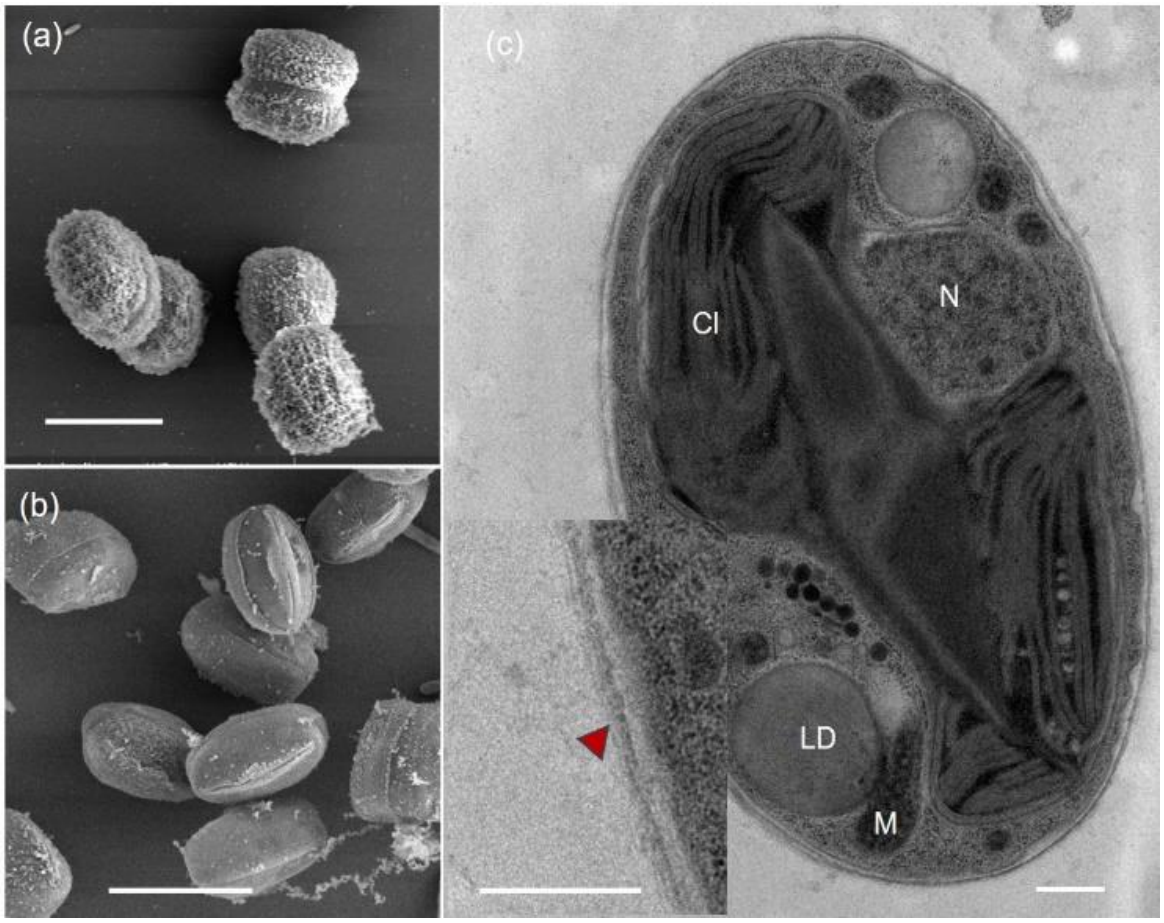

Figure 4.5. Representative SEM images of (a) freshly harvested *Navicula sp.* cells and (b) cells subjected to 1-min ultrasonication. The scale bars represent 5 µm. (c) TEM image of a *Navicula sp.* cell ultrasonicated for 1 min, revealing a cell wall lacking attached extracellular polymeric substances (M = mitochondria; N = nucleus; C = chloroplast). The scale bars represent 500 nm. Additional SEM and TEM images are provided in appendices (Figure 7.9 and 7.10).

To further investigate the role of EPS on biphasic lipid extraction from *Navicula*, measurements were obtained of the dynamic interfacial tension between hexane and suspensions of *Navicula* cells that had the mucilaginous EPS removed by ultrasonication prior to hexane contact (Figure 4.6). Implementing the established DIFT protocol, the effect of EPS removal on the behaviour of *Navicula* cells at the water-hexane interface was examined using suspensions of *Navicula* cells subjected to ultrasonication for different durations (0, 5, 30, and 60 s). This represented a graded series of EPS removal, as the muciliginous EPS could be expected to be progressively released to the supernatant during ultrasonication, which was then removed via centrifugation prior to DIFT measurements.

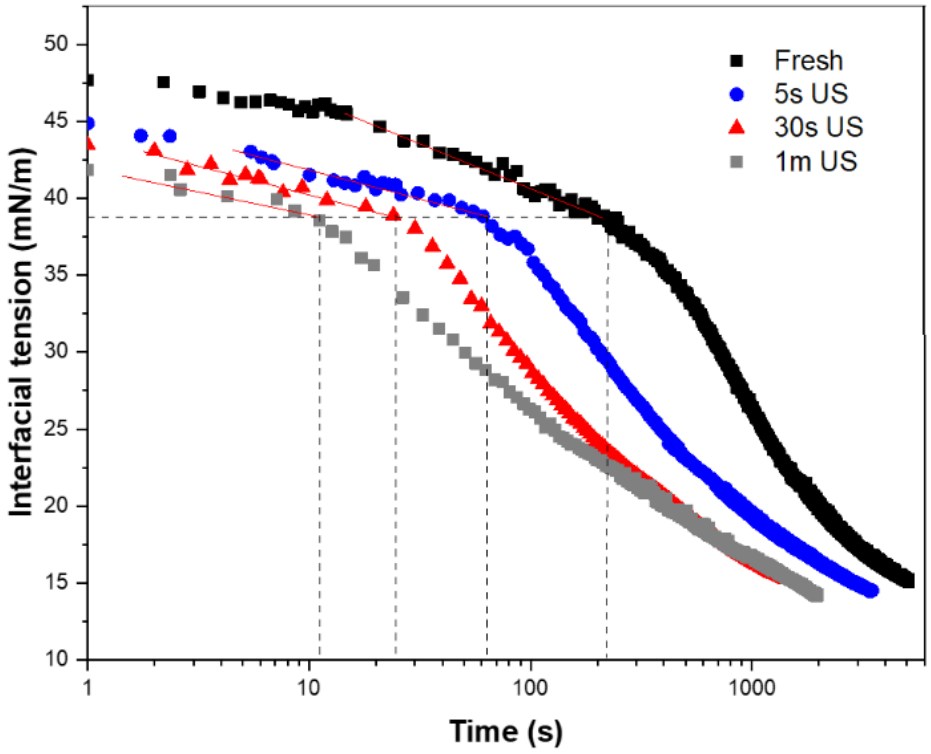

Figure 4.6: Dynamic interfacial tension (DIFT) profiles between hexane and suspensions of *Navicula* sp. cells (1.5% solids) in relation to prior treatment with ultrasound (for 5 s, 30 s, or 1 min) to remove bound EPS. Trendlines in red indicate the DIFT in regime III. Dashed lines indicate the times and IFT associated with the onset of regime IV.

The previous DIFT measurements (Figure 4.3) were performed at a low cell concentration (0.1 wt%), in order to reveal the entire progression of the interfacial dynamics (i.e. well-separated kinetic regimes). However, the next set of DIFT measurements were performed using a 1.5% solids suspension of cells to highlight the effect of EPS removal on the final regime IV (i.e. interfacial lipid uptake) that was previously revealed. At such solids concentrations, it could be expected that the water-hexane interface would be instantly saturated by the *Navicula* cells upon pendant drop formation before the commencement of data acquisition, thus not revealing regimes I and II (Law et al., 2018). As a result, the profiles commenced with a relative linear IFT decrease (Figure 4.5) representative of regime III, as presented in previous studies (Law et al., 2018, Mnif and Ghribi, 2015). The removal of EPS reduced the initial IFT (from ~48 mN/m to ~42 mN/m after 1 min sonication), indicating that the progressive removal of the chemically complex, amphiphilic EPS (Klein et al., 2014) altered the surface activity and interfacial wetting behaviour of the cells,

apparently increasing the relative hydrophobicity of the cells. The increased hydrophobicity can be attributed to the removal of the more hydrophilic mucilaginous capsule, exposing the more hydrophobic organic 'skin' layer coating the silica valve. Cleaned diatom frustules have in fact been shown to be capable of selective protein adsorption from aqueous protein solutions, even at neutral pH values, confirming their moderate hydrophobicity (Lim et al., 2015).

Consistent with the low cell concentration DIFT profile (Figure 4.2), a final stage of rapid, yet decelerating IFT reduction (i.e. regime IV) was observed for all samples. The removal of EPS both reduced the time taken to reach regime IV (from 3 min, to 70 s, 25s, and 7 s for 0 s, 5 s, 30 s, and 1 min of ultrasonication, respectively). For all samples, there was a significant reduction in the IFT of over 20 mN/m during regime IV, compared to a prior reduction of less than 10 mN/m from the interfacial wetting by the cells. This is consistent with the results obtained at a lower cell concentration (Figure 4.2). As discussed, the dramatic drop in IFT can be attributed to intracellular, surface-active lipids being extracted out of the cells due to the contact with hexane. The lead time observed in the onset of the lipid-releasing stage (regime IV) for fresh untreated cells is consistent with the idea that the EPS initially acts as a barrier for the transfer of lipids from the cells to the hexane phase. The application of ultrasonication to remove the muciliginous EPS layer from the cell surface without affecting the internal structure or composition of the cells, therefore, reduces the time for the hydrophobic hexane to directly contact the organic layer coating the frustules, penetrate the cells and ultimately extract the lipids.

Interestingly, the onset of the lipid-releasing stage (regime IV) occurred at approximately the same IFT (~39 mN/m) regardless of the amount of EPS initially present. This suggests that the interfacial layer is similar in composition at this point, which could reflect the removal of the EPS barrier between the frustules and the hexane, allowing complete contact between the two. As such, this IFT value (39 mN/m) appears to represent the minimum IFT obtainable from the interfacial stabilisation by 'naked' cells, stripped of the hydrophilic/steric mucilaginous EPS layer. Based on the TEM images in Figure 4.3, it appears that hexane contact removes the mucilaginous EPS layer, which is apparently a necessary precursor to the onset of the lipid-releasing stage (regime IV). The earlier onset for the pre-ultrasonicated cells therefore indicates that ultrasonication assists in the pre-removal of the mucilaginous EPS barrier to advance the commencement of lipid mass transfer between the cells and hexane phase. However, as ultrasonication for 1 min in the presence of

hexane was seen to rupture the cells (Figure 4.1d), it is likely that EPS removal was not the primary reason for the faster extraction kinetics observed in Figure 4.1). Rather, these experiments reveal that mucilaginous EPS provides a barrier to biphasic extraction from unruptured *Navicula* cells.

The current results are not sufficient to provide a conclusive discussion about the nature of the mucilaginous EPS removal by hexane nor its exact role as a barrier. More detailed characterisation of the chemistry of the EPS would be needed to understand the relative influence of potential steric and hydrophobic shielding effects and the nature of the removal of EPS by hexane contact. Interestingly, in Figure 4.3c, there is evidence of partial and localised removal of EPS, indicative of the cell surface being partially wetted by hexane. However, it is not clear whether the hexane chemically alters the EPS (e.g. removes critical hydrophobic components to enable release and solubilisation of the EPS) or simply displaces it from the cell surface.

It has been shown here that the combination of hexane and high shear results in cell rupture, but that the cells remain whole if exposed to either in isolation. The reason the cells become susceptible to shear forces in the presence of hexane is not completely clear, but must be related to the adsorption of the cells at the hexane/water interface. For instance, the removal of intracellular lipids from cells located at the hexane/water interface could mechanically weaken the cells, in particular the structures connecting the frustules. In addition, the droplet break-up and recoalescence events occurring when the emulsions are subjected to shear could exert increased mechanical stresses on the cells.

4.3.5 Overall mechanism of biphasic lipid extraction from *Navicula* sp.

Based on the observations herein, the mechanism of lipid extraction from *Navicula* sp. is proposed as described below and summarised schematically in Figure 4.7.

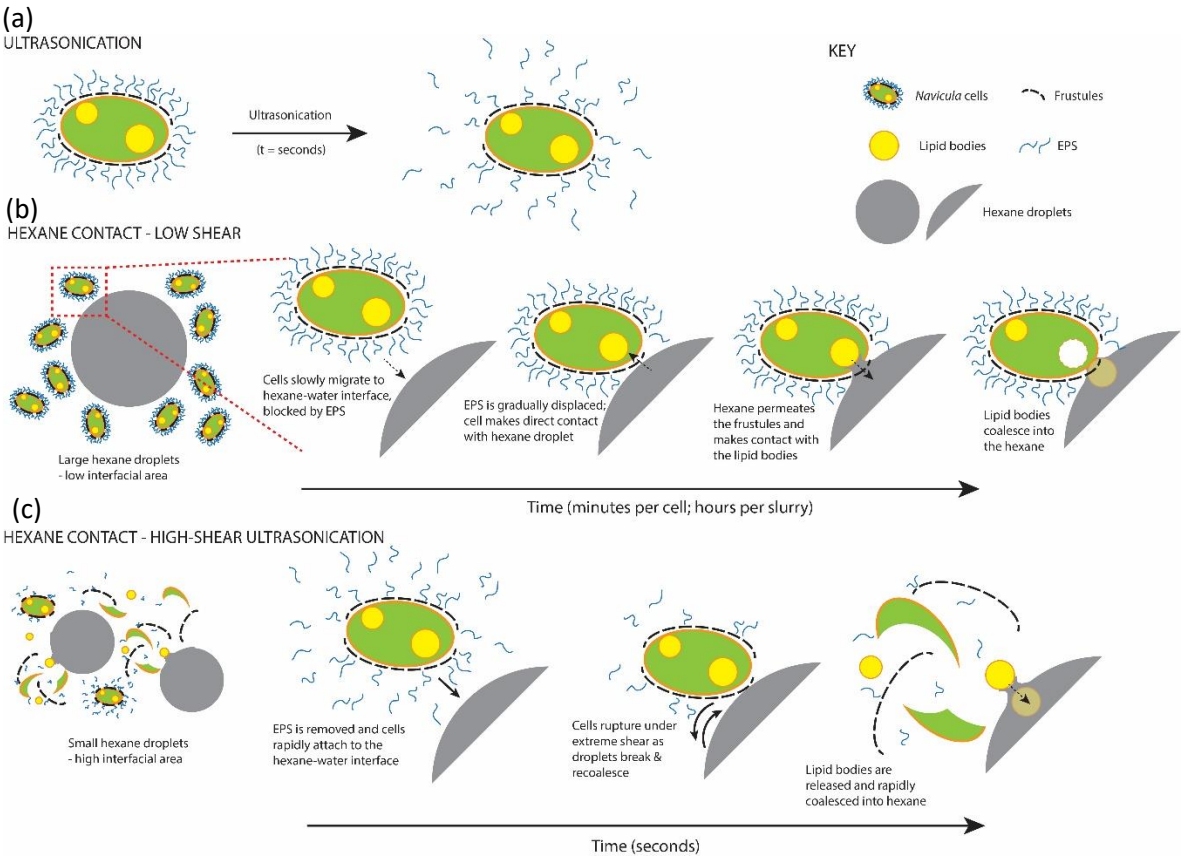

Figure 4.7: Schematic of the proposed mechanism of biphasic lipid extraction from the diatom *Navicula* with and without high shear forces. A detailed description of the mechanism is included in the main text.

First, the high-intensity shear forces provided by ultrasonication in the absence of hexane removes mucilaginous EPS while leaving the cells otherwise intact (Figure 4.7a). In the absence of shear forces, lipid extraction is possible, although very slowly (Figure 4.7b). The cells adsorb onto the hexane droplets, with the mucilaginous EPS presenting a barrier to intimate contact between the frustules and solvent. After several minutes, hexane wets the organic layer coating the frustules, diffuses into the cells via the pores, and coalesces with the lipid bodies inside the cells. This process continues to extract lipids from different cells within the culture over many hours, to eventually recover high yields of lipids. The application of ultrasound in the presence of hexane, removes the mucilaginous EPS from cell surfaces and decreases the size of the hexane droplets (Figure 4.7c). This increases the direct contact of cells with hexane due to the removal of EPS barrier and the available surface area for the contact with hexane via the formation of emulsions with small droplets. The continual coalescence and reformation of small hexane droplets due to the rapid

mixing in the presence of ultrasonication results in the complete rupture of the diatoms due to high mechanical stresses imposed on the cells.

According to these mechanisms, biphasic extraction of lipids from diatoms such as *Navicula* can be achieved either through direct contact of the cells with hexane or more rapidly following cell rupture that can occur in-situ during extraction performed under high-shear. Smaller emulsion droplets are preferred in order to increase the surface area available for the cells to contact with hexane (Dong et al., 2016a). Ultrasonication not only assists in forming tight emulsions (Li et al., 2018a) but also removes the EPS layer covering the cell surface (Figure 4.5), which facilitates the direct contact of the cells with hexane. Cells are susceptible to rupture when subjected to both hexane contact and shear forces (Figure 4.4). This could be due to mechanical weakening of the cells exposed to hexane (Hejazi et al., 2004) or increased mechanical forces at the interface resulting from the breakage and collision of emulsion droplets under shear (Li et al., 2018a). Importantly, this is different behaviour to what has previously been observed for *Nannochloropsis* sp., which has a cellulosic cell wall. For *Nannochloropsis* sp., neither direct lipid extraction from intact cells (Law et al., 2017a, Olmstead et al., 2013b) nor cell rupture during ultrasonic biphasic lipid extraction was observed (Appendix). The different mechanisms revealed here for *Navicula* appear related to the physicochemical properties and porosity of its cell wall structure. It would be interesting in the future to study other diatoms to see how universal these mechanisms are in this class of algae given their similarity in cell wall structure and differences in surface and physiological characteristics (Hoagland et al., 1993).

4.4 Conclusions

Biphasic lipid extraction from unruptured cells of the diatom *Navicula* sp. was investigated in relation to cell structure, interfacial behaviour and the application of shear. Importantly and unexpectedly, prior cell rupture was observed to be unnecessary for lipid extraction. However, extraction was very slow, taking over 40 hours to extract >80% of the total neutral lipids. Interfacial tension measurements revealed that the intact cells were able to make direct contact with hexane phase without the application of shear resulting in a significant reduction of the interfacial tension from 40 mN/m to 18 mN/m. Contact with the hexane droplets enabled the removal of intracellular lipid bodies, as shown in TEM images and attributed to passage via pores in the frustule of the cells. This process was slow, taking several minutes for an initial population

of cells, and was impeded by the presence of mucilaginous EPS on the cell surface. The application of shear by rotor-stator mixing and ultrasonication greatly increased the rate of lipid extraction, with 75% of the total neutral lipids recovered in approximately 70 min or 1.5 min, respectively. Ultrasonication in the absence of hexane was unable to rupture the cells effectively, but was instead able to remove the mucilaginous EPS covering the cell surface. In the presence of hexane, ultrasonication could rupture the cells, resulting in extraction of > 95% of the neutral lipids in <5 minutes. This study revealed different mechanisms for biphasic lipid extraction from the diatom *Navicula* to those previously observed with algae such as *Nannochloropsis* and *Chlorella* which possess impermeable cellulosic cell walls. These insights will assist future efforts to develop effective biphasic lipid extraction and EPS recovery from diatomaceous microalgae species.

4.5 References

AGUIRRE, A.-M., BASSI, A. & SAXENA, P. 2013. Engineering challenges in biodiesel production from microalgae. *Critical reviews in biotechnology,* 33**,** 293-308.

BENSALEM, S., LOPES, F., BODÉNÈS, P., PAREAU, D., FRANÇAIS, O. & LE PIOUFLE, B. 2018. Understanding the mechanisms of lipid extraction from microalga Chlamydomonas reinhardtii after electrical field solicitations and mechanical stress within a microfluidic device. *Bioresource technology,* 257**,** 129-136.

BERNAERTS, T. M. M., GHEYSEN, L., FOUBERT, I., HENDRICKX, M. E. & VAN LOEY, A. M. 2019. Evaluating microalgal cell disruption upon ultra high pressure homogenization. *Algal Research,* 42.

BEVERUNG, C., RADKE, C. J. & BLANCH, H. W. 1999. Protein adsorption at the oil/water interface: characterization of adsorption kinetics by dynamic interfacial tension measurements. *Biophysical chemistry,* 81**,** 59-80.

BIELSA, G. B., POPOVICH, C. A., RODRÍGUEZ, M. C., MARTÍNEZ, A. M., MARTÍN, L. A., MATULEWICZ, M. C. & LEONARDI, P. I. 2016. Simultaneous production assessment of triacylglycerols for biodiesel and exopolysaccharides as valuable co-products in *Navicula* cincta. *Algal research,* 15**,** 120-128.

CARTENS, M., MOLINA GRIMA, E., ROBLES MEDINA, A., GIMÉNEZ GIMÉNEZ, A. & IBÁNEZ GONZALEZ, J. 1996. Eicosapentaenoic acid (20:5n-3) from the Marine Microalga Phaeodactylum tricornutum. *JAOCS, Journal of the American Oil Chemists' Society,* 73**,** 1025-1031.

CHAUTON, M. S., SKOLEM, L. M., OLSEN, L. M., VULLUM, P. E., WALMSLEY, J. & VADSTEIN, O. 2015. Titanium uptake and incorporation into silica nanostructures by the diatom Pinnularia sp.(Bacillariophyceae). *Journal of applied phycology,* 27**,** 777-786.

COONEY, M. J., YOUNG, G. & PATE, R. 2011. Bio-oil from photosynthetic microalgae: Case study. *Bioresource Technology,* 102**,** 166-177.

DERWENSKUS, F., METZ, F., GILLE, A., SCHMID-STAIGER, U., BRIVIBA, K., SCHLIEßMANN, U. & HIRTH, T. 2019. Pressurized extraction of unsaturated fatty acids and carotenoids from wet Chlorella vulgaris and Phaeodactylum tricornutum biomass using subcritical liquids. *GCB Bioenergy,* 11**,** 335-344.

DOGHRI, I., LAVAUD, J., DUFOUR, A., BAZIRE, A., LANNELUC, I. & SABLÉ, S. 2017. Cell-bound exopolysaccharides from an axenic culture of the intertidal mudflat *Navicula* phyllepta diatom affect biofilm formation by benthic bacteria. *Journal of Applied Phycology,* 29**,** 165-177.

DONG, T., KNOSHAUG, E. P., PIENKOS, P. T. & LAURENS, L. M. 2016. Lipid recovery from wet oleaginous microbial biomass for biofuel production: a critical review. *Applied energy,* 177**,** 879-895.

GILBERT-LÓPEZ, B., BARRANCO, A., HERRERO, M., CIFUENTES, A. & IBÁÑEZ, E. 2017. Development of new green processes for the recovery of bioactives from Phaeodactylum tricornutum. *Food Research International,* 99**,** 1056-1065.

HEJAZI, M., KLEINEGRIS, D. & WIJFFELS, R. 2004. Mechanism of extraction of β-carotene from microalga Dunaliellea salina in two-phase bioreactors. *Biotechnology and bioengineering,* 88**,** 593-600.

HOAGLAND, K. D., ROSOWSKI, J. R., GRETZ, M. R. & ROEMER, S. C. 1993. Diatom extracellular polymeric substances: function, fine structure, chemistry, and physiology. *Journal of phycology,* 29**,** 537-566.

HORST, I., PARKER, B. M., DENNIS, J. S., HOWE, C. J., SCOTT, S. A. & SMITH, A. G. 2012. Treatment of Phaeodactylum tricornutum cells with papain facilitates lipid extraction. *Journal of Biotechnology,* 162**,** 40-49.

KANDA, H., HOSHINO, R., MURAKAMI, K., ZHENG, Q. & GOTO, M. 2020. Lipid extraction from microalgae covered with biomineralized cell walls using liquefied dimethyl ether. *Fuel,* 262**,** 116590.

KLEIN, G. L., PIERRE, G., BELLON-FONTAINE, M.-N., ZHAO, J.-M., BRERET, M., MAUGARD, T. & GRABER, M. 2014. Marine diatom *Navicula* jeffreyi from biochemical composition and physico-chemical surface properties to understanding the first step of benthic biofilm formation. *Journal of Adhesion Science and Technology,* 28**,** 1739-1753.

KRISHNAN, S., WANG, N., OBER, C. K., FINLAY, J. A., CALLOW, M. E., CALLOW, J. A., HEXEMER, A., SOHN, K. E., KRAMER, E. J. & FISCHER, D. A. 2006. Comparison of the fouling release properties of hydrophobic fluorinated and hydrophilic PEGylated block copolymer surfaces: attachment strength of the diatom *Navicula* and the green alga Ulva. *Biomacromolecules,* 7**,** 1449-1462.

KWAK, M., KANG, S. G., HONG, W.-K., HAN, J.-I. & CHANG, Y. K. 2018. Simultaneous cell disruption and lipid extraction of wet Aurantiochytrium sp. KRS101 using a high shear mixer. *Bioprocess and biosystems engineering,* 41**,** 671-678.

KWAK, M., ROH, S., YANG, A., LEE, H. & CHANG, Y. K. 2019. High shear-assisted solvent extraction of lipid from wet biomass of Aurantiochytrium sp. KRS101. *Separation and Purification Technology*.

LAW, S. Q., CHEN, B., SCALES, P. J. & MARTIN, G. J. 2017. Centrifugal recovery of solvent after biphasic wet extraction of lipids from a concentrated slurry of *Nannochloropsis* sp. biomass. *Algal research,* 24**,** 299-308.

LAW, S. Q., METTU, S., ASHOKKUMAR, M., SCALES, P. J. & MARTIN, G. J. 2018. Emulsifying properties of ruptured microalgae cells: Barriers to lipid extraction or promising biosurfactants? *Colloids and Surfaces B: Biointerfaces*.

LI, W., LEONG, T. S., ASHOKKUMAR, M. & MARTIN, G. J. 2018a. A study of the effectiveness and energy efficiency of ultrasonic emulsification. *Physical Chemistry Chemical Physics,* 20**,** 86-96.

LI, W., LEONG, T. S. H., ASHOKKUMAR, M. & MARTIN, G. J. O. 2018b. A study of the effectiveness and energy efficiency of ultrasonic emulsification. *Physical Chemistry Chemical Physics,* In press.

LIM, G., LIM, J., AHMAD, A. & CHAN, D. 2015. Influences of diatom frustule morphologies on protein adsorption behavior. *Journal of Applied Phycology,* 27**,** 763-775.

MARTIN, G. J. O. 2016. Energy requirements for wet solvent extraction of lipids from microalgal biomass. *Bioresource Technology,* 205**,** 40-47.

MCDONALD, K. L. & WEBB, R. I. 2011. Freeze substitution in 3 hours or less. *Journal of Microscopy,* 243**,** 227-233.

MINHAS, A. K., HODGSON, P., BARROW, C. J. & ADHOLEYA, A. 2016. A review on the assessment of stress conditions for simultaneous production of microalgal lipids and carotenoids. *Frontiers in microbiology,* 7**,** 546.

MNIF, I. & GHRIBI, D. 2015. High molecular weight bioemulsifiers, main properties and potential environmental and biomedical applications. *World Journal of Microbiology and Biotechnology,* 31**,** 691-706.

NIXON, S. J., WEBB, R. I., FLOETENMEYER, M., SCHIEBER, N., LO, H. P. & PARTON, R. G. 2009. A single method for cryofixation and correlative light, electron microscopy and tomography of zebrafish embryos. *Traffic,* 10**,** 131-136.

NOGUEIRA, D. A., DA SILVEIRA, J. M., VIDAL, É. M., RIBEIRO, N. T. & VEIGA BURKERT, C. A. 2018. Cell Disruption of Chaetoceros calcitrans by Microwave and Ultrasound in Lipid Extraction. *International Journal of Chemical Engineering,* 2018.

OLMSTEAD, I. L., HILL, D. R., DIAS, D. A., JAYASINGHE, N. S., CALLAHAN, D. L., KENTISH, S. E., SCALES, P. J. & MARTIN, G. J. 2013a. A quantitative analysis of microalgal lipids for optimization of biodiesel and omega-3 production. *Biotechnology and bioengineering,* 110**,** 2096-2104.

OLMSTEAD, I. L., KENTISH, S. E., SCALES, P. J. & MARTIN, G. J. 2013b. Low solvent, low temperature method for extracting biodiesel lipids from concentrated microalgal biomass. *Bioresource technology,* 148**,** 615-619.

PODDAR, N., SEN, R. & MARTIN, G. J. 2020. Bacterial abundance and diversity in Microchloropsis salina (formerly *Nannochloropsis* salina) cultures in response to the presence of ammonium, nitrate and glycerol. *Journal of Applied Phycology,* 32**,** 839-850.

POPOVICH, C. A., PISTONESI, M., HEGEL, P., CONSTENLA, D., BIELSA, G. B., MARTÍN, L. A., DAMIANI, M. C. & LEONARDI, P. I. 2019. Unconventional alternative biofuels: Quality assessment of biodiesel and its blends from marine diatom *Navicula* cincta. *Algal Research,* 39.

RAMÍREZ FAJARDO, A., ESTEBAN CERDÁN, L., ROBLES MEDINA, A., ACIÉN FERNÁNDEZ, F. G., GONZÁLEZ MORENO, P. A. & MOLINA GRIMA, E. 2007. Lipid extraction from the microalga *Phaeodactylum tricornutum*. *European Journal of Lipid Science and Technology,* 109**,** 120-126.

REDDY, S. & FOGLER, H. 1980. Emulsion stability of acoustically formed emulsions. *The Journal of physical chemistry,* 84**,** 1570-1575.

ROSENGARTEN, G. & HERRINGER, J. 2017. Interactions of Diatoms with Their Fluid Environment. *Diatom Nanotechnology.*

SPIDEN, E. M., SCALES, P. J., YAP, B. H., KENTISH, S. E., HILL, D. R. & MARTIN, G. J. 2015. The effects of acidic and thermal pretreatment on the mechanical rupture of two industrially relevant microalgae: Chlorella sp. and *Navicula* sp. *Algal research,* 7**,** 5-10.

SPIDEN, E. M., YAP, B. H. J., HILL, D. R. A., KENTISH, S. E., SCALES, P. J. & MARTIN, G. J. O. 2013. Quantitative evaluation of the ease of rupture of industrially promising microalgae by high pressure homogenization. *Bioresource Technology,* 140**,** 165-171.

UNDERWOOD, G. J. & PATERSON, D. M. 2003. The importance of extracellular carbohydrate productionby marine epipelic diatoms. *Advances in botanical research,* 40**,** 183-240.

VANDAMME, D., GHEYSEN, L., MUYLAERT, K. & FOUBERT, I. 2018. Impact of harvesting method on total lipid content and extraction efficiency for Phaeodactylum tricornutum. *Separation and Purification Technology,* 194**,** 362-367.

VILKHU, K., MAWSON, R., SIMONS, L. & BATES, D. 2008. Applications and opportunities for ultrasound assisted extraction in the food industry—A review. *Innovative Food Science & Emerging Technologies,* 9**,** 161-169.

WALTHER, P. & ZIEGLER, A. 2002. Freeze substitution of high-pressure frozen samples: the visibility of biological membranes is improved when the substitution medium contains water. *Journal of Microscopy,* 208**,** 3-10.

WANG, J.-K. & SEIBERT, M. 2017. Prospects for commercial production of diatoms. *Biotechnology for biofuels,* 10**,** 16.

WANG, Y., CHEN, Y., LAVIN, C. & GRETZ, M. R. 2000. Extracellular matrix assembly in diatoms (Bacillariophyceae). iv. ultrastructure of Achnanthes longipes and Cymbella cistula as revealed by high-pressure freezing/freeze substituton and cryo-field emission scanning electron microscopy. *Journal of Phycology,* 36**,** 367-378.

YAO, S., METTU, S., LAW, S. Q. K., ASHOKKUMAR, M. & MARTIN, G. J. O. 2018. The effect of high-intensity ultrasound on cell disruption and lipid extraction from high-solids viscous slurries of *Nannochloropsis* sp. biomass. *Algal Research,* 35**,** 341-348.

YAP, B. H., CRAWFORD, S. A., DUMSDAY, G. J., SCALES, P. J. & MARTIN, G. J. 2014. A mechanistic study of algal cell disruption and its effect on lipid recovery by solvent extraction. *Algal Research,* 5**,** 112-120.

YAP, B. H. J., CRAWFORD, S. A., DAGASTINE, R. R., SCALES, P. J. & MARTIN, G. J. O. 2016a. Nitrogen deprivation of microalgae: effect on cell size, cell wall thickness, cell strength, and resistance to mechanical rupture. *Journal of Industrial Microbiology and Biotechnology,* 43**,** 1671-1680.

YAP, B. H. J., MARTIN, G. J. O. & SCALES, P. J. 2016b. Rheological manipulation of flocculated algal slurries to achieve high solids processing. *Algal Research,* 14**,** 1-8.

YI, Z., XU, M., DI, X., BRYNJOLFSSON, S. & FU, W. 2017. Exploring valuable lipids in diatoms. *Frontiers in Marine Science,* 4**,** 17.

ZHANG, F., CHENG, L.-H., GAO, W.-L., XU, X.-H., ZHANG, L. & CHEN, H.-L. 2011. Mechanism of lipid extraction from Botryococcus braunii FACHB 357 in a biphasic bioreactor. *Journal of biotechnology,* 154**,** 281-284.

Chapter 5

5. Ultrasound-assisted EPS removal from the diatom *Navicula* sp.: A route to functional polysaccharides and more efficient algal biorefineries

This chapter follows from the discoveries in the previous chapter that ultrasound treatment seemed to remove the EPS layer in the diatom *Navicula* sp. This chapter investigates the application of power ultrasound to remove EPS as a potential co product with the aim of maximizing EPS extraction while minimizing cell rupture. Further to this, the processability of the slurries following EPS removal is investigated specifically looking at the dewaterability, rheology and biphasic lipid extraction for efficient biorefineries.

This chapter has been published as below.

"Ultrasound-Assisted Extracellular Polymeric Substance Removal from the Diatom *Navicula* sp.: A Route to Functional Polysaccharides and More Efficient Algal Biorefineries" by Yatipanthalawa BS., Ashokkumar M, Scales PJ, Martin GJ (2022). ACS Sustainable Chemistry & Engineering 10 (5), 1795-1804.

5.1 Introduction

Microalgae are a diverse group of photosynthetic organisms that have great potential as a highly productive feedstock for biorefineries that can produce biofuels, food ingredients and nutraceuticals (Yatipanthalawa and Martin, 2021, Vanthoor-Koopmans et al., 2013, Eppink et al., 2019). Diatoms are a large sub-group of microalgae characterised by their unique siliceous cell walls, known as frustules. Importantly, a number of diatoms have shown promise for commercial application due to their ability to produce large amounts of lipids rich in polyunsaturated fatty acids. In addition, diatoms produce carbohydrate-rich substances known as EPS.

EPS is a general term for polymeric substances that are produced by a range of microorganisms, including bacteria and microalgae. While highly diverse, they are often carbohydrate-rich polymers that can be characterized as quite bulky and hydrophilic (Henderson et al., 2010, Henderson et al., 2008b). As such, microbial EPS has found application as thickeners, for example bacteria-derived xanthan gum (Ikeda et al., 2019). The similar functional properties of microalgae EPS, suggests they could also be used as active thickeners or texturizing agents (Pierre et al., 2019). Microalgal EPS has also been found to bind with heavy metals, which could enable its application in water treatment (Naveed et al., 2019). Beyond these, based on the composition and properties of microalgal EPS it has been suggested for use as moisturizing agents, immune stimulants, aggregating agents and plant elicitors, or simply used as a feedstock for ethanol fermentation (Xiao and Zheng, 2016, Pierre et al., 2019, Gargouch et al., 2021). Despite the broad potential, microalgal EPS is currently expensive to produce and is used only in high-value niche markets of food and nutraceutical, cosmetic and pharmaceutical applications (Pierre et al., 2019).

The cost of producing microalgal EPS could be reduced if it could be efficiently recovered as a co-product with lipid production. Microalgal EPS can be released out from or bound to the cells, and different approaches have been taken to remove or extract bound EPS, including physical, chemical or a combination of physical and chemical methods. A challenge to consider is how to remove bound EPS without rupturing the cells. Cell rupture is disadvantageous since the EPS fraction will be contaminated with DNA, intercellular proteins, lipids and polysaccharides, while the loss of these components into EPS product stream would reduce the amount of lipid or protein available to be extracted in the subsequent processes. Takahashi et al. (2009) explored different combinations of physical and chemical methods for EPS extraction from the diatom *Navicula jeffreyi* while minimizing cell rupture. However, the extracted carbohydrate/polysaccharide

content was too low to be used commercially. Conversely, physical methods such as cation exchange resins, heating (Lv et al., 2019) and ultrasonication (Han et al., 2013) have shown the potential to give higher EPS extraction yields.

The interaction between ultrasound waves and bubbles in a liquid may lead to acoustic cavitation under certain conditions (Li et al., 2019). Strong shear forces are generated by acoustic cavitation when low frequency (20 kHz) ultrasound is used. The shear forces can facilitate removal of EPS, but also potentially cause cell rupture. Compared with other physical extraction methods, ultrasonic extraction is very rapid, however the energy consumption and scalability need to be considered. In this study, the first aim was to investigate the application of ultrasound to remove bound EPS while minimizing cell rupture and energy consumption. The purpose is to isolate pure EPS fractions for use in food or nutraceuticals, leaving behind a biomass that is rich in lipids for the production of biodiesel or for food applications.

Another possible benefit of upstream removal of EPS that has yet to be explored, is improving the flow properties of the concentrated diatom slurry in relation to downstream processing and lipid extraction. For diatoms, EPS is secreted out from the raphe (slits in the two valves, or plates, that comprise the frustule), becoming hydrated and swollen, which represents a hydrated polymeric layer surrounding the cells (Stal and Défarge, 2005). The presence of such a polymer layer (e.g. EPS) surrounding the surface of particles (e.g. diatom cells) is expected to induce repulsive forces between particles due to a volume restriction effect on the polymer conformations and the osmotic effect caused by high concentrations of overlapped polymer elements between the particles (Usher, 2005). Further, this layer contributes to extending the effective hydrodynamic volume occupied by the cells, which would be expected to increase the viscosity of cell slurries. Consistent with this idea, Ekstrand et al. (2020) observed the viscosity of anaerobic bacterial sludges to be increased with an increase in EPS content.

Based on these general observations, the presence of EPS surrounding diatom cells is likely to influence the packing and interactions between diatoms and therefore affect the rheology of these slurries. Thus, the removal of EPS improves the processability of the slurries, by facilitating concentration and dewatering. Such effects have previously been shown for bacteria, with a reduction in viscosity and improved dewaterability of sewage sludge resulting when EPS was dislocated from large aggregates of cells into the bulk aqueous solution (Ruiz-Hernando et al., 2013). However, the effect of EPS removal from diatoms has still not been properly investigated

in terms of the resultant suspension rheological properties nor the dewaterability of these suspensions. In a previous study, we showed that the bound EPS on the diatom *Navicula* sp. potentially hindered the lipid extraction from these cells in a biphasic system and that ultrasound was capable of removing the bound EPS (Yatipanthalawa et al., 2021). Therefore, apart from the potential effect on the rheological properties and hence the processability, the presence of EPS appears to affect lipid extraction efficiency as well.

In this study, 20 kHz ultrasound at different power densities and intensities were examined in order to optimise the extraction of EPS from the diatom *Navicula* sp. while minimising cell rupture and energy use. In addition, the effects of EPS removal on the processability of the residual algal slurry, including its rheological properties, dewatering and lipid extraction efficiencies were investigated. The results are aimed at providing new fundamental understanding that will enable efficient recovery of both EPS and lipids as value-added products from diatomaceous algae.

5.2 Materials and methods

5.2.1 Algae growth and harvest

A previously studied strain of the diatom *Navicula* sp. was grown in a modified *f* medium with added silica (Yatipanthalawa et al., 2021). The cultures were grown in 15 L carboys as described in Section 4.2.1 and harvested after a 10-day growth period using a disc stack centrifuge (Separator OTC 2-02-137, GEA Westfalia, Italy) operated at 10,000 rpm. The solids concentration of the harvested biomass was determined by drying overnight at 60 °C in an oven (with residual salt accounted for at 3% w/w of the evaporated water). Where applicable, the dry weight of the dilute suspensions was also verified by filtering the samples through pre-weighed Whatman GF/C (47 mm; glass microfiber) filters using a vacuum filtration unit, washing the filters containing samples using ammonium formate (0.5 M) and then drying at 60 °C overnight before taking the dry weight measurements.

5.2.2 Ultrasonication and EPS removal

For the first part of the study involving ultrasonic EPS removal, 20 mL of the cell suspensions with 1.0 ± 0.1% solids concentration were ultrasonicated at 20 kHz in 50 mL conical centrifuge tubes for 5 s, 15 s and 30 s. The treatments were done in an ice water bath to minimize the heating effects during ultrasonication. During ultrasonication, the high intensity shear forces will be localized immediately adjacent to the transducer face (Leong et al., 2009). This could have an

impact on the energy efficiency as well as the effectiveness of EPS removal. To investigate this effect of ultrasonic power intensity (power per unit transducer area), two Branson digital sonifiers fitted with two different ultrasonic transducers were used: 1) a transducer with a 12 mm diameter horn tip (No.102C) connected to a sonifier (Model No. 450, nominal power 400 W, Branson, Connecticut) and 2) a micro tip horn with a 3 mm diameter connected to a sonifier (Model No. 450, nominal power 400 W, Branson, Connecticut). The average power density (the average energy dissipated per unit time and unit volume) is another measure of the strength of the turbulence, understanding of which could minimise the energy requirement while maximizing the benefits. The calorimetric power was determined by measuring the temperature increment increase of a 100 ml water bath after ultrasonicating for 1 min. Based on these parameters, three different treatments to observe the different effects of power intensity and densities are described as detailed in Table 5.1.

Table 5.1. Ultrasound parameters used in three different EPS removal treatments.

Horn tip diameter (mm)	Nominal Power (W)	Calorimetric power (W)	Power intensity Level	Power intensity (MW/m^2)	Power density Level	Power density (W/ml)
12	40	13.8	Low	0.12	Low	0.688
12	80	30	Medium	0.27	High	1.5
3	120	30	High	4.24	High	1.5

Following ultrasonication, cell suspensions were centrifuged for 10 mins at 4000 g using a benchtop centrifuge (Allegra X-30R, fixed-angle rotor F0685, Beckman Coulter, Victoria, Australia). To obtain a consistent solids concentration of 5% w/w, a pre-determined volume of the supernatant layer was pipetted out from each sample and discarded, assuming the supernatant removed was equivalent to 3% salt water. The separated supernatant was centrifuged twice to ensure it was free from cells. Centrifugation of the supernatant was performed at 6000 g for 10 min for the first round and at 10,864 g for 10 mins for the second round using a benchtop centrifuge (Allegra X-30R, fixed-angle rotor F0685, Beckman Coulter, Victoria, Australia).

5.2.3 Polysaccharide measurement

The polysaccharide content of the separated supernatant was quantified following the phenol sulphuric method developed by Dubois et al. (1956) using glucose as the standard. Briefly, the supernatants were diluted with 3% sea water, and mixed with a 5% phenol solution and concentrated sulphuric acid at a ratio of 1:1:5. The tubes were left at room temperature for 10 minutes, after which they were shaken and placed in a water bath at 25 °C for 20 minutes. The absorbance was measured using a UV-Vis spectrophotometer (Cary 3E UV-Vis absorbance spectrophotometer, Agilent Technologies, Mulgrave, VIC, Australia) at a wavelength of 490 nm. This measured polysaccharide concentration was converted to an extracted EPS content based on the dry weight of the suspensions.

5.2.4 Quantification of cell rupture

The extent of cell rupture caused by ultrasonication was quantified using cell counting. The cell suspensions were diluted with 3% synthetic sea water (Red Sea Coral Pro Salt, Red Sea, USA) by x100 times and 10 µl of the diluted suspension was placed in a standard Neubauer hemocytometer, and imaged using Olympus BX51 microscope (Olympus, Australia). From these images, the number of whole cells was manually counted. The absorbance at 260 nm, which gives a rough estimation of the DNA content, was also measured as an indication of the extent of cell rupture (Spiden et al., 2013a). The maximum absorption corresponding to complete cell rupture was found by subjecting the cells to prolonged ultrasonication at 2 min, 5 min and 10 min intervals, with the absorbance after 5 min ultrasonication found to give the highest absorption. This was used as a reference and the percent cell rupture after ultrasonication was calculated using the following equation. The samples were diluted using modified F medium with added silica (Spiden et al., 2015) where necessary to obtain an absorbance value below 0.6.

$$\%Cell\ Rupture = \frac{Absorbance\ at\ 260nm}{Absorbance\ at\ 260nm\ after\ 5\ \mathrm{min}\ ultrasonication} \times 100.$$

5.2.5 Shear dependent viscosity measurement

The shear rate-dependent viscosity of slurries of *Navicula* sp. at various solid concentrations was measured using a rheometer (MCR 702 Twin Drive from Anton-Paar) with shear rates from 0.5 s^{-1} to 300 s^{-1}. Two different setups were used for the measurement of shear dependent viscosity of the algae slurries before and after EPS removal. The viscosity of the slurries prior to EPS removal were measured at different solid concentrations using a vane in cup geometry (ST10 &

C-CC30, Anton-Paar). The viscosity of the slurries after EPS removal was measured using a cup and bob geometry (Cup diameter 28mm and bob, Anton-Paar), as the viscosity was too low to be measured using the vane in cup geometry. The concurrence of results from the two systems was compared by using an algae suspension of 5% solids concentration and measuring the shear dependent viscosity of the slurry using both geometries. The viscosity measurements were obtained at least in duplicate. The shear dependent viscosity of the dilute supernatants containing the EPS fractions was measured using a double gap measuring system (DG26.7 & DG26.7/T200/SS) with shear rates applied from 0.5 s^{-1} to 300 s^{-1}.

5.2.6 Dewatering of suspensions after EPS extraction

The kinetics of centrifugal separation of the diatom cells from the supernatant was observed using a benchtop centrifuge with an integrated photo analyser (LUMiFuge®, L.U.M. GmbH, Berlin, Germany). 1.3±0.1 ml samples were put into the LUMiFuge tubes (10 mm optical path length, part no. 110-135XX, L.U.M. GmbH, Berlin, Germany) and were centrifuged at 2330 g for 20 mins in order to observe the dewatering of the diatom cells. Duplicate analyses were done for process triplicates. The separation efficiency was calculated based on the length between the two interfaces (air-supernatant and supernatant-algae) as tracked by an integrated photo analyser (Law et al., 2017b).

5.2.7 Shear-assisted lipid extraction

The kinetics of biphasic lipid extraction from concentrated suspensions of *Navicula* using hexane was studied as a function of EPS removal using a previously described method (Yatipanthalawa et al., 2021). Briefly, 10 ml of 5% w/w algae slurry (untreated or ultrasonicated) was combined with 10 ml of hexane in a 50 ml plastic tube and subjected to lipid extraction using one of two mixing methods: low-shear mixing or high-shear ultrasonication. Low shear mixing was achieved by rotating the tubes at 8 rpm using a rotator (Labquake, Barnstead International, Iowa, USA). The extraction temperature was maintained at 24 ± 1 ºC by placing the mixer in an incubator (Unimax 1010 & Incubator 1000, Heidolph Instruments, Germany). High-shear mixing was performed by ultrasonicating the algae/hexane mixture using a high-intensity ultrasonic transducer with a 3 mm diameter microtip horn. The tip was placed at the initial hexane-biomass interface to uniformly distribute the ultrasound through the sample. The tubes were submerged in ice cold water bath during ultrasonication to avoid heating of the samples.

To determine the lipid extraction kinetics, representative 1.5 ml aliquots of the emulsion were periodically removed and centrifuged at 2330 g for 10 min in a benchtop centrifuge (5424 Eppendorf, Germany). The lipid rich hexane layer was pipetted and diluted appropriately using n-hexane and the absorbance was measured at 450 nm using a UV-Vis spectrophotometer (Cary 3E UV-Vis absorbance spectrophotometer, Agilent Technologies, Mulgrave, VIC, Australia). The lipid concentration was obtained using a calibration curve obtained for known lipid concentrations vs the absorbance at 450 nm following the same method as (Yatipanthalawa et al., 2021). In brief, the calibration curve was obtained by redissolving a known mass of lipids in hexane that was extracted from *Navicula* sp. using hexane and dried under a nitrogen stream. The absorbance at 450nm of known lipid concentrations were measured. To further validate the measurements, the absorbance values were rechecked with the gravimetric lipid content where possible. The gravimetric lipid concentration was obtained by pipetting out a known volume of lipid rich hexane layer following lipid extraction into a clean weighed glass vial. This was dried at 60 °C under a stream of nitrogen (Olmstead et al., 2013a) to obtain the gravimetric lipid concentration.

5.2.8 Experimental reproducibility and analysis

All experiments were performed at least in duplicates. Ultrasound-assisted EPS removal was performed as triplicated experiments, for each time point. Polysaccharide content measurement and cell rupture quantification were performed in duplicates for each triplicated experiment. Shear-dependent viscosity measurements were performed in duplicates for each experiment.

Dewaterability measurements were carried out as duplicated analysis for triplicated experiments. For clarity, only representative separation kinetics were selected and presented. The final biomass concentrations were obtained as previously explained using the data from the replicates for dewaterability measurements. Lipid extractions were performed on triplicated experiments. For the quantitative data, the mean and the standard deviation were calculated based on the replicates. A single-factor analysis of variance (ANOVA) analysis was performed for the lipid yield data using Excel to see if the treatments have caused significant differences. A confidence interval of 99% ($\alpha = 0.01$) was used for the comparison of means. Following the ANOVA test, t-tests with a 95% confidence interval were performed to confirm the effects at each time interval for all the treatments.

5.3 Results and discussion

5.3.1 Removal of EPS and cell rupture as a function of ultrasonication parameters

It was previously shown that the presence of EPS surrounding *Navicula* sp. cells hindered biphasic lipid extraction and that ultrasonication could remove EPS from the cell surfaces (Yatipanthalawa et al., 2021). As noted above, when using ultrasound to recover EPS as a product it is important to decrease the extent of cell rupture while increasing the extraction yield of EPS. In addition, to reduce energy consumption, the ultrasonication time and power should be minimised. The first aim of this study was to investigate how ultrasonic EPS removal could be optimised by determining the relative extent of EPS removal and cell rupture and the energy consumption in relation to three important ultrasonic processing variables: time, power density (W/ml), and power intensity (W/m^2).

Power density determines how well the Higher power intensities will lead to highly localized turbulent forces whereas at lower intensities, the ultrasound waves would be comparatively distributed. Therefore, high intense treatment could lead to more cell rupture and hence worthwhile playing around the applied ultrasound intensities.

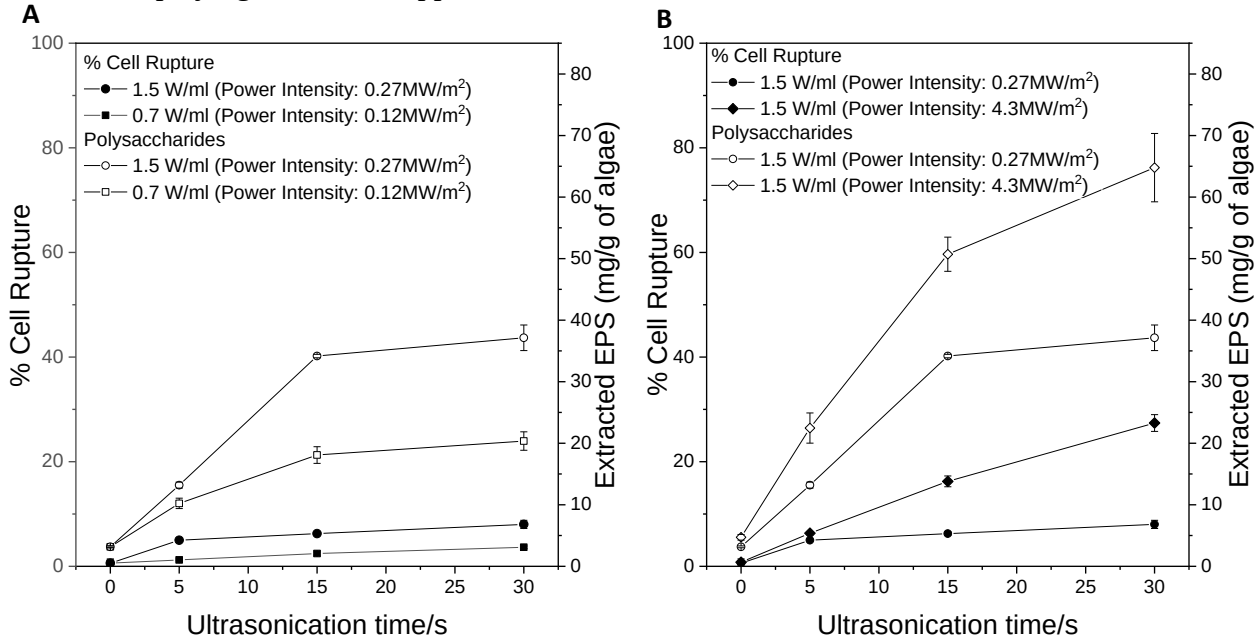

Figure 5.1: Extracted EPS (as estimated by the polysaccharide content of the supernatant) and cell rupture as a function ultrasonication time at (A) two different power densities and intensities and (B) at two different power intensities at the same power density of 1.5 W/ml. The data points and error bars represent the average and standard deviation of process triplicates, respectively. The same 1.5 W/ml, 0.27 MW/m^2 data is presented in both panels to facilitate comparisons.

Figure 5.1 shows the quantity of EPS polysaccharides extracted over time at different power densities and intensities and the corresponding percentage of cell rupture. The results show that with increasing ultrasonication time, both the amount of EPS extracted and the percentage of cell rupture increased for all combinations of ultrasound power intensity and density. Further, when the power density was increased at the same power intensity (Figure 5.1A), or conversely when the power intensity was increased at the same power density (Figure 5.1B), both cell rupture and extracted EPS increased. To help understand the influence of ultrasound parameters, the data was presented in terms of the selectivity of EPS removal relative to cell rupture (Figure 5.2A) and energy consumption (Figure 5.2B).

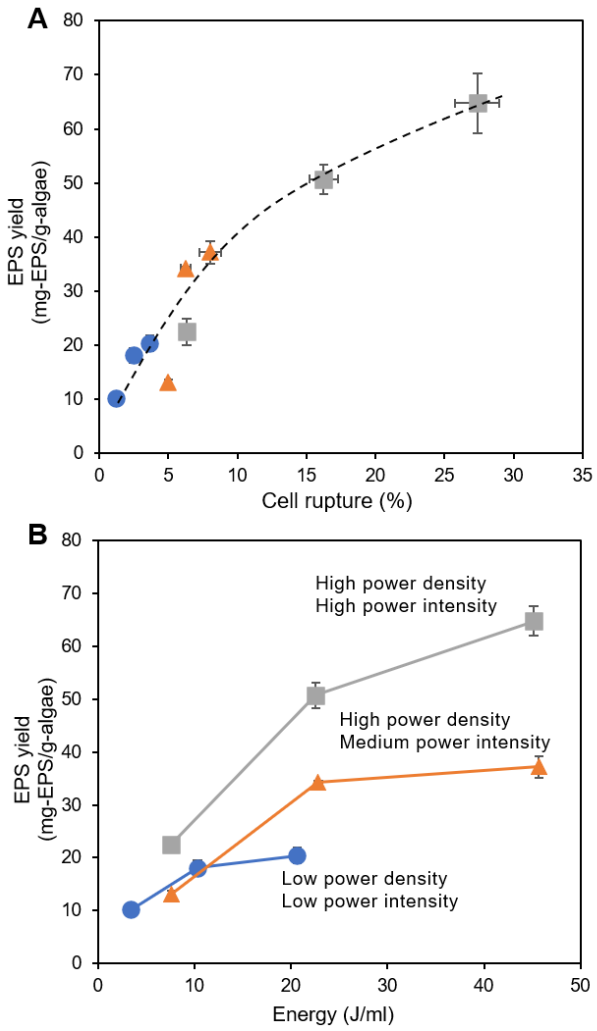

Figure 5.2: EPS recovery yield (as estimated by the supernatant polysaccharide content) in relation to cell rupture (A) and energy use (B) as a function ultrasound power intensity (low = blue circles = 0.12 MW/m^2; medium = orange triangles = 0.27 MW/m^2; high = grey squares = 4.24 MW/m^2) and power density (low = 0.688 W/mL; high = 1.5 W/mL). The data points and the error bars represent the average and standard deviation of process triplicates.

The relationship between EPS yield and cell rupture did not appear to vary with the ultrasound intensity or the power density used (Figure 5.2A). Rather, the EPS yield was approximately proportional to the % of cell rupture up to a certain extent, beyond which the relative increase in EPS yield diminished with respect to increasing % cell rupture. This is similar to a previous observation that 'loosely bound' EPS could be extracted from activated sludge with minimal cell disruption using ultrasonication (Han et al., 2013). The increase in the relative cell rupture at higher

extents of EPS removal (Figure 5.2A) can be attributed to more tightly bound EPS that is more difficult to extract without also causing cell rupture. The results indicate that, for *Navicula*, the trade-off between EPS yield and the cell rupture cannot be readily resolved by manipulation of the ultrasound parameters, suggesting that the level of shear needed to dislodge tightly bound EPS is commensurate with that needed to break the cells.

Importantly, the results show that the energy efficiency of EPS recovery could be improved by increasing ultrasound power density and intensity (Figure 5.2B). Using a higher power density for a shorter time almost doubled the amount of EPS extracted from 18 to 34 mg-EPS/g-algae using a similar amount of energy (21-22 J/mL), thus improving the energy efficiency of the process. Similarly, increased power density has previously been found to be more energy efficient in producing emulsions with a given average droplet diameter (Li et al., 2018a). Moreover, using a higher power intensity (at the high power density) also increased the EPS extraction yield by 48-74% for a given energy input (Figure 5.2B). In these experiments, ultrasonication power density was varied by changing the input power, while the power intensity was changed by using ultrasonic horns with different tip diameters. For a given power output, a smaller tip means the acoustic intensity is more intensely focussed, and the energy dissipation zone is limited to the area around and under the tip of the transducer (Li et al., 2019). This concentrated dissipation of energy results in more intense shear forces and better mixing, thus dislodging EPS and rupturing the cells more efficiently in terms of energy input. Across all tested combinations of power intensity and density, the EPS yield per unit energy (slope of Figure 5.2B) decreased at higher EPS yields. This can be attributed to increased ultrasound attenuating due to an increase in the viscosity of the continuous aqueous phase resulting from the release of EPS as well as intracellular protein and DNA from cell rupture (Yao et al., 2018b).

5.3.2 Effect of US assisted EPS removal on slurry rheology

Having confirmed ultrasonication releases bound EPS, the effect of the removal of EPS on the processability of the microalgae suspension was investigated. For this, the rheology of the suspensions was characterised with respect to the biomass concentration and the EPS content, which was removed to different extents by controlled ultrasonic pre-treatment. Based on the higher energy efficiency of EPS extraction, a power intensity of 4.3 MW/m^2 and a power density of 1.5 W/ml were selected in this part of the study.

First, the shear dependent viscosity of untreated *Navicula* sp. suspensions at different solid concentrations was measured to provide a baseline of the rheology of EPS-containing *Navicula* sp. (Figure 5.3A). At high solid concentrations, suspensions of microalgae such as *Nannochloropsis* have been found to behave as shear thinning liquids, for which the viscosity reduces as the shear rate increases (Yap et al., 2016a, Yao et al., 2018b). Similarly, at solid concentrations above 3% *Navicula* sp. slurries were seen to be shear thinning (Figure 5.3A). Notably, the shear dependent viscosity of this diatom was comparatively higher than slurries of other algae reported in previous works, including *Nannochloropsis sp.* (Yao et al., 2018b), *O. aurita, A. platensis, Schizochytrium sp., P. tricornutum* (Bernaerts et al., 2017). For example, when comparing with the previous literature, at a shear rate of 100 s^{-1}, the viscosity of the 8% *Navicula* slurry is 3 times, 10 times and 30 times higher than equivalent slurries of *O.aurita*, *A.platensis* and *Nannochloropsis sp.*, respectively. The rheological properties of algae slurries are influenced by the solids concentration, the content of polymeric substances dissolved in the medium, the temperature, the surface properties and interactions of the algae cells, and the pH and ionic strength of the liquid phase (Wileman et al., 2012). The much higher viscosity of slurries of *Navicula* sp. compared to the other microalgae species mentioned above, is likely due to the EPS produced by *Navicula*. This could include a contribution to the bulk viscosity by soluble EPS, and strong surface interactions between cells due to the presence of bound EPS.

To investigate if the removal of EPS from these diatoms could reduce the slurry viscosity, algae suspensions were ultrasonicated and the dislodged EPS were removed by centrifugation before measuring the shear dependent viscosity of the resulting slurries. As expected, the removal of EPS using ultrasonication reduced the viscosity by orders of magnitude, with the slurry viscosity decreasing with an increase in ultrasonication time (Figure 5.3B). As shown in Figure 5.1, longer ultrasonication increases the removal of bound EPS. These results provide strong evidence that the EPS is the main cause for the high viscosity of slurries of the diatom *Navicula* sp., and indicate that considerable improvements in the processability of the biomass can result from even a very short amount of ultrasonication.

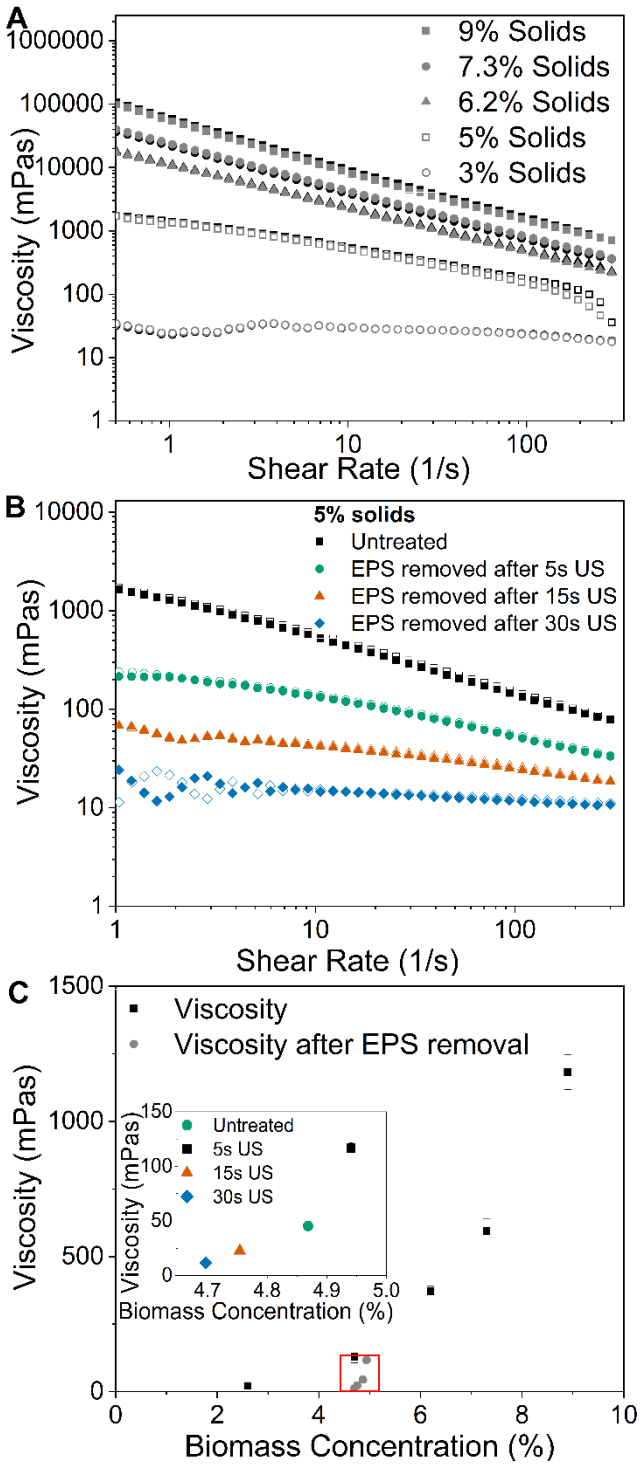

Figure 5.3: (A) Shear dependent viscosity of *Navicula* sp. slurries at increasing shear rates from 1 to 300 s^{-1} and different solid concentrations. (B) Shear dependent viscosity of *Navicula* sp. slurries following removal of EPS by ultrasonication for different time periods (power intensity = 4.24 MW/m^2; power density = 1.5 W/mL) and removal of the EPS-rich supernatant to obtain a solids

concentration of approximately 5%. (C) The viscosity at a shear rate of 145 s^{-1} as a function of the biomass concentration of untreated *Navicula* slurries (■) and following ultrasonic and centrifugal EPS removal (●). The slight decrease in biomass concentration following ultrasonication is due to mass loss associated the EPS are removal. In (A) and (B), duplicated measurements are shown for each data set, in coloured and empty symbols. In (C), the data points and error bars represent the average and standard deviation of duplicate measurements, respectively.

Figure 5.3C presents the viscosity data from Figure 5.3A and B at 145 s^{-1}, as a function of biomass concentration. This shear rate is representative of the slurry being exposed to shear forces during biomass processing, such as pumping and ultrasonication. The viscosity increases exponentially with solid concentration, which is consistent with rheological theory of particulate suspensions (Rutgers, 1962).

Recently, Guadayol et al. (2021) observed that the relative viscosity near the cell surface of the diatom *Chaetoceros affinis* (of which the frustules are made of silica) was much higher than that near the surface of glass shards, indicating the effect of EPS on the surface of diatom frustules on the surrounding hydrodynamics. The coverage of diatom cells by large amounts of EPS increases the hydrodynamic volume and resistance to particle motion, thereby directly increasing the slurry viscosity. Further, this EPS can entangle and act as a 'glue' that fixes the diatom cells together in a network structure that will increase the viscoelasticity of the system (Figure 7.3). The removal of bound EPS using ultrasound reduces both the hydrodynamic volume of the cells and interparticle network, to greatly lower the suspension viscosity.

5.3.3 Effect of EPS removal on the dewaterability of microalgae

As observed and discussed earlier, the removal of EPS leads to better flow properties (lower viscosity) of the microalgal suspension. Apart from the effect on the viscosity, the presence of these polymers is also expected to affect the ability to remove water from the suspensions. This in turn affects the separation efficiency when concentrating the cells using compressional processes such as filtration and centrifugation (Ekstrand et al., 2020). Disintegrating or detaching the EPS from the particle surface is expected to reduce the water holding capacity of the suspension and improve dewaterability (Raynaud et al., 2012). To confirm this, the dewaterability of the *Navicula* suspension at a starting biomass concentration of 1% w/w was studied using a LUMiFuge centrifugal separator. The device allows the user to track both the rate and the extent of a separation event. The separation rate and extent (highlighted as a separation efficiency herein) was tracked

by observing the interface between the aqueous phase and the microalgae suspension. The dewatering rate decreased as a function of increasing cake solid fraction in the kinetic profile (Figure 5.4A) which was typical to dewatering of a compressible material.

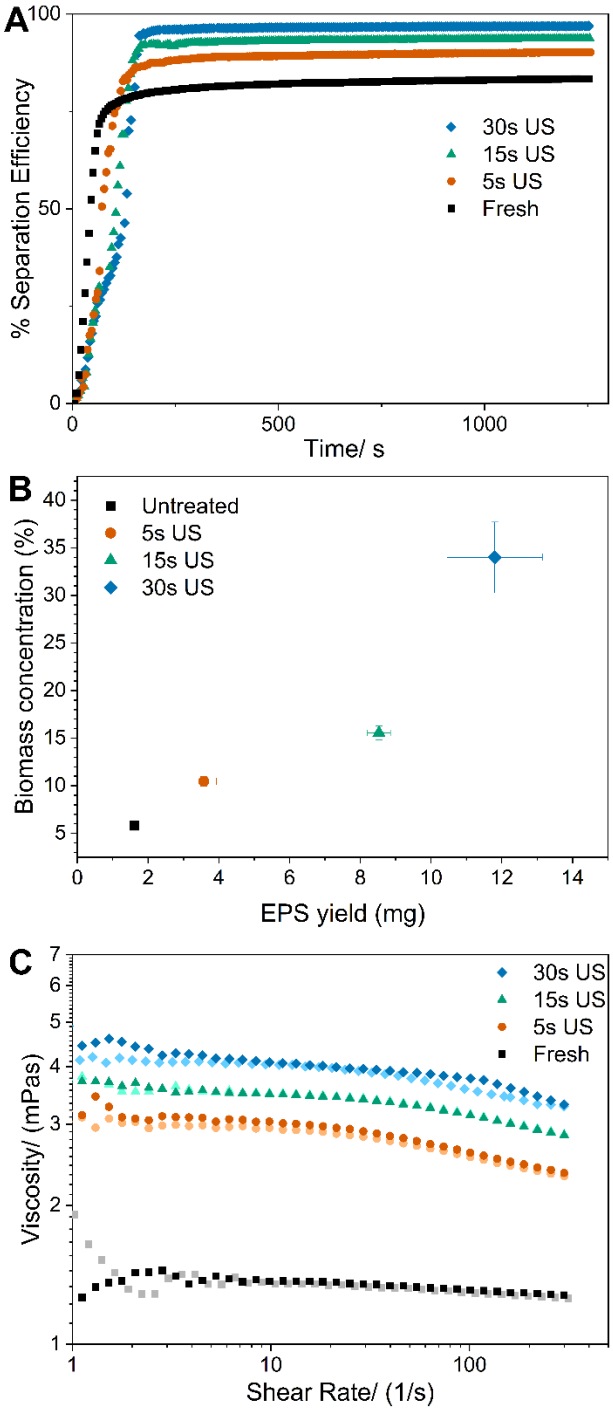

Figure 5.4: (A) The effect of ultrasonic removal of EPS on the rate of separation efficiency (defined as the percentage of water removed from the biomass). (B) The final biomass concentration

obtained after centrifugation for 20 min at 2330 g as a function of the amount of EPS removed/dislodged using ultrasonication for 5 s, 15 s, or 30 s (power intensity = 4.3 MW/m^2; power density = 1.5 W/ml). (C) Shear dependent viscosity of the EPS fractions separated by centrifugation after ultrasonication.

Upon centrifugation, the *Navicula* suspensions reached higher final separation efficiencies (representing dewatering to higher concentrations) with increasing ultrasonication time (Figure 5.4A), although the rate of separation was slightly slower with increasing ultrasonication time. EPS is involved in the agglomeration of microalgae cells and affects solid-liquid separation (Henderson et al., 2008a, Rao et al., 2020). EPS can aggregate diatom cells into large flocs, which leads to larger particle sizes and higher initial settling velocities (Xiao and Zheng, 2016). This can explain the faster settling rates observed for the cells not subjected to ultrasonic EPS removal. In addition, the slower settling rates observed after EPS removal using ultrasound could be partially due to an increase in viscosity of the continuous aqueous phase (due to the released EPS), thereby hindering the settling of the cells. Consistent with this, the shear dependant viscosity of the EPS-containing supernatants following ultrasonication was indeed higher when the ultrasonication time was increased (Figure 5.4C). The viscosity was increased 3-4 fold, which would reduce the initial settling rate proportionally, thereby potentially accounting for the observed differences. It is important to note however, that the decrease in settling rate of ultrasonicated cells is unlikely to have much practical consequence. The cells will have already been undergone gravity settling prior to ultrasonic EPS removal, and the effect of a slightly slower initial settling rate during subsequent centrifugation will have little impact on efficiency.

In contrast, an improvement in the final extent of dewatering would be of significant practical benefit for processing. After centrifuging for 20 min at 2330 g, a separation efficiency of only around 80% could be achieved in the case of untreated suspensions whereas a separation efficiency of around 98% could be obtained after dislodging the EPS using ultrasound for 30s (Figure 5.4A). The improvement in separation efficiency resulting from EPS removal translates to a dramatic increase in the final biomass concentration achieved following centrifugation (Figure 5.4B). Ultrasonicating for 5 s, 15 s and 30 s progressively removed EPS allowing the solids concentration to increase from only 6% up to 11%, 15% and almost 35%, respectively.

This increase in the separation efficiency and therefore the final biomass concentration (up to a 7-fold increase) represents a significant reduction in the processing volume. This in turn would lead

to an intensified and more energy efficient process when considering microalgal biorefineries using wet microalgal biomass (Martin, 2016b).

5.3.4 Effect of EPS removal on lipid extraction

Previously we observed that biphasic lipid extraction from *Navicula* sp. was possible even without prior cell rupture, and the application of ultrasonic shear during extraction increased the rate of lipid extraction (Yatipanthalawa et al., 2021). This improvement could be attributed to a number of factors, including increased mass transfer, increased cell rupture, and removal of EPS as a barrier between the cells and the hexane droplets. Thus, in this work we investigated whether the removal of EPS, which was previously shown to hinder the contact between the cells and hexane droplets (Yatipanthalawa et al., 2021) could itself improve the lipid yield and the lipid extraction kinetics. To test this, the EPS fraction was removed by ultrasonication prior to extraction, with the cells then concentrated to remove the released EPS, and subsequently subjected to lipid extraction. In the previous study, it was seen that using ultrasonication/high shear mixing during hexane extraction significantly improved the kinetics compared with low shear mixing (Yatipanthalawa et al., 2021). To facilitate comparisons, the effects of EPS removal on the lipid extraction was tested again using both high shear (ultrasonic-assisted extraction) and low shear mixing regimes. Figure 5.5 presents the neutral lipid extraction kinetics (in terms % lipid yield) obtained for low and high shear mixing.

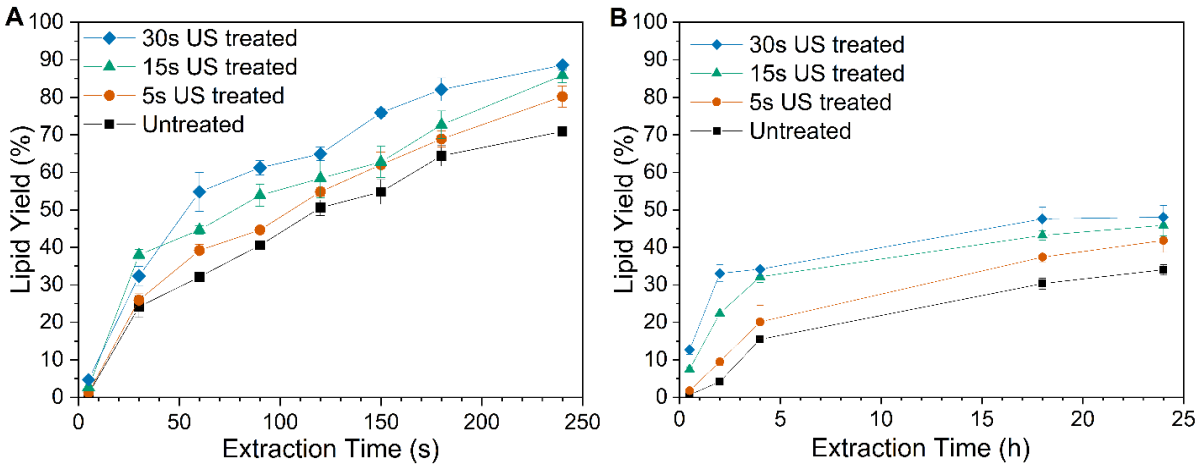

Figure 5.5: Biphasic lipid extraction kinetics from suspensions of the diatom *Navicula* sp. with EPS removed by ultrasound pretreatment and concentrated to 5% solids. Lipid yields represent the % of total neutral lipids in the algae that were recovered. (A) Extraction kinetics under high shear

mixing using ultrasonication. (B) Extraction kinetics under low shear mixing. Both sets of data were obtained at room temperature. The data points and error bars represent the average and standard deviation of triplicated experiments.

Similar to our previous study (Yatipanthalawa et al., 2021), extraction under low shear took hours whereas ultrasonic-assisted extraction took minutes (Figure 5.5). The removal of EPS improved the lipid extraction kinetics and yield under both low-shear and high-shear mixing, with the increased rate being more pronounced for the low shear extractions. The improvements can firstly be attributed to the reduction in viscosity (as identified above) that facilitates more efficient emulsification of the hexane, creating more interfacial area for contact between the cells and hexane droplets. High viscosities rapidly attenuate ultrasound waves and thus the ability for ultrasound to properly emulsify the system (Yao et al., 2018b). In addition, the detachment of EPS removes a barrier to direct contact between the permeable diatom cell frustules and the hexane. (Yatipanthalawa et al., 2021).

When low shear mixing is considered, although the overall lipid yield is not increased considerably, lipid extraction kinetics are greatly improved, minimising the time required to reach a specific lipid yield. For instance, reaching a lipid yield of 30% takes 18 h for the algae suspension in the presence of EPS, but this is reduced to 12 h, 3.5 h and 2 h after removing the EPS by ultrasonicating for 5 s, 15 s and 30 s intervals, respectively.

Although the improvement during high shear mixing may appear to be slight, significant reductions in the overall energy required are possible. For example, the time taken to reach a 60% lipid yield during this process was found to be approximately 166 s, 142 s, 132 s and 86 s for the suspensions with no EPS removal, 5 s, 15 s and 30 s of ultrasonication assisted EPS removal, respectively. The overall ultrasonication time required (including ultrasonic pretreatment and extraction) is almost halved when the system is subjected to a pre-EPS removal step by subjecting them to 30 s of ultrasonication compared with that with no pre-EPS removal. Beyond the energy savings for ultrasonication, the decrease in extraction time reduces the vessel size and operational costs of extraction.

5.3.5 General discussion

A schematic overview of the mechanistic insights from this study is shown in Figure 5.6. The bound EPS are released from the cells using ultrasonication, which leads to a reduction in the viscosity as a result of a reduced role of polysaccharides that otherwise act as a glue and a thickener

to bind the cells together and hinder the particle motion (Henderson et al., 2008a). In combination, the decrease in the viscosity, improved settling and dewatering, and the increased rate of lipid extraction represent a considerable reduction in the energy, capital, and operational costs associated with this process. While the incorporation of the pre-EPS removal step represents an additional cost, it allows the possibility of recovering EPS as a valuable co-product for use in food and nutraceutical applications. The released EPS are recovered as a separate fraction, which has the potential to be used as a high value additive in food and nutraceutical applications, due to avoidance of contamination with organic solvents during lipid extraction. Overall, this method appears to have a lot of practical potential, with a detailed cost and energy analysis implied as an obvious next step.

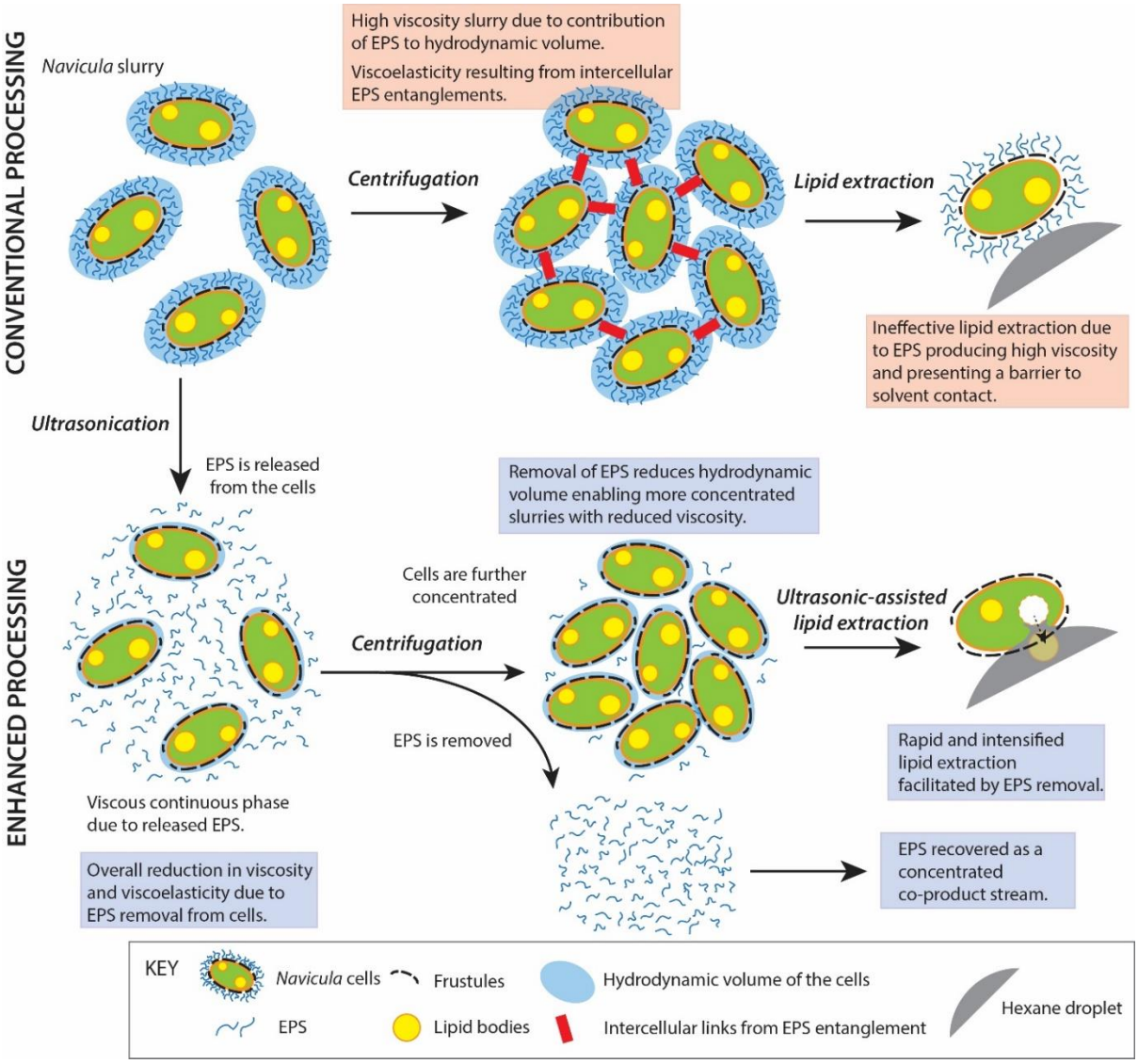

Figure 5.6: Summary of the improvements to a biorefinery enabled by ultrasonic pre-treatment to remove EPS. This process results in a concentrated EPS stream and improves the processability of the microalgae suspension by decreasing the overall suspension viscosity, by enabling higher solids concentration slurries to intensify processing, and by accelerating lipid extraction.

5.4 Conclusion

In this work, ultrasonic EPS removal and its effect on the processability of algal suspensions of the diatom *Navicula* sp. were investigated. While manipulation of ultrasonic parameters did not appear to influence the extent of cell rupture for a given EPS yield, it was found that more intense ultrasound could improve energy efficiency and produce higher EPS yields. Ultrasound assisted EPS removal was shown to decrease the viscosity of the cell suspensions by orders of magnitude and to improve the extent of dewaterability to allow up a 7-fold increase in the concentration of slurries that can be processed. Lipid extraction kinetics using both high and low shear mixing was also improved after EPS removal. Ultrasound was therefore shown to be promising as a method for EPS removal, which in turn can greatly enhance the processability of algae suspensions.

5.5 References

BERNAERTS, T. M., PANOZZO, A., DOUMEN, V., FOUBERT, I., GHEYSEN, L., GOIRIS, K., MOLDENAERS, P., HENDRICKX, M. E. & VAN LOEY, A. M. 2017. Microalgal biomass as a (multi) functional ingredient in food products: Rheological properties of microalgal suspensions as affected by mechanical and thermal processing. *Algal research,* 25**,** 452-463.

DUBOIS, M., GILLES, K. A., HAMILTON, J. K., REBERS, P. T. & SMITH, F. 1956. Colorimetric method for determination of sugars and related substances. *Analytical chemistry,* 28**,** 350-356.

EKSTRAND, E.-M., SVENSSON, B. H., ŠAFARIČ, L. & BJÖRN, A. 2020. Viscosity dynamics and the production of extracellular polymeric substances and soluble microbial products during anaerobic digestion of pulp and paper mill wastewater sludges. *Bioprocess and biosystems engineering,* 43**,** 283-291.

EPPINK, M. H. M., OLIVIERI, G., REITH, H., VAN DEN BERG, C., BARBOSA, M. J. & WIJFFELS, R. H. 2019. From current algae products to future biorefinery practices: A review. *Advances in Biochemical Engineering/Biotechnology.*

GARGOUCH, N., ELLEUCH, F., KARKOUCH, I., TABBENE, O., PICHON, C., GARDARIN, C., RIHOUEY, C., PICTON, L., ABDELKAFI, S., FENDRI, I. & LAROCHE, C. 2021. Potential of exopolysaccharide from porphyridium marinum to contend with bacterial proliferation, biofilm formation, and breast cancer. *Marine Drugs,* 19.

GUADAYOL, Ò., MENDONCA, T., SEGURA-NOGUERA, M., WRIGHT, A. J., TASSIERI, M. & HUMPHRIES, S. 2021. Microrheology reveals microscale viscosity gradients in planktonic systems. *Proceedings of the National Academy of Sciences,* 118.

HAN, X., WANG, Z., ZHU, C. & WU, Z. 2013. Effect of ultrasonic power density on extracting loosely bound and tightly bound extracellular polymeric substances. *Desalination,* 329**,** 35-40.

HENDERSON, R., PARSONS, S. A. & JEFFERSON, B. 2008a. The impact of algal properties and pre-oxidation on solid–liquid separation of algae. *Water research,* 42**,** 1827-1845.

HENDERSON, R. K., BAKER, A., PARSONS, S. A. & JEFFERSON, B. 2008b. Characterisation of algogenic organic matter extracted from cyanobacteria, green algae and diatoms. *Water research,* 42**,** 3435-3445.

HENDERSON, R. K., PARSONS, S. A. & JEFFERSON, B. 2010. The impact of differing cell and algogenic organic matter (AOM) characteristics on the coagulation and flotation of algae. *Water research,* 44**,** 3617-3624.

IKEDA, S., MURAYAMA, D., TSURUMAKI, A., SATO, S., URASHIMA, T. & FUKUDA, K. 2019. Rheological characteristics and supramolecular structure of the exopolysaccharide produced by Lactobacillus fermentum MTCC 25067. *Carbohydrate polymers,* 218**,** 226-233.

LAW, S. Q. K., CHEN, B., SCALES, P. J. & MARTIN, G. J. O. 2017. Centrifugal recovery of solvent after biphasic wet extraction of lipids from a concentrated slurry of *Nannochloropsis* sp. biomass. *Algal Research,* 24**,** 299-308.

LEONG, T., WOOSTER, T., KENTISH, S. & ASHOKKUMAR, M. 2009. Minimising oil droplet size using ultrasonic emulsification. *Ultrasonics sonochemistry,* 16**,** 721-727.

LI, W., GAMLATH, C. J., PATHAK, R., MARTIN, G. J. & ASHOKKUMAR, M. 2019. Ultrasound–The Physical and Chemical Effects Integral to Food Processing. *In:* KNOERZER, K. & MUTHUKUMARAPPAN, K. (eds.) *Innovative Food Processing Technologies.* Elsevier.

LI, W., LEONG, T. S., ASHOKKUMAR, M. & MARTIN, G. J. 2018. A study of the effectiveness and energy efficiency of ultrasonic emulsification. *Physical Chemistry Chemical Physics,* 20**,** 86-96.

LV, J., ZHAO, F., FENG, J., LIU, Q., NAN, F. & XIE, S. 2019. Extraction of extracellular polymeric substances (EPS) from a newly isolated self-flocculating microalga Neocystis mucosa SX with different methods. *Algal Research,* 40**,** 101479.

MARTIN, G. J. O. 2016. Energy requirements for wet solvent extraction of lipids from microalgal biomass. *Bioresource Technology,* 205**,** 40-47.

NAVEED, S., LI, C., LU, X., CHEN, S., YIN, B., ZHANG, C. & GE, Y. 2019. Microalgal extracellular polymeric substances and their interactions with metal (loid) s: A review. *Critical Reviews in Environmental Science and Technology,* 49**,** 1769-1802.

OLMSTEAD, I. L., HILL, D. R., DIAS, D. A., JAYASINGHE, N. S., CALLAHAN, D. L., KENTISH, S. E., SCALES, P. J. & MARTIN, G. J. 2013. A quantitative analysis of microalgal lipids for optimization of biodiesel and omega-3 production. *Biotechnology and bioengineering,* 110**,** 2096-2104.

PIERRE, G., DELATTRE, C., DUBESSAY, P., JUBEAU, S., VIALLEIX, C., CADORET, J.-P., PROBERT, I. & MICHAUD, P. 2019. What is in store for EPS microalgae in the next decade? *Molecules,* 24**,** 4296.

RAO, N., GRANVILLE, A., WICH, P. & HENDERSON, R. 2020. Detailed algal extracellular carbohydrate-protein characterisation lends insight into algal solid-liquid separation process outcomes. *Water research,* 178**,** 115833.

RAYNAUD, M., VAXELAIRE, J., OLIVIER, J., DIEUDÉ-FAUVEL, E. & BAUDEZ, J.-C. 2012. Compression dewatering of municipal activated sludge: effects of salt and pH. *Water research,* 46**,** 4448-4456.

RUIZ-HERNANDO, M., MARTINEZ-ELORZA, G., LABANDA, J. & LLORENS, J. 2013. Dewaterability of sewage sludge by ultrasonic, thermal and chemical treatments. *Chemical Engineering Journal,* 230**,** 102-110.

RUTGERS, I. R. 1962. Relative viscosity and concentration. *Rheologica Acta,* 2**,** 305-348.

SPIDEN, E. M., SCALES, P. J., KENTISH, S. E. & MARTIN, G. J. 2013. Critical analysis of quantitative indicators of cell disruption applied to Saccharomyces cerevisiae processed with an industrial high pressure homogenizer. *Biochemical engineering journal,* 70**,** 120-126.

SPIDEN, E. M., SCALES, P. J., YAP, B. H., KENTISH, S. E., HILL, D. R. & MARTIN, G. J. 2015. The effects of acidic and thermal pretreatment on the mechanical rupture of two industrially relevant microalgae: Chlorella sp. and Navicula sp. *Algal research,* 7**,** 5-10.

STAL, L. J. & DÉFARGE, C. 2005. Structure and dynamics of exopolymers in an intertidal diatom biofilm. *Geomicrobiology Journal,* 22**,** 341-352.

TAKAHASHI, E., LEDAUPHIN, J., GOUX, D. & ORVAIN, F. 2009. Optimising extraction of extracellular polymeric substances (EPS) from benthic diatoms: comparison of the efficiency of six EPS extraction methods. *Marine and Freshwater Research,* 60**,** 1201-1210.

USHER, S. P. 2005. *Suspension dewatering: characterisation and optimisation.* University of Melbourne (Australia).

VANTHOOR-KOOPMANS, M., WIJFFELS, R. H., BARBOSA, M. J. & EPPINK, M. H. 2013. Biorefinery of microalgae for food and fuel. *Bioresource technology,* 135**,** 142-149.

WILEMAN, A., OZKAN, A. & BERBEROGLU, H. 2012. Rheological properties of algae slurries for minimizing harvesting energy requirements in biofuel production. *Bioresource technology,* 104**,** 432-439.

XIAO, R. & ZHENG, Y. 2016. Overview of microalgal extracellular polymeric substances (EPS) and their applications. *Biotechnology Advances,* 34**,** 1225-1244.

YAO, S., METTU, S., LAW, S. Q. K., ASHOKKUMAR, M. & MARTIN, G. J. O. 2018. The effect of high-intensity ultrasound on cell disruption and lipid extraction from high-solids viscous slurries of Nannochloropsis sp. biomass. *Algal Research,* 35**,** 341-348.

YAP, B. H., MARTIN, G. J. & SCALES, P. J. 2016. Rheological manipulation of flocculated algal slurries to achieve high solids processing. *Algal Research,* 14**,** 1-8.

YATIPANTHALAWA, B., LI, W., HILL, D. R., TRIFUNOVIC, Z., ASHOKKUMAR, M., SCALES, P. J. & MARTIN, G. J. 2021. Interplay between interfacial behaviour, cell structure and shear enables biphasic lipid extraction from whole diatom cells (Navicula sp.). *Journal of Colloid and Interface Science,* 589**,** 65-76.

YATIPANTHALAWA, B. & MARTIN, G. 2021. Conventional and novel approaches to extract food ingredients and nutraceuticals from microalgae. *In:* LAFARGA, T. & ACIÉN, G. (eds.) *Cultured Microalgae for the Food Industry.* Elsevier.

Chapter 6

6. Conclusions and Future recommendations

In this chapter, insights from the thesis are summarised and brought together to present an overall understanding of the downstream processing of microalgae for the recovery of high-value components including lipids, proteins and polysaccharides. This thesis helps to bridge the existing knowledge on wet microalgal processing, biphasic lipid extraction and EPS extraction from microalgae.

6.1 Key conclusions

The key conclusions from the thesis are summarised as below.

1. *Nannochloropsis* sp. cells switch to glycolytic and fermentative pathways during dark anoxia and the cells undergo proteolysis and lipolysis leading to eventual cell weakening and autolysis.

In Chapter 3, a previously introduced dark anoxia incubation method used to weaken the cell walls of the microalgae *Nannochloropsis* sp. was studied in detail with regards to the effects on the biomacromolecules and the underlying cellular responses. It was seen that dark anoxia imposes several stress conditions on *Nannochloropsis*, leading the cells actively switching to alternate energy generating and fermentative pathways. This adaptation leads to reduced ATP production, the accumulation of various fermentative end products, and eventually the loss of cellular membrane integrity. The switch to dark anoxic metabolism involved the induction of several proteins with specific functions and the removal or degradation of others. In general, the changes in the proteome were more pronounced in the early stages of incubation, consistent with an active metabolic response, while longer time periods lead to the uncontrolled loss of membrane integrity and inadvertent degradation of cellular biomacromolecules including the proteins and lipids to form peptides and free fatty acids respectively. This is a particularly important finding for potential industrial application of this method for production of proteins and lipids. Considering the degradation of the proteins and lipids it is important to optimise the dark anoxia incubation time in order to minimise the degradations while maximising the cell weakening.

2. Biphasic lipid extraction from the diatom *Navicula* sp. can be achieved without prior cell rupture and the application of shear enables efficient lipid extraction.

Chapter 4 investigated biphasic lipid extraction from unruptured cells of the diatom *Navicula* sp. in relation to cell structure, interfacial behaviour and the application of shear. Prior cell rupture is generally considered necessary for biphasic lipid extraction from wet slurries of microalgal cells. However, due to difference in their cell structure, prior cell rupture was found to be not necessary for biphasic lipid extraction from *Navicula* sp. Intact diatom cells were able to make direct contact with hexane droplets, enabling the removal of intracellular lipid bodies. Application of shear greatly improved lipid extraction by minimising the time required to achieve a certain lipid yield.

Chapter 3 proposes a mechanism for biphasic lipid extraction from *Navicula* sp. based on its cell wall structure, interfacial behaviour and the application of shear. The presence of EPS was found to hinder biphasic lipid extraction from *Navicula* and the application of power ultrasound effectively removed the EPS layer without leading to significant cell rupture. This chapter resulted in new insights into the extraction of lipids from diatoms, with important implications for large-scale lipid producing from these algae.

3. Ultrasound assisted EPS removal improves the processability of wet microalgal slurries of the diatom *Navicula* sp.

Having shown the ability of power ultrasound to remove the EPS layer from the diatom *Navicula* sp. without causing significant cell rupture in Chapter 4, Chapter 5 looked at EPS removal and its effect on the processability of algal suspensions of the diatom *Navicula* sp. The removal of EPS improved the processability of the microalgal slurries by reducing the viscosity, improving the dewaterability and increasing the efficiency of biphasic lipid extraction. This experimental chapter also showed that the use of high-intensity power ultrasound for EPS removal from the diatom *Navicula* sp. improves the energy efficiency and produce high lipid yields. The findings open new possibilities to produce a potentially valuable polysaccharide product from diatoms, while simultaneously enhancing the subsequent recovery of the lipids.

6.2 Recommendations and future studies

The following is a collection of outstanding research questions and recommendations for future research.

1. Understanding the impact of protein hydrolysis on the functional and nutritional value of microalgal proteins.

Protein degradation, or specifically protein hydrolysis (the breakdown of proteins into smaller peptides) can have various impacts on the nutritional and flavour profiles of microalgal protein fractions. As dark anoxia incubation leads to proteolysis, the functional and nutritional properties of the protein fraction as a function of incubation time are likely to change and should therefore be investigated. As an example, the bioactivity of the protein fraction, such as the antioxidant capacity can be investigated. Further, the emulsification ability can also be investigated as a important functional property, as protein hydrolysis was previously seen to decrease the emulsification ability of microalgal proteins (Medina et al., 2015).

2. Scaling up cell weakening via dark anoxia incubation.

Given the ability to weaken the cell walls of Nannochloropsis sp. using dark anoxic incubation as seen in chapter 3, this method appears to have the potential to be used commercially at an industrial scale. Scale up of this method will need careful consideration of the vessel design and mixing regime to ensure a uniform temperature and anoxic environment. It was previously seen that dark anoxic incubation was dependant on mixing, although the mechanism was not elucidated (Halim

et al., 2016a). When it comes to scale up, the effectiveness of mixing will affect the homogeneity of temperature and metabolites, and therefore the extent of localised differences in the metabolism of the cells. Also, as the cell walls of Nannochloropsis weaken over time, the turbulence and shear forces introduced by different methods of mixing could have an impact on the integrity of the weakened cells. Therefore, further investigations into these aspects will be needed to identify the optimal mixing regime, and the design of large-scale incubation vessels.

3. In-depth characterisation of Navicula frustules and EPS.

From chapter 4, it was seen that lipids inside the cells were extracted into the hexane droplets over time. Through studying the hexane water interface, the cells were seen to be interacting directly with hexane. In order for such phenomena to occur, the EPS fraction must firstly have some surface activity (as polysaccharides are seen to be surface active) and secondly the frustules themselves should have some hydrophobic properties. Although Klein et al. (2014) have shown that cells of the diatom *Navicula jeffreyi* are moderately hydrophobic, it would be worth studying the cell surface and EPS fraction in *Navicula* sp. to get a further in depth understanding on the mechanism of biphasic lipid extraction. This would also provides useful insights into the potential application of the frustule and EPS components.

4. Generalising findings on Naviula to other diatoms.

The pores present in the frustules of *Navicula* were proposed to be facilitating the biphasic lipid extraction in Chapter 4. Since the frustule pores are common to all diatoms, it would be worth studying if the mechanism of biphasic lipid extraction from *Navicula* is common to other diatom species, including both pennate and centric cells. As a starting point, another pennate diatom and a centric diatom could be used.

5. Optimising lipid extraction from the diatom Navicula.

The biphasic lipid extraction process from the diatom *Navicula* sp. can further be optimised considering important processing parameters such as the solvent-to-biomass ratio and solids concentration of the slurry to obtain a more efficient lipid extraction process. Also, another important factor to consider is the separation of the lipid-rich hexane layer following lipid extraction. Physical solvent separation using centrifugation is required to minimise energy consumption, however it is challenging when stable emulsions are present (Law et al., 2017a). Understanding how to balance the need for emulsion formed during biphasic lipid extraction with the separation efficiency for this type of cells, will be critical to maximising the overall energy efficiency of processing.

6. Investigation into possible lipid degradation during lipid extraction from Navicula sp.

Coupling the observations made in the chapters 3 and 4, the lipases present in the cells could act on the lipids if the conditions are favourable during biphasic lipid extraction. Hence it would be

worth investigating effect of exposure to ultrasound or prolonged high-shear mixing on the quality of the lipids extracted using hexane.

7. Navicula EPS as a functional polysaccharide.

Having demonstrated the ability of power ultrasound to remove the EPS fraction efficiently and the improvement seen on the processability of the microalgal slurries, it is worth investigating the feasibility of using this separated EPS fraction as a value-added by product. In particular, the nutritional and functional properties of the *Navicula* EPS fraction is worth studying. Functional properties such as thickening ability, gel-stabilisation capacity and its nutritional profile could be analysed in relation to both algal cultivation and subsequent ultrasonic harvesting to determine the potential use of EPS as functional polysaccharides.

8. An in-depth analysis considering the scalability and energy consumption of ultrasound-assisted EPS and lipid extraction processes.

The ultrasound-assisted EPS and lipid extraction processes studied in the Chapter 6 showed great promise as a new biorefinery approach for diatoms. Before considering this for commercialisation, an overall energy assessment would be required, along with a technical analysis of what is required for scale-up of the process.

9. Investigation into the presence of bacteria and their interactions with the diatoms and diatomaceous EPS.

The diatom *Navicula* sp. that was investigated in Chapter 4 and 5 was not grown as pure axenic cultures. It has been seen that *Nannochloropsis* sp. coexists with small amounts of bacteria in lab scale photoautotrophic cultures (Poddar et al., 2018), and bacteria will co-exist with Navicula, possibly supported by the increased abundance of EPS. Previous work in the literature has found that diatoms closely interact with a diverse array of bacteria, and the EPS produced by diatoms acts as a source of food for the bacteria. This coexistence of diatoms with bacteria has previously seen to result in increased amounts of EPS and varying effects on cell growth rates depending on the species (Koedooder et al., 2019, Johansson et al., 2019). Therefore, it will be worth investigating the interactions between the studied diatom *Navicula* sp. and its associated bacteria, to see if any and how it affects the production and composition of EPS and the processability of cell slurries.

References

HALIM, R., WEBLEY, P. A. & MARTIN, G. J. 2016. The CIDES process: fractionation of concentrated microalgal paste for co-production of biofuel, nutraceuticals, and high-grade protein feed. *Algal Research,* 19**,** 299-306.

JOHANSSON, O. N., PINDER, M. I., OHLSSON, F., EGARDT, J., TÖPEL, M. & CLARKE, A. K. 2019. Friends with benefits: Exploring the phycosphere of the marine diatom Skeletonema marinoi. *Frontiers in microbiology,* 10**,** 1828.

KLEIN, G. L., PIERRE, G., BELLON-FONTAINE, M.-N., ZHAO, J.-M., BRERET, M., MAUGARD, T. & GRABER, M. 2014. Marine diatom Navicula jeffreyi from biochemical composition and physico-chemical

surface properties to understanding the first step of benthic biofilm formation. *Journal of Adhesion Science and Technology,* 28**,** 1739-1753.

KOEDOODER, C., STOCK, W., WILLEMS, A., MANGELINCKX, S., DE TROCH, M., VYVERMAN, W. & SABBE, K. 2019. Diatom-bacteria interactions modulate the composition and productivity of benthic diatom biofilms. *Frontiers in Microbiology,* 10**,** 1255.

LAW, S. Q., CHEN, B., SCALES, P. J. & MARTIN, G. J. 2017. Centrifugal recovery of solvent after biphasic wet extraction of lipids from a concentrated slurry of Nannochloropsis sp. biomass. *Algal research,* 24**,** 299-308.

MEDINA, C., RUBILAR, M., SHENE, C., TORRES, S. & VERDUGO, M. 2015. Protein fractions with techno-functional and antioxidant properties from Nannochloropsis gaditana microalgal biomass. *Journal of Biobased Materials and Bioenergy,* 9**,** 417-425.

PODDAR, N., SEN, R. & MARTIN, G. J. 2018. Glycerol and nitrate utilisation by marine microalgae Nannochloropsis salina and Chlorella sp. and associated bacteria during mixotrophic and heterotrophic growth. *Algal Research,* 33**,** 298-309.

Chapter 7

7. Appendices

Supporting experiments were done to better understand the physicochemical mechanisms of mechanical cell rupture and biphasic lipid extraction from *Nannochloropsis* and *Navicula* sp. carried out in the thesis. While these research questions were beyond the key research questions addressed in the thesis, they will be appended to the thesis for completeness. Each additional experimental section includes a short introduction, details of the experiments, a description of the results and a summary of the key findings. Further, following these separate supporting experimental sections, additional images supporting the observations and conclusions of the experimental chapters are included following the separate experimental sections.

7.1 The effect of the presence of hexane on the rupture efficiency of *Nannochloropsis* using ultrasonication.

In Chapter 4, it was seen that ultrasonication greatly improved the biphasic lipid extraction from the diatom *Navicula* sp. The application of ultrasound to a biphasic lipid extraction system of *Navicula* resulted in complete cell rupture. Such an effect had not been previously observed in microalgae with cellulosic cell walls such as *Nannochloropsis* sp. Therefore, experiments were carried out to confirm the effects on the extent of cell rupture in *Nannochloropsis* sp. in a biphasic system.

For this *Nannochloropsis* sp. was grown and harvested following the same methods described in Section 3.2.1 and rediluted using artificial sea water to obtain a solids concentrations of around 2% (w/w). 10 ml of the cell suspensions were put into centrifuge tubes. In order to observe the effects of ultrasonication and ultrasonication in the presence of hexane two sets of experiments were carried out. To determine the extent of cell rupture following ultrasonication in the presence of hexane, 10 ml of hexane was added to the tube and the procedure explained for ultrasound assisted biphasic lipid extraction in Section 4.2.3 was followed. To determine the extent of cell rupture when subjected to ultrasonication alone, 10 ml of artificial sea water was added to the tube and the same method was followed as in Section 4.2.8. Following ultrasonication for different time intervals, 500 µl of the suspensions were collected in separate tubes. The extent of cell rupture was measured by obtaining the cell counts using a standard Neubauer hemocytometer, and imaged using Olympus BX51 microscope (Olympus, Australia) after appropriate dilutions.

The results obtained showed that the presence of hexane did not affect the extent of cell rupture of *Nannochloropsis* when subjected to ultrasonication (Figure 7.1).

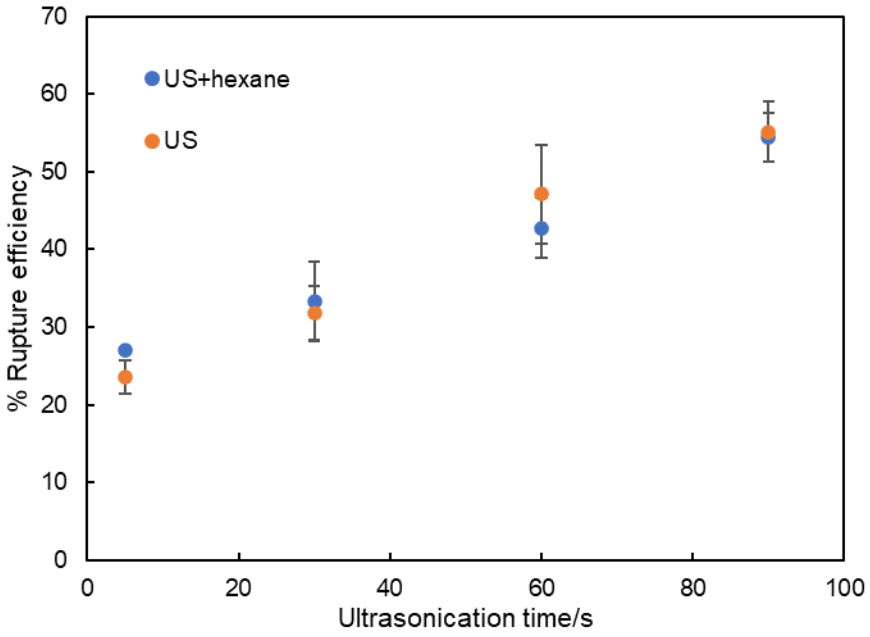

Figure 7.1: Rupture efficiency of *Nannochloropsis* sp. subjected to ultrasonication in the presence and absence of hexane as determined by cell counting using a haemocytometer. The cell density and the power density were maintained constant in order to avoid any effect on the rupture efficiency. The error bars represent the standard deviation of process triplicates.

7.2 Comparison of two cell rupture quantification methods for *Navicula* sp.

Cell count and the absorbance measured at 260 nm have both been used previously to quantify the extent of cell rupture in different microorganisms. In order to verify the comparability of the two methods for *Navicula* sp., experiments were performed.

Navicula sp. suspensions that were subjected to ultrasonication at different time intervals were used to obtain cell counts using a Neubauer hemocytometer and the absorbance at 260 nm using a UV-Vis spectrophotometer. Data obtained using both the measurement methods correlated well (Figure 7.2).

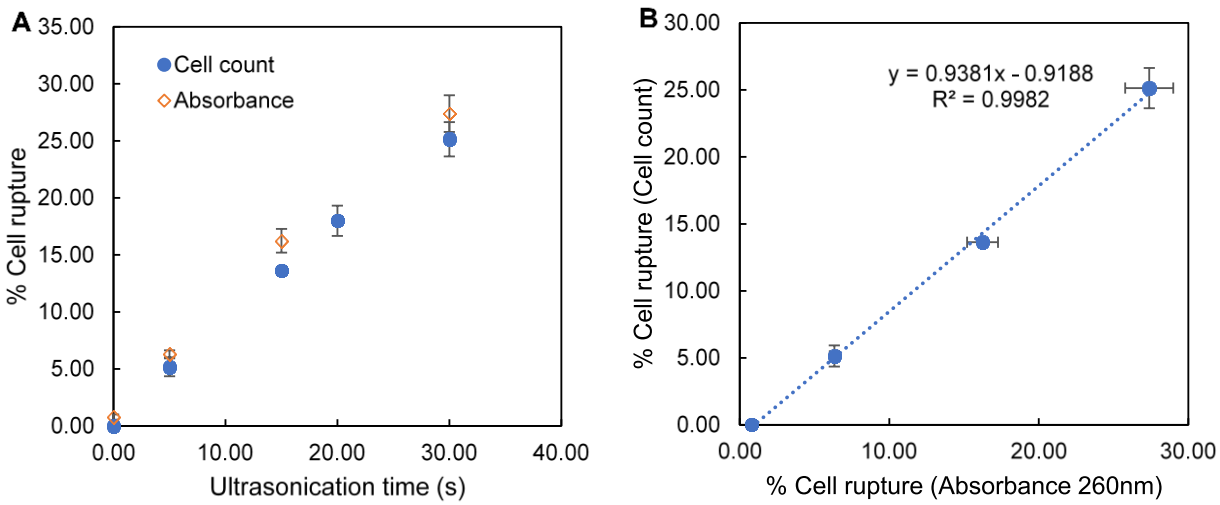

Figure 7.2: Extent of cell rupture of *Navicula* sp. measured by manual cell counting using a haemocytometer and by measuring the absorbance at 260 nm, (A) as a function of ultrasonication time, and (B) as a correlation of the two measurements

7.3 Viscoelasticity of the *Navicula* sp. slurries.

Viscoelasticity is the ability for a material to behave as both a solid and a liquid (i.e. showing both viscous and elastic behaviour). The storage modulus G' represents the elastic portion of the viscoelastic behaviour, that is the solid-state behaviour of a sample. The loss modulus G" describes the viscous portion of the viscoelastic behaviour, that is the liquid-state behaviour of the sample. A strain sweep at a constant angular frequency of 1 rad/s was performed using a rheometer at different solid concentrations of the diatom Navicula sp.

Similar to other viscoelastic materials, an initial elastic region (G'>G") is observed followed by a viscous flow (G">G'). Figure 7.3 shows how the linear viscoelastic region changes with the increasing solid concentration. As the solids concentration becomes higher the liquid shows a gel-like behaviour, and as the solid concentration reduces the liquid-like behaviour increases. The force required to disturb the network structure and make the material flow increases with the increasing solids concentration, thereby confirming the increased viscoelastic behaviour. The suspensions below 3.6% (w/w) concentrations showed pure viscous behaviour (G">G').

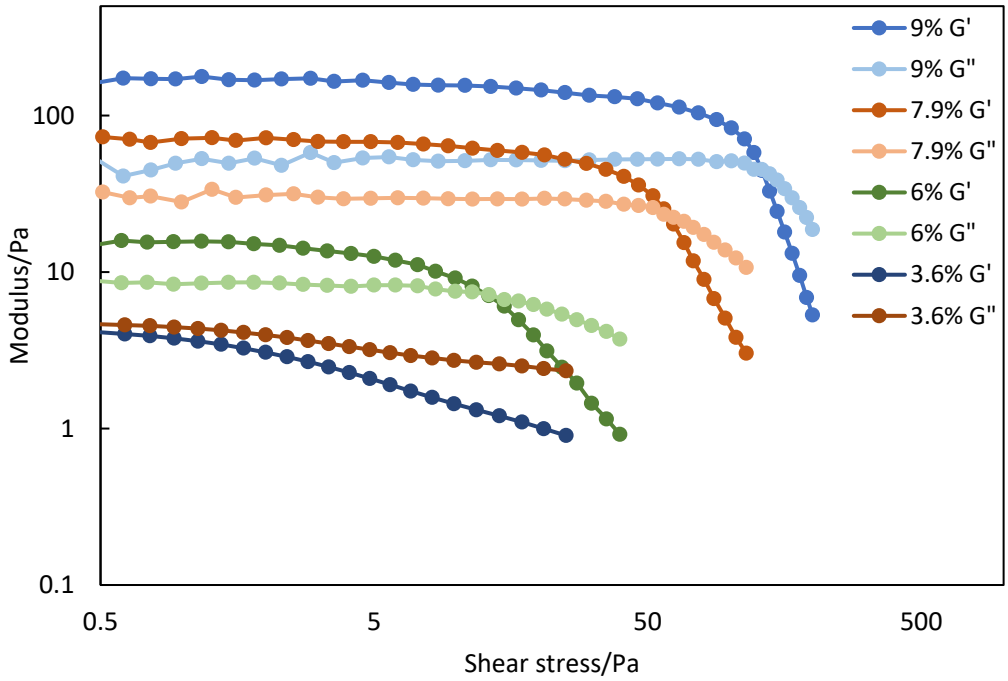

Figure 7.3: Strain sweep at a constant angular frequency of 1 rad/s indicating the linear viscoelastic range (LVE).

7.4 Supporting figures for the experimental chapters.

Additional figures for supporting the experimental chapters are included below.

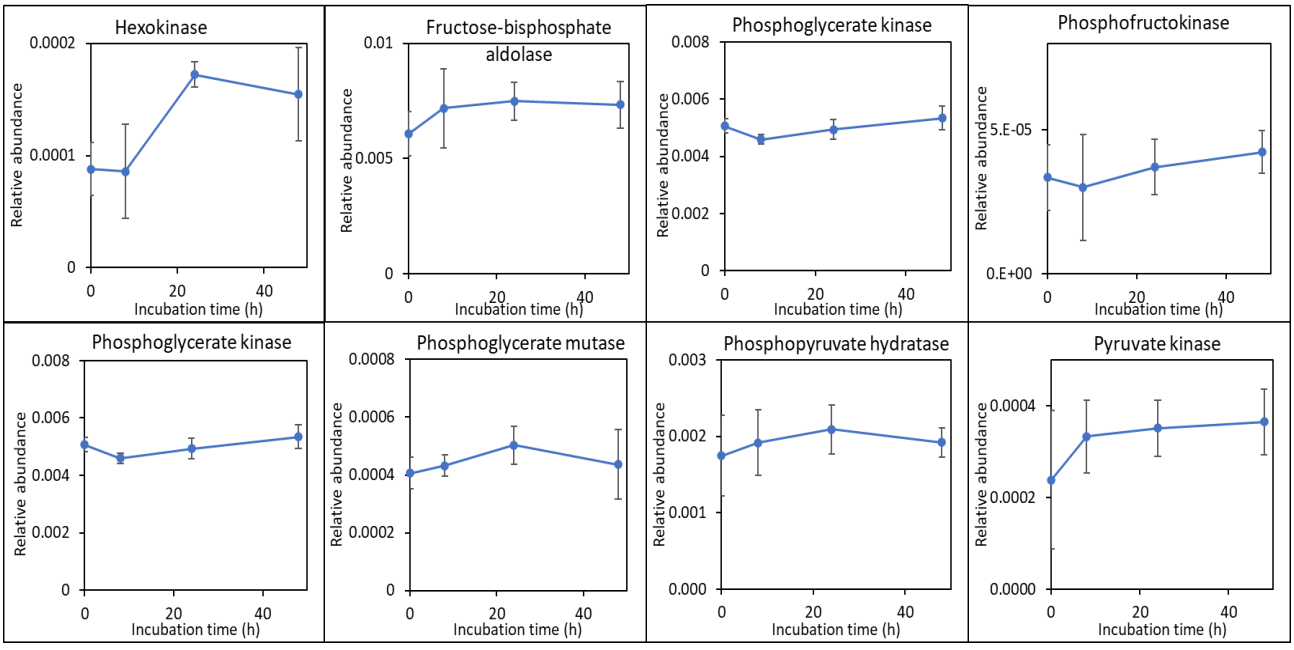

Figure 7.4: The average sum of the relative abundance of protein involved in the glycolytic pathway as explained in Figure 3.5.

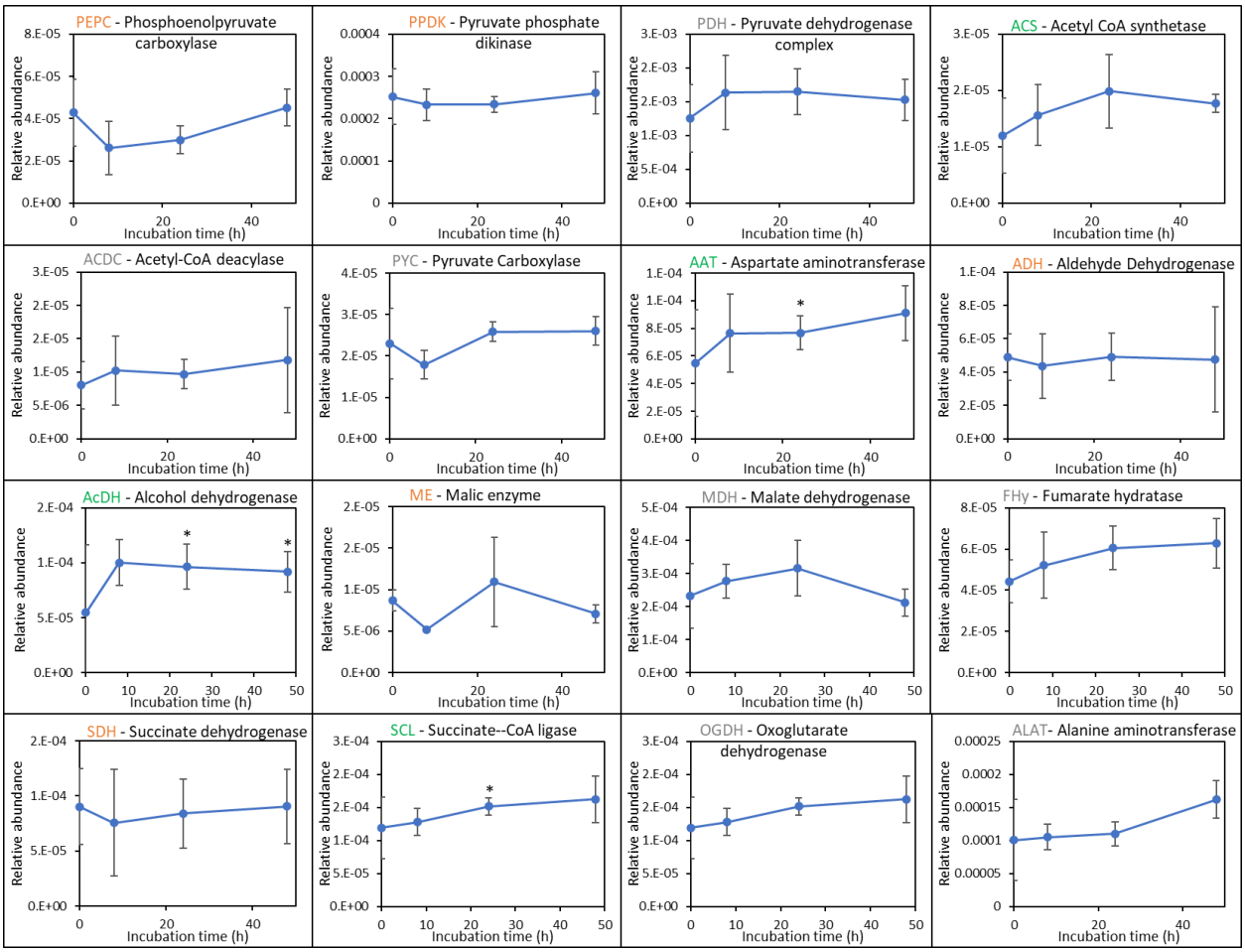

Figure 7.5: The average sum of the relative abundance of proteins involved in the fermentative pathways as explained in the Figure 3.6. Error bars represent the standard deviation of duplicated samples of triplicated experiments. Green: significantly increased. Grey: increased but not significantly. Orange: decreased but not significantly Black: not found. Asterisk symbols represent statistically significant differences compared to the t = 0 time point.

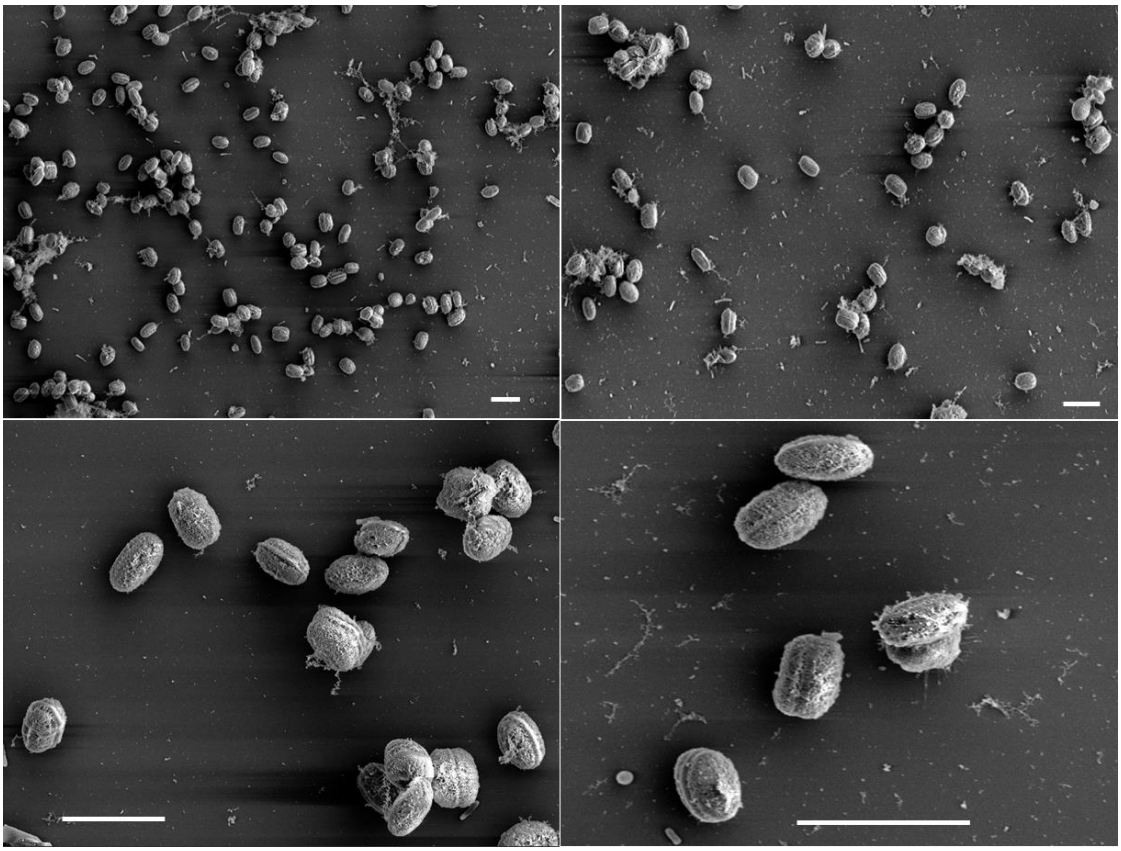

Figure 7.6: SEM images of *Navicula* sp. cells freshly harvested by centrifugation to support the observation in the Figure 4.1. The scale bars represent 10 µm.

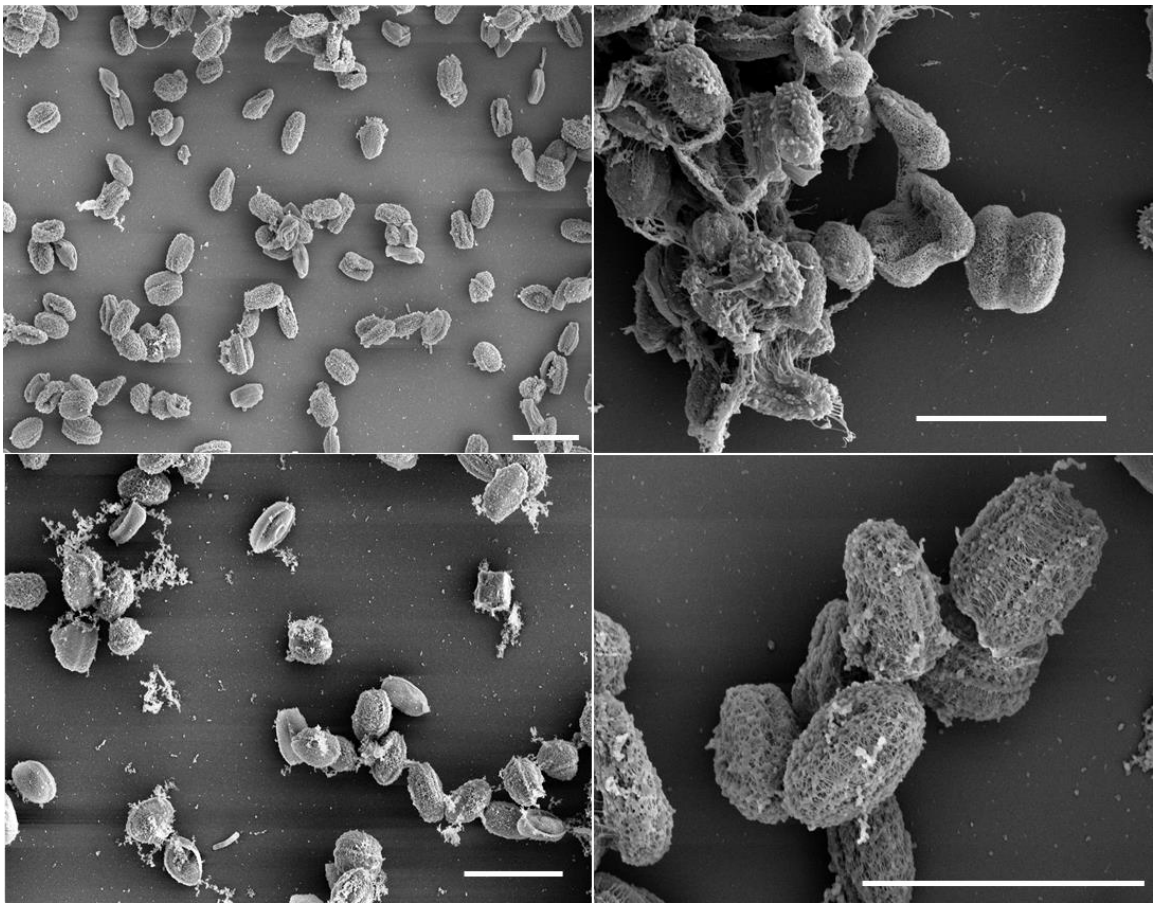

Figure 7.7: Additional SEM images of *Navicula* sp. cells mixed with hexane for 23h to support the observations in Figure 4.1. The scale bars represent 10 µm.

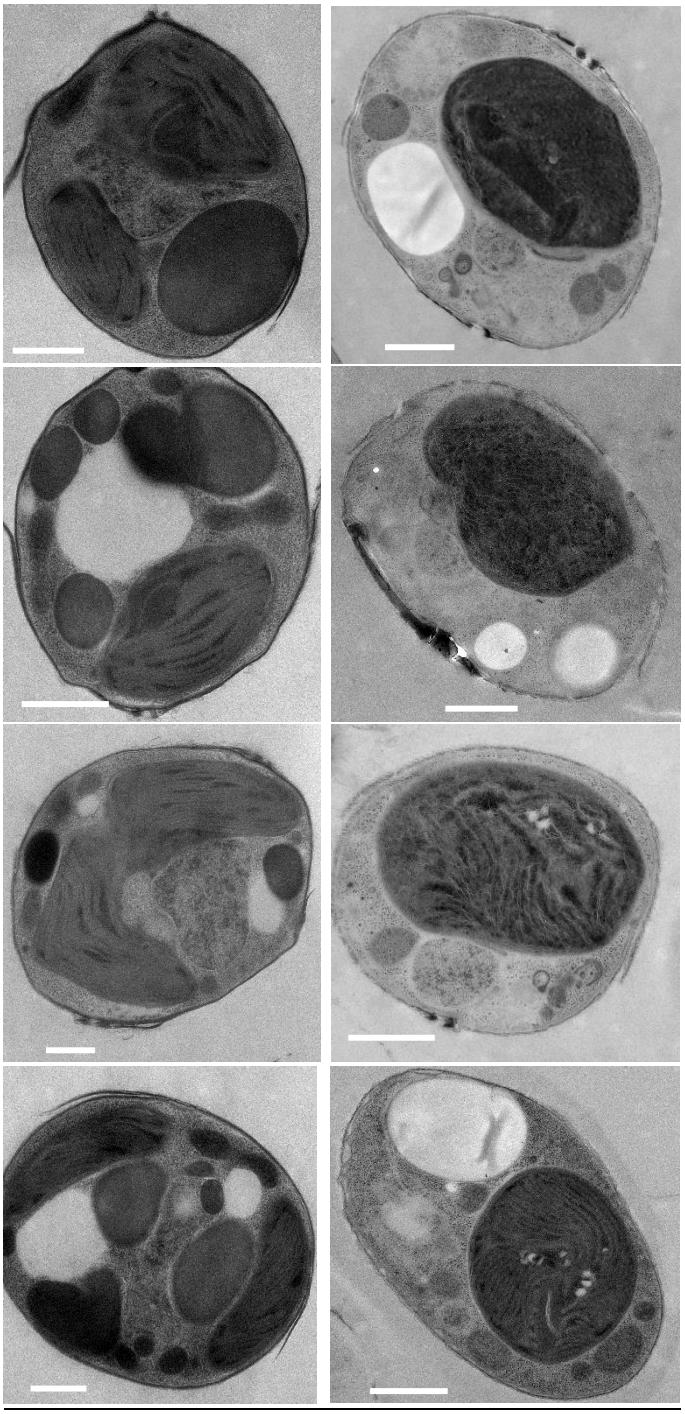

Figure 7.8: Additional TEM images of freshly harvested *Navicula* sp. cells (left panel) and cells contacted with hexane for 2 h without high-shear mixing (right panel) to support the observations in Figure 4.3. The scale bars represent 1 μm.

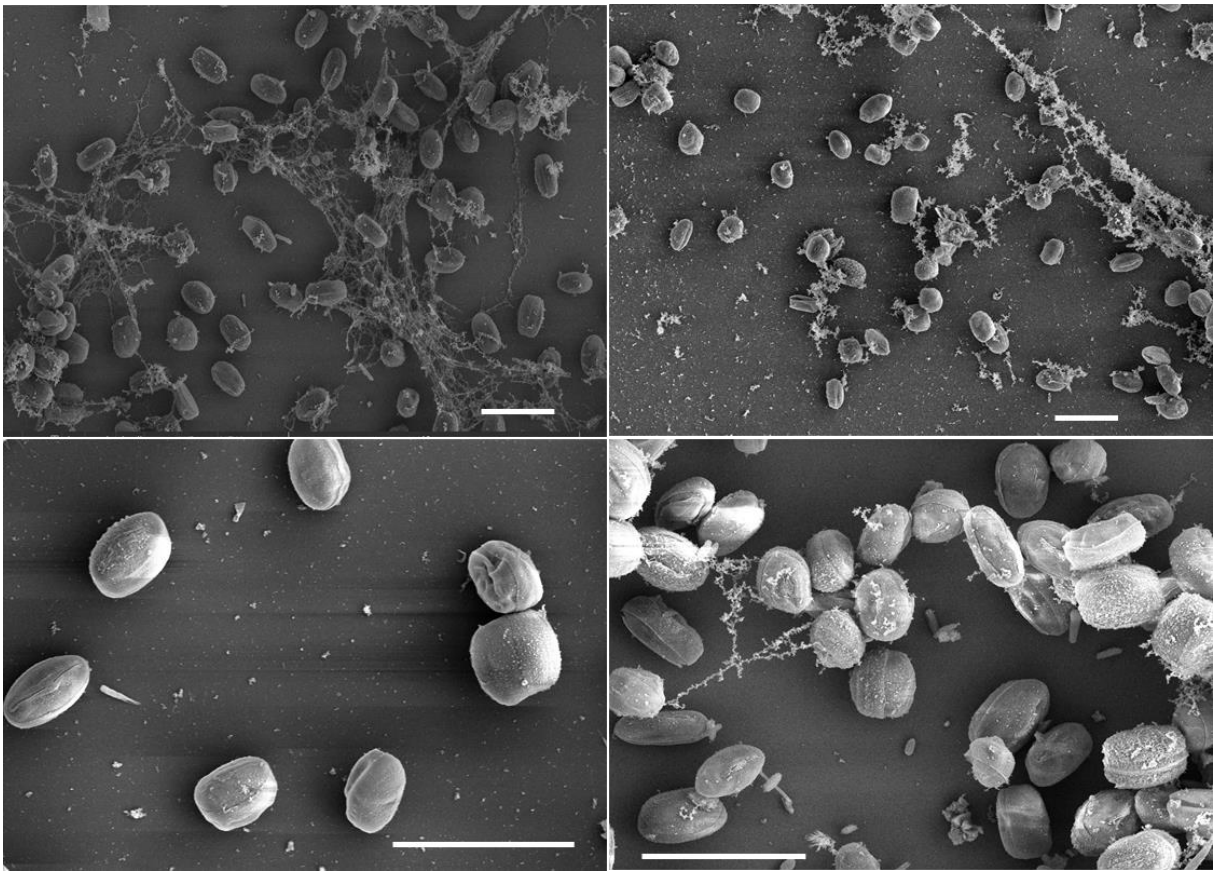

Figure 7.9: Additional SEM images of *Navicula* sp. cells ultrasonicated for 1 min to support the observations in Figure 4.5. The scale bars represent 10 µm.

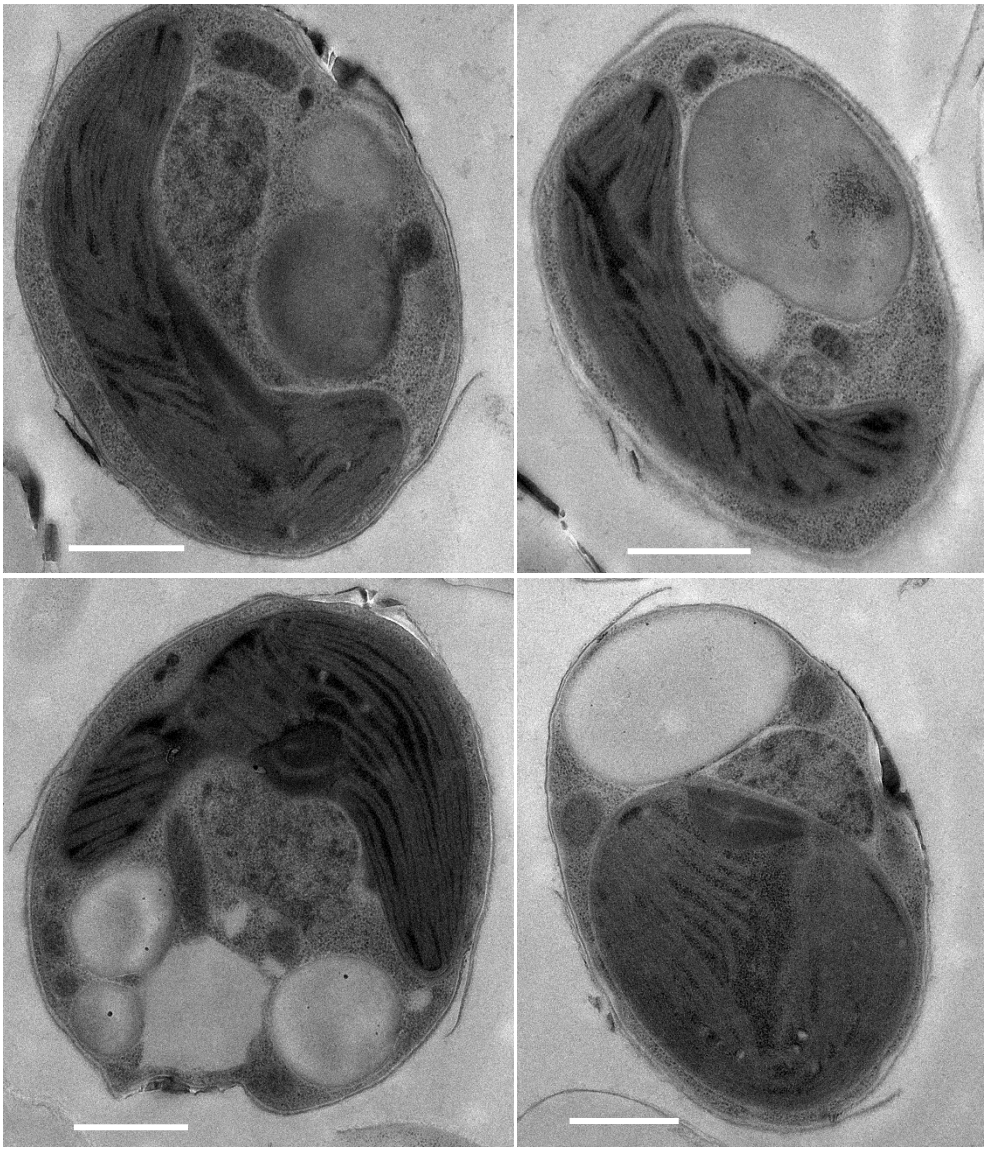

Figure 7.10: Additional TEM images of *Navicula* sp. ultrasonicated for 1 min to support the observations in Figure 4.5. The scale bars represent 1 µm.